



Norwegian University of  
Science and Technology

# a Four Wheel Drive System for a Formula Style Electric Racecar

**Peder August Aune**

Industrial Design Engineering

Submission date: February 2016

Supervisor: Johannes Sigurjonsson, IPD

Norwegian University of Science and Technology  
Department of Product Design



# Foreword

This master thesis is the culmination of a fantastic four year career in Revolve NTNU. It ended up becoming a true passion project that really challenged both my creative ability and my skill in design and engineering. The result of this process is thoroughly recorded within this stack of paper. What is not recorded is all the long nights, frustrations and failures required in order to finally end up with a working product at this level. It is a well known fact that the bigger the challenge is, the larger the number of failures will be before one is able to finally achieve success. The success will however also be proportionally more satisfying. This is very descriptive of my experience with this project.

The focused mentality, creative environment and dedication experienced during my time in Revolve NTNU have left me deeply appreciative of the organization and all of its members. I consider myself very lucky in having been provided the resources and arena needed in order to realize this project. In ending i will therefore extend a thank you to Revolve NTNU team 2016 for providing me with the experience of a lifetime.

# Abstract

This is a master thesis detailing the development and design of a four wheel drive transmission system for a formula style race car using four electric motors to achieve asynchronous power output to each wheel. First an in depth analysis was performed in order to identify key system performance parameters. A concept development phase was used to come up with a system layout based on the performance requirements. The transmission system was then designed and calculated using KISSSoft. Topology optimization in OptiStruct was used to design the gearbox/wheel upright. Results have been evaluated, showing significant reduction in weight and increase in performance over existing systems. Manufacturing documentation has been designed for every part of the system. A discussion on commercial viability of such a system has then been discussed.

# Table of content

<b>Master thesis</b>	<b>1</b>
<b>Acknowledgment</b>	<b>2</b>
<b>The author</b>	<b>4</b>
<b>Formula Student</b>	<b>6</b>
<b>Revolve NTNU</b>	<b>12</b>
<b>Project overview</b>	<b>16</b>
<b>User analysis</b>	<b>18</b>
-Primary user	18
-Secondary user	20
Vehicle dynamics	22
Torque vectoring	23
System overview	24
Collaboration	25
<b>Motor Analysis</b>	<b>27</b>
-Initial assessment	27
-Moment of inertia	29
-Difference in efficiency	32
-Lap time simulation: Acceleration	38
-Lap time simulation: Autocross	40
-Energy limitations and KERS	42
<b>Transmission ratio</b>	<b>44</b>
-Analysis of logged data	44
-Lap time simulation: Acceleration	46
-Lap time simulation: Autocross	48
<b>Drivetrain concepts</b>	<b>50</b>
-An evaluation of different mechanical concepts	50
-Different gear trains	52
-Examples	54
-Concept 1	56
-Concept 2	58
-Concept 3	60
-Choice of drivetrain concept	62
<b>Planetary systems</b>	<b>64</b>
-Design space	64
-Standard planetary system	66
-Double planetary system	67
-Compound planetary system	68
-Choice of solution	69
-Load spectrum for gear simulation	70
-Additional limitations in gear design	73
-Choosing gear material	74

<b>KISSSoft</b>	<b>76</b>
-Introduction	76
-Overview of system	78
-Main line shaft design and simulation	80
-Planet shaft design and simulation	82
-Bearing calculations	84
-Wheel bearing calculation	86
-Sizing of gear stage 1	88
-Sizing of gear stage 2	89
-Gear misalignment	90
-FEM simulation of planet carrier assembly	92
-Gear calculation	94
-Modification result evaluation	101
-Polygon connection	102
<b>System design</b>	<b>104</b>
-Planet shaft assembly	104
-Full gear assembly	106
-Full transmission system assembly	108
<b>Upright design</b>	<b>110</b>
-On designing for additive manufacturing	110
-3D printing with metallic materials	112
-Microstructures workflow verification	116
-Microstructure in upright center	118
-Topology optimization	120
-Front upright optimization result	122
-Front upright finished CAD model	123
-Rear upright optimization result	124
-Rear upright finished CAD model	125
-FEM verification of front upright	126
-FEM verification of rear upright	128
<b>Final design</b>	<b>130</b>
-Motor cooling block	130
-Front assembly	132
-Rear assembly	134
-Front wheel	136
-Rear wheel	137
-Drivetrain and suspension layout	138
-Hard data	140
-Evaluation of data	142
-Non quantifiable results	143

<b>Manufacturing design</b>	<b>144</b>
-Sun gear	146
-Planet gear 1	148
-Planet gear 2 (0, 120 and 240 deg.)	150
-Ring gear	152
-Planet pin shaft	154
-Hub	156
-Planet carrier	158
-Motor adapter plate	160
-Prevention nut	162
-Front upright	164
-Rear upright	166
<b>Commercial viability</b>	<b>168</b>
-Prototype cars	168
-Formula student prototypes	169
-Performance and implementation	170
-Disruptive effect	171
-Serviceability	172
-Torque vectoring and self driving cars	173
<b>Sources</b>	<b>174</b>
<b>Appendix</b>	<b>175</b>
-Polygon calculation	176
-Wheel bearing calculation	178
-Ring gear shear pin calculation	185
-Hardening depth gear stage 1	187
-Hardening depth gear stage 2	189
-Main line shaft calculation	191
-Planet shaft calculation	210
-Gear stage 1 calculation	220
-Contact analysis gear stage 1	230
-Gear stage 2 calculation	241
-Contact analysis gear stage 2	252



## Master Thesis for Student Peder August Aune

### A four wheel drive system for a formula style electric racecar.

*Firehjuls fremdrifts-system for en elektrisk racerbil*

Electric cars may be the future of personal transportation. Looking past the current challenges of battery technology, electric cars are one of the leading concepts for a sustainable, high performance future for the automotive industry.

Prototype race car development is, and has always been in the forefront of innovation and technology development for the automotive industry. While not cost efficient in their own right, these prototype programs have created, and will continue to create substantial future value for the industry.

The student organization Revolve NTNU designs and develops a new formula style race car each year in order to compete in the student engineering competition series known as Formula Student.

This master project will be conducted in cooperation with Revolve and working version of the results is planned to be implemented in the 2016 car.

The project will entail the design and development of a four wheel drive system for a formula style electric racecar. It is intended that the system will utilize four electric motors, one driving each wheel, enabling true asynchronous regulation of power output. The focus will be on design and development of the transmission, connecting the motors to the wheels with a speed reduction, as well as the whole wheel packaging in and of itself. A brief assessment of the commercial potential and future implications of automotive design will be included.

The project includes:

- Assessment of different four-wheel drive solutions
- Choice of solution
- Development of design parameters for the system
- Design and FEM analysis of the selected concept
- Detailing and manufacturing drawings of the final design.
- Assessment of commercial viability and future implications on automotive design

Responsible supervisor: Jóhannes B. Sigurjónsson  
Supervisor:

Start date: August 28. 2015  
Delivery date: January 22. 2016

Jóhannes B. Sigurjónsson  
Responsible supervisor

Trondheim, NTNU, August 28. 2015

Casper Boks  
Head of Department

# Acknowledgments

## Contributors

This project would have had a slim chance of success without the important and generous contributions of the following key partners.

Thanks to NTNU Department of Product Design with special mention to my faculty adviser Johannes Sigurjonsson for giving me the chance to work on this project for my master thesis.

Thanks to Revolve NTNU with special mention to Lennard Bosch and Kurt Erik Nesje.

Thanks to Benjamin Cach at Transtech for advising on gear design.

Thanks to Viggo Norum at Kongsberg Devotek for advising on gear design.

Thanks to Andre Thuswaldner at Novagear for advising on gear design.

Thanks to Amir Rasekhi Nejad at NTNU Department of Marine Technology for advising on gear design.

Thanks to ProNor for providing free licenses to Solidworks and EnterpricePDM software.

Thanks to KISSSoft AG for providing free student licenses and tech support.

Thanks to Materialise for providing free software licenses for 3D-printing software.

Thanks to Altair for providing free licenses on Hyperworks and OptiStruct software.

Thanks to Tronrud Engineering for sponsoring with titanium 3D printing production.

Thanks to Sandvik Teeness for sponsoring with free manufacturing of a large number of parts.

Thanks to SKF for sponsoring all bearings used in the project.

Thanks to Seal Engineering for sponsoring all O-rings and lip seals for this project.





Department of Product Design

**devotek**<sup>®</sup>

**NOVAGEAR**



Department of Marine Technology



ProNor



Altair



# The author

## Educational focus and past exploits



**Name:** Peder August Aune

**Born:** 1987

**City of origin:** Drammen

### **Educational focus:**

I have chosen to focus my education in industrial design engineering towards performance based product design. The choice was made from my love of functional, high performance design where high end materials synergized with smart engineering solutions and creative design. I also felt at home in the competitive multidisciplinary environments needed to succeed in this branch of product design. It is easy for me to become inspired by the need for ever improving skill and knowledge within this field. The prospect of never ending learning is my main motivational factor

## **Career in Formula Student:**

### **Revolve NTNU 2013:**

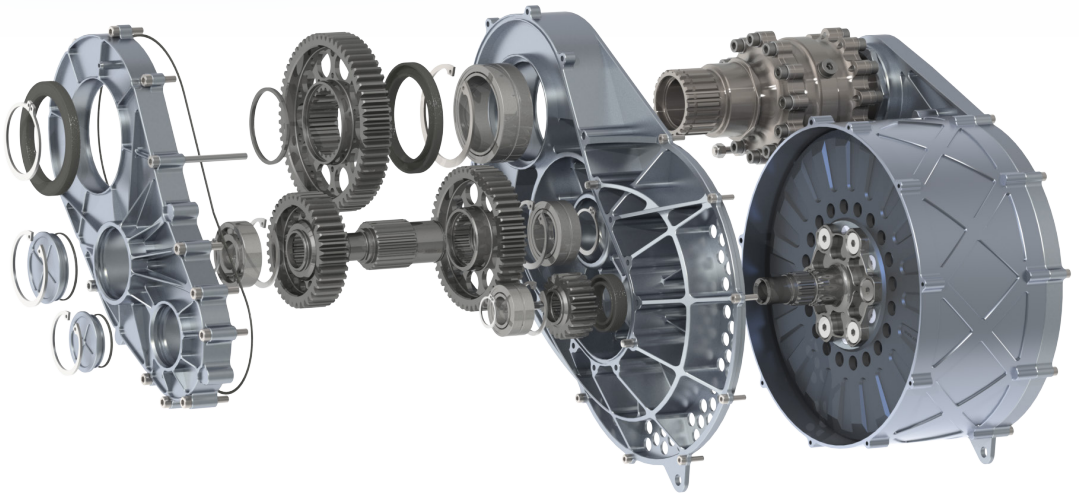
I had the role of lead digital designer responsible for the main assembly of the car. I was also tasked with designing the carbon fiber bodywork covering the steel space frame. I ended up also getting involved in the design of the motor plenum and CNC machine manufacturing of parts.

### **Revolve NTNU 2014:**

I had the role of lead digital designer responsible for overall vehicle design, assembly and the design of the carbon fiber monocoque chassis. I also did the manufacturing design and was heavily involved in the actual manufacturing of the chassis together with other key members. In addition to this, i manufactured a large number of parts in the CNC milling machine. This year Revolve developed Norway's first electric race car.

### **Revolve NTNU 2015:**

This year i was responsible for the design of the rear wheel drive transmission system. This task reduced organizational responsibilities from the years before in exchange for more focused project with a significantly higher grade of theoretical challenges. This project was done as my project thesis. Without the knowledge gathered during this project, the following master thesis would have been impossible to realize.



*Revolve NTNU major design contributions 2013 to 2015 from top to bottom.*

# Formula Student

## The worlds largest engineering competition for students

*"Formula Student is a testing ground for the next generation of world-class Engineers; a competition that attracts thousands of entrants and spectators from across the globe, with competitions in the United States, Australia and Germany as well as the United Kingdom, Formula Student is one of the world's biggest student events."*

*"The competition aims to inspire and develop enterprising and innovative young engineers. Universities from across the globe are challenged to design and build a single-seat racing car in order to compete in static and dynamic events, which demonstrate their understanding and test the performance of the vehicle."*

### **Formula Student is:**

*"A high-performance engineering project that is extremely valued by universities and usually forms part of a degree-level project"*

*"Viewed by the motorsport industry as the standard for engineering graduates to meet, transitioning them from university to the workplace."*

*"The kite-mark for real-world engineering experience"*

### **The Mission:**

*"The mission is to excite and encourage young people to take up a career*

*in engineering. It seeks to challenge university students to conceive, design, build, cost, present and compete as a team with a small single-seat racing car in a series of static and dynamic competitions. The format of the event is such that it provides an ideal opportunity for the students to demonstrate and improve their capabilities to deliver a complex and integrated product in the demanding environment of a motorsport competition."*

The task set by the competition is asking students to design and develop an open cockpit, single seat, open wheel, formula style race car. The car, knowledge and experience produced in the project is then used in a competition against other students. The competition entails the following static and dynamic events:

### **Business presentation:**

The event is structured as a pitch meeting with potential investors, where you have 10 minutes to convince them to invest in your business idea built on the criteria of manufacturing 1000 units of your car each year.

### **Cost event:**

Every part of the car needs to be documented in a cost document that specifies method and cost of both manufacture and assembly. The event is a control of the

correctness of this document with follow up questions with focus on the knowledge on manufacturing and sustainability.

### **Design event:**

This event is a 40 minute presentation, explaining the theory and thought behind the design and development of the car to a panel of world class engineering judges. Winning this event directly describes your teams superior knowledge of engineering. Winning this event is therefore considered almost as prestigious as an overall event victory.

### **Acceleration:**

A 75 meter drag race event that is designed to show the cars acceleration performance.

### **Skid pad:**

In this event, the car is to drive a full right hand circle and then a full left hand circle. The average time between the two circles is then used to describe the vehicles steady state cornering performance.

### **Autocross:**

This one round time trial event is the most technically challenging of all the dynamic events. This is where the skill of the driver has significant impact on the result. This is also the most prestigious of all the dynamic events as it best compares the maximum track pace of each vehicle.

### Endurance:

A 22 Km race over 20 laps with a pit stop and driver change at 11 km. This event is meant to test vehicle reliability, fuel management and race strategy. This is the event that most teams fear due to the fact that all competing vehicles are highly unreliable prototypes, and as a result, the number of teams able to finish the endurance race is low. It is also the event that awards the highest amount of points, making it impossible to place high in the overall standings without a finish.

### Efficiency:

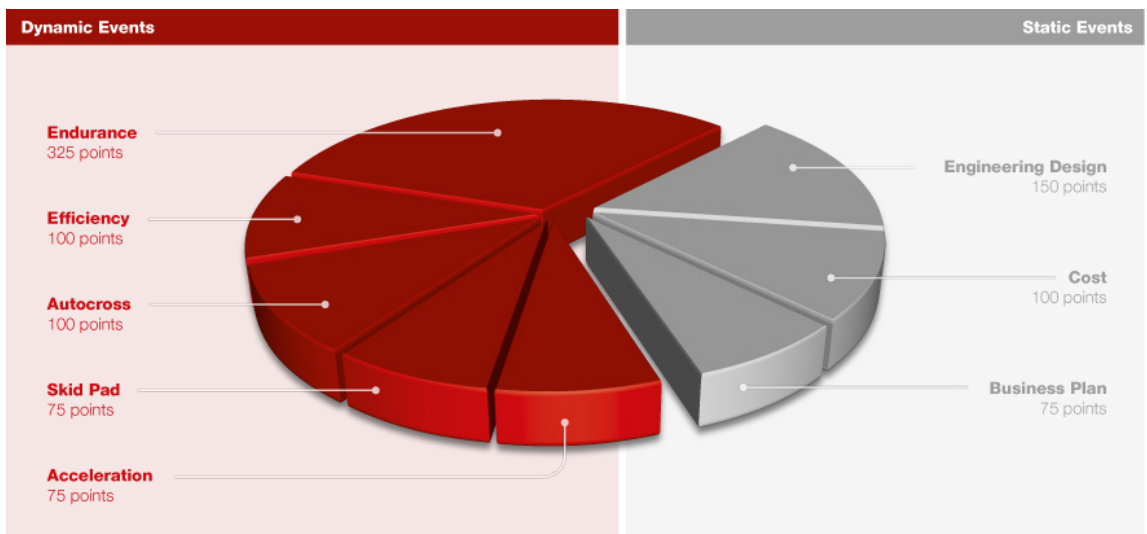
You are scored in efficiency based on the energy the car

consumed during the 22 km of the endurance race. The efficiency scoring is based on a combination of track pace and energy consumption. Focusing solely on energy spent per meter driven would severely punish the faster driving cars and would undermine the racing aspect of the competition.

In addition, there is an extensive technical control of every car making sure everything is in accordance with the competition rule set. A rule set mainly consisting of technical regulations that ensures driver safety in the event of a crash. This rule set is the only restrictive effort

imposed on the students when designing their car. The result is a plethora of different and creative design solutions in the hunt for more performance.

The competition is scored as seen below with a total of 1000 points spread unevenly over the 8 different events. The uneven point distribution shows the significance of each event, indicating that the most important parameter of the car is the combination between performance and reliability. No team yet has been able to score a perfect 1000 points.







# Formula Student

The cars







**Type:** Open wheel formula style car  
**Size:** 1600/1400 wheel base/track  
**Weight:** 150-200kg dry weight  
**Fuel type:** Electric  
**Power:** 80kW (rules restricted)  
**0-100 kph:** Under 3 seconds  
**Lateral maximum:** 2.3g  
**Range:** +22 km @ race pace.

# Revolve NTNU

## From theory to practice

Revolve NTNU is an independent organization operated by students at the Norwegian University of Science and Technology in Trondheim. It was founded in 2010 and has since 2012 produced a new formula student race car each year. The intention of the organization is to give engineering students a practical counterpart to the classroom theory preached by the university. This is done through the glory and passion of high technology race car engineering. The intended outcome is to produce better engineers for the future.

The first car designed by Revolve NTNU took an overall 19th place and was awarded best newcomer at Silverstone (FSUK) 2012. KA Borealis R was as such the important starting point of an impressive progression in project development.

The 2013 car saw the introduction of aerodynamic devices in the form of wings. KA Aquilo R was able to place 11th at Silverstone (FSUK) this season. Both car design and performance was as such a natural progression from the year before.

For the 2014 season, Revolve NTNU designed, manufactured and raced Norway's first custom built electric race car, taking home a strong 8th place during the Silverstone competition in England. This season saw a huge push towards a more advanced, refined and light weight car

that was able to deliver truly impressive track performance. The 4th place in the autocross event at Formula Student Germany was a testament to the pace of this car.

The 2015 project focused on refining the design and improving the reliability of the 2014 design. The team was able to save an additional 10 kg of weight, producing one of the lightest cars in the competition. The improved design of Vilje was able to grab a 3rd place in the design event at Silverstone (FSUK) and a truly astonishing 4th overall at Formula Student Austria.

A new team is recruited each year with project startup in August and a following 8 month design and manufacturing frenzy resulting in a brand new car come May. The team consists of around 50 students from over 10 different areas of engineering education spanning from mechanical engineering through cybernetics to industrial economics and management.

The project has significant similarities with a medium sized high end technology company paired with a top athlete mentality. It is this fearless "just do it" mindset that has seen Revolve NTNU progress from newcomer to among the best teams in the world in only 4 seasons.

Revolve NTNU is offering students a truly inspiring and innovative environment where they are able to develop both their practical and theoretical skill set.

## KA Borealis R (2012)

**82**  
BHP

**260**  
kg

**4.0**  
0-100 kph

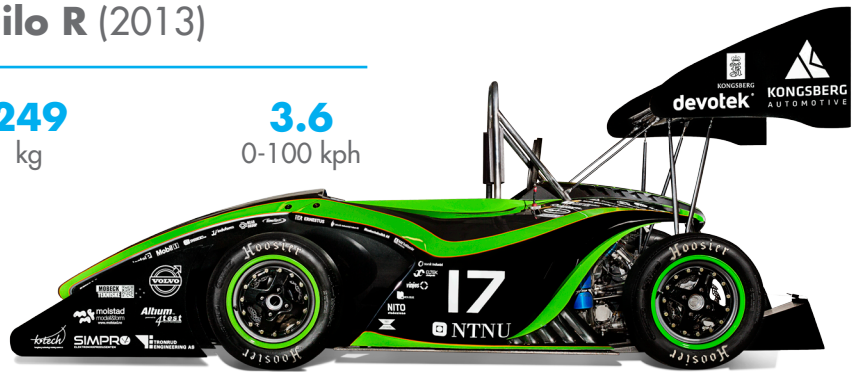


## KA Aquilo R (2013)

**85**  
BHP

**249**  
kg

**3.6**  
0-100 kph



## KOG Arctos R (2014)

**115**  
BHP

**185**  
kg

**2.9**  
0-100 kph

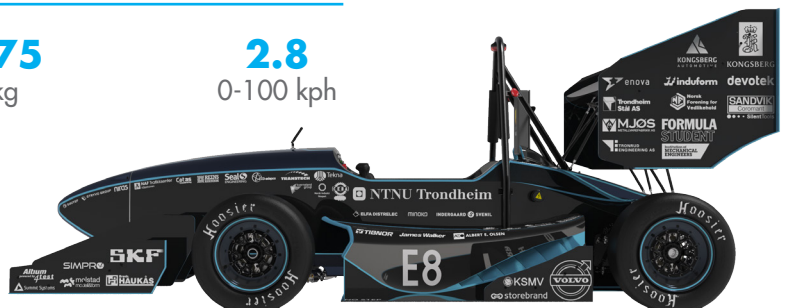


## Vilje (2015)

**107**  
BHP

**175**  
kg

**2.8**  
0-100 kph





**KONGSBERG**  
AUTOMOTIVE

revolve

**FORMULA**  
**STUDENT**  
INTERNATIONAL  
TECHNICAL  
ENGINEERING

KONGSBERG

**evotek**

KONGSBERG

**evotek**

KONGSBERG

**evotek**

KONGSBERG

**evotek**



# Project overview

## Definition of limitations and success criteria

For the last two years, Revolve NTNU has been using a single electric motor as the power plant of the car. More specifically, the cars have been designed with an Emrax 228 electric motor coupled to a limited slip differential running the rear wheels. This concept has been very successful so far, mainly because of the high reliability and fairly high performance such systems produce. The downside is that only 2 of the 4 available tires are used for traction in high acceleration situations.

As Revolve NTNU as an organization wants to keep pushing the boundaries of car design for the Formula Student competitions, it has been decided that a four wheel drive system is to be developed for the 2016 car. In addition to being a four wheel drive system, each wheel is to be actuated by a separate motor. Having a system of four individual motors enables asynchronous torque output to each wheel. This opens up to the possibility for active regulation of torque output for each tire, potentially optimizing track grip and acceleration in every situation.

The potential performance improvement from such a system is nothing less than significant. It is however an additional factor to this concept that is of equal importance. By opening up for the implementation of smart electronic systems that actively regulate individual wheel torque, Revolve NTNU enters into a world where development of extremely complex vehicle dynamics designs only currently used in super and hyper cars are made possible. This will increase the academic output of the project immensely. This strengthens the intention that Revolve NTNU is an educational program set on educating the best engineers in Norway.

The task of developing this four wheel actuated drivetrain is, as previously described in the official thesis description, the objective of the author. The thesis description does little to contextualize the project. A design brief that better specify the context, limitations and success criteria was developed to have a reference for evaluation of different concepts and design further into the project.

- 1 The system needs to comply with the restrictions set by the 2016 FSAE rules.
- 2 The system needs to use 4 AMK DD5-14 servo motors.
- 3 The system needs to fulfill its primary function of transferring torque from the motors to the wheels with an added appropriate rotational speed reduction mechanism.
- 4 The system needs to deliver the same or better torque performance compared to the 2015 system.
- 5 The system needs to weigh the same or less compared to the 2015 system.
- 6 The system needs to be designed within the financial limitations of Revolve NTNU and the manufacturing competence of involved sponsors.
- 7 Full manufacturing documentation needs to be created for all parts.
- 8 The system needs to be manufactured.
- 9 The manufactured system needs to deliver the performance specified in the design documentation.
- 10 The system has to last the whole season without needing replacement of parts.

# User analysis

## Primary user

The primary user of the proposed drive train will be the driver. It is this interface between human and machine that will determine the actual overall success of the system no matter how impressive the theoretical numbers or performance specifications are. Following is a breakdown of the most important criterion in fulfilling the primary user needs:

### Performance:

The system must deliver high performance in order to make it possible for the driver to achieve a high pace. High acceleration performance results in a car that is much more forgiving to driver mistakes. A system that delivers high torque will therefore help the driver perform better.

### Weight:

A light weight system will help keep the total mass of the car down. A lighter car will accelerate quicker in every direction. The driver will perceive the car as more agile and easier to control. The car will as such enable the driver to run at higher pace with increased control. Low weight is as such a major contributor to improved primary user experience.

### Predictability:

The driver needs to be able to predict the behavior of the system in high stress situations. A system with a high degree of compliance will be perceived as unpredictable and slow reacting to driver input. Predictability will build confidence in the user. Confidence in the equipment is a fundamental criteria for success in every equipment based sporting competition.

### Reliability:

The system needs to be reliable for many of the same reasons as with predictability. A system that breaks down often will not inspire any confidence in the user.

### Efficiency:

Limitations in available energy is one of the major struggles in Formula Student. Loosing even more of this scarce resource to low mechanical efficiency significantly reduce the maximum average pace of the driver. By focusing on efficiency, one can ensure that the driver is able to drive at maximum pace for a longer time before having to go into energy conservation mode. The driver will as such be able to focus more on his primary tasks and the user experience is improved.

### Reliability:

This was a more difficult criterion to evaluate. On the one side, concept 3 has less parts, less connections and less that can go wrong. On the other side, concept 3 will probably end up very compact and the final design may therefore see some compromises in reliability. In the end this was called as a small victory to concept 3.

### Synergy:

If the solution is designed with focus on a high degree of synergy with interfacing systems, the overall driving experience is greatly increased. The car needs to feel like one unit and not as a collection of well performing sub systems. Only then will the user be able to achieve a synergy with the car and achieve truly remarkable performance numbers.





KONGSBERG



KONGSBERG

revolve  
RCTOS

TRS

TRS

E11

ÅRDAL  
maskinering

KONGSBERG  
AUTOMOTIVE

transnova devotek  
- for bærekraftig mobilitet

Trondheim  
Stål AS

KONGSBERG  
AUTOMOTIVE

ÅRDAL  
maskinering

devotek transnova  
- for bærekraftig mobilitet

Trondheim  
Stål AS

# User analysis

## Secondary users

In addition to fulfilling the needs of the primary user, the system needs to fully or partially fulfill the needs of several secondary users.

### **Race engineer:**

The race engineer is tasked with finding the optimal car setup for every situation and weather condition in order to ensure the best possible performance from the driver. The key in ensuring good usability from a race engineers standpoint is to design solutions for setup variations of the system that are very easy and simple to use. If changing to a different setting is taking two hours of work in the pit, this setting will in most situations remain as is, regardless of performance. Focusing on the needs of the race engineer will ensure good teamwork between him and the driver and eventually increase the performance potential of the car.

### **Mechanics:**

All high end prototype race cars needs constant maintenance in order to perform to design specifications. This means that the mechanics are faced with a significant workload from when the car runs its first meters and until the end of the competition season. In designing the system with reliability and easy maintenance in mind, it is possible to make the life of the pit

crew easier. If able to reduce the stress on these users, the risk of human error in maintenance and reassembly is also reduced. The chance for success is thus increased.

### **Marketing:**

Revolve NTNU is a project that in large part is made possible by external sponsors that find the project and its participants interesting. An important factor in ensuring continued interest is to make sure that the design of every car is pushing the envelope of innovation further than the car before. The more innovative concepts should therefore be given high priority as long as primary user requirements are fulfilled. An interesting, different and innovative car will greatly help the marketing team in fulfilling their task of funding the project.

### **Designer:**

The systems designer is also a Revolve NTNU participant. The fulfillment of his user need is based on the level of academic improvement that the project brings. The choice of concept should therefore ensure the use of creativity, design methodology and engineering to ensure academic improvement within the field of product design.



# Vehicle dynamics

## Omitted theory

Vehicle dynamics is the theory behind vehicle motion. Looking at forces and torque to predict the behavior of different vehicle designs is key in designing high performance race car suspensions. Power output and power distribution are elements that affects vehicle dynamics. The synergy between suspension and drivetrain is therefore the reason why references to vehicle dynamics can be found throughout this thesis.

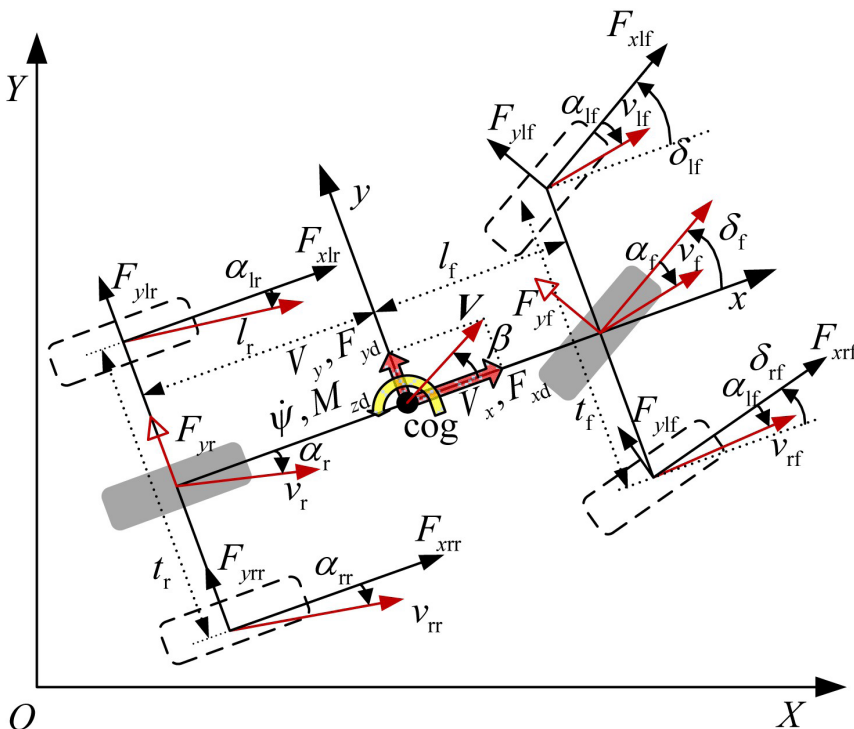
The theoretical foundation of race car vehicle dynamics will not be explained in this thesis despite the fact that it is being extensively used to evaluate data and design solutions. This is in part because the theory is quite complex, having to take up significant space in an already long thesis. It is also not the focus of the thesis and it is therefore expected that the reader has some general understanding of vehicle dynamics, including kinematics and tire theory in order to fully understand all the arguments presented later on.

The suspension design developed by the vehicle dynamics engineer for the 2016 Revolve car is

an unequal double wishbone, push rod actuated suspension with torsion bar spring anti roll bar in the front and the back. The steering geometry is a progressive Ackerman configuration. It is designed on the vehicle dynamics principles found in the book "Race Car Vehicle Dynamics" by the Milliken brothers.

Included in vehicle dynamics is tire theory. All references to tire performance used in this thesis was developed by the vehicle dynamics engineer from test data available through the "Tire Test Consortium" (TTC). The tire tests were performed by Calspan. The data has been processed using the "magic formula" tire model developed by Hans Bastiaan Pacejka in order to precisely specify the overall vehicle longitudinal and lateral friction capacity for all slip angles and slip ratios.

The theoretical basis for all claims relating to vehicle dynamics and tire performance included in this thesis is therefore very strong. This understanding was critical in developing a high performance system.



# Torque vectoring

## Vehicle dynamics and yaw behaviour

The biggest design challenge within classical vehicle dynamics is to find the perfect balance between conflicting performance attributes. In the search for both stability and agility there will always be a compromise between the two. Torque vectoring is a power distribution concept that has the potential to significantly reduce the conflict between these two parameters. This concept is best suited to electric vehicles because of the more instantaneous torque response and the ability to more easily achieve independent power output at each wheel.

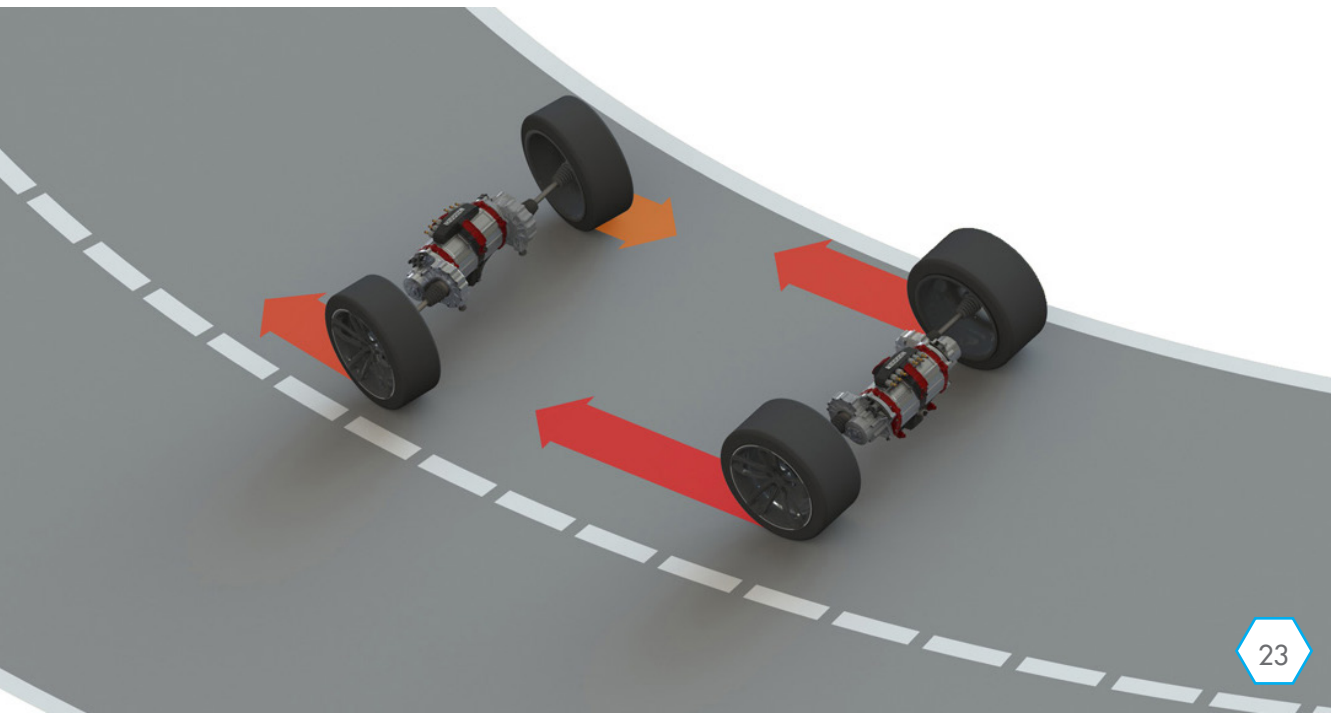
Generally, a vehicles reaction to steering input is to change direction, also referred to as yaw. This direction change is however not an instantaneous reaction but is delayed by the time it takes the tire to develop the required lateral force. This delay, especially at rapid steering input, can result in an overshoot in requested yaw rate. The vehicle yaw rate will oscillate as a result before settling on a steady value. The driver will perceive the car as being unstable and will adjust steering input to regain control.

Conventional race car suspension designs use passive tuning parameters to create stability and prevent yaw oscillation. The price tag of

increased stability is, as previously mentioned, reduced vehicle agility. This will always lead to a compromise between the two.

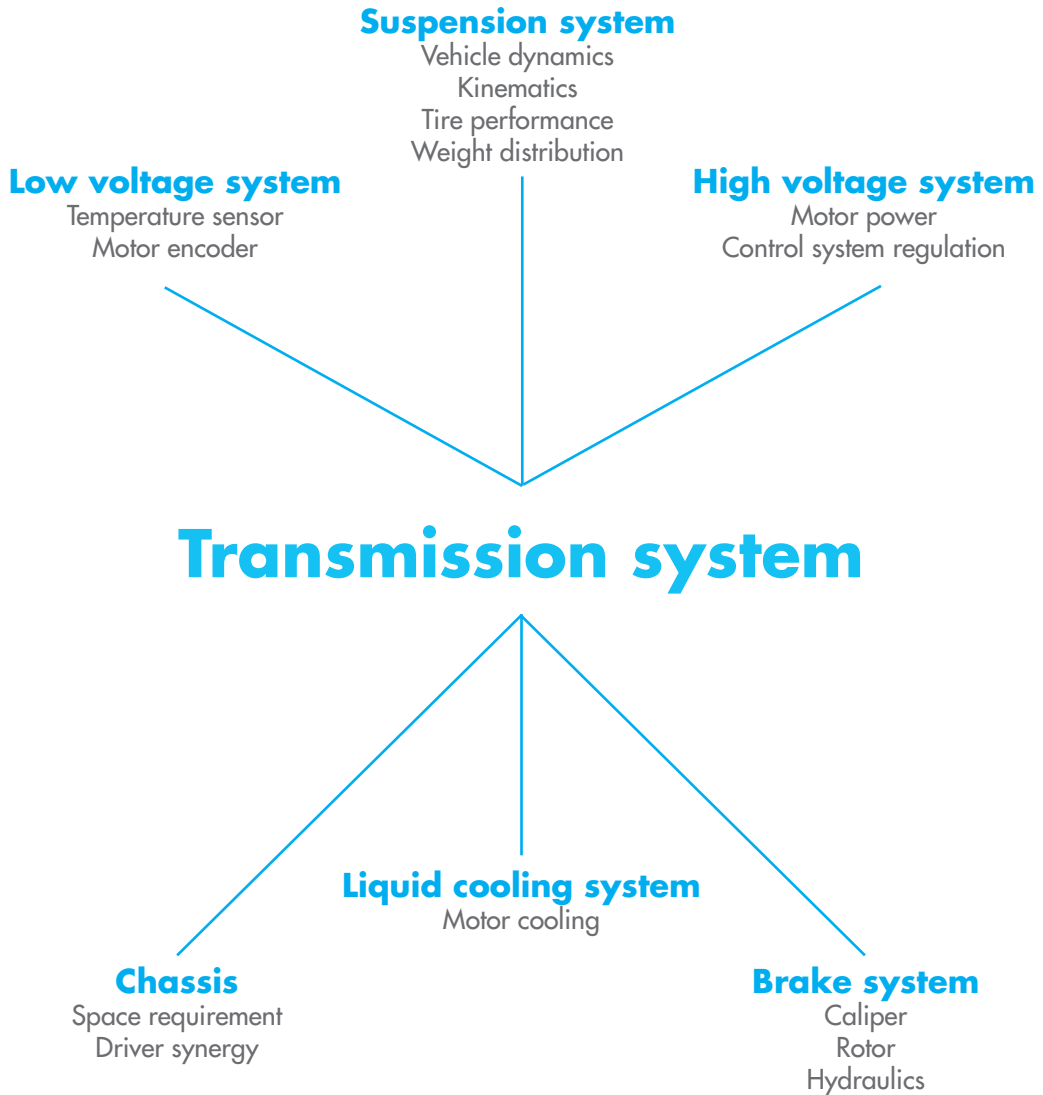
The ability to independently regulate torque at each wheel opens up to the possibility of active regulation of yaw response. By increasing torque at the outer wheels while applying brake torque to the inner wheels, it is possible to create instantaneous yaw response from steering input. The yaw behavior would as such be much more predictable and the car would feel more stable. Torque vectoring therefore has the potential to eliminate the required compromise in suspension characteristics. The end result is a significant improvement in overall track performance.

The main premise of this thesis is to develop a high performance transmission system using four electric motors to independently control torque output to each wheel. This will enable the implementation of a torque vectoring system with the intention of improving vehicle yaw behavior. It is expected that this will greatly improve the cars performance potential, bringing Revolve NTNU closer to an overall competition victory.



# Systems overview

Interfacing components and key design drivers



# Collaboration

## Major contributors

Parts of this thesis is the product of direct collaboration with other members of Revolve NTNU. The size and scope of the project demands teamwork across disciplines in order to achieve optimal results. Following are the involved members with accreditation to their contribution to this thesis.



**Lennard Bosch**

Simulation engineer, responsible for all FEM simulation and topology optimization done in Hyperworks mentioned in this thesis. Also responsible for upright load case development and FEM theory.



**Kurt Erik Nesje**

Vehicle dynamics engineer and suspension designer. Has been a key player in ensuring synergy between suspension and drivetrain design.



**Bjørn Omholt**

Control systems engineer responsible for development of the torque vectoring system. Has provided theoretical input on the synergy between the transmission and control system.



**Vetle Espeseth**

Fluid dynamics engineer, has provided theoretical input on motor cooling block parameters and performed computational fluid dynamic analysis to verify the design.





# Motor analysis

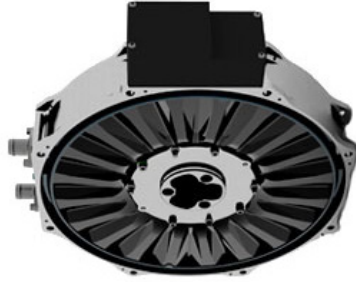
## Initial assessment

As Revolve NTNU currently lack the resources to develop bespoke motors that perfectly fit our needs, we are left to wander the commercial market in the search for fitting motor solutions. Extensive research into commercially available motors that fit with our specific performance requirements has only produced a single viable result. A German company called AMK has agreed to supply the motors for the 2016 project. They manufacture customized motors as a part of their Formula Student sponsorship initiative.

Only having one motor option is however not optimal from a designers point of view as decisions are made for you and are not based on technical evaluation of performance. In any case, it is important to document the difference in performance from other drive concepts. The following chapter will therefore entail an in depth evaluation of commercially available electric motors for automotive use and benchmark their performance against the motors provided by AMK. The intention is to find if the base premise of this project is negatively affected by having no choice in what kind of motors to use.



A selection of 5 commercially available motors has been evaluated. All the motors are permanent magnet synchronous motors. While the AMK DD5-14-10 motors are configured in the classical radial flux array, both the Yasa and the Emrax motors are configured in what is known as axial flux arrays. What this means is that the magnets are mounted side by side with, instead of inside the stator. This increases the radial size of the motors, but also enables high torque/low RPM configurations. The axial flux motors are larger in volume because of this, but needs a smaller transmission ratio and is generally more efficient. Each parameter category is rated by color code.



Yasa 750

Red is a low score, blue is mid range and green is the best score. Geared torque is calculated for a top speed of 110 kph.

The Yasa 750 and 400 motors are developed for racing application in larger vehicles and is therefore not suited as a solution as the torque, while extremely high, is outside what our rear tires can handle in a 2WD setup. In addition, the weight of both of the motors is far too high compared to the other options under evaluation.

The Emrax 207 was evaluated for the 2015 car and was discarded in place of the 228. The main



Emrax 207 and Emrax 228

reason for this being that the max power output was less than is the limit in the competition. This limit is 80kW. In order to evaluate the Emrax 228 on equal terms with the AMK 4 motor setup, the weight of a differential was added to the total weight. A single motor 2WD concept needs a differential to distribute power output between the two wheels while this will happen electronically with 4 individual motors. From this simple choice matrix, the 4WD system seems the stronger option. The next step will be to take a more in depth look at both the Emrax 228 and the AMK DD5-14-10 in order to make a more informed assessment of the differences seen here.



AMK DD5-14-10

Motor	Weight [kg]	Torque [Nm]	Geared torque [Nm]	Power [kW]	Torque/Weight	Size [m <sup>3</sup> ]	Diameter [mm]	Moment of inertia [kg*cm <sup>2</sup> ]
Yasa 750	33	790	2013	200	61	0,007	350	Very high
Yasa 400	24	360	2117	165	88	0,006	280	High
Emrax 207 w/Differential	11,4	140	768	70	67	0,003	207	256
Emrax 228 w/Differential	14,4	240	1116	100	78	0,004	228	421
4x AMK DD5-14-10	14,2	84	1303	148	93	0,003	96	10.96

Simple choice matrix for different motor options

# Motor analysis

## Moment of inertia

Before going deeper into the difference between the two electric motors, there is one parameter in the matrix that demands a more elaborate explanation. Rotational moment of inertia in isolation seems like a very abstract value. It is of course not hard to visualize how radial moment of inertia reduces the angular acceleration of the rotating mass. It is however very hard to visualize to what extent a difference in rotational moment of inertia will affect performance. In order to show this without doing any complex computational exercises, we do a simplified calculation of the loss of torque in spinning both motors from 0 to half speed in 1.75 seconds with no load at constant acceleration. A more complete analysis will follow later on.

We use the equation:

$$T = a * I$$

Where **T** is torque, **a** is angular acceleration and **I** is rotational moment of inertia.

And the equation:

$$\dot{\omega} = \dot{\omega}_0 + at$$

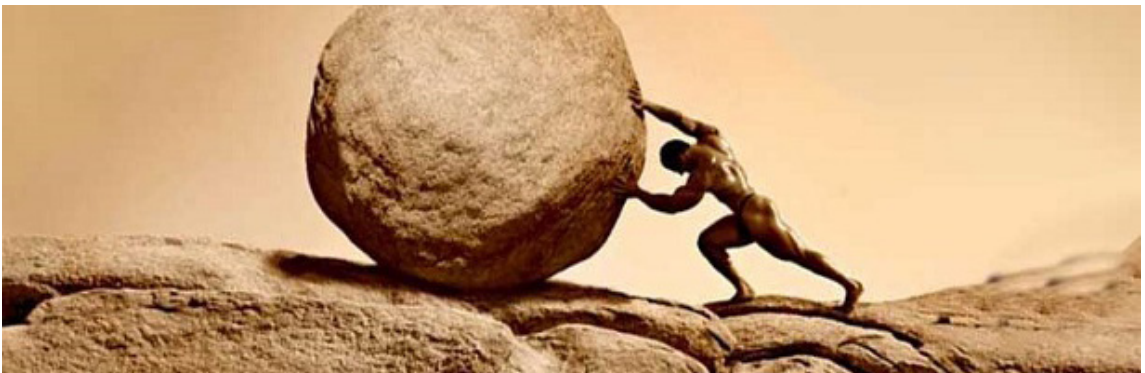
Where  $\dot{\omega}$  is angular velocity,  $\dot{\omega}_0$  is initial angular velocity and **t** is time.

Combining these equation, we are able to calculate the no load torque required to accelerate the motors from 0 to 55 kph car speed. This is equivalent to 3000 RPM and 10000 RPM for the Emrax 228 and the AMK DD5-14-10 respectively.

As is evident from the below

matrix, the higher rotational moment of inertia of the Emrax 228 motor needs 7.55 Nm of torque just to spin itself from 0 to 3000 RPM in 1.75 seconds. The four AMK motors only need 0.66 Nm of torque to perform the same operation from 0 to 10000 RPM. The torque lost from moment of inertia is 4 times higher for the Emrax 228 motor compared to four AMK DD5-14-10 motors. The corresponding difference in geared torque gives us the visualized difference from the different values of rotational moment of inertia in a unit and quantity that is much more tangible. The conclusion is that there may be a significant difference in loss of performance due to the difference in rotational moment of inertia of the two motors.

Motor	I [kg*cm <sup>2</sup> ]	$\dot{\omega}$ [Rad/s]	t [s]	T [Nm]	% of motor torque	Geared torque loss [Nm]
Emrax 228	421	314	1,75	7,55	3,15	35,57
AMK DD5-14-10	10,96	1047	1,75	0,66	0,78	10,17



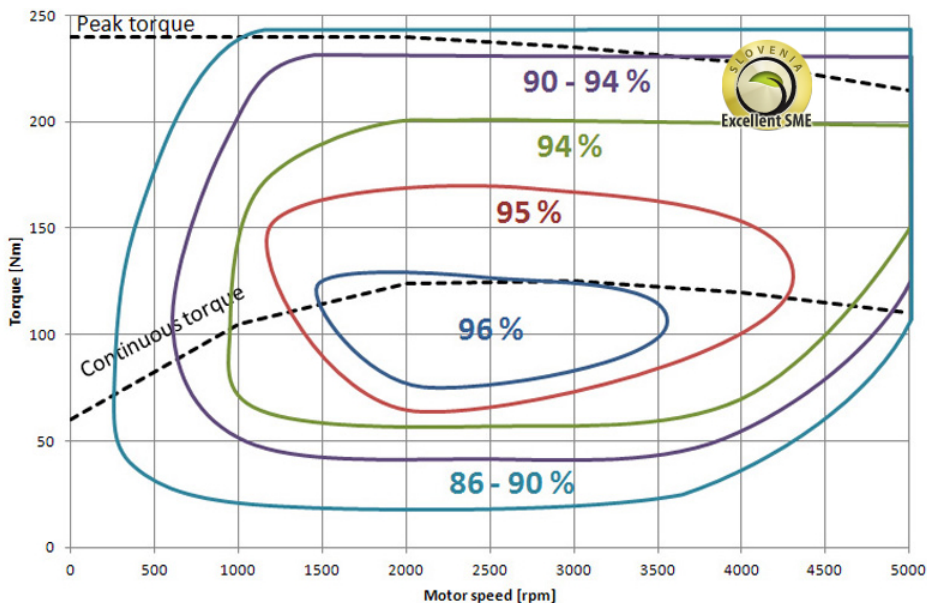
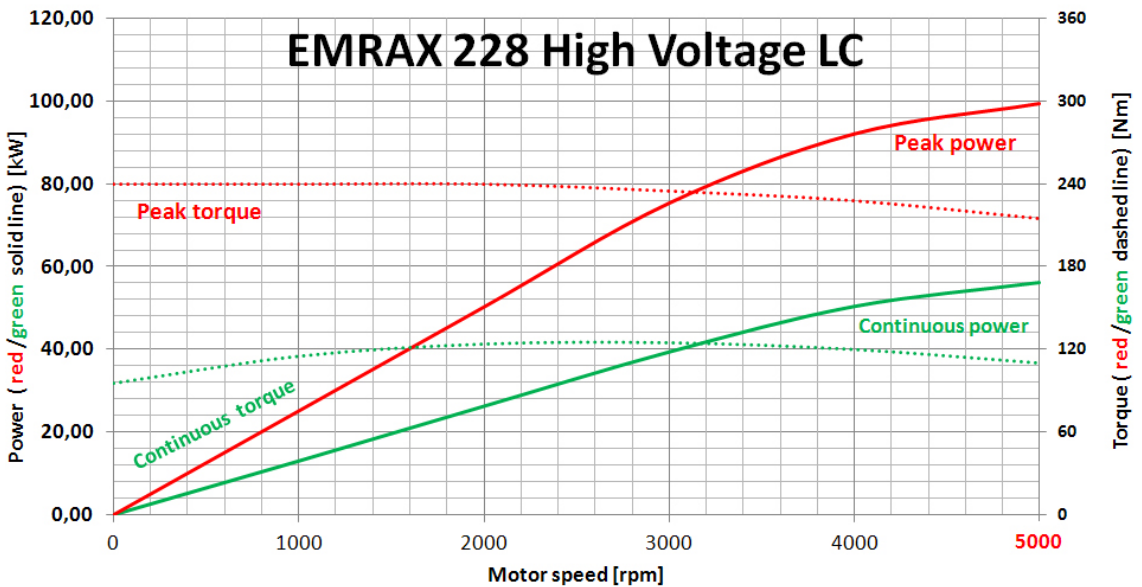
In order to assess the difference between the two drive choices, a detailed analysis of the output parameters of both motors has to be performed. We start by looking at the performance data sheet of the Emrax 228. An important thing to note right away is that the diagram only runs to 5000 RPM while the newest version of the motor can operate to 6000 RPM. The motor peaks out at 240 Nm of torque. With

a final drive resulting in a vehicle top speed of ~110 kph, the final torque output is peaking at 1116 Nm.

110 kph is used as a comparative value because this is the top speed of the 2015 car. One can then assume that the 2016 car will have a similar top speed. Using 110 kph as a general value in this comparative study of motor parameters is increasing the contextual

value of the data. It also enables easy visualization of the difference in performance from the 2015 car.

The efficiency plot shows that the motor rarely operate below 86% efficiency. This is considered as very high efficiency numbers. It is in line with what was previously mentioned about axial flux motors generally being more efficient than their radial flux counterparts.



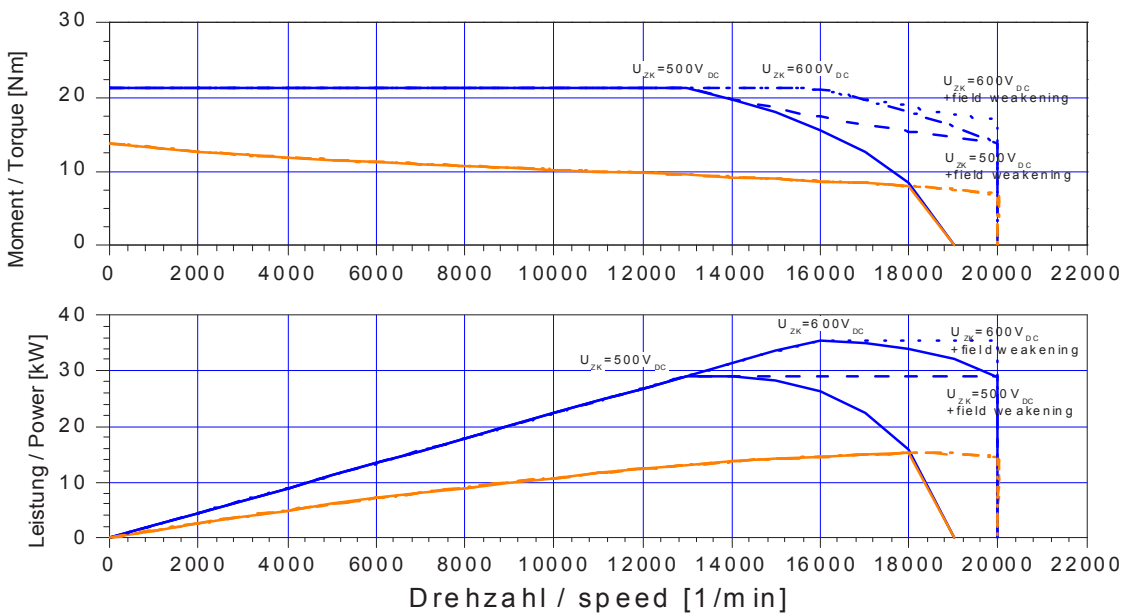
The AMK DD5-14-10 is a different monster entirely. Where the Emrax 228 has a speed range limit of 6000 RPM, the AMK motor peaks out at 20000 RPM. One factor to note is in regards to the dashed lines at the end of the RPM spectrum denoted by "field weakening". This means that the magnetic field will significantly weaken at these speeds. In order to get the output graphed by the dashed lines, a field weakening compensation needs to be implemented in the motor controller. It is given that this will be implemented by the motor controller department working with the controller. The dashed line indicated

by 600 volts is therefore the expected performance of the motor.

The high peak RPM seen in combination with the torque output visualizes the previously mentioned difference between axial and radial flux quite well. While the output torque of the AMK motor is a meager 21 Nm, compared to the 240 Nm of the Emrax 228, the geared output at ~110 kph clocks in at a peak value of 1303 Nm. This is just shy of a 17% increase in peak torque output compared to an Emrax driven RWD system. 17% can be considered an extreme increase in performance when you also factor in the

improvement in traction and vehicle control that also comes with a 4WD system.

Looking at the efficiency plot there is a significant difference in values compared the Emrax 228. While the Emrax maintains a fairly high efficiency at peak torque throughout the whole RPM spectrum, the AMK does not. At peak torque, the AMK has a maximum efficiency of 79%. In the lower end of the RPM spectrum, the values drop significantly. The Emrax is operating at peak efficiency in its RPM mid-range. This clearly differs as the AMK motor has its peak efficiency at maximum RPM.



Torque [Nm]	speed [rpm]									
	500	1000	2000	3000	4000	6000	10000	12000	15000	19000
1,3	64,37	71,33	73,64	74,70	75,43	76,57	77,00	77,08	77,56	78,14
2,7	58,42	70,48	77,57	80,40	82,01	83,92	85,16	85,44	85,97	86,50
5,4	44,94	60,81	73,35	78,82	81,94	85,43	88,20	88,88	89,71	90,44
7,9	35,59	51,90	67,02	74,26	78,54	83,42	87,58	88,65	89,84	90,86
10,4	29,14	44,78	61,01	69,41	74,57	80,62	85,93	87,34	88,86	90,16
12,5	24,17	38,71	55,22	64,39	70,24	77,30	83,73	85,48	87,37	88,98
14,4	20,41	33,76	50,04	59,65	65,99	73,88	81,33	83,42	85,66	87,59
16,0	17,31	29,40	45,10	54,87	61,55	70,10	78,56	80,97	83,56	85,81
17,4	14,82	25,75	40,67	50,41	57,28	66,34	75,70	78,40	81,34	83,91
18,5	12,81	22,67	36,72	46,30	53,25	62,67	72,77	75,75	79,02	81,91
19,6	11,17	20,05	33,21	42,51	49,44	59,09	69,82	73,06	76,63	79,83

# Motor analysis

## Difference in efficiency

In order to compare the two drive systems, the motor parameters have to be adjusted for the power output limitation set by the FSAE competition rules document:

**“EV2.2.1** The maximum power drawn from the battery must not exceed 80kW. This will be checked by evaluating the Energy Meter data.”

The torque curves of both drive systems were graphed out using the aforementioned top speed of ~110 kph. The resulting gear ratio needed is 1:4,65 for the Emrax 228. The AMK motor needs a ratio of 1:15,5 to achieve the same output speed.

In order to properly visualize how the difference in

efficiency is impacting the torque performance of the two systems, loss needs to be considered. Working with last year's efficiency limitation for the Emrax 228 as a starting point yields the graph seen below. Here, both the efficiency of the power electronics and the motor itself was taken into consideration in order to find the motors maximum mechanical power output in kilowatts while staying within the rules set by the competition. The efficiency was then calculated as follows:

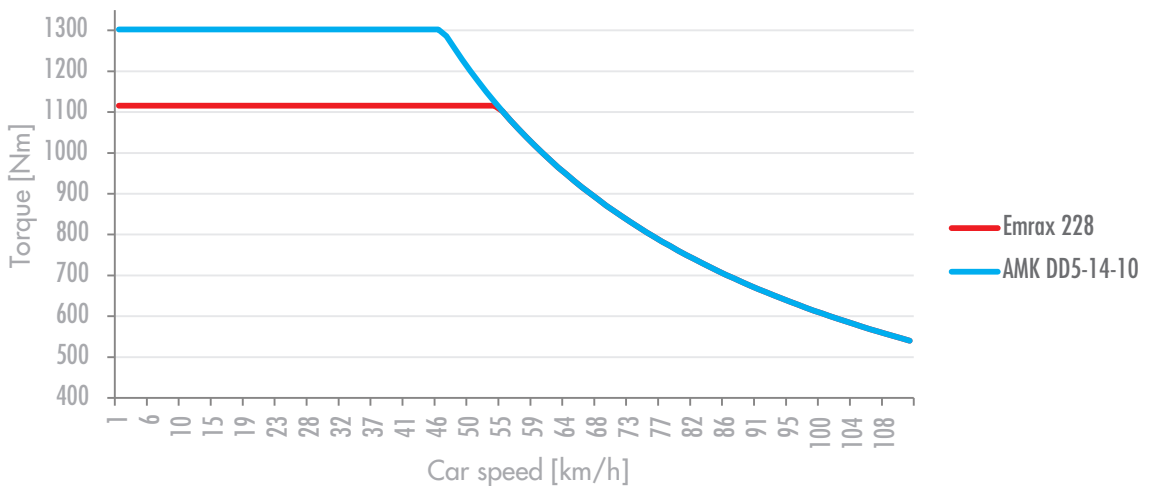
- 79kW of maximum draw
- 1% loss of power from the power electronics
- 7% loss of power from the motor at peak torque

This results in a conservative

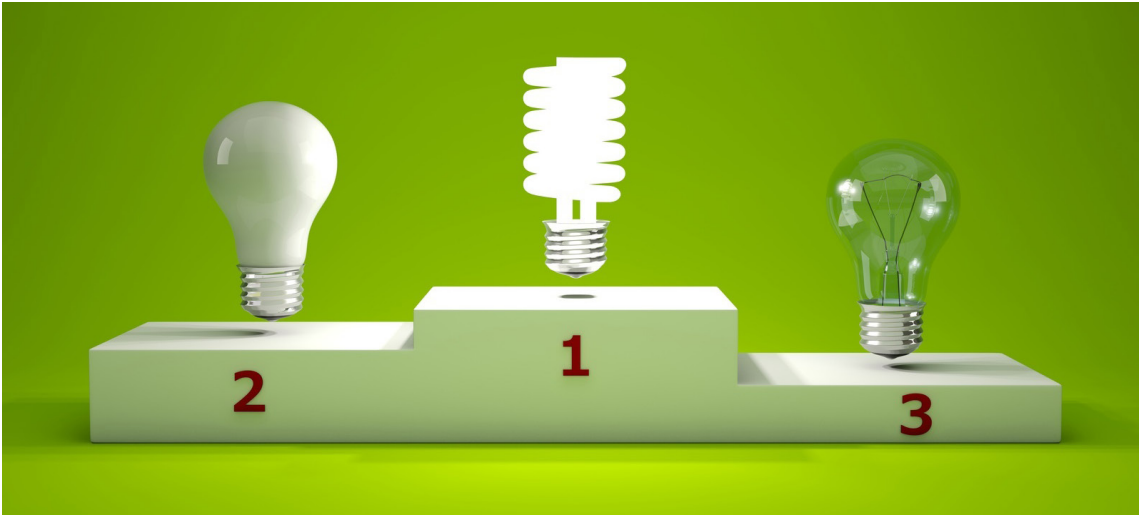
estimate of a maximum of 73 kilowatts of mechanical power being produced by the motor or motors. Conservative, meaning that the actual number will be less as there is a considerable risk of disqualification involved in running the car close to a 80 kilowatt power draw. The loss of power in the Emrax motor at peak torque is also for the most part higher than 7% (see efficiency diagram).

The conclusion on performance so far is identical to what was seen in the initial assessment. This is however, as already stated, not a correct evaluation of the efficiency difference between the two systems. Further adjustment of the data is needed to show the actual difference in mechanical output between

AMK 4WD vs. Emrax 228 RWD



Torque output of 4x AMK DD5-14-10 vs one Emrax 228 adjusted to 73kW of max output.



the two systems.

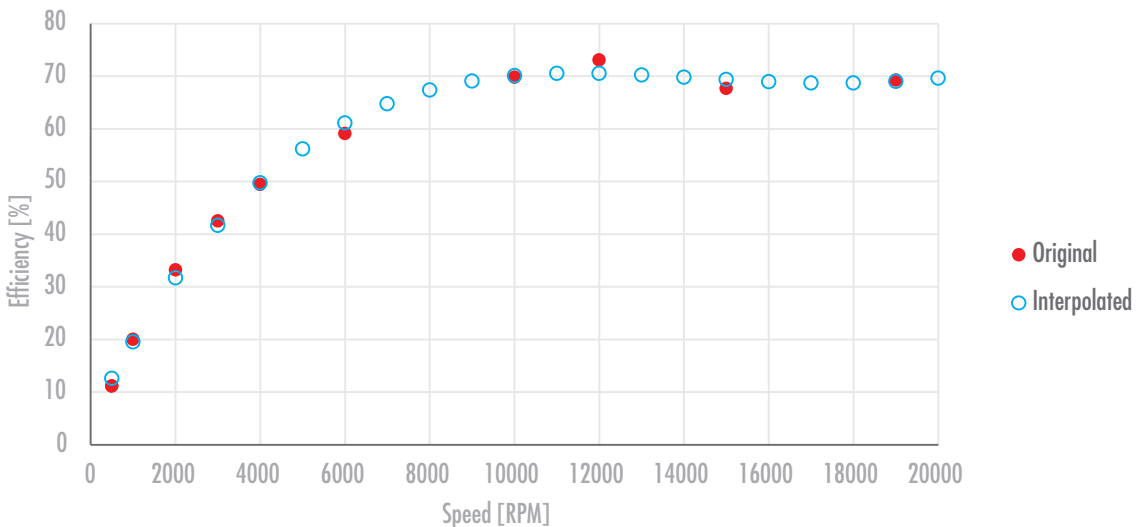
In order to improve the quality of the mechanical output data for the AMK motor, the numbers needed to be adjusted according to the specifications of the efficiency chart (See previous page). The chart does however appear problematic to read. The pseudo logarithmic scale used for the motor speed axis is resulting in a very coarse

dataset. A correct torque value adjustment would be very hard to do with this kind of data resolution.

For this reason, the dataset needed to be edited. Using Microsoft Excel, the resolution was doubled. This was done by running the initial data through a 4th degree polynomial interpolation algorithm. The graph shows the curve fit for the dataset

at maximum torque. The tolerance of the interpolation in regards to the original efficiency values is considered within reasonable limits. Using this method, the motor speed axis was made linear in order to improve readability. The next step will be to calculate the absolute output values of output power for a peak input power of 20 kW.

### Polynomial: 4th degree



Original data vs interpolated values for the 21 Nm torque string of the data set.

Efficiency [%]	Speed[RPM]																				
	500	1000	2000	3000	4000	5000	6000	7000	8000	9000	10000	11000	12000	13000	14000	15000	16000	17000	18000	19000	20000
<b>1.3</b>	66.61	68.99	72.60	74.93	76.30	76.95	77.13	77.03	76.80	76.57	76.45	76.47	76.68	77.06	77.56	78.11	78.60	78.87	78.75	78.02	76.44
<b>2.7</b>	62.00	67.25	75.23	80.44	83.51	85.03	85.49	85.31	84.84	84.35	84.05	84.06	84.44	85.17	86.14	87.20	88.09	88.50	88.04	86.25	82.58
<b>5.4</b>	49.16	57.41	70.10	78.58	83.81	86.64	87.79	87.91	87.52	87.02	86.72	86.83	87.42	88.49	89.90	91.42	92.70	93.30	92.65	90.09	84.85
<b>7.9</b>	39.49	48.98	63.76	73.86	80.32	84.07	85.91	86.52	86.47	86.23	86.13	86.39	87.13	88.35	89.91	91.57	93.00	93.70	93.11	90.51	85.10
<b>10.4</b>	32.49	42.42	58.04	68.94	76.14	80.54	82.96	84.05	84.41	84.49	84.63	85.06	85.91	87.18	88.77	90.46	91.91	92.68	92.21	89.84	84.78
<b>12.5</b>	26.93	36.87	52.66	63.90	71.55	76.46	79.38	80.97	81.76	82.20	82.62	83.25	84.21	85.52	87.11	88.77	90.21	91.03	90.73	88.70	84.23
<b>14.4</b>	22.65	32.34	47.90	59.18	67.06	72.33	75.68	77.70	78.91	79.71	80.41	81.24	82.31	83.67	85.23	86.85	88.27	89.14	89.01	87.35	83.53
<b>16</b>	19.08	28.33	43.35	54.44	62.40	67.92	71.62	74.05	75.66	76.82	77.81	78.84	80.04	81.43	82.98	84.55	85.94	86.85	86.89	85.61	82.47
<b>17.4</b>	16.19	24.94	39.29	50.05	57.94	63.60	67.56	70.33	72.29	73.79	75.08	76.34	77.68	79.13	80.65	82.12	83.35	84.07	83.95	82.56	79.41
<b>18.5</b>	13.80	22.08	35.71	46.05	53.76	59.41	63.53	66.54	68.82	70.65	72.06	73.80	75.33	76.85	78.31	79.54	80.34	80.41	79.40	76.85	72.28
<b>19.6</b>	12.60	19.54	31.67	41.66	49.75	56.16	61.10	64.78	67.39	69.10	70.52	70.52	70.52	70.25	69.82	69.35	68.95	68.70	68.69	68.98	69.65
<b>21</b>	9.10	14.27	24.08	33.05	41.01	47.84	53.47	57.85	60.99	62.93	63.76	63.58	62.57	60.93	58.90	56.76	54.84	53.50	53.14	54.22	57.20

Efficiency data for AMK DD5-14-10 expanded by 4th degree polynomial interpolation

The increased resolution of the efficiency dataset will increase the detail of the overall mechanical output assessment of the AMK motor. The chart does however contain many redundant data points. This is because the AMK motor can be run up to an input power of 37 kW (See motor data sheet). As we are limiting the analysis to

consider input power values up to 20 kW, some data points can be eliminated.

Initially, power values are calculated as a function of motor torque and speed with the same data resolution as the efficiency chart. We then have input power for the whole dataset, not adjusted

for efficiency. Power values of over 20 kW are marked as non-applicable. Continuing, the input power values were then adjusted with the values from the interpolated efficiency chart. This further increased the number of non applicable data points.

Power [kW]	Speed[RPM]																				
	500	1000	2000	3000	4000	5000	6000	7000	8000	9000	10000	11000	12000	13000	14000	15000	16000	17000	18000	19000	20000
<b>1.3</b>	0.07	0.14	0.27	0.41	0.54	0.68	0.82	0.95	1.09	1.23	1.36	1.50	1.63	1.77	1.91	2.04	2.18	2.31	2.45	2.59	2.72
<b>2.7</b>	0.14	0.28	0.57	0.85	1.13	1.41	1.70	1.98	2.26	2.54	2.83	3.11	3.39	3.68	3.96	4.24	4.52	4.81	5.09	5.37	5.65
<b>5.4</b>	0.28	0.57	1.13	1.70	2.26	2.83	3.39	3.96	4.52	5.09	5.65	6.22	6.79	7.35	7.92	8.48	9.05	9.61	10.18	10.74	11.31
<b>7.9</b>	0.41	0.83	1.65	2.48	3.31	4.14	4.96	5.79	6.62	7.45	8.27	9.10	9.93	10.75	11.58	12.41	13.24	14.06	14.89	15.72	16.55
<b>10.4</b>	0.54	1.09	2.18	3.27	4.36	5.45	6.53	7.62	8.71	9.80	10.89	11.98	13.07	14.16	15.25	16.34	17.43	18.51	19.60	20.69	21.78
<b>12.5</b>	0.65	1.31	2.62	3.93	5.24	6.54	7.85	9.16	10.47	11.78	13.09	14.40	15.71	17.02	18.33	19.63	20.94	22.25	23.56	24.87	26.18
<b>14.4</b>	0.75	1.51	3.02	4.52	6.03	7.54	9.05	10.56	12.06	13.57	15.08	16.59	18.10	19.60	21.11	22.62	24.13	25.64	27.14	28.65	30.16
<b>16</b>	0.84	1.68	3.35	5.03	6.70	8.38	10.05	11.73	13.40	15.08	16.76	18.43	20.11	21.78	23.46	25.13	26.81	28.48	30.16	31.83	33.51
<b>17.4</b>	0.91	1.82	3.64	5.47	7.29	9.11	10.93	12.75	14.58	16.40	18.22	20.04	21.87	23.69	25.51	27.33	29.15	30.98	32.80	34.62	36.44
<b>18.5</b>	0.97	1.94	3.87	5.81	7.75	9.69	11.62	13.56	15.50	17.44	19.37	21.31	23.25	25.19	27.12	29.06	31.00	32.93	34.87	36.81	38.75
<b>19.6</b>	1.03	2.05	4.11	6.16	8.21	10.26	12.32	14.37	16.42	18.47	20.53	22.58	24.63	26.68	28.74	30.79	32.84	34.89	36.95	39.00	41.05
<b>21</b>	1.10	2.20	4.40	6.60	8.80	11.00	13.19	15.39	17.59	19.79	21.99	24.19	26.39	28.59	30.79	32.99	35.19	37.38	39.58	41.78	43.98

Calculated input power as a function of torque and speed for the AMK DD5-14-10 motor.



Power [kW]	Speed[RPM]																				
	500	1000	2000	3000	4000	5000	6000	7000	8000	9000	10000	11000	12000	13000	14000	15000	16000	17000	18000	19000	20000
<b>1.3</b>	0.10	0.20	0.38	0.55	0.71	0.88	1.06	1.24	1.42	1.60	1.78	1.96	2.13	2.30	2.46	2.61	2.77	2.93	3.11	3.32	3.56
<b>2.7</b>	0.23	0.42	0.75	1.05	1.35	1.66	1.98	2.32	2.67	3.02	3.36	3.70	4.02	4.32	4.60	4.86	5.14	5.43	5.78	6.23	6.85
<b>5.4</b>	0.58	0.98	1.61	2.16	2.70	3.26	3.86	4.50	5.17	5.85	6.52	7.16	7.76	8.31	8.81	9.28	9.76	10.30	10.99	11.93	13.33
<b>7.9</b>	1.05	1.69	2.60	3.36	4.12	4.92	5.78	6.69	7.65	8.63	9.61	10.53	11.39	12.17	12.88	13.55	14.23	15.01	15.99	17.37	19.44
<b>10.4</b>	1.68	2.57	3.75	4.74	5.72	6.76	7.88	9.07	10.32	11.60	12.87	14.08	15.21	16.24	17.18	18.06	18.96	19.98	21.26	23.03	25.69
<b>12.5</b>	2.43	3.55	4.97	6.15	7.32	8.56	9.89	11.32	12.81	14.33	15.84	17.30	18.65	19.90	21.04	22.12	23.22	24.45	25.97	28.04	31.08
<b>14.4</b>	3.33	4.66	6.30	7.64	8.99	10.42	11.96	13.58	15.29	17.03	18.75	20.42	21.98	23.43	24.77	26.04	27.33	28.76	30.49	32.80	36.11
<b>16</b>	4.39	5.91	7.73	9.23	10.74	12.34	14.04	15.84	17.72	19.63	21.53	23.38	25.12	26.75	28.27	29.72	31.19	32.80	34.71	37.18	40.63
<b>17.4</b>	5.63	7.30	9.28	10.92	12.58	14.33	16.18	18.14	20.16	22.22	24.27	26.25	28.15	29.93	31.63	33.28	34.98	36.84	39.07	41.94	45.89
<b>18.5</b>	7.02	8.77	10.85	12.62	14.42	16.30	18.30	20.38	22.52	24.68	26.81	28.88	30.86	32.77	34.64	36.53	38.58	40.96	43.92	47.89	53.61
<b>19.6</b>	8.14	10.50	12.96	14.78	16.50	18.27	20.15	22.18	24.37	26.73	29.28	32.02	34.92	37.98	41.15	44.39	47.63	50.79	53.79	56.53	58.94
<b>21</b>	12.08	15.41	18.27	19.96	21.45	22.98	24.68	26.61	28.84	31.45	34.49	38.05	42.18	46.92	52.27	58.12	64.16	69.88	74.48	77.07	76.89

Motor input power adjusted for efficiency for the AMK DD5-14-10 motor.

The domain of the data set is now limited to a maximum motor input value of 20 kW. Looking at the chart, it is now very clear that maximum torque output is significantly more limited from motor efficiency at lower ends of the RPM spectrum than what the initial limitation of 73 kW

would have us believe.

The input power, although interesting, is not really relevant in terms of assessing absolute motor performance. The numbers that are of interest is describing how much force that is actually acting

on the wheels of the car. The final operation is to calculate the power output adjusted for efficiency from the interpolated efficiency plot. The values shown clearly visualize the significant impact that motor efficiency has on the overall performance of the vehicle.

Power [kW]	Speed[RPM]																				
	500	1000	2000	3000	4000	5000	6000	7000	8000	9000	10000	11000	12000	13000	14000	15000	16000	17000	18000	19000	20000
<b>1.3</b>	0.07	0.14	0.27	0.41	0.54	0.68	0.82	0.95	1.09	1.23	1.36	1.50	1.63	1.77	1.91	2.04	2.18	2.31	2.45	2.59	2.72
<b>2.7</b>	0.14	0.28	0.57	0.85	1.13	1.41	1.70	1.98	2.26	2.54	2.83	3.11	3.39	3.68	3.96	4.24	4.52	4.81	5.09	5.37	5.65
<b>5.4</b>	0.28	0.57	1.13	1.70	2.26	2.83	3.39	3.96	4.52	5.09	5.65	6.22	6.79	7.35	7.92	8.48	9.05	9.61	10.18	10.74	11.31
<b>7.9</b>	0.41	0.83	1.65	2.48	3.31	4.14	4.96	5.79	6.62	7.45	8.27	9.10	9.93	10.75	11.58	12.41	13.24	14.06	14.89	15.72	16.55
<b>10.4</b>	0.54	1.09	2.18	3.27	4.36	5.45	6.53	7.62	8.71	9.80	10.89	11.98	13.07	14.16	15.25	16.34	17.43	18.51	19.60	20.69	21.78
<b>12.5</b>	0.65	1.31	2.62	3.93	5.24	6.54	7.85	9.16	10.47	11.78	13.09	14.40	15.71	17.02	18.33	19.63	20.94	22.25	23.56	24.87	26.18
<b>14.4</b>	0.75	1.51	3.02	4.52	6.03	7.54	9.05	10.56	12.06	13.57	15.08	16.59	18.10	19.60	21.11	22.62	24.13	25.64	27.14	28.65	30.16
<b>16</b>	0.84	1.68	3.35	5.03	6.70	8.38	10.05	11.73	13.40	15.08	16.76	18.43	20.11	21.78	23.46	25.13	26.81	28.48	30.16	31.83	33.51
<b>17.4</b>	0.91	1.82	3.64	5.47	7.29	9.11	10.93	12.75	14.58	16.40	18.22	20.04	21.87	23.69	25.51	27.33	29.15	30.98	32.80	34.62	36.44
<b>18.5</b>	0.97	1.94	3.87	5.81	7.75	9.69	11.62	13.56	15.50	17.44	19.37	21.31	23.25	25.19	27.12	29.06	31.00	32.93	34.87	36.81	38.75
<b>19.6</b>	1.03	2.05	4.11	6.16	8.21	10.26	12.32	14.37	16.42	18.47	20.53	22.58	24.63	26.68	28.74	30.79	32.84	34.89	36.95	39.00	41.05
<b>21</b>	1.10	2.20	4.40	6.60	8.80	11.00	13.19	15.39	17.59	19.79	21.99	24.19	26.39	28.59	30.79	32.99	35.19	37.38	39.58	41.78	43.98

Motor output power adjusted for efficiency for the AMK DD5-14-10 motor.

The numbers describing peak mechanical output for the motor can then be used to update the peak torque output data. The resulting graph is a significantly more correct visualization of the difference between an Emrax 228 driven RWD concept and an AMK DD5-14-10 driven 4WD concept.

The main change from the initial assessment is that the mid-range peak torque output of the AMK motor has been reduced dramatically because of the lower efficiency numbers. The result is that the Emrax motor performs better from 40 to 80 kph. The difference in absolute peak torque is still almost 17% in favor of the 4WD concept. Considering the off the line traction limitation of a RWD

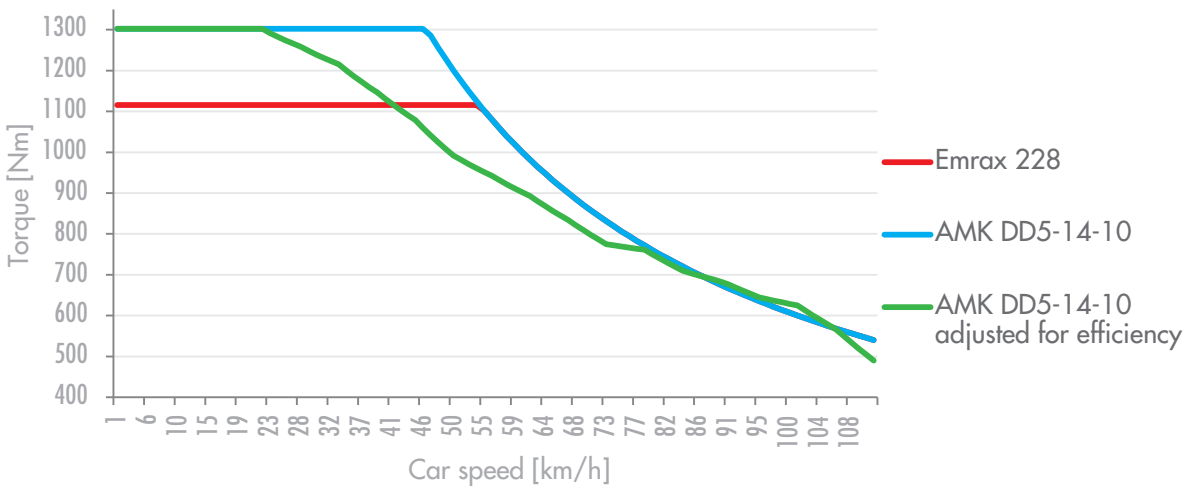
concept compared to a 4WD concept, the real difference will be higher. This is because two tires does not have the friction capacity to transfer 1116 Nm of torque into the ground. This is verified through the traction model in Optimum Lap. Graphs showing the relationship between the tractive force on the wheels and the traction limit are shown on the next page. As the car weight shifts towards the rear wheel during acceleration, the front wheel traction contribution is less than that of the rear wheels. Adjusting for this, total traction was increased by a factor of 1.6 as a conservative estimate. Even then, the difference in traction capacity will yield two very different results in actual vehicle performance.

From this we can conclude that a 4WD system driven by four AMK DD5-14-10 motors will perform significantly better than a RWD system driven by an Emrax 228 motor in stationary and low speed start acceleration situations.

At higher speeds, specifically from 80 kph and up, there is an insignificant difference in mechanical output between the two concepts. The question then becomes if the better low speed performance weights up for the loss in mid-range performance for the 4WD system? Additional considerations regarding the RWD system needs to be pointed out before an answer can be given.

First off, the efficiency adjustment done to the Emrax

### AMK 4WD vs. Emrax 228 RWD



Torque output of 4x AMK DD5-14-10 vs one Emrax 228 adjusted to 73kW of max output vs. 4x AMK DD5-14-10 adjusted for correct efficiency.

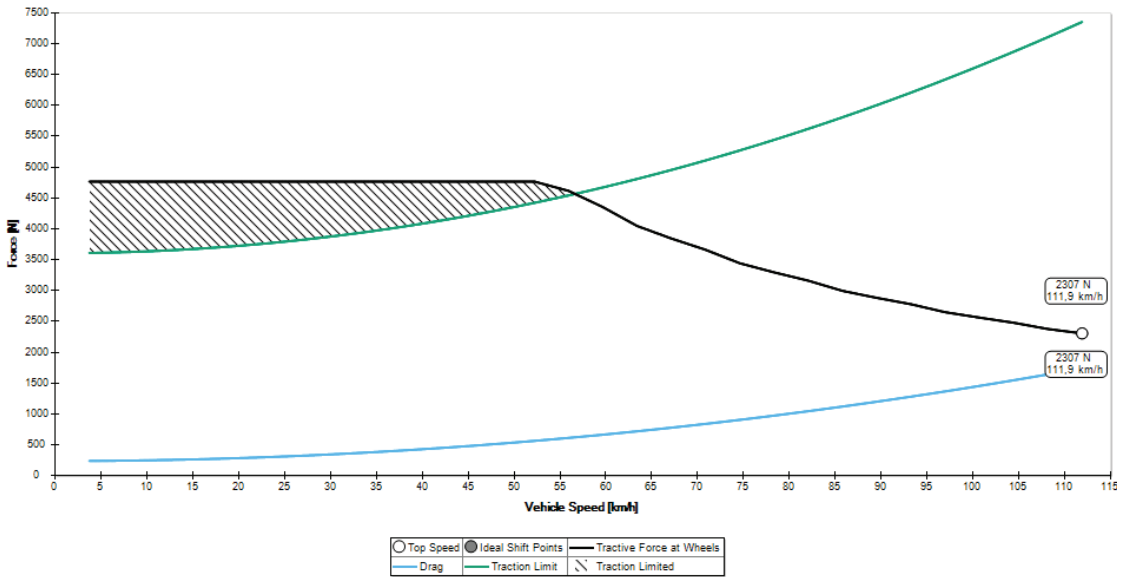
motor data is an optimistic simplification. A more precise adjustment would result in more conservative values. This means that the two motors are closer at mid-range vehicle

speed than what is implied by the graph.

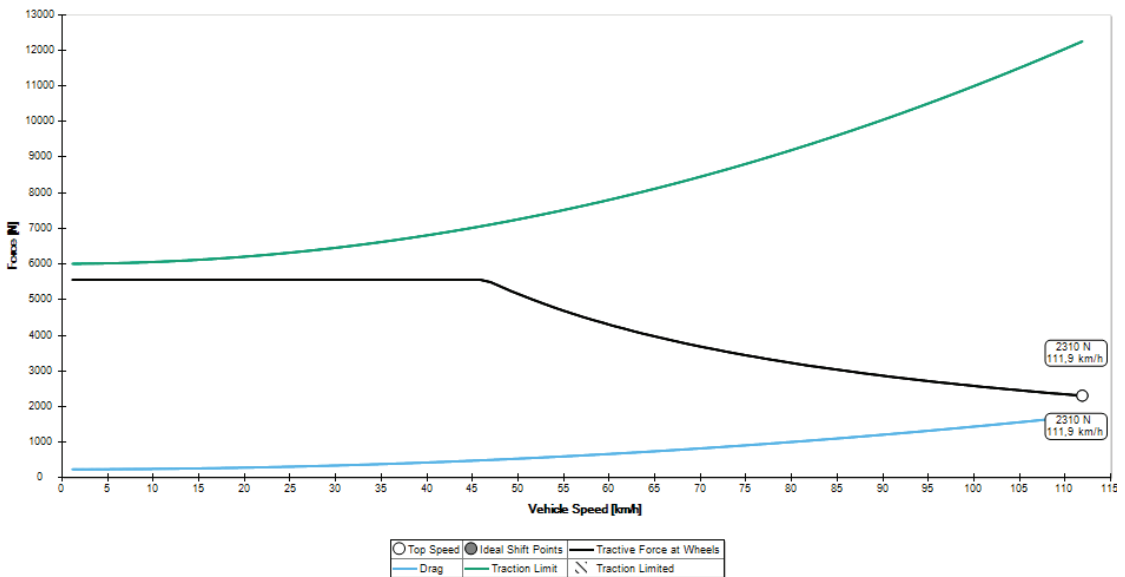
Secondly, The Emrax 228 needs a mechanical differential to split power

between the rear wheels. This differential has between 2% and 5% of mechanical loss that you wont have with a motor driving each wheel separately.

### Traction capacity vs. torque RWD



### Traction capacity vs. torque 4WD



# Motor analysis

## Lap time simulation: Acceleration

Working from these premises it would be easy to assume better performance from the 4WD system and stop the analysis here. It would however result in a conclusion based on isolated performance parameters of the drive systems in question. Actual difference in vehicle performance has, to a very low degree, been considered in the analysis. A vehicle performance analysis is therefore needed in order to further expand the scope of this analysis.

A popular tool for vehicle analysis is a type of software called "lap time simulators". This kind of software breaks the technical specifications of a vehicle down into mathematical parameters. These parameters are then used to simulate a potential lap time within the computational boundaries of the software. It is then easy to compare two different parameter values within a subsystem of a car

as a function of the time each variation takes to complete a lap at a given course.

In order to further verify that the indications given from the analysis so far are in fact representative of actual vehicle performance, a lap time simulation software was used. Optimum Lap from OptimumG is a basic but strong tool for use at this level of engineering. This software only takes into account basic parameters like tire friction, power output, transmission ratio and aerodynamic coefficients while more advanced programs lets you mathematically model the whole car. Advanced lap time simulations are not beyond the reach of what Revolve NTNU can do, but as a subtask it is not feasible as the time required to set up these types of calculations would be a primary design task in and of itself.

Using Optimum Lap, the

two drive systems have been compared. The comparison has been made during both a 0 to 75 meter acceleration event and a single lap (auto cross) event. These are the two events of the competition where motor performance has a significant impact on overall performance.

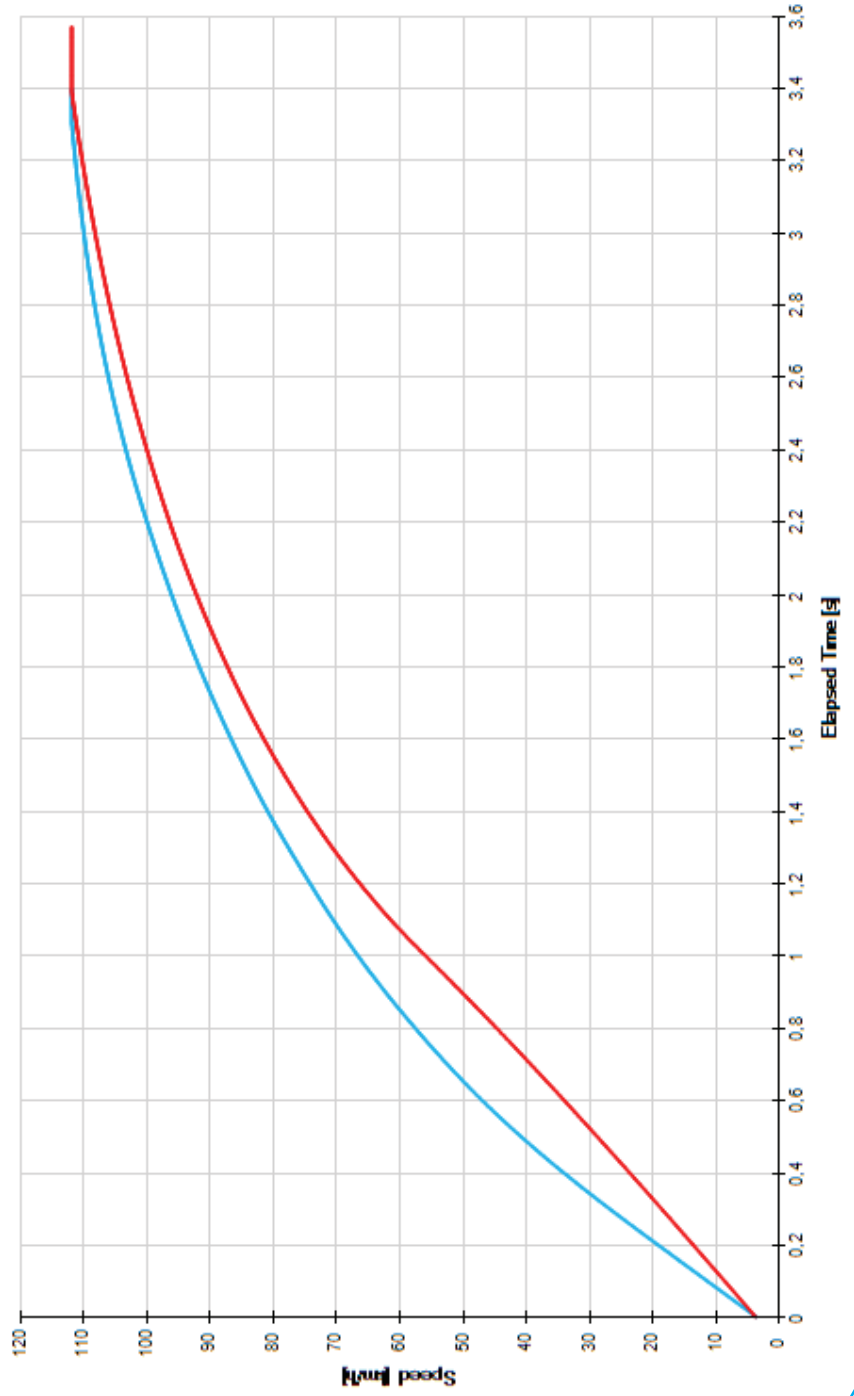
First, we look at the acceleration event simulation. Here we can see a dramatic difference in off the line performance. The difference in mid range torque does however even out the difference substantially. The end result is a 0.17 seconds advantage in favor of the 4WD system. This might seem a small advantage, but when you take into account that Optimum Lap models a perfect traction control for situations when the torque overcomes the traction capacity of the wheels, the result further confirms the superior performance of the 4WD system.

## Traction control RWD vs. 4WD 0-75 meters



Traction control activity during simulated 0 to 75 meter acceleration event for 4WD vs. RWD concept.

## Time/Speed RWD vs. 4WD 0-75 meters



Selected Results	
[3.57]	110 km/h top speed RWD, Drag
[3.40]	110 km/h top speed 4wd, Drag

# Motor analysis

## Lap time simulation: Autocross

Performance in a single lap auto cross event is a defining factor for the overall on track success of the car. High straight line acceleration performance is important to an extent, but track driving is where the majority of the dynamic event takes place. This is true both in driving time and points awarded. The single lap simulation results are weighted more because of this.

The result of the simulation is displayed in the graph to the right. It shows that the 4WD car drives a lap 0.64 seconds faster than the RWD car. Keeping in mind that both cars are identical in regards to all other parameters, weight, aerodynamics etc, over half a

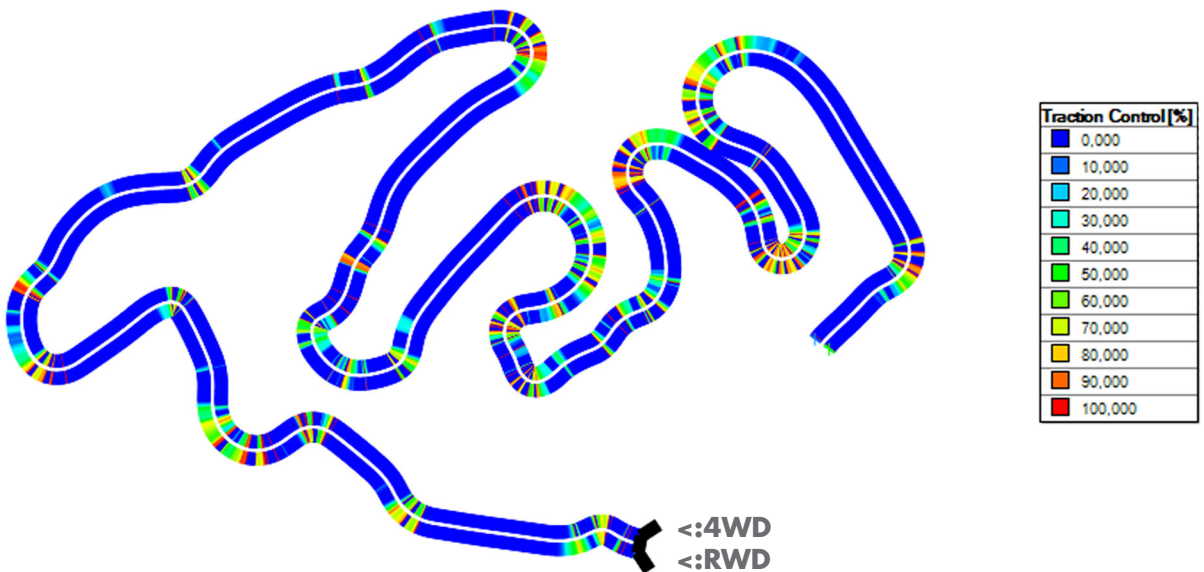
second of reduction in lap time is a significant improvement on its own. It does however become more interesting when looking at the traction control plot.

One would from the acceleration simulation results assume that the 4WD car would be faster at the start of every straight line of road. This assumption is of course true as can be seen in the graphic. It is however only part of the difference displayed. Looking at the turns, we can see that the lateral traction capacity of the 4WD car is higher than that of the RWD car. This especially holds true in the wider curves with higher speeds where the traction control is significantly

more active for the RWD car. This shows an improvement in both longitudinal and lateral capacity from driving all four wheels compared to just two.

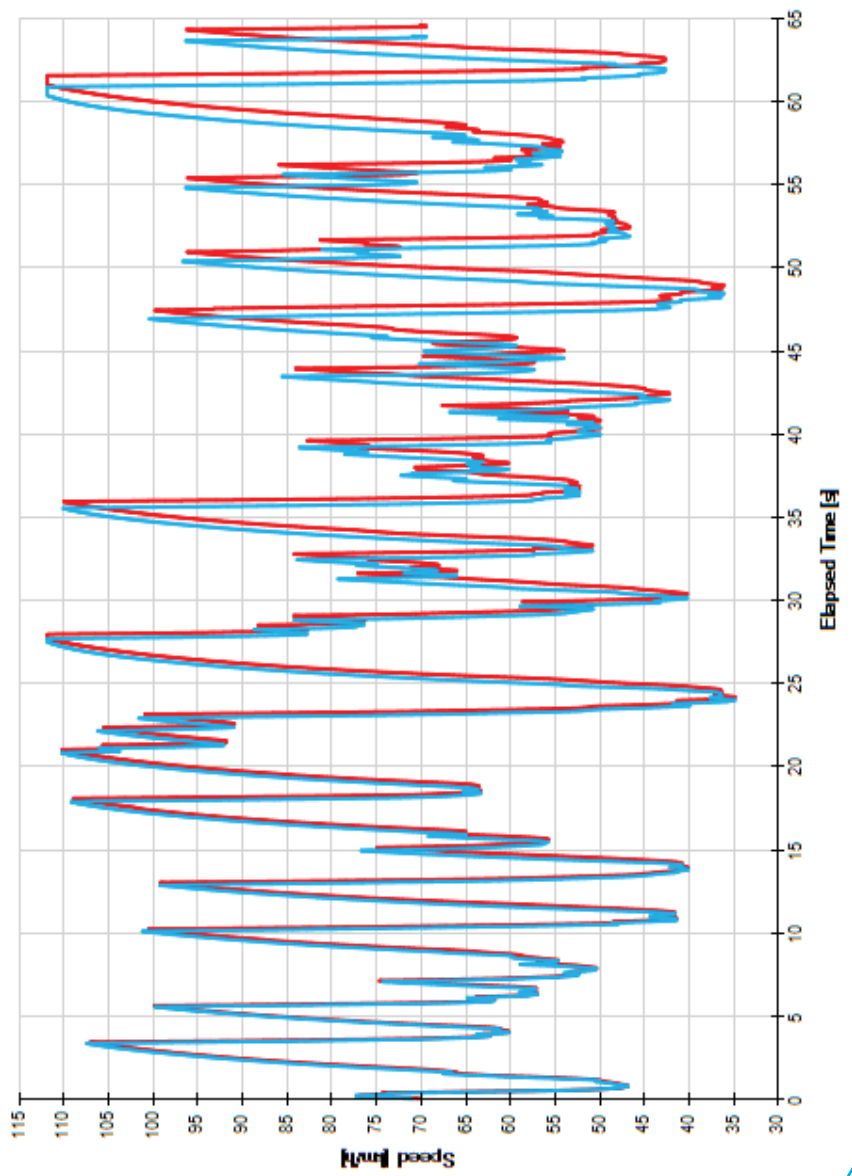
From this we can conclude that the 4WD system has overall higher performance than what the RWD system has. We can also conclude that the higher traction capacity, both longitudinal and lateral, results in a car that is easier for the driver to control. We are then able to say, with a larger amount of certainty than was initially present, that a 4WD car driven by four AMK DD5-14-10 motors will outperform a RWD car driven by an Emrax 228 motor with a mechanical limited slip differential.

### Traction control RWD vs. 4WD single lap



Traction control activity during simulated single lap auto cross event for 4WD vs. RWD concept.

## Time/Speed RWD vs. 4WD single lap



**Selected Results**  
— [63,94] 110 kmh top speed 4wd, F.SAE Autocross Germany 2012  
— [64,58] 110 kmh top speed RWD, F.SAE Autocross Germany 2012

# Motor analysis

## Energy limitations and KERS

We have so far clearly established that a 4WD system based on the AMK DD5-14-10 motor outperforms the other options available within the scope of this project. This conclusion is however purely based on an analysis of the propulsive capacity of the system. We have yet to discuss the difference between the two analyzed systems in the context of the fundamental difference between an internal combustion system and an electric powered system.

Internal combustion engine driven vehicles inside the Formula Student competition run on either 95% unleaded petrol or 85% ethanol. The high energy density of these fossil fuels results in a very low trade off in weight and volume from significantly extending the driving range of the car. Some cars run fuel tanks of only 3,5 liters.

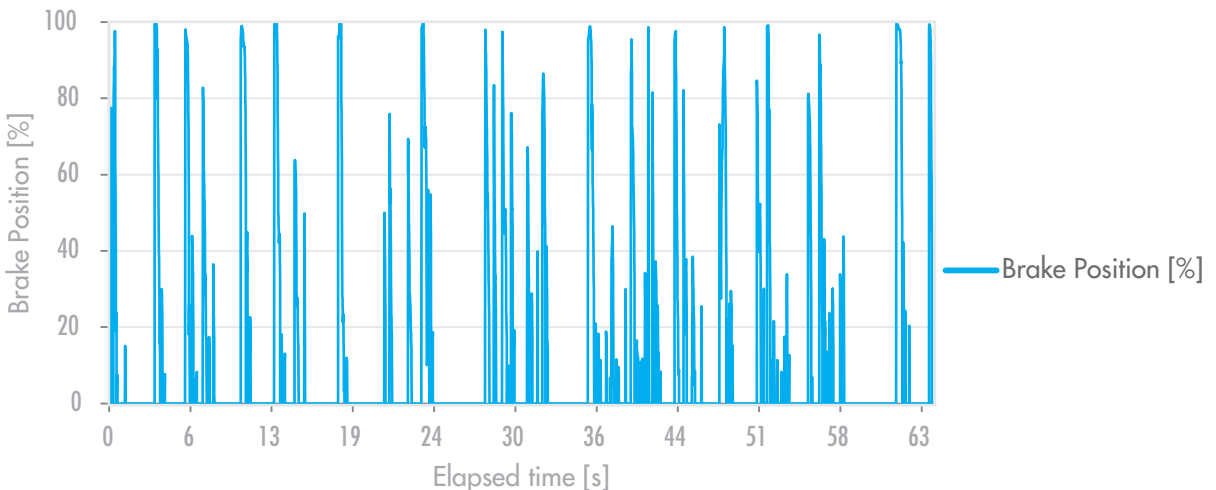
Increasing the range of the car by 50% only adds 1 liter of petrol. This results in high freedom in design of available energy. Thus, the range of the vehicle is never really limited by energy within the context of the competition.

With the electric vehicles, its a different story altogether. Here we are faced with similar challenges that are currently present in the world of commercial automotive engineering in that we need batteries to store energy. The energy density of lithium ion batteries is abysmal compared to that of fossil fuels. This results in the need to carry large and heavy battery packs, weighing in at between 40 and 50 kg. That is almost one third of the total weight of the car only in batteries. And even then, the car is still severely energy limited during the endurance competition.

Increasing the size of the battery pack beyond this is also not an option because of the increase in weight, size, cost and design limitations. The question that needs to be answered in light of this is how the two concepts compare in absolute energy efficiency.

At first glance one might be compelled into thinking that the Emrax 228 motor is significantly more efficient than the AMK DD5-14-10 motor as has been shown. This is true before we consider one of the defining differences between an electric motor and an internal combustion engine. In an internal combustion engine, mechanical energy is created through a non-reversible process. The only way to get more energy is to put more fuel in the tank. With electric motors, energy can go both ways. This is because an electric motor and an electric

## Brake Performance



Brake position during a single lap event in Optimum Lap



generator is one and the same. From this follows that we can use the motor as a generator in situations when it is possible to absorb energy.

By using the motor as a generator while breaking, we are able to charge the battery pack with the kinetic energy otherwise absorbed by the braking system. Instead of hot brake disks, we are able to spend the energy on propulsion later on. This is a well known solution for electric vehicles described as kinetic energy recovery system, or KERS for short. By utilizing KERS, electric vehicles are able to further improve energy efficiency over internal combustion cars beyond the difference in motor efficiency.

To show the difference in KERS performance between a 4WD system and a RWD system,

break position data was extracted from the Optimum Lap single lap data. The plot of breaking performance shows a significant amount of hard breaking situations, indicating the possibility to absorb a substantial amount of kinetic energy.

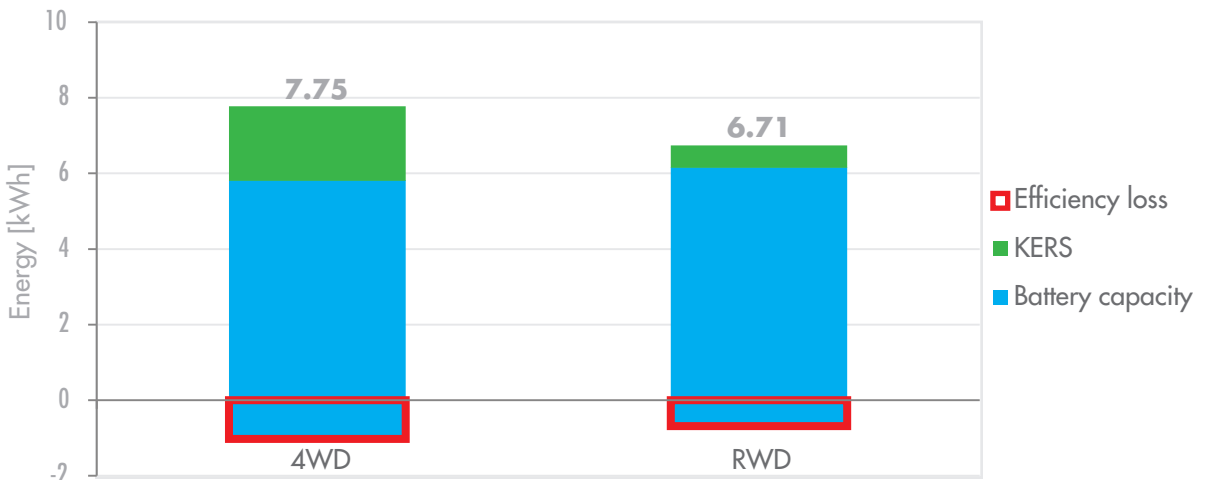
In order to calculate the maximum amount of kinetic energy each system can recover, the maximum breaking power of the motor was multiplied with the brake position factor for each data point. The maximum motor breaking power is limited in turn by the maximum charging capacity of the battery pack. The cells currently in use enable a maximum burst charge of 45 kW of power. Using 45 kW, each point of recovery data was added together to get the total recuperated energy for one lap. The energy was then

multiplied by 18 laps, making the result equivalent to a 22 km endurance event.

The next step is to account for break balance for the RWD car. Formula student cars tend to break around 70% on the front tires. This is because the weight of the car is shifting forward in the volatile breaking situations shown in the graph. More weight on the front wheel increases tire grip while the opposite happens to the rear wheels.

The energy data is finally adjusted for the difference in efficiency. It is here assumed that the RWD is 90% efficient and that the 4WD is 50% less efficient at 85%. Using 6.8 kWh as the battery capacity, we see that the 4WD system ideally has over 1 kWh or 15% more mechanical energy available during the course of an endurance race.

### Total available mechanical energy



Total available mechanical energy with energy recuperation with a total battery capacity of 6.8 kWh.

# Transmission ratio

## Analysis of logged data

The fundamental functional performance of a transmission system for automotive racing applications is to transform a range of speed and torque input to a corresponding range of speed and torque output. In order to fulfill the vehicles overall performance goals, an optimization of the described power transformation is of great importance.

To gather a sufficient understanding of optimization requirements, it is essential to look at the practical racing situations and how much an optimized system may affect the overall outcome. **Within a design and production time frame of only 8 months, starting out by identifying the optimization factors that will yield the most "bang for buck" is key in designing competitive performance.**

With this in mind, a starting point was to look at the aforementioned acceleration event. Common sense dictates that this event constitutes the situation that is most torque sensitive. It then follows that a transmission designed for optimal torque performance for this particular event may yield significant competitive gain. Looking at the acceleration performance of Arctos, the 2014 car, 35 to 40 points were lost to the best teams during this event. Many of those points were lost due to the already explained

performance differences between a 4WD and a RWD car. As driving 75 meters from stationary without changing gears is more performance than driver skill based, we are able to analyze the requirements of event competitiveness in isolation. We may then, through a strategic design approach, close the gap that the best all wheel drive cars currently have in the acceleration event.

Using sensor data logged during the events, we were able to plot every acceleration run completed during competition in Silverstone and Hockenheim in 2014. A 3rd degree polynomial function was used to graph a continuous line for a better graphical representation of the full acceleration run. By comparing these runs with logged data for power output from the accumulator (battery), some obvious elements of improvement presented themselves.

What follows is a summation of these elements divided into three main points. These points are intended to form a basis for further investigation and choice of focus regarding the design solution.

### 1 Energy input

Peak input is only 73 kW. The curve is also not as steep as the motor data permits, resulting in around 20% loss of torque compared to what the system is designed for.

The reason for this lies with the controlling electronics and is of little interest. What is of interest is that this extra performance, if used, could have reduced the gap in the acceleration event. Optimally, this means that the advantage up to the best cars is actually less than 35-40 points. **Note:** *Cyan and yellow dataset have significant wheel spin off the line, resulting in high power output without a corresponding mechanical output during the first second or so.*

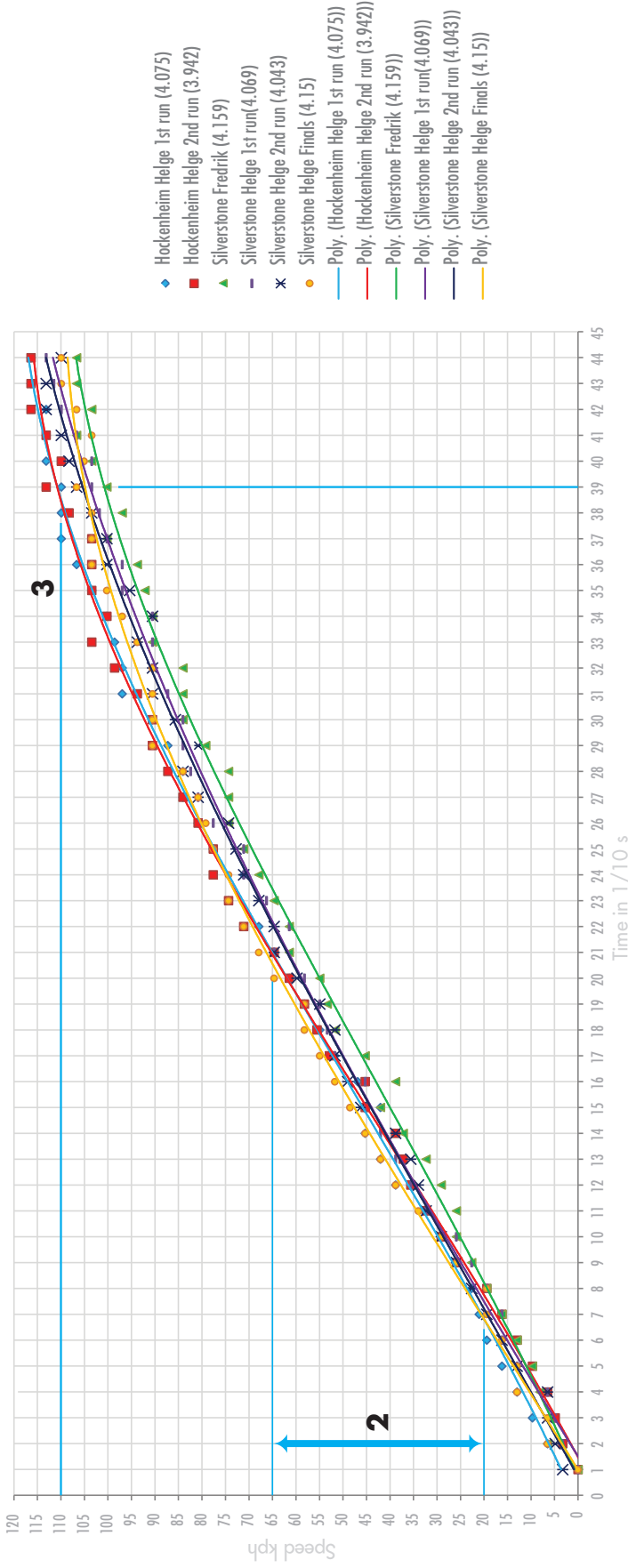
### 2 Peak acceleration

The steepest part of the curve is from 20 to 65 kph. By increasing the traction capacity, the car is able to accommodate more torque through increasing the gear ratio. The steeper profile would result in a larger area under the curve, more time at higher speeds before reaching 75 meter, and thus potentially a better time.

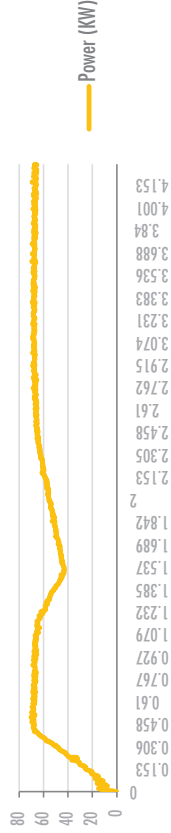
### 3 Top Speed

Looking at the top speed for each run, 110 +/- 2 km/h is the logged maximum when hitting the finish line. The gearing for a max speed of 120 kph may seem excessive in light of the possible added benefits of more low end torque. This may be an especially interesting prospect in terms of how it may change the performance in the other events. After all, overall performance gain is the goal.

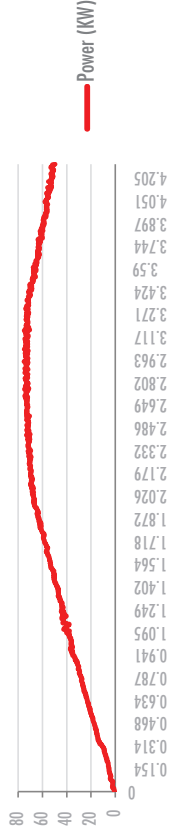
# Acceleration runs Revolve NTNU 2014



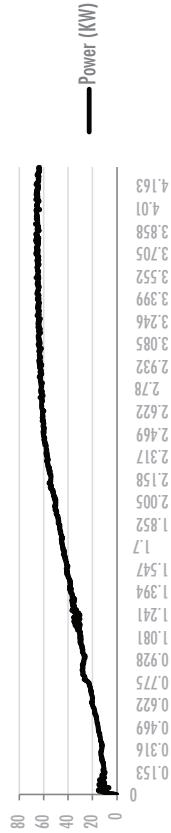
Silverstone Helge Finals (4.15)



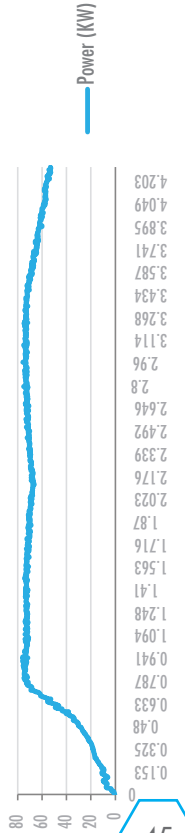
Hockenheim Helge 2nd run (3.942)



Silverstone Helge 2nd run (4.043)



Hockenheim Helge 1st run (4.075)



# Transmission ratio

## Lap time simulation: Acceleration

Some assumptions were made during the analysis of the logged acceleration data on the previous page. While these assumptions were based on common engineering sense, that alone is not enough to determine if a change in the fundamental parameter of a system will produce the performance increase that one “hopes” for. An attempt has to be made to objectively verify that the initial assumption holds true. Real world testing would demand the design and manufacture of a system for each design variation. This is obviously neither cost, nor time efficient. Within the allotted time frame, a computational approach is the method that will produce the best objectively comparable data.

Using OptimumLap lap time simulator, we were able to compare three different

final drive values that each represents a distinct difference in final performance. The three representations are top speed oriented, torque oriented and a tradeoff between the two. They are represented using the top speed limitation of each variation:

- 1**: 120 kph @ 20000 RPM
- 2**: 100 kph @ 20000 RPM
- 3**: 110 kph @ 20000 RPM

We start by evaluating how the results from the acceleration event are affected by the different final drive variations. The one dimensional format of this event is perfectly suited to evaluate the overall performance difference from different gearing ratios.

We see that **1** has the worst off the line and mid range performance. The higher top speed capacity is not able to compensate for

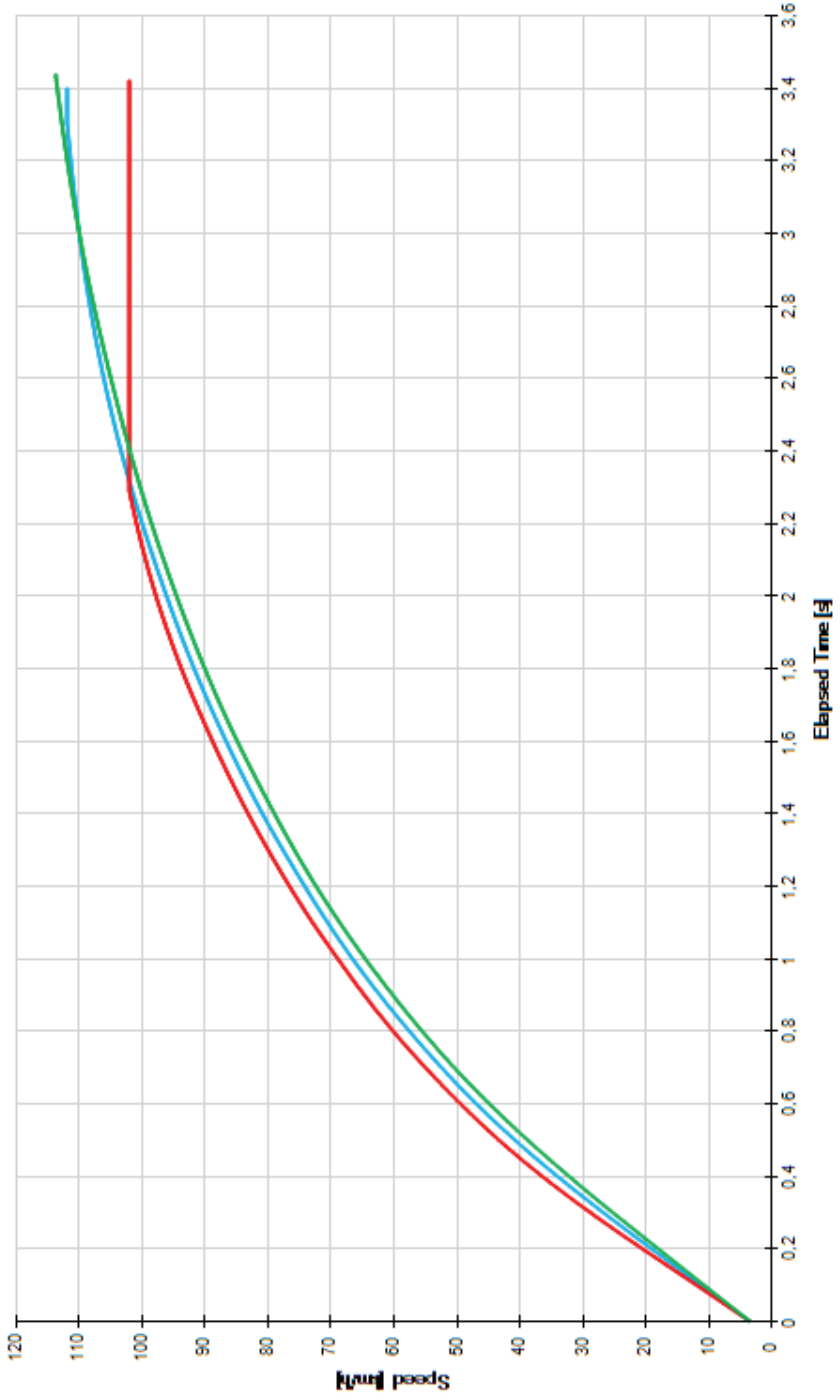
this performance gap. **1** is therefore yielding the worst result of the three at 0.04 seconds behind the best. **2** is by far the best setting for low and mid range speed performance. The limited top speed is unfortunately hampering the overall performance significantly, yielding a result of 0.02 seconds behind. **3** is found to perform well both at high and low speeds. It can logically be seen as an average between **1** and **2**. For this reason it is also the performance winner at 0.02 and 0.04 seconds ahead of **2** and **1** respectively.

The numbers are indeed small, but the comparative value is substantially more important here than the absolute value. The software agrees that there are competitive gains from a tradeoff between top speed and torque.



Optimum lap acceleration track shape speed plot.

# Time/Speed plot of acceleration event for different gear ratios



Selected Results	
[3.44]	120 km/h top speed 4wd, Drag
[3.42]	100 km/h top speed 4wd, Drag
[3.40]	110 km/h top speed 4wd, Drag

# Transmission ratio

## Lap time simulation: Autocross

We now know that gearing for a top speed of 110 kph @ 20000 RPM yields the best overall performance in the acceleration event. The acceleration event is, although very relevant, only a small and isolated part of the dynamic competition. Taking this into account, we are forced to verify that the results from the acceleration analysis holds true also during normal track racing. This is especially important since the largest amount of dynamic points is awarded in events evolving around regular track racing situations. If we found that option **1** or **2** would give better results in this driving situation, we would have to perform a trade off analysis to see what would be the best overall choice.

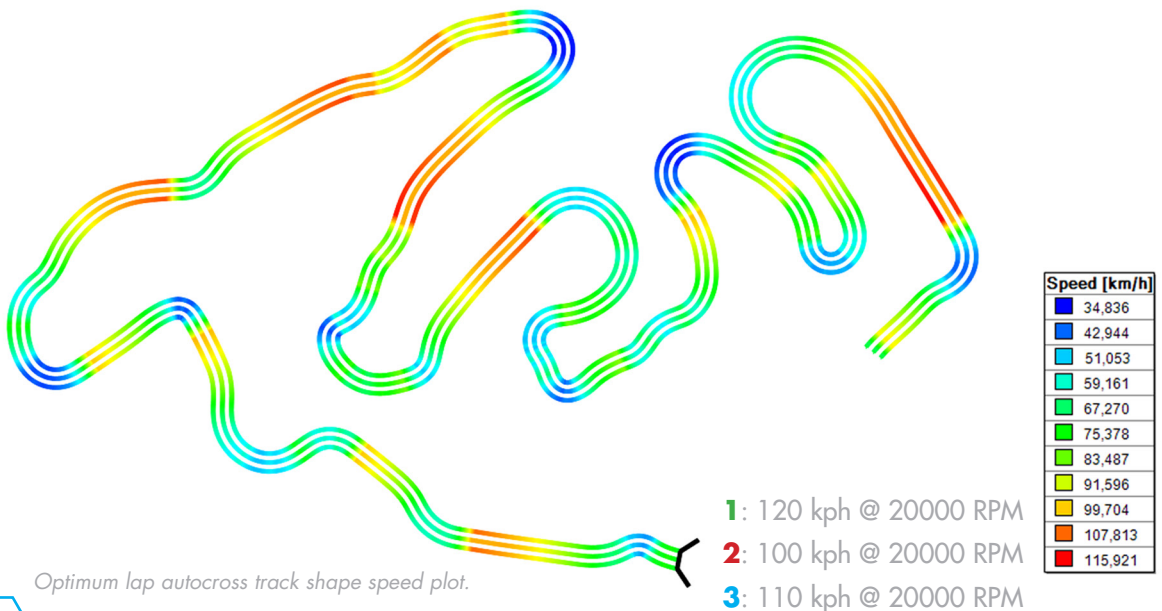
Again, using Optimum Lap we run a simulation on option **1**, **3** and **2** during an autocross

event. As the endurance event is 18 laps of the autocross, we are able to use the results to assess the difference in performance for both events. The weakness of this analysis is that the tracks differ between England, Germany and Austria. Optimally, we would have to simulate and compare results across the different tracks. Optimum Lap does only have the German track as standard and building the other two tracks would be too time intensive. In any case we are still left with a solid indication of which of the three final drive options that results in the faster car.

Evaluating the results of the autocross analysis we see the exact same trends as was present in the acceleration analysis. Option **1** has the peak top speed but lacks the low end torque to keep up with **3** and **2**. **2** falls short

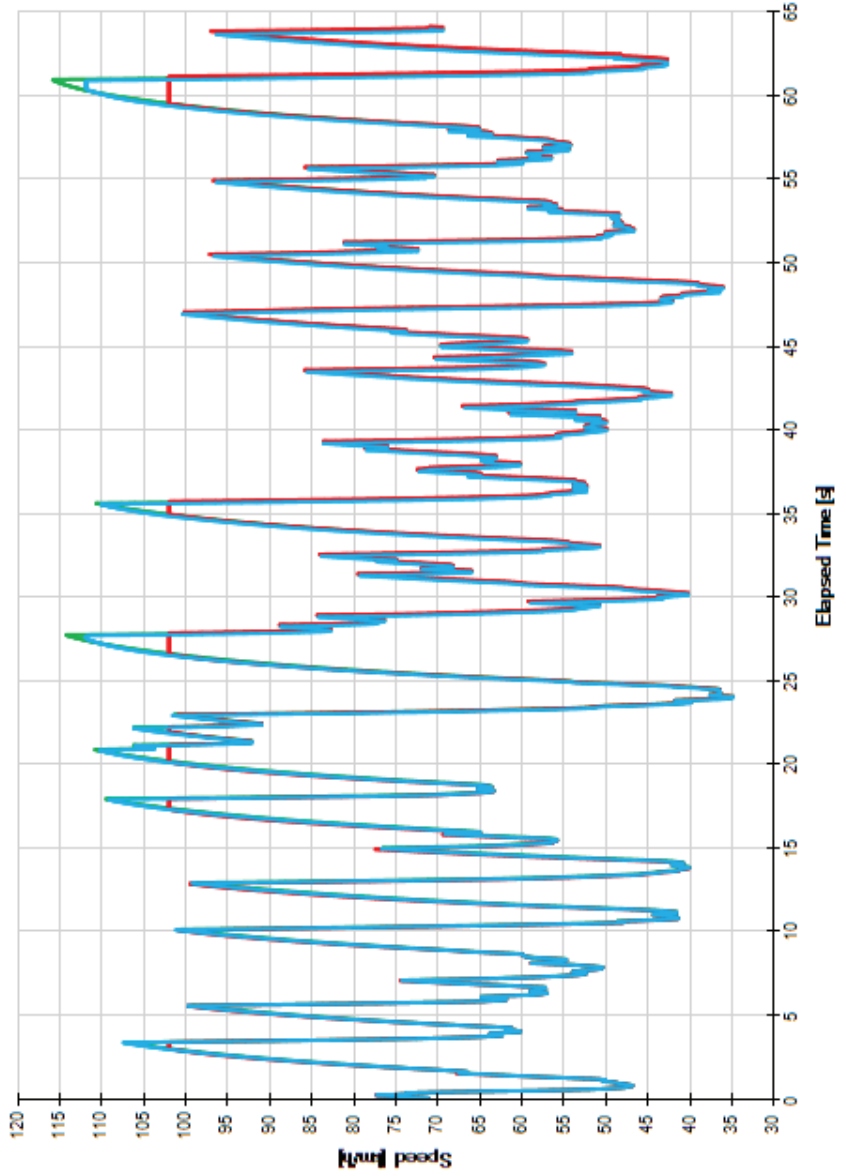
due to the loss sustained from the limited top speed. The flat tops in the graph peaks visualize this effectively. **3** is again left as the winner, 0.09 seconds and 0.19 seconds in front of **1** and **2** respectively. The fact that **2** places last here compared to 2nd in the acceleration analysis is indicating the importance of analyzing both cases.

Extrapolating the data for a full endurance race based on the autocross analysis results give a time difference of 1.62 seconds and 3.42 seconds for **1** and **2** respectively. Through these, and the acceleration analysis results we have shown that implementing a final drive ratio of around 1:15.5 will yield the higher total performance. Reducing or increasing the gearing ratio from this point is shown to reduce the overall vehicle performance.



Optimum lap autocross track shape speed plot.

# Time/Speed plot of autocross event for different gear ratios



# Drivetrain concepts

## An evaluation of different mechanical concepts

Looking at different concepts for force transfer in a transmission system, there are three distinct design options that stand out. These are chain, belt and gear drives respectively. The chain drive is a popular concept for FSAE combustion cars as these are mainly based around motorcycle engines with an internal gearbox that contributes most of the total gearing ratio and enables gear shifts. The simplicity of a chain system has many advantages. It is inexpensive, mechanically crude and designs itself from standard parts. The belt drive can be seen as an extension in complexity of the chain drive, somewhat more exotic in regards to both design and manufacture. Both of these work using toothed sprockets that directly mesh with a perforated area of the chain or belt, transferring power and thus creating locomotion. Looking more in detail at these rather similar options some critical points has to be raised.

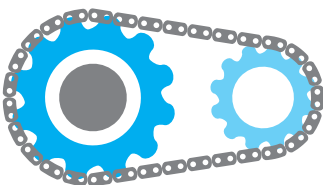
Firstly, chain and belt drives

suffer from something called the “chordal effect”, describing the situation where the non tension side of the belt or chain system is lifted towards the center of said system(see figure). What happens is essentially that the non tension part of the chain or belt is riding on the sprocket tooth, producing significant movement, resulting in loss of power. This is prevalent more so in chains than belts because the steel material the chain is made of has a higher moment of inertia than what an equivalent belt made of reinforced polymer would have.

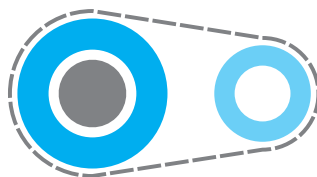
Secondly, the fact that these systems have a tension and a non tension side has implications when rapidly inverting the driver and driven part. What results is a significant backlash in the system. Comparing this to a theoretical non backlash system we can conclude that significant backlash has a negative effect on the handling precision of the car. Looking at lap time simulations and logged data, we see that these

situations happen all the time and backlash is therefore not just a theoretical problem but rather something that should be minimized. The backlash creates impact forces in the system when reversing the torque. These impacts can cause damage to the system if not kept to a minimum. What is more is that belt drives in particular are not designed for rapid and significant variations in torque and speed as they depend more on friction for torque transfer. The contact force from the sprocket teeth on the chain has a significantly higher torque transfer capacity.

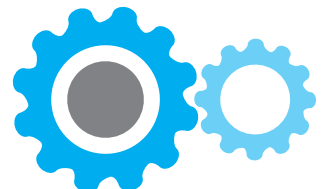
Thirdly, in order for the chain to mesh properly with the toothed sprockets and for the belt to have the required amount of frictional surface contact, the chain or belt needs to be designed with a relaxed angle from the centerline of the system. This demands belts or chains of such a length as would create a large distance between the driver and the driven axis of rotation. This means that designing a compact



Chain drive



Belt drive



Gear drive



belt or chain system with a ratio of 1:15.5 will be near impossible.

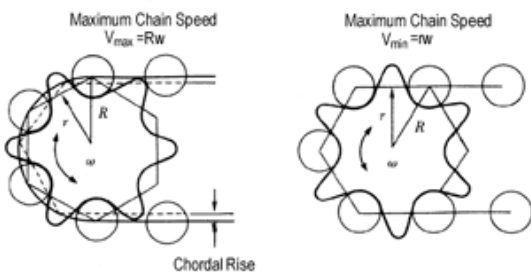
To sum up, chain and belt systems, while less complex to design, have too much backlash, are mechanically inefficient and can not be made compact. It is therefore concluded that these systems are not suited for the current conceptual application based on the design requirements previously stated. This is true even when considering the low cost of these systems.

Gear drives consist of toothed steel cylinders that when meshed together are able to transfer power as contact force with high load capacity and precision. Unlike chain and belt sprockets, the teeth of gears can be customized in order to better suit a specific application. As these geared cylinders are in direct

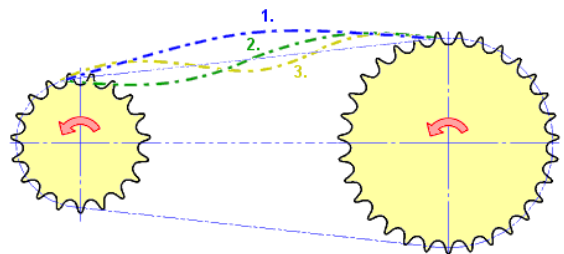
contact the total volume of the system is significantly smaller compared to that of the belt or chain drive system. There are in addition many ways to compound several of these gear pairs in order to design compact systems with a high gearing ratio. If the gears are designed properly, the precise contact dynamic of the teeth will yield a more efficient transfer of power than in a belt or chain drive. The downside is that gear design is much more elaborate and time consuming than with gears and belts. Manufacturing of high performance gears are also commonly associated with a high price tag. Despite this, gear drives remain the preferred solution for most machinery and automotive applications because of its high precision and overall performance.

By selecting gears as the basis

for speed reduction between the motor and the wheel we can expect to be able to design the most compact and efficient system of the three. Backlash is virtually non-existent in a geared drive, resulting in very crisp and precise car handling. One has to cautiously presuppose that one is able to overcome the extensive economic and intellectual price tag that follows this choice. It is however made clear that it is the only viable option of the three that are mentioned. This means that the choice to use a gear drive was baked into the decision to implement a 4WD drive system. This does not come as a surprise as the described characteristics are clear indications of why this system is exclusively used in automotive transmission applications.



Chordal rise of a chain on a sprocket.



Chordal effect of a chain or a belt.

# Drivetrain concepts

## Different gear trains

In the evaluation of mechanical concepts, toothed gear trains are presented as two cylindrical gears with meshing teeth. This is an oversimplification in order to streamline the argument. In actuality, there exist many different forms of gear systems that each solve a specific mechanical challenge. Rack and pinion converts rotational movement to linear movement. Bevel gears can transfer torque over non parallel axis of rotation. Face gears can transfer torque via axial contact. Systems can be designed where gear ratios can be changed, as is present in most, if not all, combustion cars. These and many more variations on a gear drive design creates much room for design optimization based on application. This superior design flexibility is further argument for the use of a gear drive.

From this we need to identify suitable design solutions for the proposed application. Based on the need for low weight and high efficiency, we can conclude that high torque density will be the primary criteria for the system. When assessing gear concepts based on torque density, two solutions stand out. These are parallel axis and epicyclic gear systems respectively. How they work and in what way they differ will be explained in this section.

### Parallel axis systems

A parallel axis gear, also known as spur gear, is what most people associate with gears, one small and one large cylindrical gear meshing, rotating on individual, parallel, axis. Two gears meshing in this way will from now on be referred to as a gear pair. A straight cut gear pair configuration has the potential for high torque density as the contact force created by the meshing teeth remains eccentric to the rotational axis. This means that the resultant force on the axis is almost exclusively in the radial direction. Load directions are complicated by an axial thrust force by the introduction of helical gear teeth. High performance designs usually sacrifice the smoother running and lower operational noise of the helical gear teeth for the controllability of the in plane contact force of the straight cut gear teeth.

The transmission ratio of the gear pair is a function of the difference in diameter between the two gears. This means that higher transmission ratios demands enormous output gears, increasing both mass, inertia and volume of the system. Parallel axis systems overcomes this challenge by linking two or more lower ratio gear pairs together in order to form a system with a high transmission ratio while keeping mass and volume to a minimum. Parallel axis

systems are as mentioned also used in most automotive vehicle gearboxes. Here they are implemented as a stack of gear pairs where only one gear pair is engaged at a time. A clutch and a gear shift mechanism enables shifting between the differing size gear pairs, enabling variation of the output speed range. This design enables high low end torque and a large output speed range from the same system.

A non shifting parallel axis system is seen as having medium design complexity. The part cost is usually kept reasonable as extremely fine tolerances are not of such importance that not having them will ruin the performance of the system. The downside of a parallel axis system is that higher gearing ratios, while more compact than a chain or a belt drive, will result in a design that takes up a fair amount of volume. It is also not a suitable design when the application demands that the input and output of the system remains on the same axis.

Transmission ratio relations for parallel axis systems:

Gear pair:

$$i = Z_2 / Z_1$$

Linked gear pairs:

$$i = (Z_2 / Z_1) * (Z_4 / Z_3) * \dots$$

Where  $i$  denote the ratio and

$Z_x$  denotes the number of teeth on each gear. There exist clear theoretical restrictions to the size difference between two meshing gears. If the size difference becomes too large, errors in the meshing dynamics will occur, resulting in a very inefficient design. A reduction ratio of over 1:8 for a single stage spur gear system is not advisable.

**Epicyclic systems**

Epicyclic gearing systems are distinctly different to parallel axis system in many ways. These systems utilize a combination of externally and internally toothed gears in order to achieve a high transmission ratio with a very low volume. The basic epicyclic system consists of an externally toothed sun gear rotating on the center axis. Concentric to this is an internally toothed annulus gear. A number of planet gears connect the sun gear to the annulus gear. One could mount the sun gear on a separate parallel axis and in contact with the annulus gear to produce a compact parallel axis system. The

key improvement created by adding the planet gears is that load is distributed over more gear teeth. By splitting the load like this, one is able to design systems with extremely high torque density while still using smaller gear teeth with a moderate force transfer capacity. The number of planets used differs greatly, from three in high ratio systems, up to 12 or more for extreme torque applications such as wind mills, offshore winches and the like. No matter the number of planets, the whole system fits inside the volume that would be created by the larger of the two gears in a conventional gear pair.

The downside with epicyclic systems is that they require very precise tolerances and flexible mechanisms in order to ensure that the load is balanced between all the planets in the system. This also adds to the design complexity of the system, requiring much more precise engineering in order to work flawlessly in relation to the parallel axis system. This initially means that the design and manufacturing

cost of epicyclic systems are equivalently higher. This is however far from true as the cost difference is negated by the smaller size of the system and the included components. Therefore, the total cost, especially for larger systems, can end up much smaller for an epicyclic system compared to a parallel axis system with the same specifications.

Transmission ratio relations for epicyclic systems:

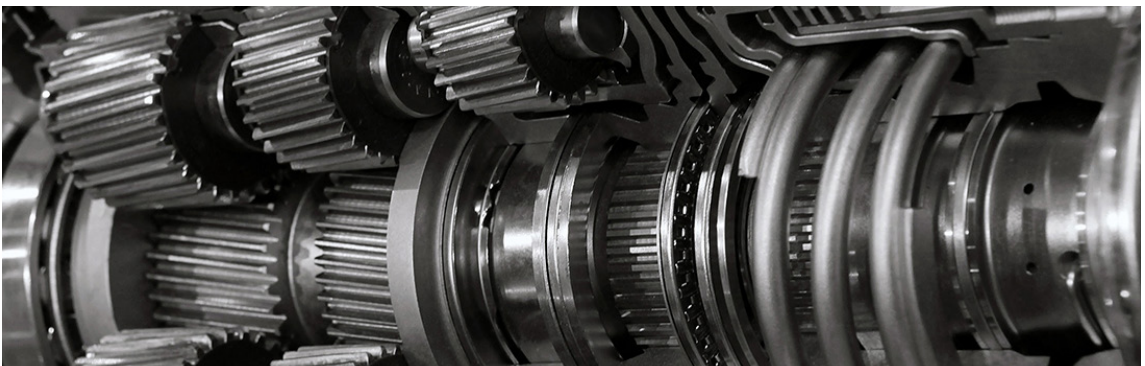
Rotating annulus gear:

$$i = Z_3/Z_1$$

Rotating planet carrier:

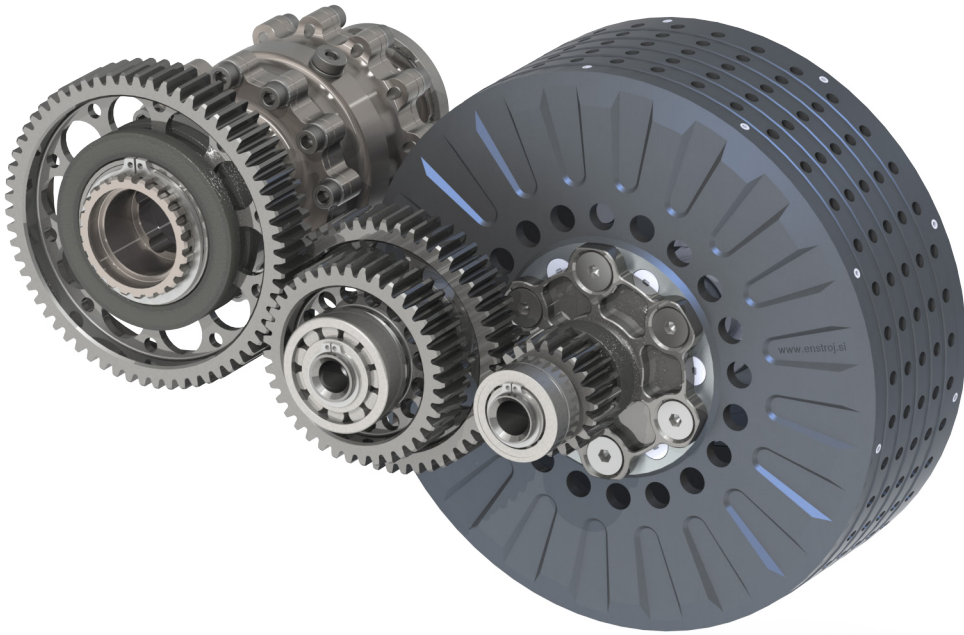
$$i = (Z_3/Z_1)+1$$

Where  $i$  denotes the ratio and  $Z_x$  denotes the number of teeth on each gear where  $Z_1$  is the sun gear and  $Z_3$  is the annulus gear while the size of the planets, denoted by  $Z_2$ , is not contributing to the value of  $i$  and is therefore not included in the equations.

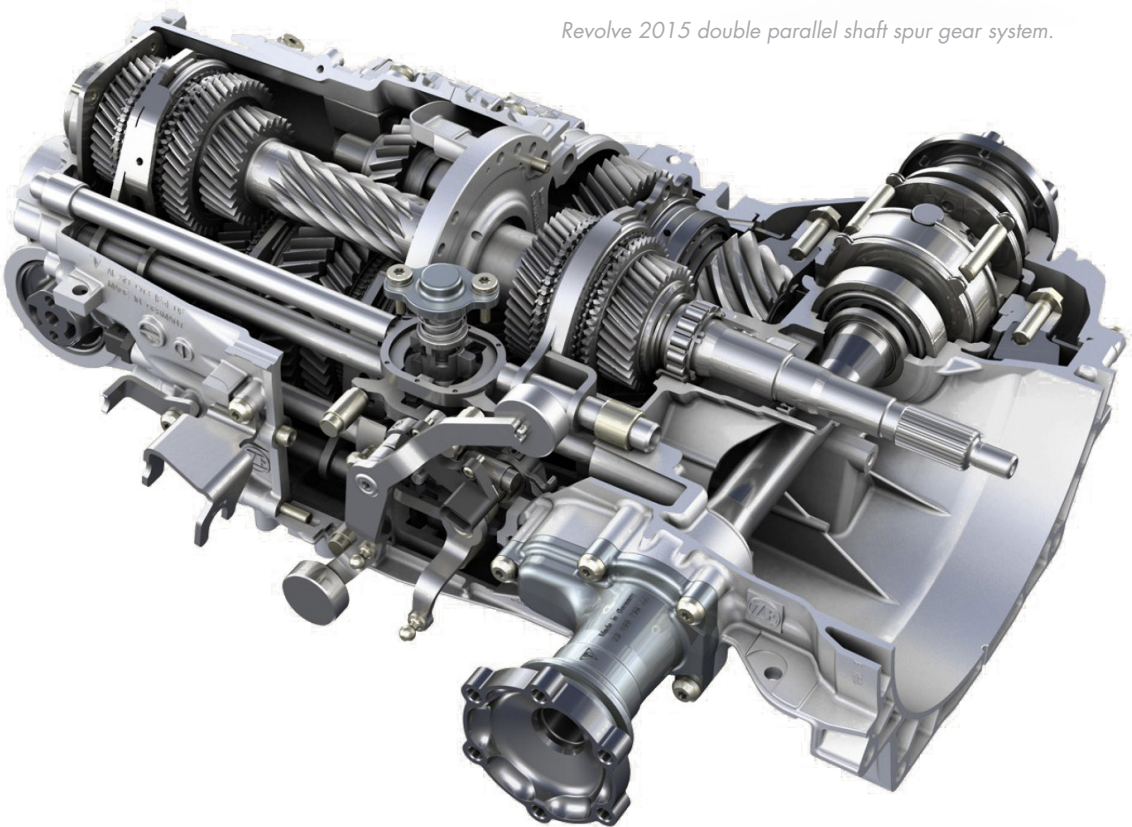


# Drivetrain concepts

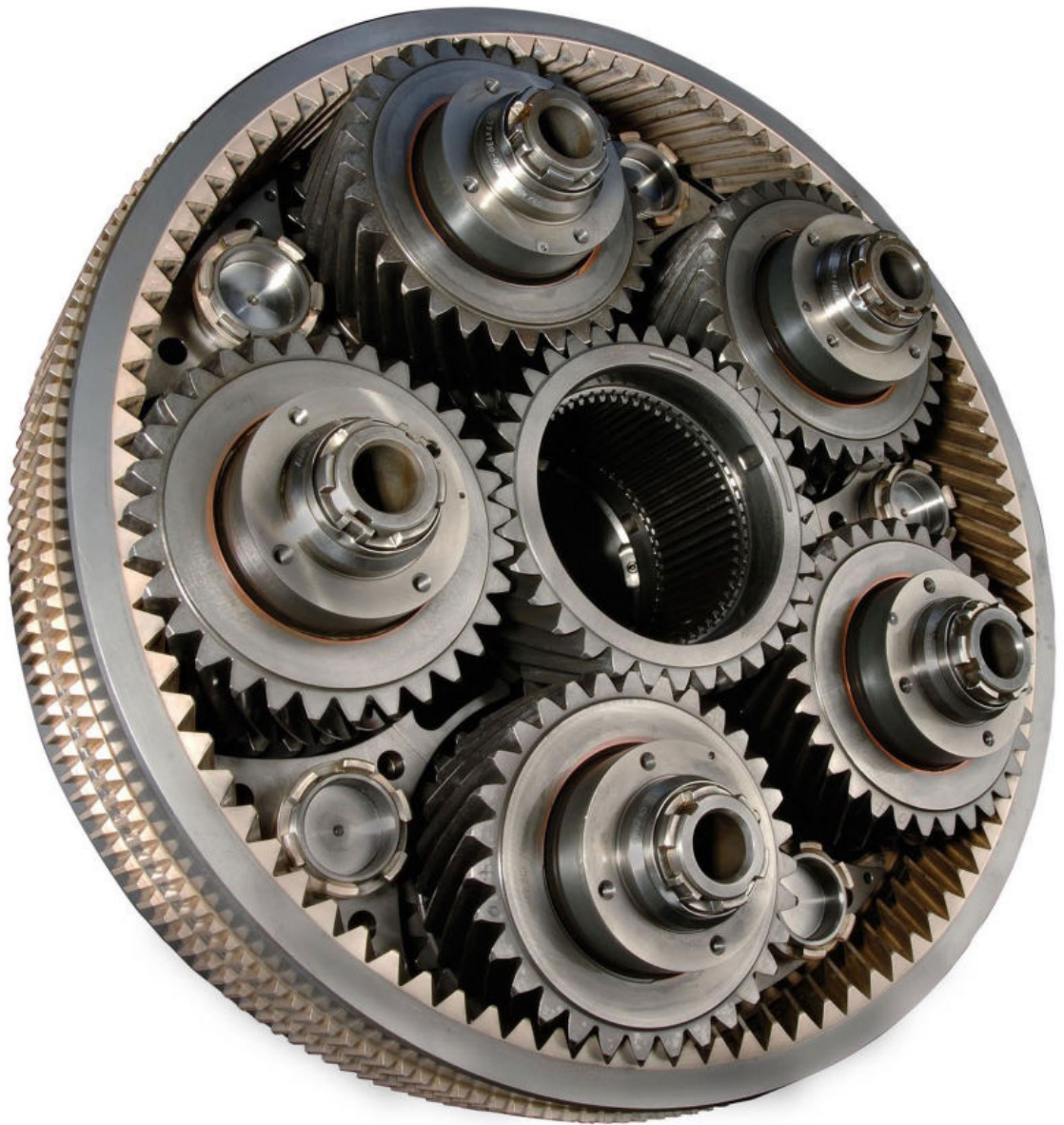
## Examples



*Revolve 2015 double parallel shaft spur gear system.*



*7 Speed sequential gearbox consisting of parallel shaft gears.*



*Planetary system using 5 planets. Force is split in 5 between the sun and ring gear.*

# Drivetrain concepts

## Concept 1

The concept of having both motors and transmission integrated into the chassis of the vehicle is in close relation to the standard automotive approach for 4WD systems. Instead of having one motor connected to one gearbox connecting to a differential that splits output for all four wheels, one motor is connected to its own gearbox at each corner of the car. The gearbox then transmits the load to the wheel via the drive shaft. The drive shaft is linked in both ends by a constant velocity joint. These joints enable movement of the wheels in relation to the chassis while still being able to transfer torque.

The motor is positioned with the center of mass as low as possible in order to reduce the height of

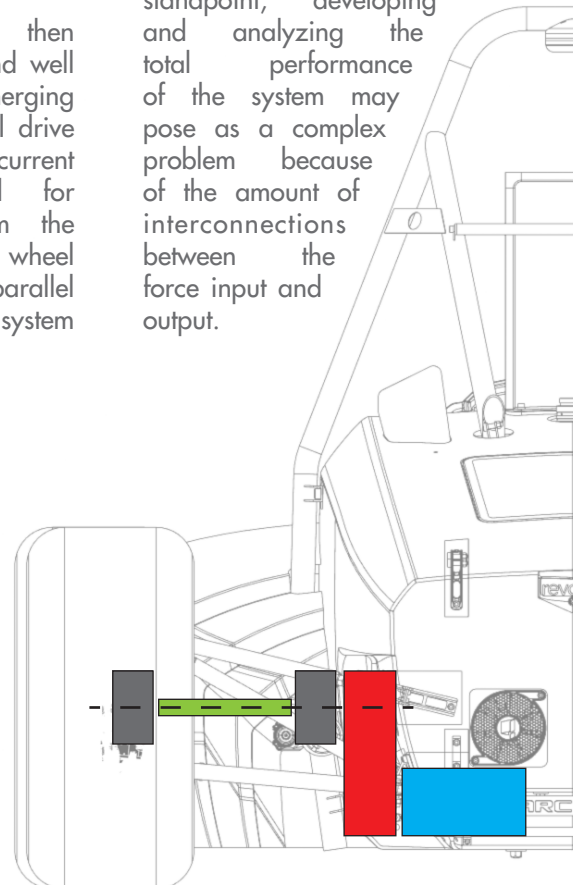
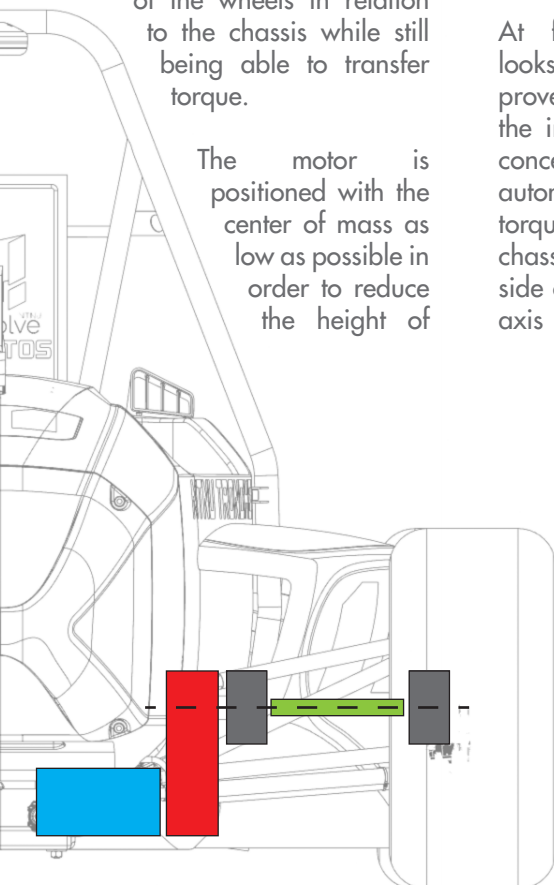
the center of gravity of the car. This will in turn ensure better kinematic performance from the suspension and better packaging opportunities for the car in general.

Running a parallel axis transmission system is shown to enable the transfer of torque from the low mounting position of the motor up to the wheel center point. The gearbox will be mounted directly to the outside wall of the chassis, simplifying the mounting points while also reducing the length of the drive shaft to a minimum.

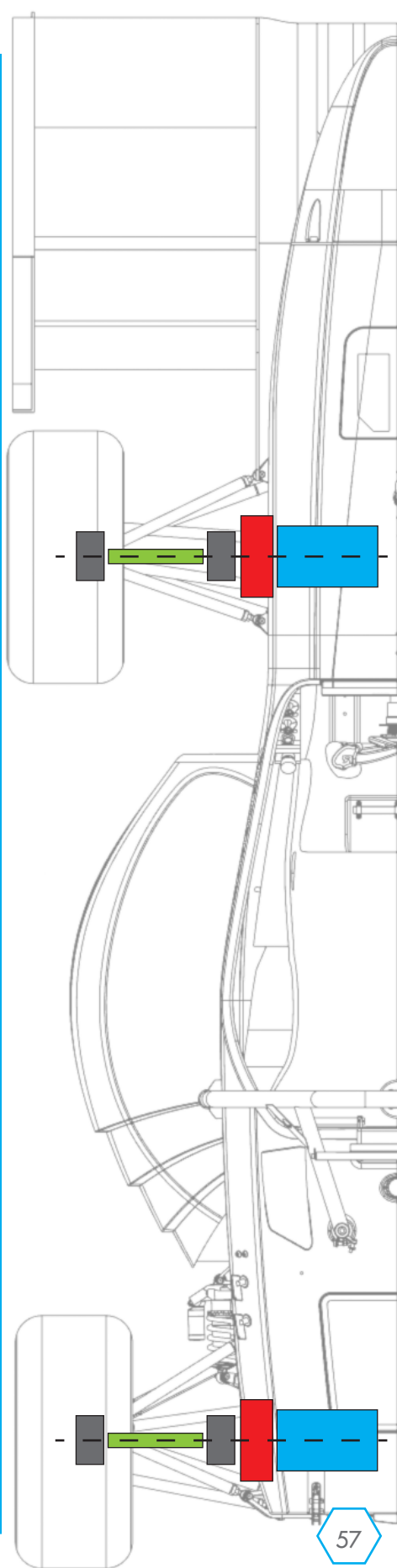
At first glance this then looks like a robust and well proven concept, merging the independent wheel drive concept with the current automotive standard for torque transfer from the chassis side to the wheel side of the vehicle. A parallel axis transmission system

is in addition well known and considered a medium complexity design task, increasing the merit of the concept seen in combination with the tight time frame of the project. Further analysis has however unveiled several factors that may be suboptimal seen in context with the other concepts.

The most glaring factor is the amount of high cost parts in the system that needs to be manufactured. This alone may pose as a significant challenge in realizing a concept like this. From a design standpoint, developing and analyzing the total performance of the system may pose as a complex problem because of the amount of interconnections between the force input and output.



# Convention

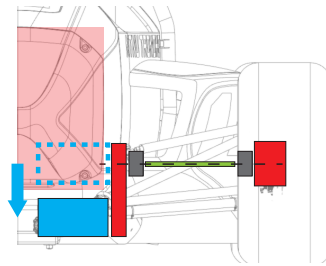


# Drivetrain concepts

## Concept 2

Further development of the first proposed concept has led to a similar, yet significantly different solution. The motor output is directly transmitted to a small shaft via a small 1:1 ratio gearbox. The optimal solution here would be to eliminate this gearbox and mount the motor directly to the shaft CV joint on the wheel rotational axis. Unfortunately, this would interfere with the cockpit area in the front, reducing the driver leg space, making the car non compliant with the competition rules. As the motors also sport significant weight, increasing the mounting height would be detrimental to the car center of gravity. As the 1:1 gearbox would be eliminated, the absolute outcome in regards to center of gravity remains unclear without further

development of the concept.

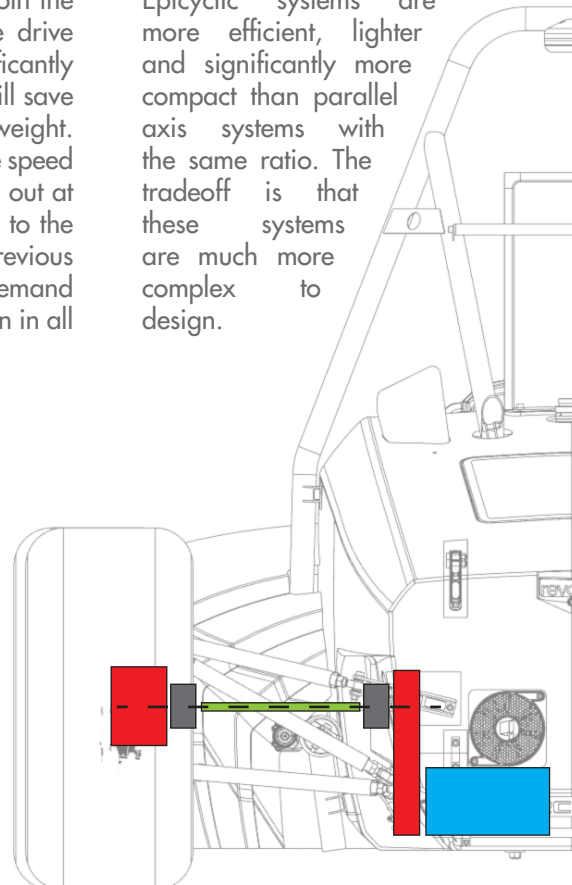
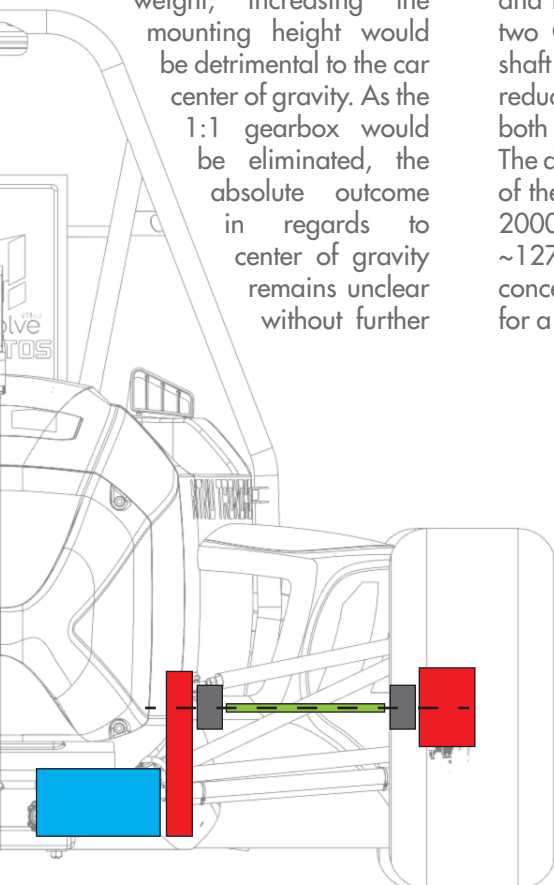


*Interference between cockpit volume and optimal motor position.*

The torque is now transmitted from the motor directly to the CV joint and the drive shaft without any form of speed reduction. What this means is that the mechanical capacity, and thus the size, of both the two CV joints and the drive shaft can be significantly reduced. This in turn will save both cost, space and weight. The downside is that the speed of the shaft now maxes out at 20000 RPM compared to the ~1270 RPM of the previous concept. This sets a demand for a very high precision in all

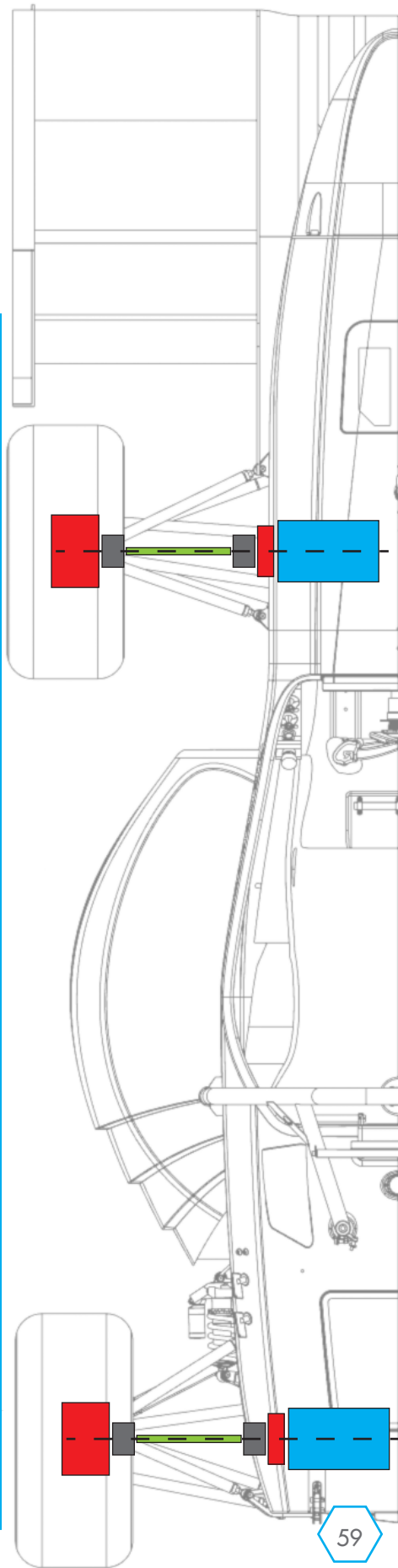
the parts. At speeds of 20000 RPM, any vibration may induce significant cavitation that can damage the system. An open system spinning at that speed would also be extremely dangerous.

The transmission system has been moved and integrated into the wheel assembly. This then enables the use of epicyclic gearing solutions, also called planetary gears. This planetary gear system is then integrated as a part of the spindle and hub assembly, eliminating the need for a separate gearbox housing. Epicyclic systems are more efficient, lighter and significantly more compact than parallel axis systems with the same ratio. The tradeoff is that these systems are much more complex to design.





# Variation



# Drivetrain concepts

## Concept 3

Concept 2 is seen as very complex, needing two gearboxes for each corner. The number of parts and the high complexity, time demand and cost that follows leaves much to be desired. The following concept has been developed to combat these factors while also improving the overall performance.

Instead of mounting the motor at the chassis side with the need for a drive shaft connected by CV joints in order to transfer power to the wheels, the motor is now mounted directly to the spindle at the wheel side. Mounting the motor in this way is not in any way a new idea. It has however just recently become a viable design option because of the accelerated development of compact

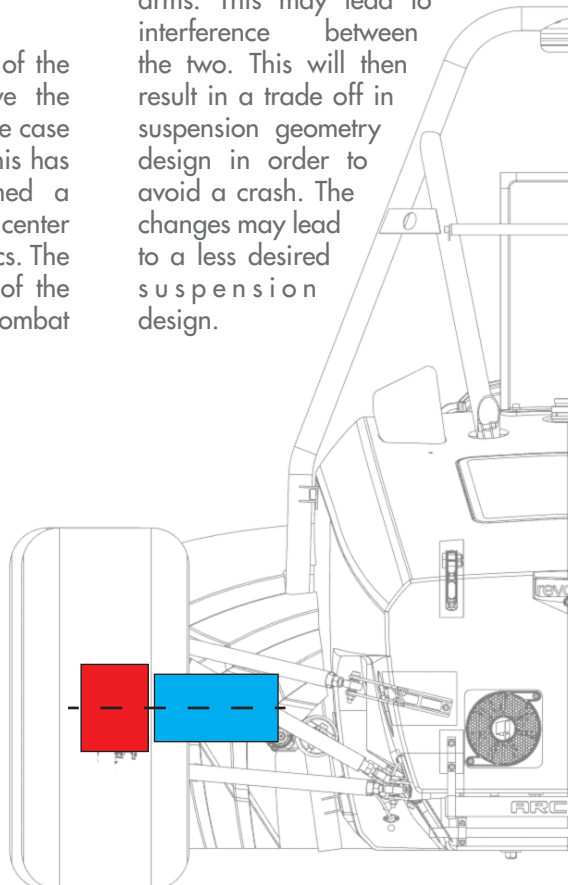
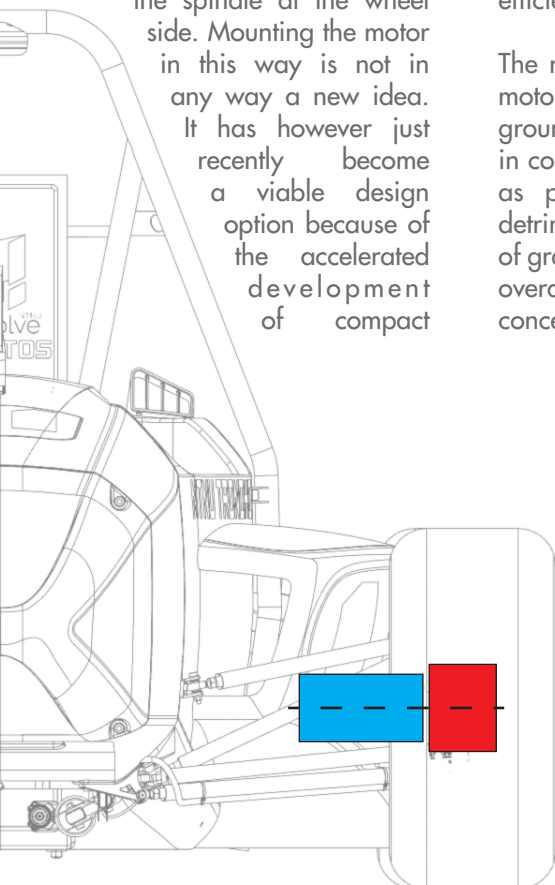
actuators with higher power to weight ratio.

The motor output is fed directly into an epicyclic gear system that has been integrated into both the hub and the spindle. This increases the complexity of both the spindle and the hub, but does not add any additional parts. Eliminating the gearbox housing, the CV joints and the drive shaft reduces both cost, complexity and weight substantially. Even more significant, the mechanical power loss from the CV joints is eliminated, increasing overall energy efficiency by 2-5%.

The mounting position of the motor is higher above the ground plane than is the case in concept 1 and 2. This has as previously mentioned a detrimental effect on car center of gravity and kinematics. The overall lower weight of the concept does a lot to combat

this effect. What is more negative is that we now have the high mass of the motors mounted unsprung. The wheel assembly moment of inertia will increase substantially as a result. Unsprung mass is not handled well by the suspension dampers. Thus, an increase in unsprung moment of inertia leads to less tire grip on uneven driving surfaces. Further investigation is needed in order to substantiate the magnitude of this trade off.

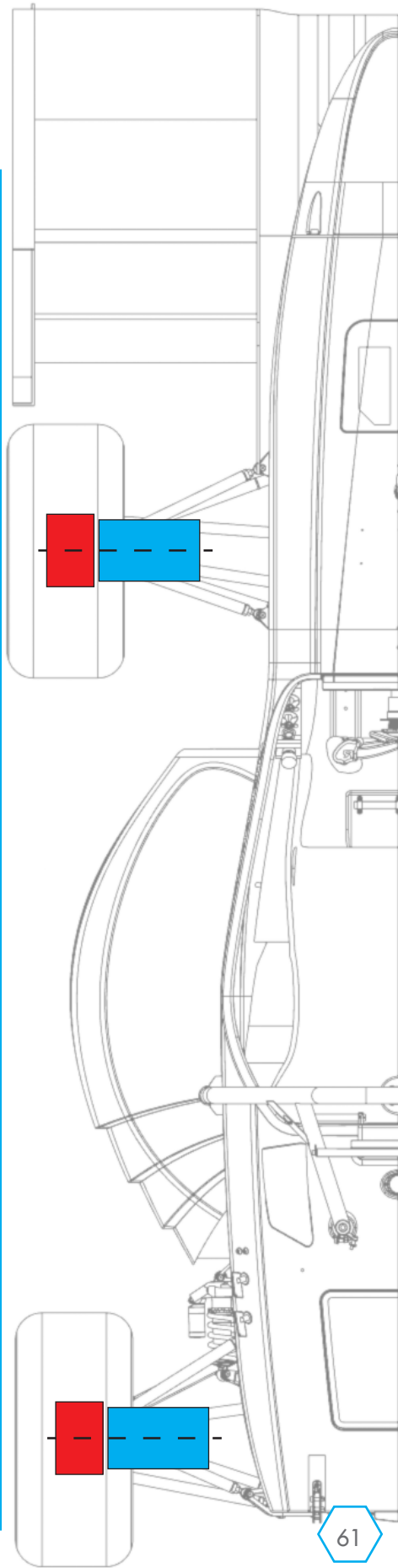
The motor is now protruding into the area regularly held by the suspension arms. This may lead to interference between the two. This will then result in a trade off in suspension geometry design in order to avoid a crash. The changes may lead to a less desired suspension design.



Motor

Transmission

# Innovation



# Drivetrain concepts

## Choice of drivetrain concept

A concept benchmark was performed to evaluate to what extent each concept was able to fulfill the projects design criteria. From this, concept 3 emerged as a clear winner and the chosen concept going forward. What follows is a breakdown of the concepts performance for each evaluation criteria.

### Rules compliance:

All three concepts were considered to be able to achieve rules compliance without any significant effort.

### Weight:

Due to the significant reduction in parts, concept 3 was evaluated to have a much larger potential for weight saving over the two other concepts.

### Cost:

Due to the significant overall reduction of parts, it was fairly easy to conclude that the price tag of concept 3 would be lower than that of the other two.

### Performance:

No significant variation in conceptual performance could be found between the concepts. All three concepts can deliver the required torque and speed to the wheels without any significant detriment to vehicle torque performance.

### Efficiency:

The elimination of the driveshafts, constant velocity joints and a reduction of load path from the motor to the wheel meant that concept 3 would be able to achieve a significantly higher mechanical efficiency than the other two concepts.

### Reliability:

This was a more difficult criterion to evaluate. On the one side, concept 3 has less parts, less connections and less that can go wrong. On the other side, concept 3 will probably end up very compact and the final design may therefore see some compromises in reliability. In the end this was called as a small victory to concept 3.

### Overall concept Feasibility:

Under this criterion, all three concepts were evaluated based on practical parameters and synergy with the rest of the car. Concept 3 has a high synergy with chassis design, moving components away from the monocoque and freeing up packing space. Moving weight out into the wheels will however increase unsprung mass and increase yaw moment of inertia. For concept 1 its the other way around. For concept 2, the potential high rotational speed of the driveshafts was considered especially problematic and resulted in a low feasibility score.

**Innovation:**

Any significant degree of innovation meant stepping away from convention. From this, only concept 3 could be classified as a truly innovative solution within the context of automotive design.

**Marketability:**

The marketing potential of a product is closely related to the products uniqueness and grade of innovation. Concept 3 will as such provide Revolve NTNU with a unique and innovative prototype concept that will create increased

interest inn the project and its participants.

**Academic challenge:**

In the spirit of providing a strong foundation for a challenging, inspiring and innovative master thesis, concept 3 was subjectively deemed the more interesting concept. The choice of concept 3 was thus also chosen for motivational reasons. This would however bear very little significance to the overall concept choice if the concept scored worse in the other choice criteria.

<b>Evaluation of transmission concepts</b>			
	<b>Concept 1</b>	<b>Concept 2</b>	<b>Concept 3</b>
Rules compliance	Blue	Blue	Blue
Weight	Red	Red	Green
Cost	Red	Red	Green
Performance	Blue	Blue	Blue
Efficiency	Red	Red	Green
Reliability	Blue	Blue	Green
Overall concept feasibility	Green	Red	Green
Innovation	Red	Red	Green
Marketability	Blue	Blue	Green
Academic challenge	Blue	Blue	Green

**Red:** Performance below requirements or weak compared to others.

**Blue:** Performance to requirements or slightly worse than best.

**Green:** Performance better than requirements or best.

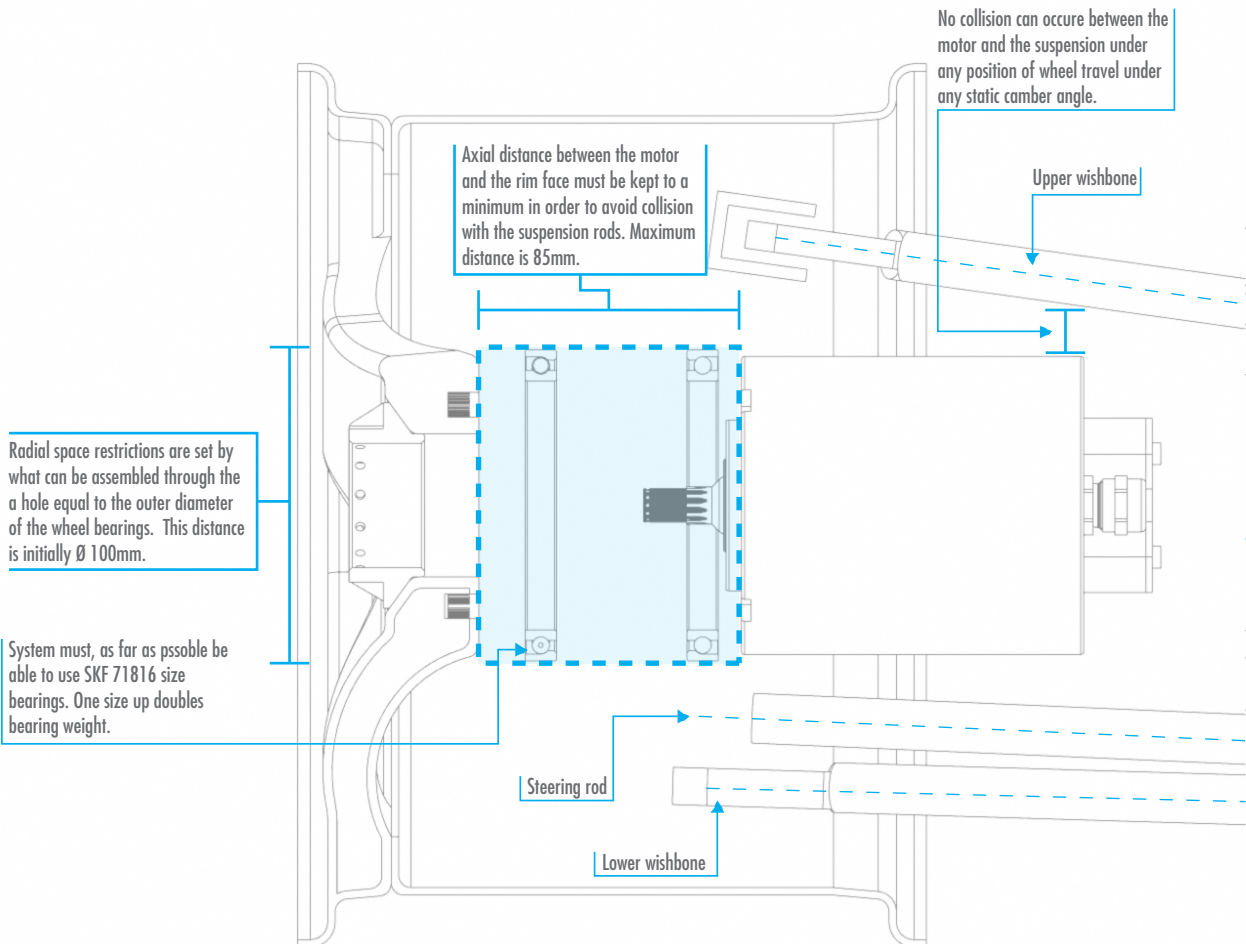
# Planetary systems

## Design space

The design space was set while working closely together with the vehicle dynamics engineer. With the main focus of finding an optimal kinematics design, a maximum design envelope for the transmission was set. This was done through an iterative co design process using crude design drafts of both systems in order to identify problems and create solutions. The process entailed using flexible CAD assemblies, looking at every type of suspension articulation for every suspension setting in order to ensure no interference between the two systems. The 30 degree steering angle movement at the front wheels emerged as the main problem

area. Ensuring clearance here required many iterations of both designs before finding a layout that was preferable for both parties.

The axial distance of the envelope was restricted to 85mm to keep the motor from crashing in the suspension system. If the system was to take up any more space, large compromises would have to be made in the kinematics design. As optimal vehicle dynamics performance was classed with a higher performance priority, any significant compromise in suspension design would not be accepted.

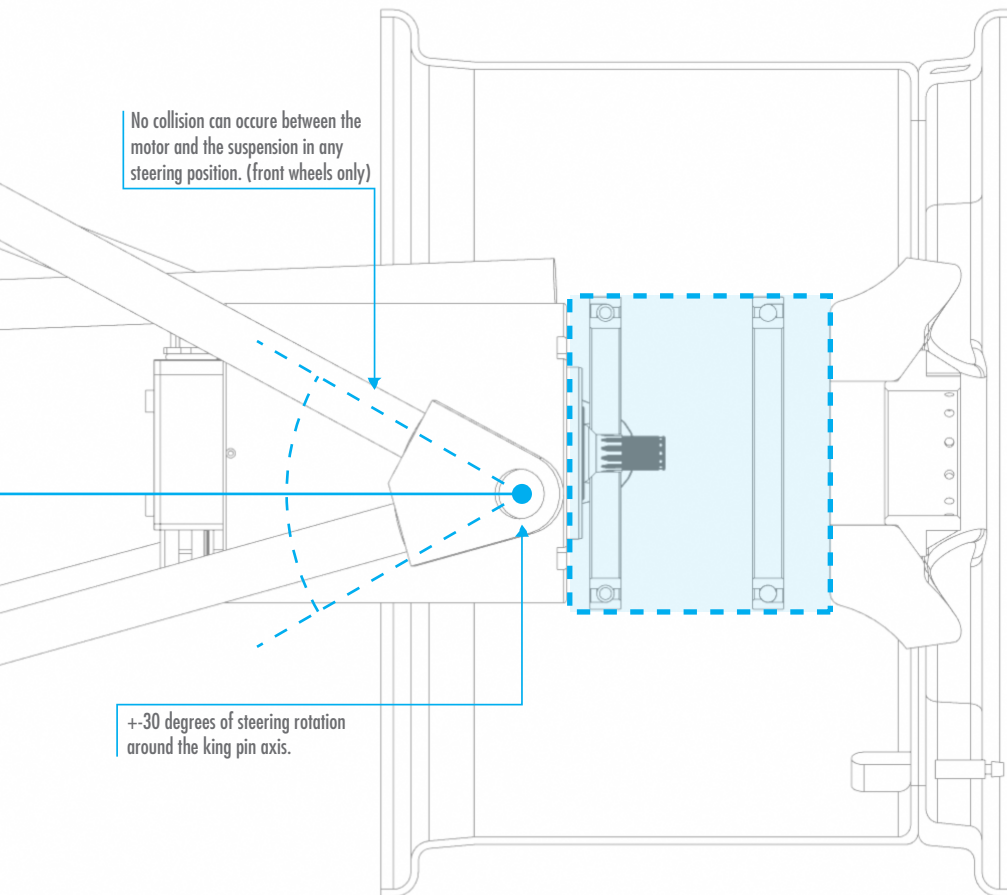


Front view of in wheel transmission design space.

The radial space for the system was set based on the most desirable choice in wheel bearings. Going up one bearing size would double the bearing weight from 150g to 300g per bearing. This would result in a total weight increase of 1.2kg or 0.7% of the total car weight. A bearing size increase would as such only be considered viable as a last resort. This meant that the transmission system had to fit inside a 100mm diameter hole, the outer diameter of the wheel bearings.

The resulting low volume of the transmission design space can be considered as very

restrictive to design freedom. It is however important to point out that restrictions like this has the ability to significantly spike creativity in the concept development phase. Increasing the difficulty of the design challenge may as such be a catalyst in ensuring a smart, well designed and high performing end product. Finding creative solutions to "impossible" problems is considered the hallmark of innovation within prototype race car engineering. This is reflected in the spirit of Revolve NTNU. The conclusion is that these restrictions are very fitting for the context of this project.



Top view of in wheel transmission design space.

# Planetary systems

## Standard planetary system

The standard planetary system offers efficient transmission performance at medium complexity. Due to the manageable design and analysis complexity, the low number of parts and therefore low weight, this would be the optimal solution not considering all the specific system requirements.

The system would be set up using a fixed ring gear configuration in order to achieve maximum transmission ratio per radial volume. As has been

described before, the ratio of such a system is calculated with the formula:

$$i = (Z_3/Z_1) + 1$$

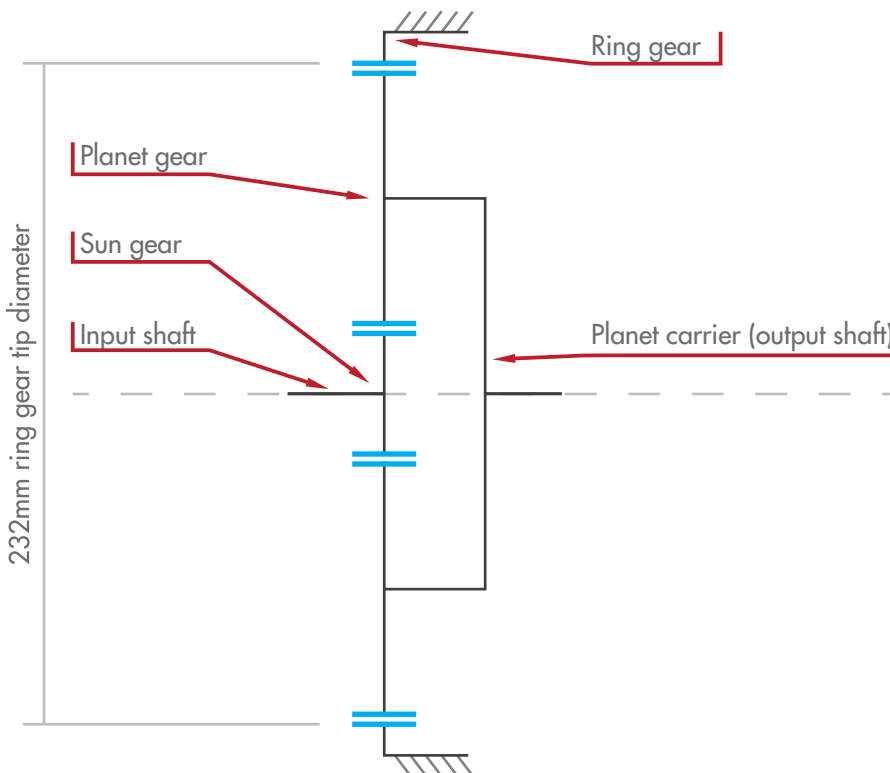
Where Z is either the number of teeth or the pitch circle diameter of the gears.

A quick calculation shows that in order to achieve a gear ratio of 15.5 with the minimum restriction on sun gear pitch circle diameter of 16mm, the ring gear pitch circle diameter needs to be 232mm or higher depending

on the tooth module of the gears.

$$15.5 = (Z_3/16) + 1$$

It will pose a significant challenge to create synergy between a gear system with that amount of radial volume and other sub systems. The design of the wheel hub, the rim and the breaking system will be severely restricted, and this is why one of the system requirements restricts radial size.



Schematic representation of a planetary system.



# Planetary systems

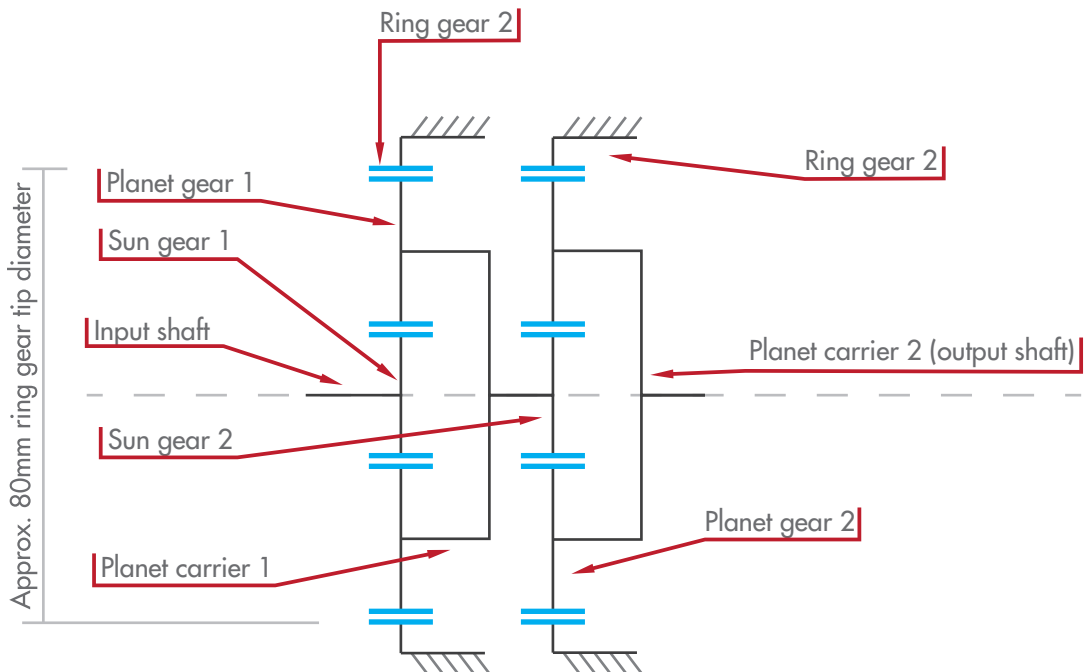
## Double planetary system

A double planetary system, consisting of two smaller standard planetary systems mounted in series, is able to achieve high ratios while still remaining radially compact. This high ratio comes at the cost of a significant increase in design and analysis complexity. The torque is increasing significantly from the input shaft to the second sun gear. The optimal system design will therefore consist of two unique planetary stages. This basically means that the total amount of design and analysis work

required is doubled from the standard planetary system. The total number of parts has also doubled, substantially increasing the cost of manufacture and weight of such a system.

The system as described in the graphics below has both ring gears fixed for maximum gearing ratio. One would most likely be able to reach the required ratio of 15.5 with one or both planet carriers fixed instead, still remaining inside the maximum radial limitation.

This freedom opens up to different solutions that can lead to smarter overall design integration with the wheel hub. The higher axial space requirements may surpass the design space limitation. This may then lead to interference with the suspension system, most likely resulting in a compromise in vehicle kinematic performance. The increased number of meshing gears will reduce the total efficiency of the system. One can expect double the amount of lost power compared to the standard planetary system.



*Schematic representation of a double planetary system.*

# Planetary systems

## Compound planetary system

This compound planetary system transfers force from the sun gear to the larger planet gear 1. This gear is connected to the smaller planet gear 2 on the same planet shaft. Planet gear 2 is meshing with the ring gear. Both planet gear 1 and planet gear 2 is connected to the planet carrier output. The total gear ratio of this system is calculated with the formula:

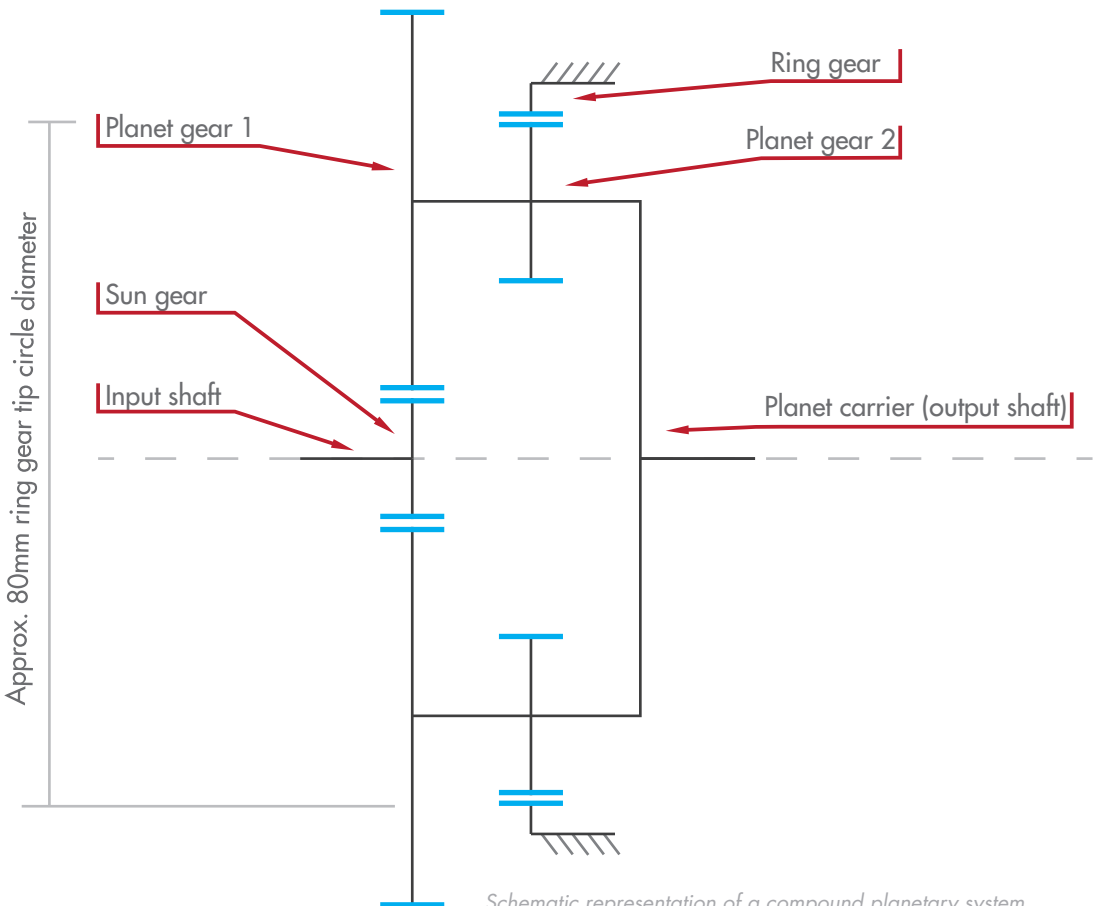
$$i = ((Z_2/Z_1) * (Z_4/Z_3)) + 1$$

Where  $Z_1$  is the sun gear,  $Z_2$  is planet gear 1,  $Z_3$  is planet gear 2 and  $Z_4$  is the ring gear.

This shows that this is a system capable of producing high gear ratios. It is able to do so while maintaining the ring gear tip diameter restriction. This is due to the fact that the larger planet gears can be larger than the upright hole diameter restriction. If a slot is designed in the upright bearing cylinder these gears can extend beyond the 100mm diameter of the upright hole. This will greatly help in achieving a 15.5 gear ratio.

planetary system, the compound system only has one planet carrier and one less sun and ring gear. Less gears means lighter weight, lower cost and better efficiency. The design and analysis complexity can be regarded the same as with a double planetary system. It is an unconventional system. This may mean that there will be harder to get input on design and calculation methods than with the other, more conventional systems.

Compared to the double



Schematic representation of a compound planetary system.

# Planetary systems

## Choice of solution

In order to properly evaluate and compare the strengths and weaknesses of each of the previously described planetary systems, a choice matrix has been implemented. Each of the systems has been evaluated based on how they are able to perform in relation to a series of different factors. These factors were chosen as they represent the most important system criteria in making a well informed concept choice going forward.

We see that the standard planetary system is going to struggle in achieving the required gear ratio. If able, it will take up too much radial space. Despite scoring highest

on efficiency, complexity, weight and cost, this system is unable to fulfill some of the absolute requirements. The system is therefore discarded.

The double planetary system, while able to operate within the system requirements, scores worst on efficiency, weight and cost. Despite being more commonly used, the double planetary systems non optimal performance leads to it being discarded.

This leaves the compound planetary system. This concept is able to fulfill the system requirements while it maintains a decent degree of performance. Only requiring one planet carrier simplifies

the integration with the wheel hub. The limited number of parts keeps both the system weight and manufacturing cost in line with overall design goals.

The choice of concept landed on the compound planetary system. None of the other two systems were able to fulfill all the physical requirements imposed by the design brief. This concept show tremendous potential in delivering the required performance parameters within the given design space restrictions.

Evaluation factors	Standard planetary system	Double planetary system	Compound planetary system
Able to achieve 15.5 ratio	Green	Green	Green
Axial space restrictions	Green	Blue	Blue
Radial space restrictions	Red	Green	Green
Efficiency	Green	Red	Blue
Design and analysis complexity	Green	Blue	Blue
Weight	Green	Red	Blue
Cost	Green	Red	Blue

# Planetary systems

## Load spectrum for gear simulation

Given that a motor and transmission system used for racing is never subjected to running at steady state force and speed, but rather subjected to a whole specter of variation in the combination of these two parameters, the dimensioning factors has to be a range of representative values within this specter. This is called a load spectrum and is a collection of power and speed data points that represents the predicted variation in forces working on the transmission system. We are then able to apply this set of data to computer aided simulations in order to find appropriate parameters for a design solution.

As the logged data from 2014 had low resolution and data point synchronization problems as stated earlier, manual editing of data was

needed. Logged data from the fastest competition lap driven in 2014 was reconciled with accurate, high resolution energy output data from the same lap.

This resulted in a 160 point load spectrum describing how the predicted car behavior during track racing is physically affecting the transmission. 160 points of data constitutes a very large load spectrum with many similar load points resulting in duplicate results during simulation. For this reason, a data point compression was deemed favorable in order to reduce simulation time down the line. The data set was then adjusted for the new final drive gear ratio and the following difference in power output. Specifically this meant that the data was adjusted from a 1:3.55 ratio

to a 1:15.5 ratio. The motor power was then split in four in order to get the load for each gearbox. No adjustment for efficiency was made. Instead the maximum mechanical output of each motor was set to 20 kW, taking into account uneven distribution of fore and aft torque as a function of vehicle weight transfer from squat and dive mechanics while driving. 20 kW of maximum mechanical output is set as a conservative estimate based on tire friction capacity.

A 7 point load spectrum was run in a comparative simulation, tweaking values until both datasets produced the same results. What started as hundreds of thousand data points has been reduced to 7 points describing the main dimensioning factors of the transmission system. Tire

<b>Torque (Nm)</b>	21
<b>Speed (RPM)</b>	9000

Load spectrum				
Frequency	Torque	Speed	Tire normal load (N)	Ym
0,4	0,35	1,32	1000	1
0,1	0,57	1,76	800	1
0,06	0,51	1,98	600	1
0,04	0,67	1,36	700	1
0,3	1	0,88	600	1
0,08	-0,34	1,76	800	0,7
0,02	-0,8	1	1000	0,7

normal loads for each load point were added. This is the force produced by the weight of the car. The variation in loads try to predict weight transfer and aerodynamic load based on the speed and torque for each bin.

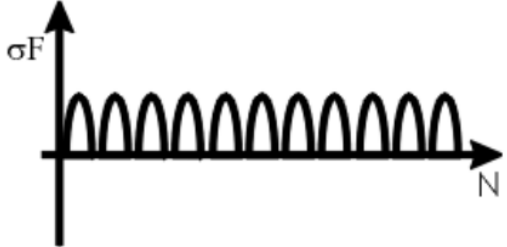
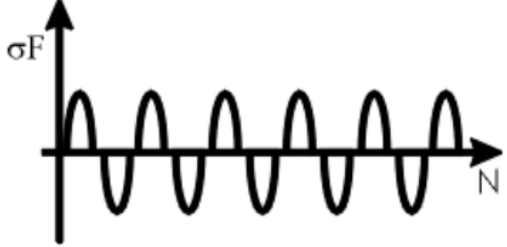
The operating mode for the mean stress influence factor was also added. This factor is describing how acceleration and motor breaking has a very different load application characteristic. While acceleration has a pulsating load application from 0 to

maximum torque, motor breaking happens when the system alternates between maximum acceleration and maximum breaking. Applying breaking force as a pulsating load would be an underestimation of the impact this force may have on the system.

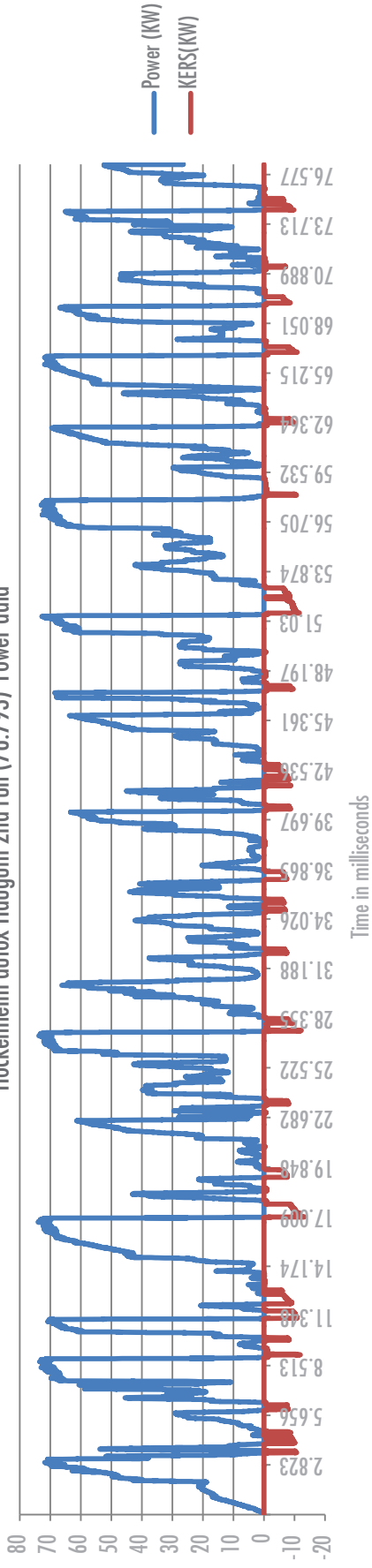
This is then the basis for the simulation and design of the gears. \*Note that the speed factor is calculated from a factor of 1 corresponding to the motor speed at which power output reaches the

peak value of 20kW @ 9000 RPM.

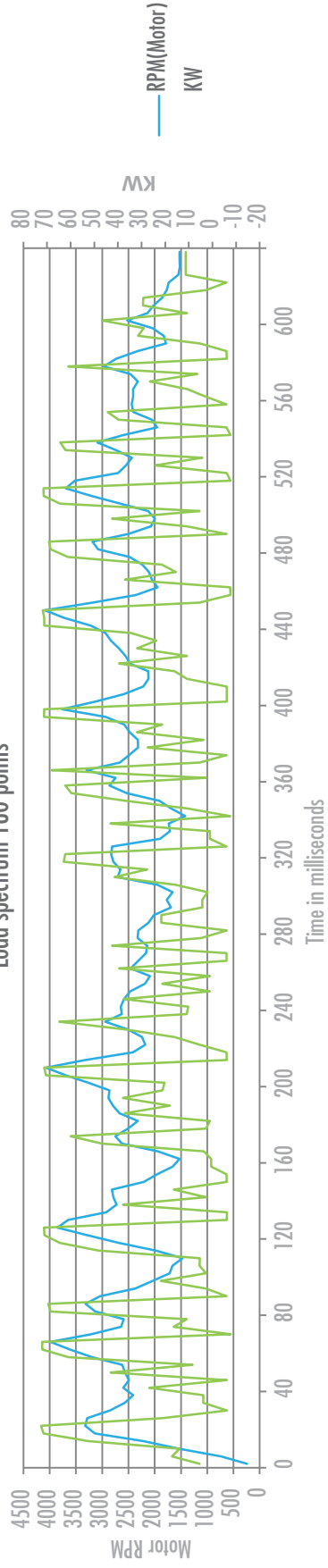
**Note:** Looking at the load spectrum, the highest speed logged during the lap is no more than 105 kph. This is somewhat lower than predicted by lap time simulations. It is however natural to assume that the increased torque performance and the extra control given by the 4WD system will bring the actual autocross top speed more in line with the lap time simulation results. (Graphs on next page)

Operating Mode	Mean Stress Influence Factor $Y_M$	Load Direction
Pulsating	1	
Alternating	0.7	

Hockenheim autotox Haugum 2nd run (76.793) Power data



Load spectrum 160 points



# Planetary systems

## Additional limitations in gear design

### Tooth geometry:

Involute tooth profiles originally designed by Leonhard Euler are the most commonly used tooth geometry for gearing. This type of tooth profile will be used in designing gears for the compound planetary system. More specifically, the ISO 53.2:1997 Profile A is the standardized tooth geometry that will be used. This is imposed by the manufacturer based on available manufacturing tools.

### Tooth module and gear rim thickness:

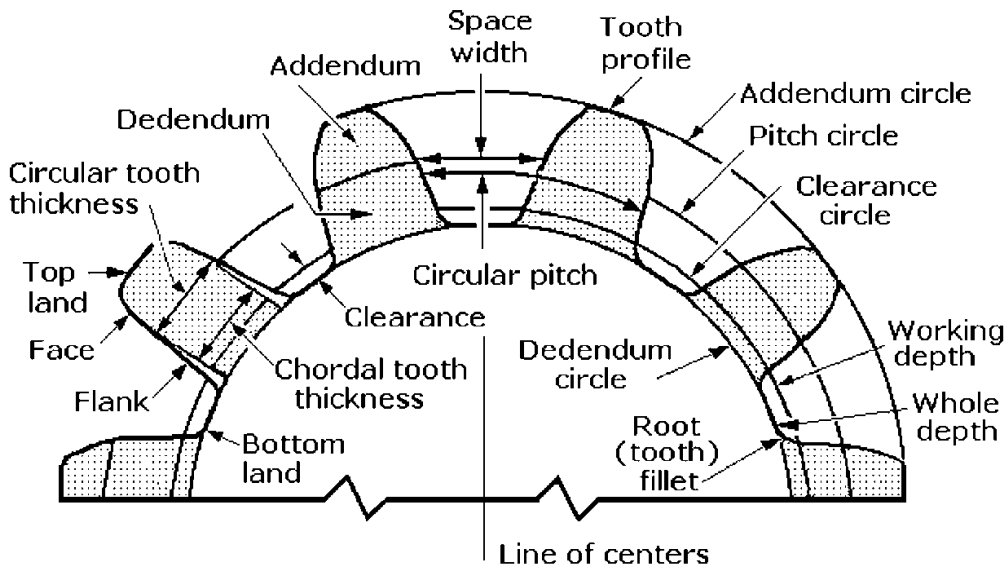
ISO has defined a gear rim thickness requirement needed to obtain sufficient tooth root stiffness based on the size of the tooth module. A gear needs to have a rim thickness of at least 2.5 times the tooth module from the root diameter to ensure sufficient stiffness of the teeth. This means two things. That smaller tooth modules means that the gear rim can be thinner, resulting in a gear that weighs less. And that gear sets with small gears mounted on shafts will be able to achieve a greater ratio with a smaller module (see sun gear mounted on splined motor shaft). The downside with smaller modules is that they are weaker than larger module gears. Small module gears will thus be used as much as possible, limited by mechanical capacity and manufacturer tool availability.

### Spur or helical gears:

Helical cut gears run smoother and with less noise compared to spur gears. Spur gears are less complex to design and only transfer radial loads to the rest of the transmission system. Only having to consider radial loads simplifies many aspects of the design. Smoothness and noise is not considered important factors in a race car transmission. The less complex and more effective solution is then to only use straight cut spur gears.

### Cooling and lubrication:

Gear systems need constant lubrication to function properly. This is to reduce contact friction and to transport heat away from the teeth. This system will use a passive oil bath to lubricate and cool the gears. This means that the gears will be partially submerged in non circulating oil. The oil that will be used is a low viscosity polyglycol oil called Klubersynth GH 6-22. Low viscosity oil is used to ensure minimum fluid drag in the rotating gears. This specific oil is also used as it has high scuffing resistance and is able to efficiently lubricate the gears up to an oil temperature of 160 degrees Celsius, far hotter than the operational temperature of the system.



# Planetary systems

## Choosing gear material

The material used in gears is of great importance, providing a foundation for their overall mechanical capacity. Gears are subjected to extreme loads, friction and impact stresses in high performance automotive transmission systems. As a result, steel is almost uniquely used for this type of application. Vanilla steel is however not able to withstand the immense stress working on the gears. To achieve the needed strength and friction resistance for this type of application, the steel needs to be hardened to 55 HRC or above. This can be done by several different methods like case hardening, nitriding and a wide variety of exotic coatings like titanium nitride, wolfram carbide and diamond like carbon.

In addition to the required hardness of the tooth surface, the rest of the gear structure has a demand for high material strength capacity. The reason for this being that it opens up for more light weight designs reducing the volume of the overall system. Heating, carburizing, quenching and tempering of steel through a case hardening process is both increasing the surface hardness and the overall strength of the material. By only hardening the outer surface of the gear, the core of the part is kept soft and flexible, preventing brittleness found in through hardened parts. Without going into

details regarding the process, the increased strength of the material is mainly due to a reduction in grain size that better prevents dislocations within the structure. In order to achieve the high hardness additional carbon is introduced to the gear surface during heating. The atoms precipitate into the molecule structure and fill interstitial voids in the surface boundary of the part. The result is a more densely packed structure and thus superior hardness.

As case hardening will yield the best overall mechanical characteristics bar very exotic coatings, types of steel with this treatment method has been evaluated. 4 different types of case hardening steels were considered, varying from medium cost, industrial grade to very high cost extreme performance grade. The table shows the 4 types of steel and their mechanical properties. 1.6587 is the baseline material. This material is considered a well performing industrial grade gear steel with good hardening performance. Hy-TUF is a steel with higher strength properties than the baseline. Unfortunately the hardening characteristics are lacking at 47 HRC maximum. 300M has the high mechanical characteristics that enable a better overall design. This material is extensively used in large airplane landing gears because of its high strength.

The availability can however be problematic.

NC3101YW was chosen as the best performing steel for this application. This is a super high performance alloy with extreme strength characteristics at a lower density than normal steel. Its hardening characteristic is optimal as this is an alloy designed for use in high performance gear solutions. These mechanical properties will give substantially more design freedom than a more normal steel as material strength becomes less of a limiting factor. The downside is a cost difference of 1000% compared to the baseline steel. Fortunately, Revolve NTNU was able to secure sponsorship for the material cost. This enables a substantial weight saving that will help in reducing weight, volume and rotational moment of inertia of the transmission system.

Looking at the table, we can see that NC3101YW has a yield strength at 1790MPa that is 228% higher than 1,6587. We see that the ultimate tensile strength of 2150MPa is also substantial higher at 195% of the high performance industrial steel 1,6587. These are extreme differences that in their own right describe the difference in potential performance of a part made from either of the two.



## Mechanical properties of 4 case hardened gear steels

Material	Density(g/ccm)		0.2% yield strength(Mpa)		Ultimate tensile strength(Mpa)		Elastic modulus(Gpa)		Elongation (%)		Post case hardening and carburizing hardness(HRC)	
	Absolute	Deviation in %	Absolute	Deviation in %	Absolute	Deviation in %	Absolute	Deviation in %	Absolute	Deviation in %	Absolute	Deviation in %
BS s155 (300M)	7,83	100	1550	197,45	2000	181,82	205	101,49	8	100	55	117,02
AMS-S-7108 (HY-TUF) 25NiSiMnMoCr7	7,78	99,36	1276	162,55	1520	138,18	202	100	10	125	47	100
1.6587 18CrNiMo7-6	7,77	99,23	785	100	1100	100	210	103,96	8	100	61	129,79
NC3101YW 40SiNiCrMoV10	7,66	97,83	1790	228,03	2150	195,45	202	100	9	112,5	59,3	126,17

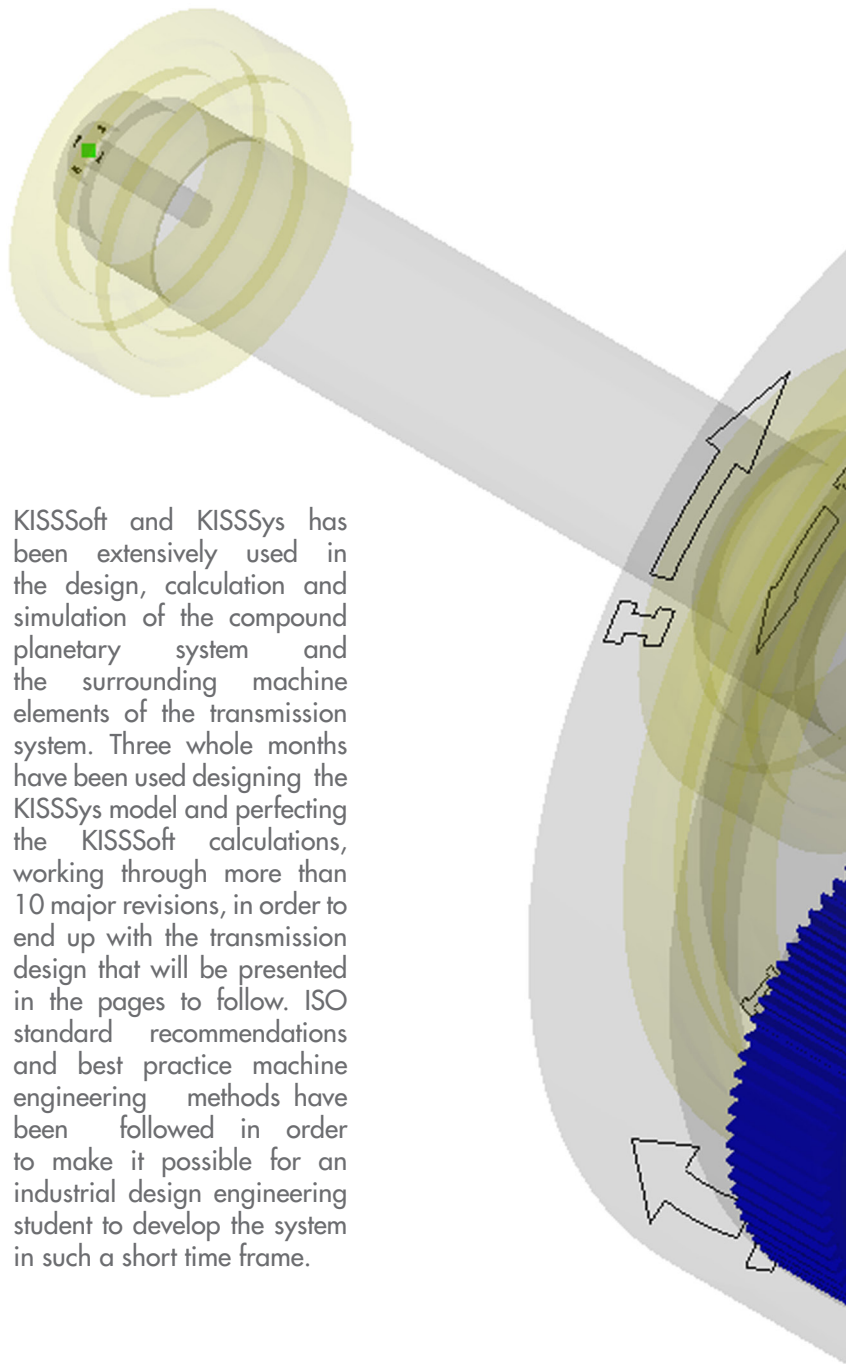


# KISSSoft

## Introduction

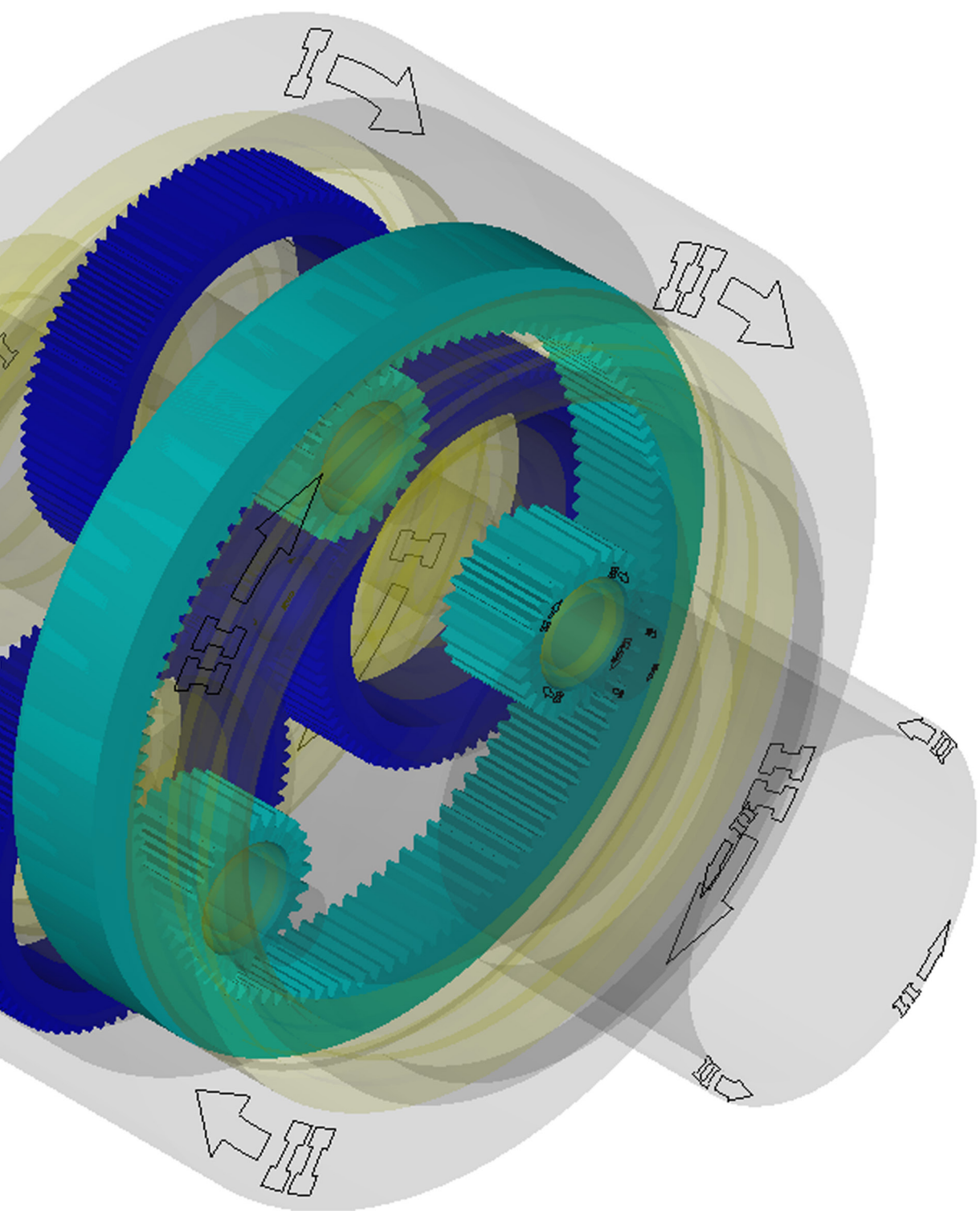
KISSSoft AG develops world leading design and analysis software for machine design application. The KISSSoft design software is used in a wide variety of fields, ranging from general industrial application, via offshore, sub sea, wind and water energy, to Formula 1 race car transmissions and aerospace solutions. The software conforms with the currently valid versions of DIN, ISO and AGMA standards and serves as a high quality tool when sizing and calculating machine elements. KISSSys is an add in provided with KISSSoft. This add in is used in design and calculation of whole drive trains where several machine elements are linked together.

KISSSoft and KISSSys has been extensively used in the design, calculation and simulation of the compound planetary system and the surrounding machine elements of the transmission system. Three whole months have been used designing the KISSSys model and perfecting the KISSSoft calculations, working through more than 10 major revisions, in order to end up with the transmission design that will be presented in the pages to follow. ISO standard recommendations and best practice machine engineering methods have been followed in order to make it possible for an industrial design engineering student to develop the system in such a short time frame.

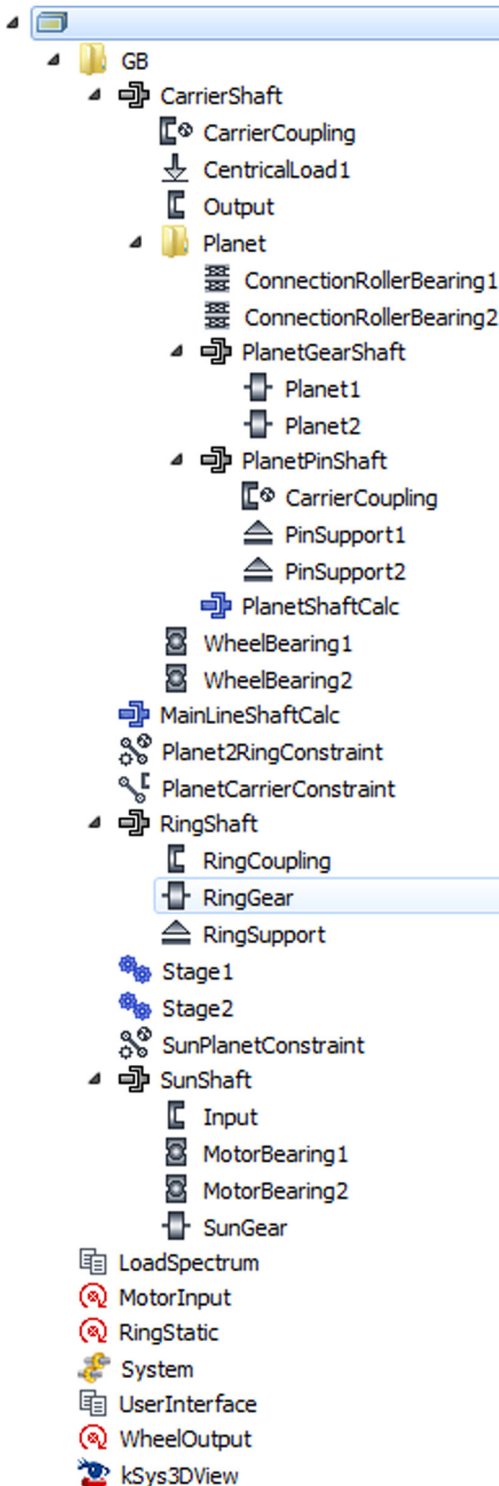


# KISSSOFT

Calculation programs for machine design



## Overview of system



The KISSSys model of the transmission system is shown in the picture on the left. The sun shaft is the rotating shaft of the motor where the sun gear is attached. It is defined as a coaxial shaft with an input coupling, two bearings and the sun gear.

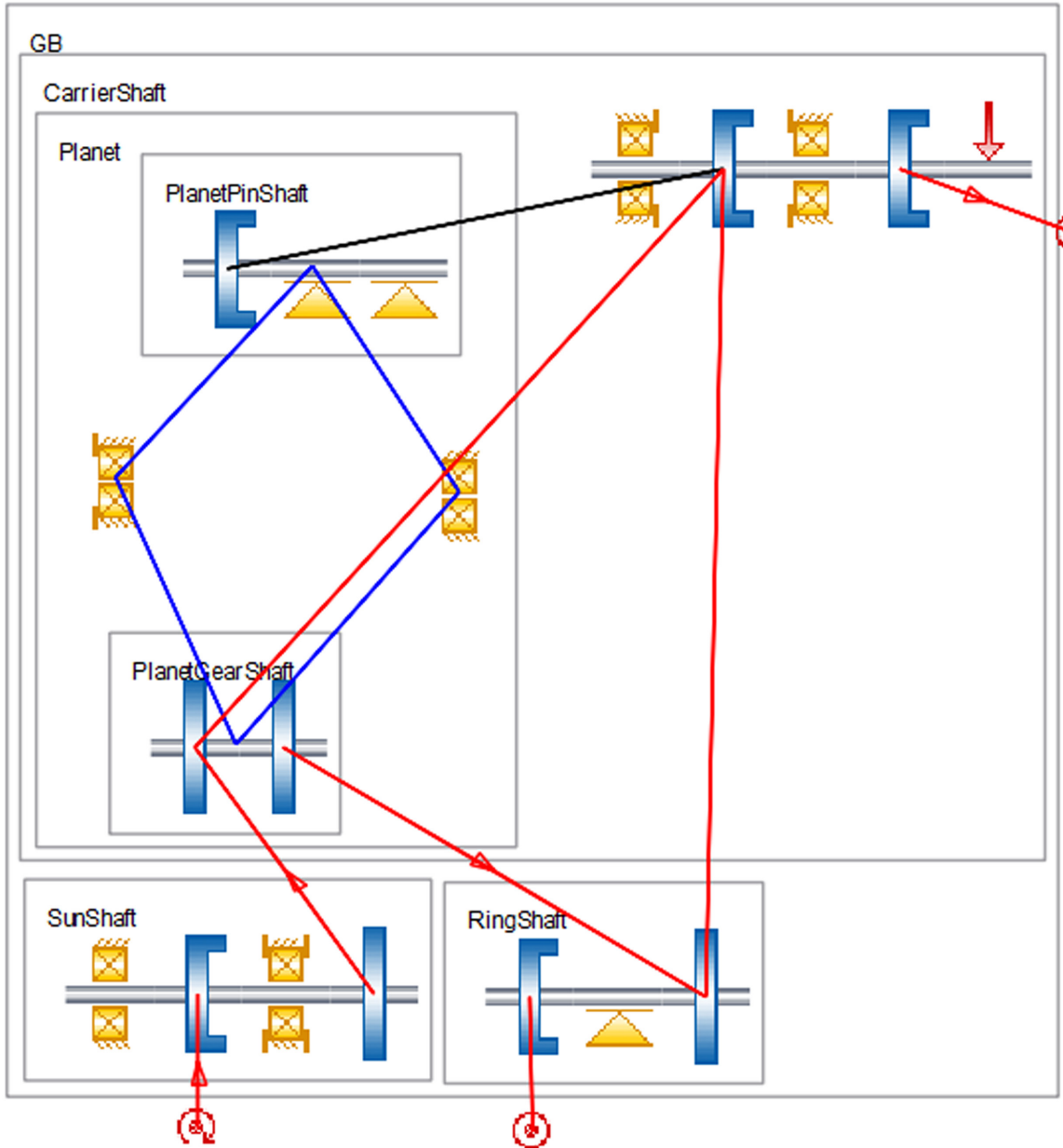
The carrier shaft is a coaxial shaft supported by two wheel bearings. It is coupled to the planet pin shaft with a planet carrier coupling. The output coupling denotes the output power to the wheel. The central load element describes the wheel normal load specified in the load spectrum.

The carrier shaft has a planet sub group containing the planet pin and planet gear shaft. These are coaxial shafts that are linked with two connecting roller bearings. The planet gear shaft holds both planet gears and rotates freely on the planet pin shaft via the connecting bearings. The planet pin shaft is rigidly connected to the carrier shaft with two standard supports. The carrier coupling denotes the interface between the carrier and the pin shaft as mentioned previously. Lastly, the subgroup contains the “PlanetShaftCalc” coaxial shaft KISSSoft calculation element.

The ring shaft is coaxially mounted with the carrier and sun shaft. It contains the ring gear element and the ring output coupling and is fixed by a general support.

The “Planet2RingConstraint” defining the connection between the second planet gear and the ring gear. The “PlanetCarrierConstraint” is defining the connection between the carrier shaft and the ring shaft. The “SunPlanetConstraint” is defining the connection between the sun gear and the first planet gear.

The “MainLineShaftCalc” element is the coaxial shaft calculation element for the sun shaft, carrier shaft and ring shaft coaxial system. The “Stage1” and “Stage2” elements are the KISSSoft calculation elements for the sun gear and the first planet gear and for the second planet gear and the ring gear respectively. Compound planetary system designs



*Kinematics diagram of KISSys model of compound planetary transmission system.*

are not supported by the planet gear calculation module in KISSSoft. Instead, the gear pair calculation module was used. Normally, this would produce a system with only one planet gear for each stage. To fix this, two additional virtual systems were created and torque was split between the three to achieve the equivalent of a planetary system.

Above is the kinematic diagram of the system. The red lines show how power flows through each element of the system. Power from the motor flows from the sun gear to the first planet gear. From there the power is split between the carrier and the second planet gear. From the second planet gear, the power flows to the fixed ring gear and into the carrier. The combined power is output from the carrier to the wheel.

## Main line shaft design and simulation

The main line shaft is defined in detail in the "MainLineShaftCalc" KISSSoft coaxial shaft calculation element.

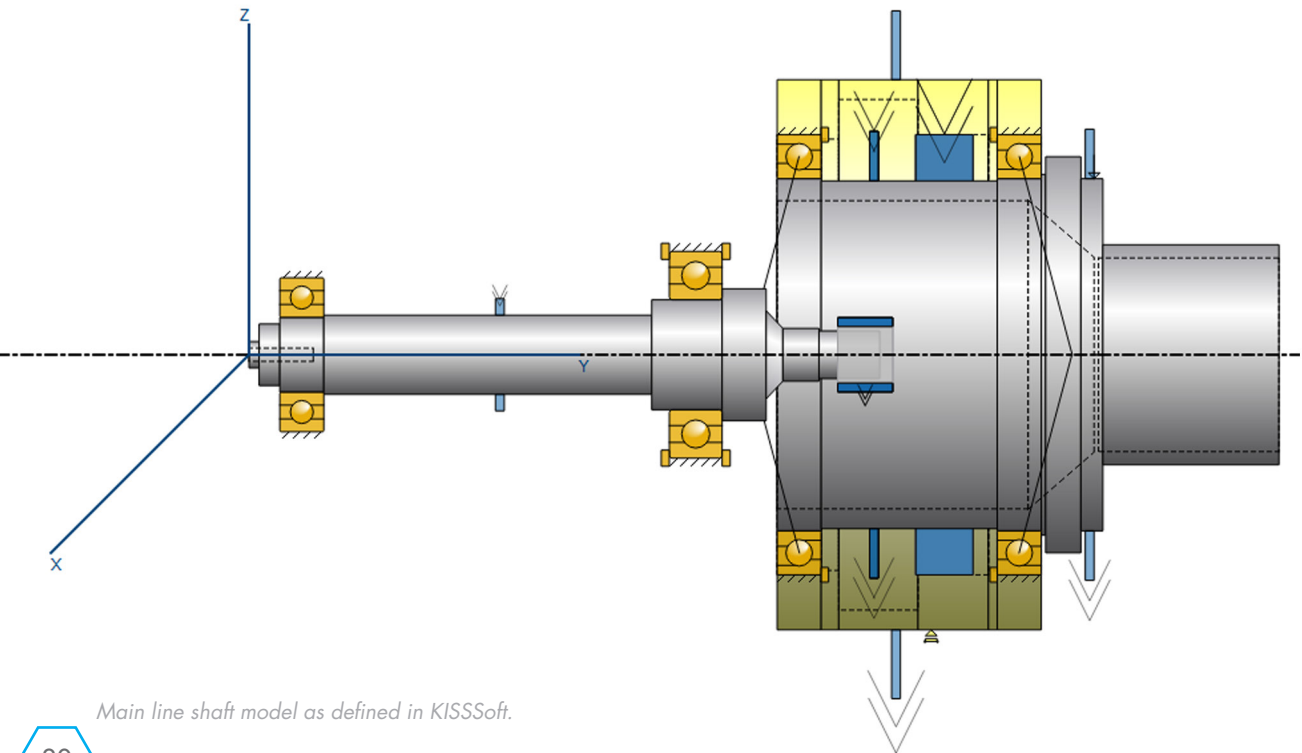
The sun shaft (motor shaft) is defined from a CAD model supplied by AMK. It is supported by two ball bearings where one is fixed in both axial directions, fixing the shaft in place. The sun gear is rigidly fixed at the end, disregarding the spline connection in order to simplify the model.

The carrier shaft and ring shaft is connected by two SKF 71816 CD/HCP4 15 degree angular contact ball bearings. These are preloaded in a <O> configuration. Were it not for the forces applied to the system by the wheel, these bearings would be redundant as the carrier would be supported solely by the balanced contact of the planet gears alone. As is shown, the <O> preloaded bearings are able to absorb and transfer both axial and radial wheel loads from the carrier shaft to the ring shaft (upright) while providing low friction system rotation.

Simulation results for the shaft elements show

very little stress at 21Nm input, as would be expected as the system is balanced with no significant bending forces applied. The central wheel normal load from the load spectrum is too low to have any significant impact. We do however lack cornering, bump, break and acceleration loads from the wheel in this analysis. The displacement results from this analysis will therefore be inconclusive. These forces will be applied in a FEM analysis of the planet carrier shaft later on.

Rotor dynamic simulations of the eigenfrequency of each shaft were done in order to evaluate if there was a risk for resonance in the system under normal operating conditions. All eigenfrequency cases with critical speeds under 20000 RPM is shown in the table. A Campbell diagram for both the sun and the carrier shaft shows the shaft frequency at the corresponding RPM value. The blue lines show the eigenfrequencies. The ring shaft is static and therefore does not have an eigenfrequency. Evaluating these results show that there is no risk of resonance occurring under normal

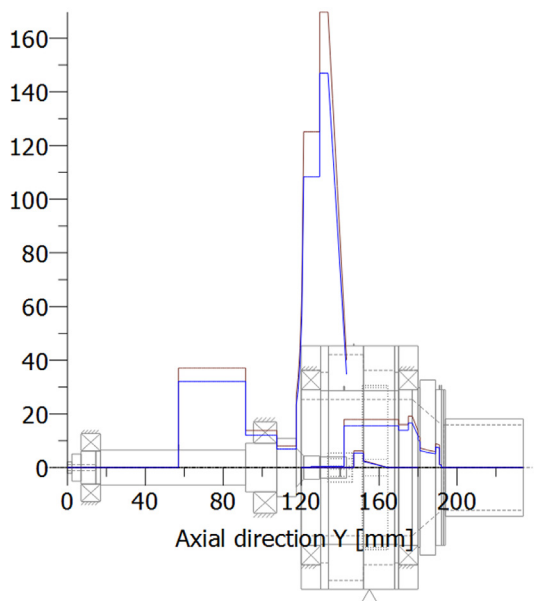


Main line shaft model as defined in KISSSoft.

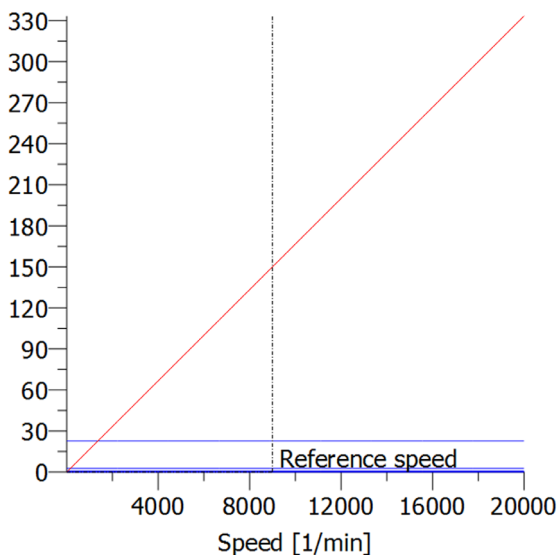
Stress [N/mm<sup>2</sup>]

operating conditions. The sun shaft YZ bending mode is the only result that is within what could be considered normal operating parameters. A critical speed of 1360 RPM does however only amount to 7.5 kph vehicle speed. The vehicle is never subjected to steady state operation at this speed. The meshing frequency of the gears will be evaluated later on in order to absolutely conclude regarding the risk of system resonance.

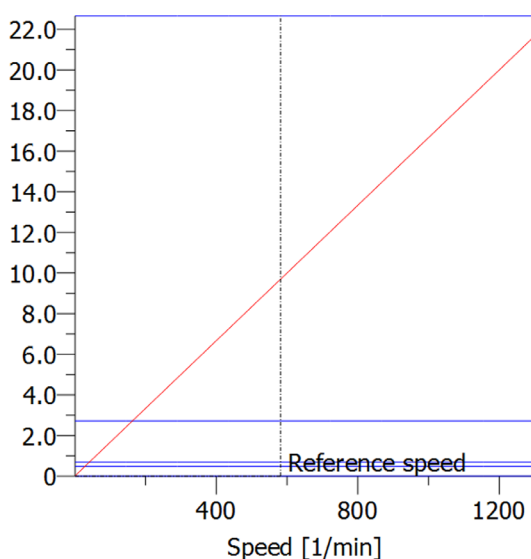
**Right:** Stress plot showing Von Mises in blue and Tresca in brown for the peak load of 21Nm. Peak stress is shown to happen as a result of torsion at the thin end of the sun shaft where the sun gear is located.



Eigenmode	Eigenfrequency	Critical speed	Mode
1	0.00 Hz	0.09 1/min	Rigid body rotation Y 'RingShaft'
2	0.48 Hz	28.69 1/min	Rigid body rotation Y 'SunShaft'
3	0.69 Hz	41.24 1/min	Rigid body rotation Y 'CarrierShaft'
4	2.71 Hz	162.87 1/min	Bending XY 'SunShaft'
5	22.66 Hz	1359.48 1/min	Bending YZ 'SunShaft'



Sun shaft Campbell diagram.



Carrier shaft Campbell diagram.

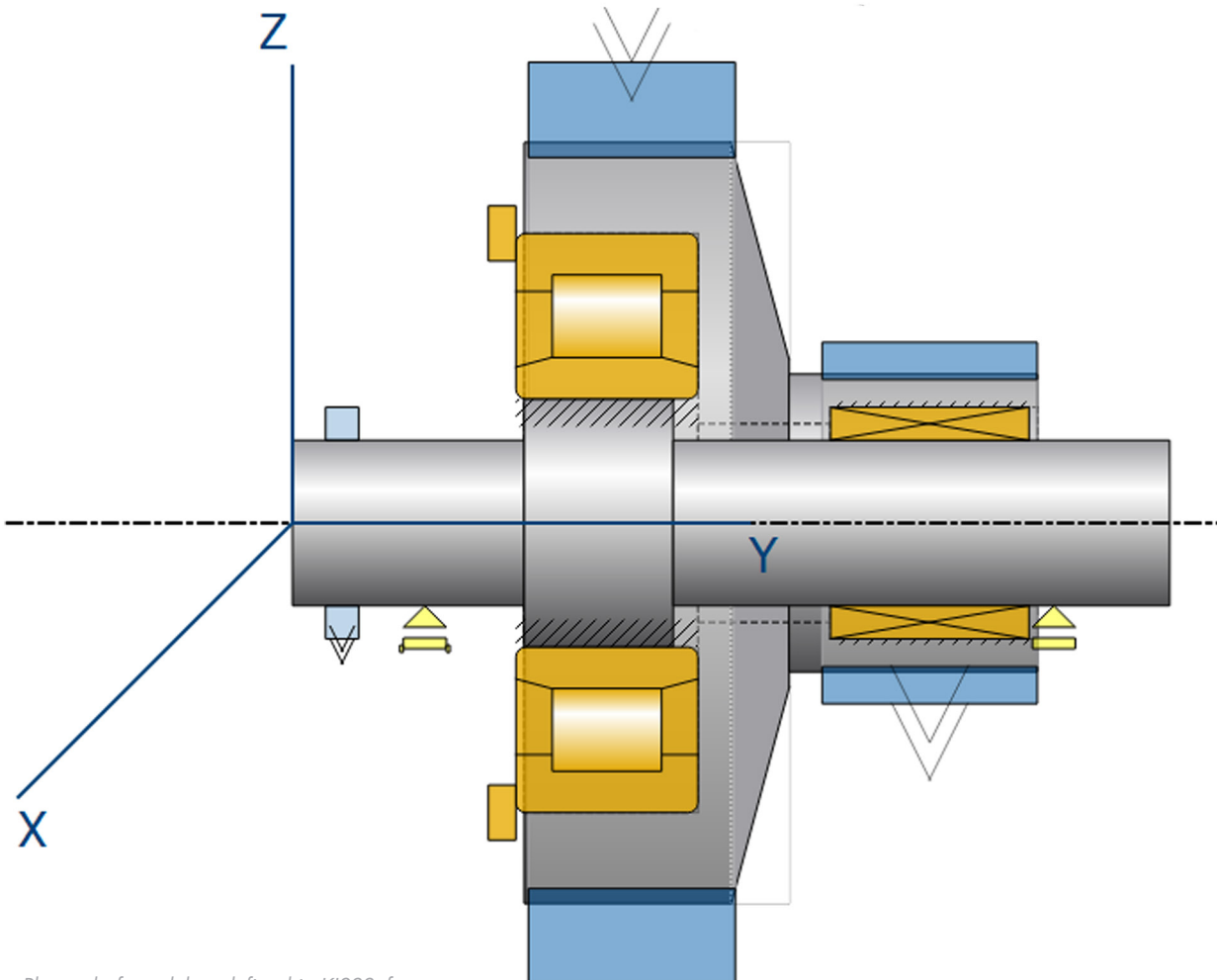
## Planet shaft design and simulation

The planet shaft group is consisting of a planet pin shaft and a coaxial mounted planet gear shaft connected by a roller bearing and a needle roller bearing. The planet pin shaft is fixed with a general support, restricting X, Y and Z translation on the left, and a general support restricting X and Z translation on the right.

The gear shaft will in reality be made up of two gears connected by a polygon connection. This connection was excluded from the KISSSoft model as it was concluded that it would not have a significant impact on the simulation results. Simplification of the model was then prioritized. Planet gear 1 is the larger planet on the left, and planet gear 2 is the smaller to the right.

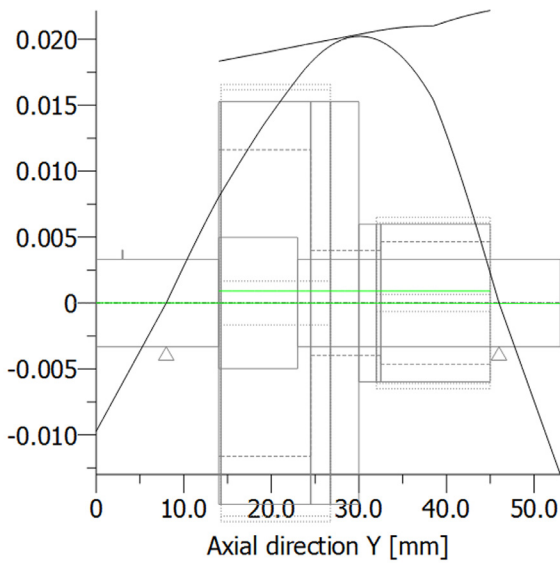
The roller bearing used is SKF RNU 202 ECP and the needle roller bearings are SKF HK 1012. These are bearings without an inner ring. Their narrow profile made it possible to design a system with a small diameter planet gear 2.

The displacement simulation shows a predictable bending displacement of the planet pin shaft, and a very small bending displacement between the two gears on the gear shaft. Torsional bending is marginal on the gear shaft. The stress plot shows peak stress from bending in the needle bearing contact area on the planet pin shaft. This was to be expected. The planet gear shaft is sustaining marginal stress, mostly from torsion between the two gears.

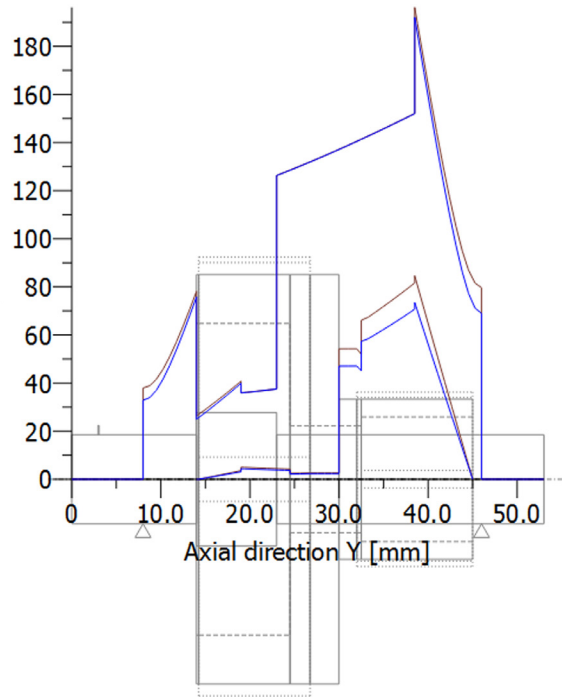


Planet shaft model as defined in KISSSoft.





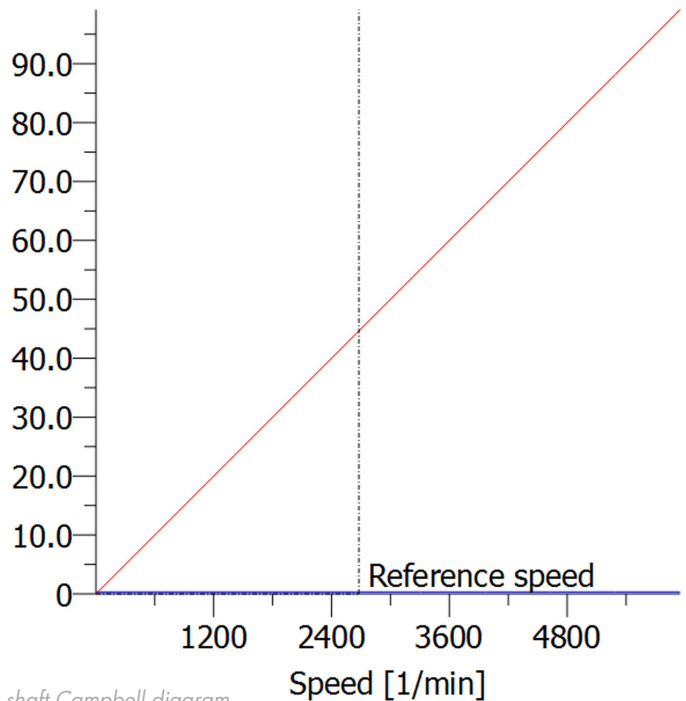
**Top:** Displacement plot of planet pin and gear shaft @ 21Nm motor torque.



**Right:** Stress plot of planet pin and gear shaft @ 21Nm motor torque. The blue graph shows Von Mises and the brown shows Tresca.

Eigenmode	Eigenfrequencies	Critical speeds	Mode
1	0.34 Hz	20.11 1/min	Rigid body rotation Y 'PlanetGearShaft'

In investigating the rotor dynamics of the planet shaft system, it was found that only one eigenmode existed that gave a critical speed under the maximum speed of 5950 RPM. Based on its critical speed value of 20 RPM, it was possible to conclude that there was no risk of resonance in the planet gear shaft. The pin shaft is static, but has high eigenfrequency in bending mode. These values were well above the maximum rotational speed of the system and were as such excluded from the evaluation.



Planet gear shaft Campbell diagram.

## Bearing calculations

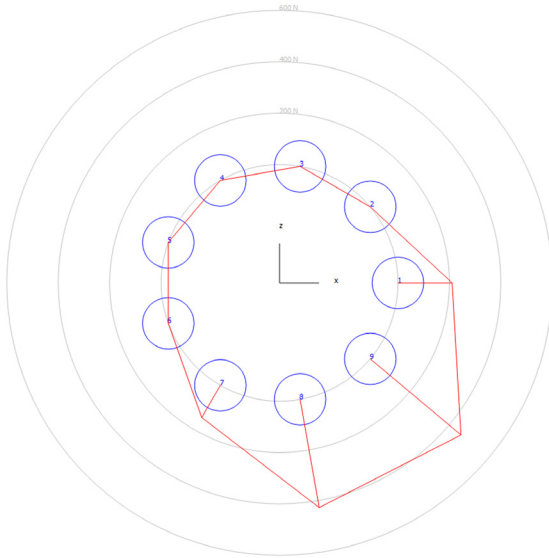
The capacity of the bearings were calculated in order to ensure smooth system operation with minimal maintenance throughout the systems 50 hour life time. Limitations in the KISSys model meant that it was not possible to do the bearing calculations based on the load spectrum. Instead, a simplified, very conservative calculation was made using a constant system input speed of 9000 RPM with 21Nm of torque and a 1000N central load from the weight of the car. The bearing life calculation algorithm is based on a 10% failure probability criterion that has a large standard deviation for results under 200 hours. Based on this, it was concluded that a conservative approach was the right choice in ensuring the performance of the system.

From the table we can confirm the previous statement that the transmission system in itself does not load the angular contact wheel bearings. The axial force ( $F_y$ ) that these bearings sustain is purely from the  $\langle O \rangle$  preload. The radial force ( $F_z$ ) on the bearings are exactly what one would expect based on the position of the central load close to the drive side

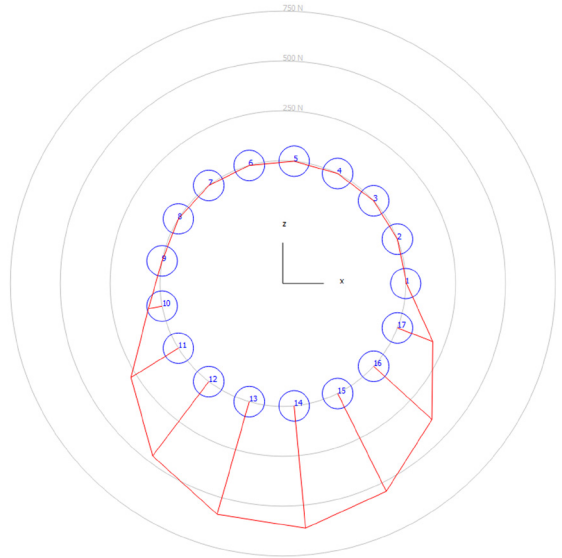
bearing and the stiffness of the carrier shaft. The low load results in very high life estimates and static safety factors. The main loads on these bearings, namely the dynamic wheel loads, will be considered in a separate calculation.

The calculation results for the roller and needle bearing on the planet shaft show a non optimal balance of loads between the two. This also results in significant misalignment of the needles. The reason for this uneven load distribution is the stringent space restriction imposed by the design space. It was then considered a reasonable trade off to load the needle bearing more than the roller bearing given that one was able to achieve sufficient calculation results. The results show significant contact pressure (3882 MPa) with a corresponding static safety factor (2.68) and bearing life estimate (54 h) for the needle bearing. Taking into account the conservative input values of the calculation, we are able to conclude, with a fair degree of confidence, that this bearing will be able to operate within system parameters for over 50 hours.

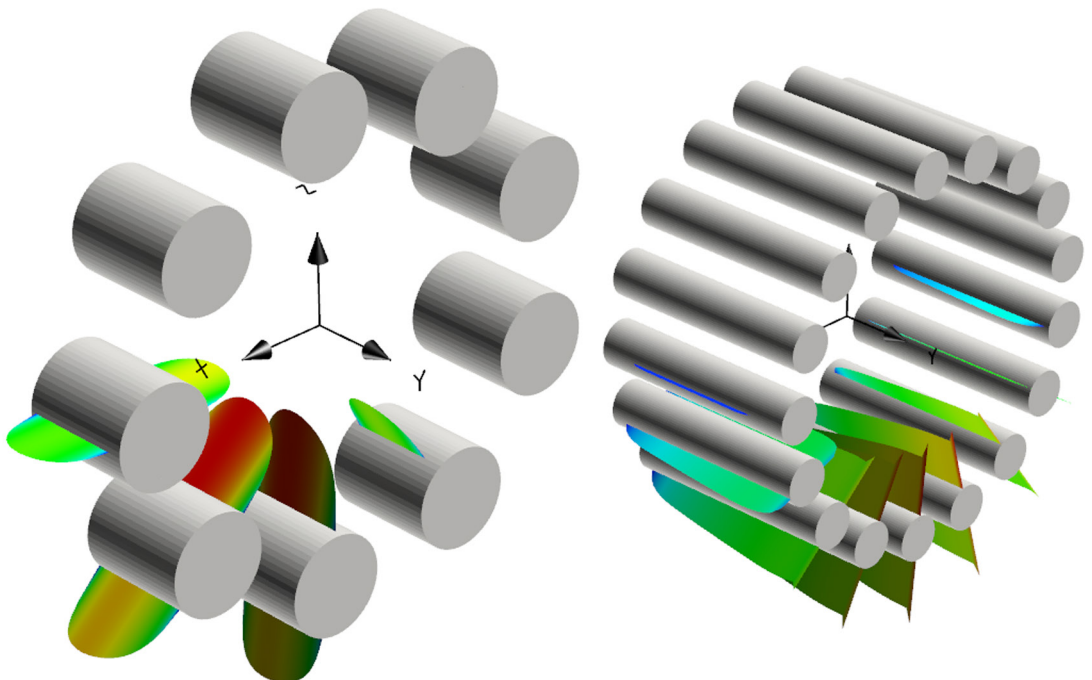
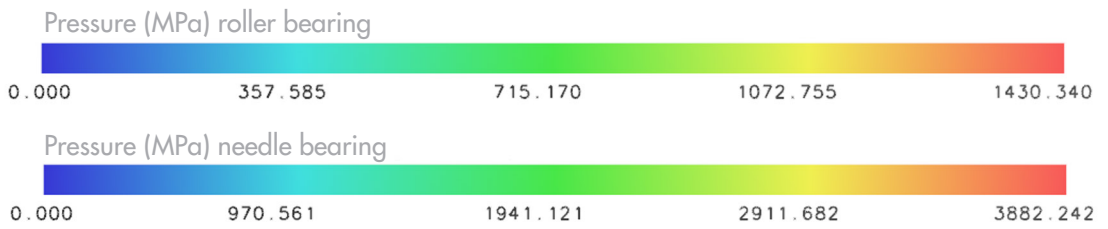
Shaft	Carrier shaft		Planet shaft	
<b>Bearing form</b>	Angular contact ball bearing		Cylindrical roller bearing	Needle roller bearing
<b>Bearing type</b>	SKF 71816 CD/HCP4		SKF RNU 202 ECP	SKF HK 1012
<b>Inner diameter (mm)</b>	80		15	10
<b>Outer diameter (mm)</b>	100		35	14
<b>Width (mm)</b>	10		11	12
	Non drive side	Drive side		
<b><math>F_x</math> (kN)</b>	0	0	-0,57	-0,03
<b><math>F_y</math> (kN)</b>	-0,31	0,31	0	0
<b><math>F_z</math> (kN)</b>	0,07	-1,07	0,84	2,54
<b><math>R_{xz}</math> (kN)</b>	0,07	1,07	1,01	2,54
<b>Bearing life <math>L_{nrh}</math>(h)</b>	>1000	>1000	>1000	54
<b>Static factor of safety</b>	134,32	22,48	10,06	2,68
<b>Contact pressure (Mpa)</b>	949	1519	1430	3882



Roller bearing force distribution



Needle bearing force distribution



Pressure distribution over rollers and needles. Notice significant edge contact in the needle bearing.

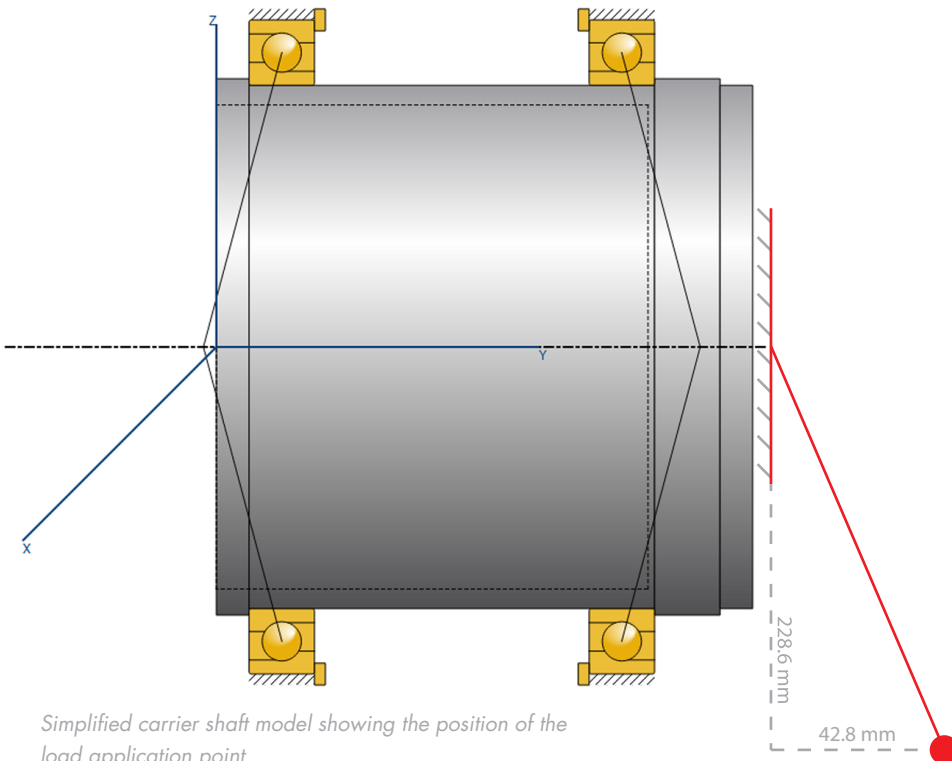
## Wheel bearing calculation

A separate calculation was done to investigate what impact the dynamic wheel loads while driving has on the angular contact wheel bearings. A simplified KISSSoft model was made of the carrier shaft and the bearings. The shaft speed was set to 700 RPM. This equals around 60 kph and is around the average speed seen in the autocross event. Additionally, an eccentric load was added with the load application point located in what would be the contact patch of the tire. From this point, the force is transferred to the center point of the face on the carrier shaft that will interface with the wheel rim. A load corresponding to the forces on the wheel in 2.3g turn (lateral) was applied to the load application point. 2.3g is the highest lateral force the vehicle is able to achieve based

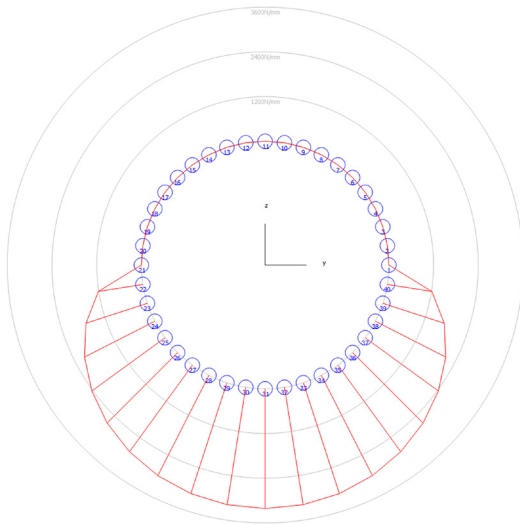
on the vehicle center of gravity, the kinematic design and the tire friction capacity. This case corresponds to peak tire loads and is the situation that would stress the wheel bearings the most.

The results show that both wheel bearings are able to sustain this load for an extended time period. The drive side bearing is, as expected, loaded considerably harder than the non-drive side bearing. This is a product of this type of application and is hard to avoid. The calculations show that both bearings perform within the system requirements and that force and pressure has a smooth distribution over the balls.

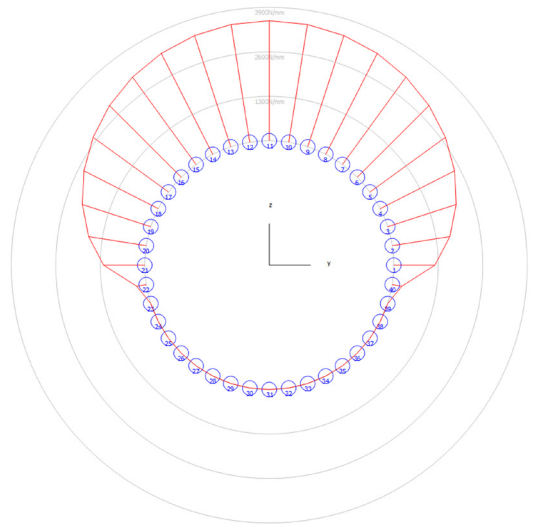
	F <sub>x</sub> (kN)	F <sub>y</sub> (kN)	F <sub>z</sub> (kN)	R <sub>xz</sub> (kN)	Static factor of safety	Bearing life L <sub>nr</sub> (h)	Contact pressure (Mpa)
Non drive side	0	-3,69	9,23	9,23	1,82	99	3212
Drive side	0	6,78	-11,79	11,79	1,43	43	3509



Simplified carrier shaft model showing the position of the load application point.



Non drive side pressure distribution

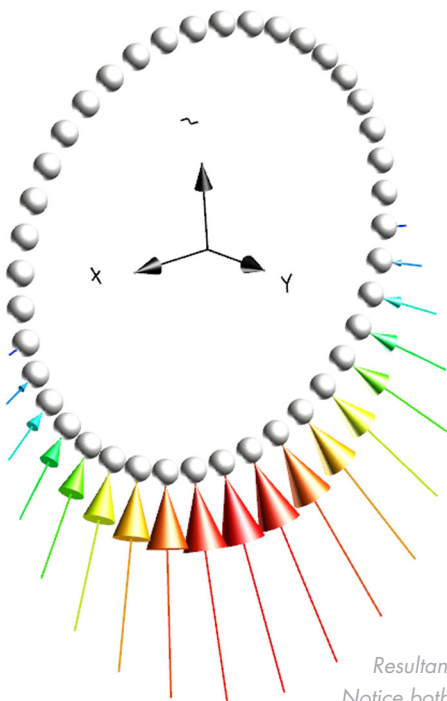


Drive side pressure distribution

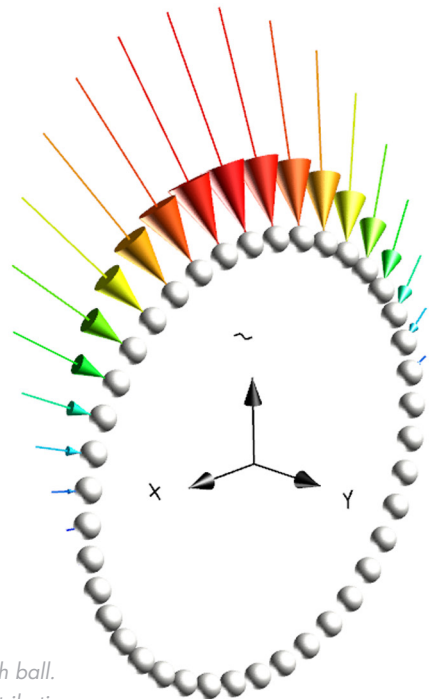
Force (N) non drive side bearing (left)



Force (N) drive side bearing (right)



Resultant force vectors on each ball.  
Notice both axial and radial contributions.



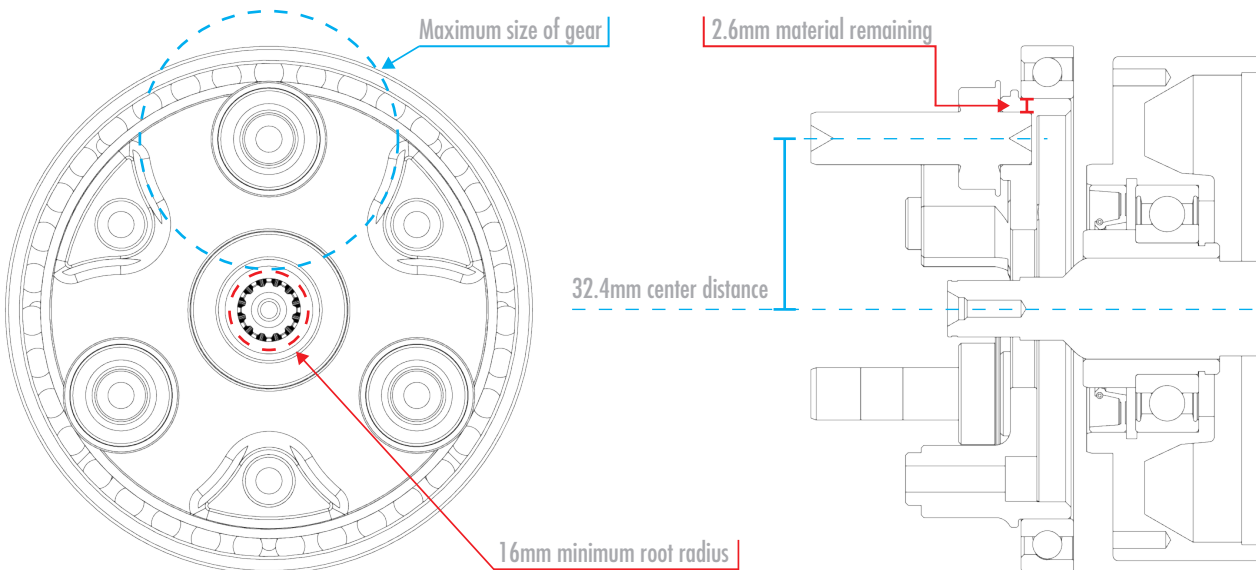
## Sizing of gear stage 1

Gear stage 1 was sized with as large a ratio as possible within the given constraints. The minimum size restriction on the root diameter of the sun gear and the minimum material thickness between the planet pin shaft and the inner wheel bearing seat on the planet carrier resulted in a maximum ratio limitation for this stage of 3.36:1. This was achieved using a normal module of 0.6 with a profile shift coefficient optimized both for strength and

extra ratio. The module was chosen based on a selection of available gear cutting tools that the manufacturer had in stock.

The gear pair was calculated in order to establish a working baseline. Marginal safety factors for both root and flank was achieved with a gear facewidth of 12.5mm.

Gear stage 1		
	Sun gear	Planet gear 1
Normal module [mn]	0,6	
Pressure angle [ $\alpha_n$ ] (deg)	20	
Helix angle [ $\beta$ ] (deg)	0	
Number of teeth [z]	25	84
Tip circle diameter (mm)	16,309	50,868
Profile shift coefficient [ $x^*$ ]	0,1094	-0,5915
Facewidth [b] (mm)	12,5	
Center distance [a] (mm)	32,4	



Shown is the relationship between the minimum sun gear size, the maximum center distance between the motor and the planet pin shaft and the resulting maximum size of the planet gear.

## Sizing of gear stage 2

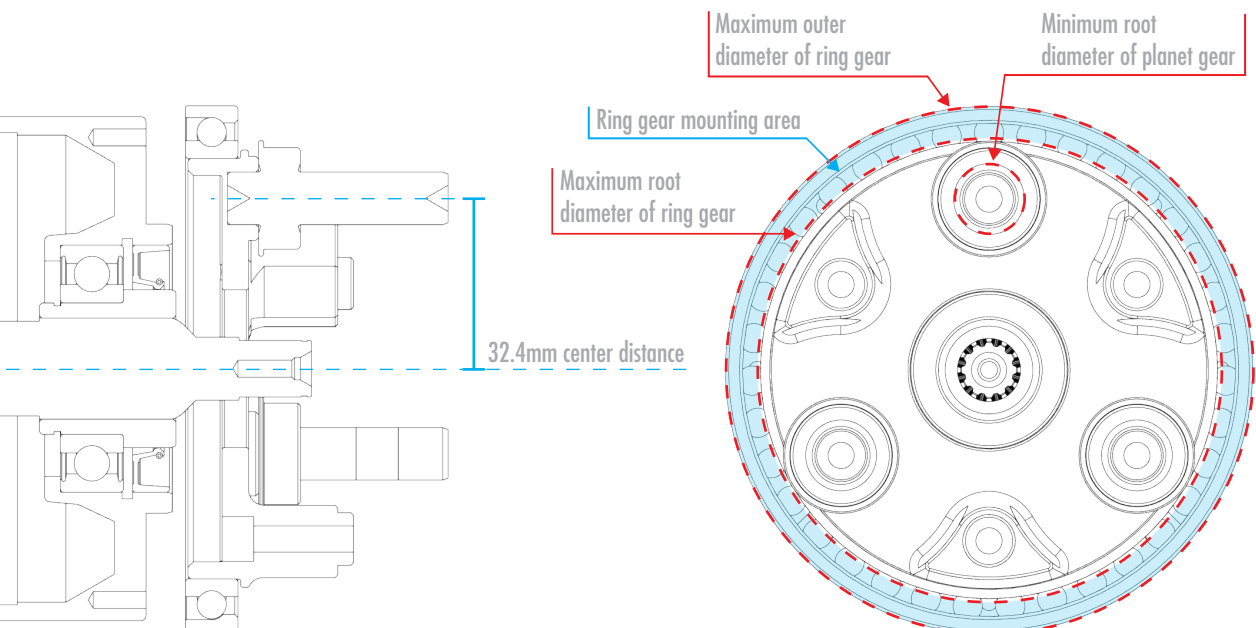
Sizing gear stage 2 proved much more choice restrictive. The center distance was already set from gear stage 1. A minimum root diameter restriction was set on the planet gear in order to ensure sufficient gear rim thickness between the outer diameter of the needle bearing and the tooth root. A maximum root diameter was set for the ring gear in order to ensure assembly.

Sizing for maximum gear ratio within these restrictions gave few viable results. A baseline

calculation of these results yielded a gear pair with a gear ratio of 4.31:1 and a facewidth of 13mm. The module was increased to 0.75 in response to the increased torque in this gear stage. This gave a total gear ratio of 15.47:1, just 0.03 shy of the 15.5 design target.

An in detail view of the initial gear calculation for gear stage 1 and 2 can be found in the appendix.

Gear stage 2		
	Sun gear	Planet gear 1
Normal module [mn]	0,75	
Pressure angle [an] (deg)	20	
Helix angle [β] (deg)	0	
Number of teeth [z]	26	-112
Tip circle diameter (mm)	21,418	-83,218
Profile shift coefficient [x*]	0,2749	-0,4784
Facewidth [b] (mm)	13	
Center distance [a] (mm)	-32,4	



*Shown is the maximum root diameter for the ring, the ring mounting area used to attach the ring gear to the ring shaft, the ring gear outer diameter and the minimum planet root radius.*

# KISSSoft

## Gear misalignment

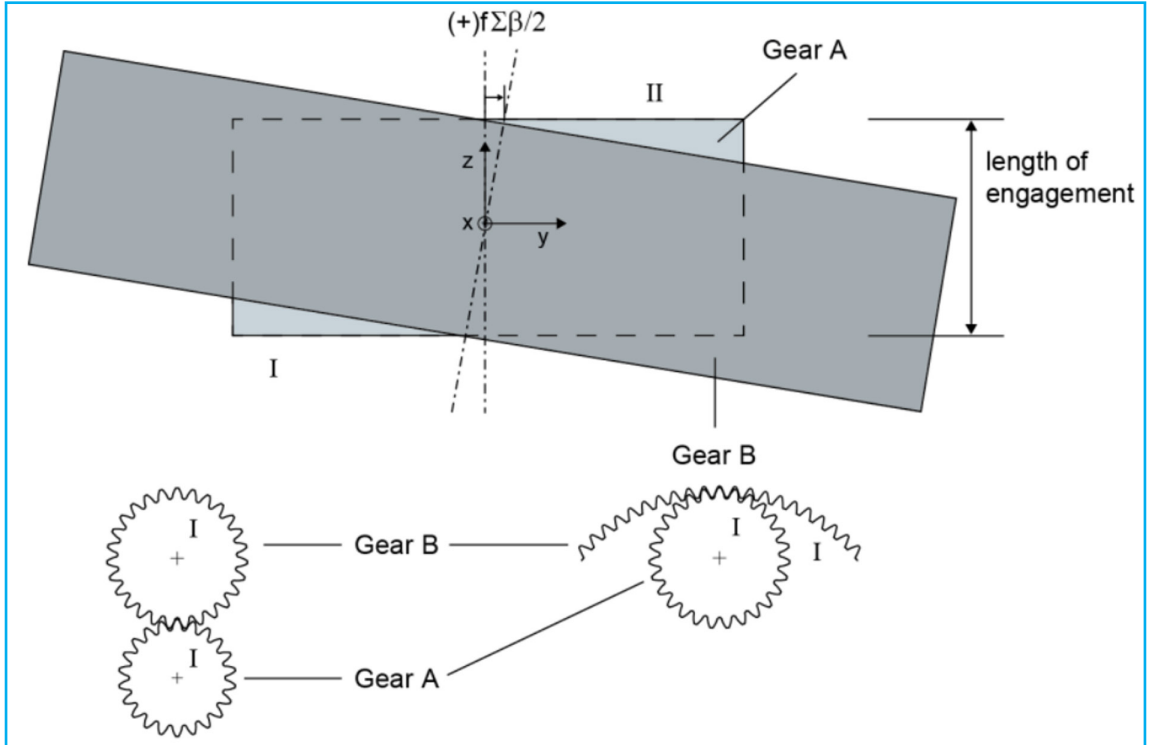
In order to perform an in depth calculation of the contact characteristics of the meshing gears in KISSSoft, the axis misalignment has to be known. This misalignment is a product of elastic deformation of parts in the transmission system. When the system is under load, the gear axes are no longer aligned, resulting in non-optimal tooth contact. This non-optimal contact will over stress the edge of the tooth and can have a wide variety of negative consequences, from reduced mechanical efficiency to gear jamming and significant gear damage. If discovered during the design phase, tooth modifications can be implemented to circumvent these negative

effects, and in some cases further improve the design.

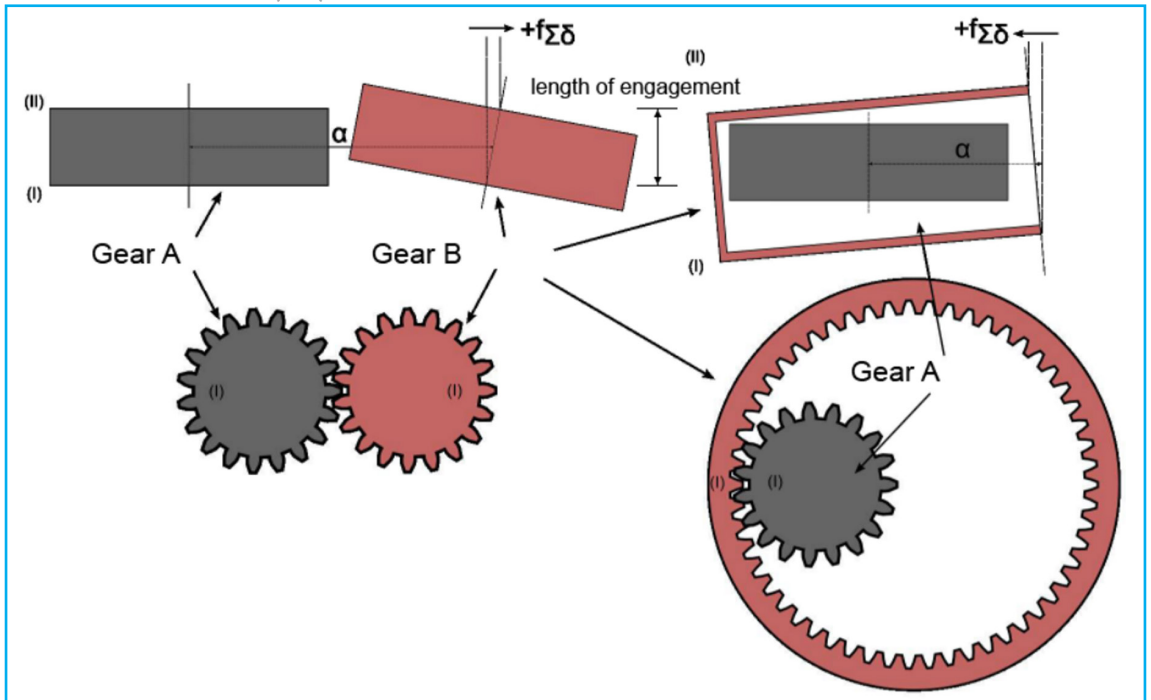
Axis misalignment is defined as deviation ( $f_{\Sigma\beta}$ ) and inclination ( $f_{\Sigma\delta}$ ) error of one axis in relation to the other. Calculating this error for a non-complex transmission system is done directly in KISSSoft. A compound planetary system is too complex, without standardized geometry for the planet carrier and other surrounding parts. An external, in detail FEM simulation is needed to establish precise values for the axis misalignment in this system.



Deviation error of axis ( $f_{\Sigma\beta}$ )



Inclination error of axis ( $f_{\Sigma\delta}$ )



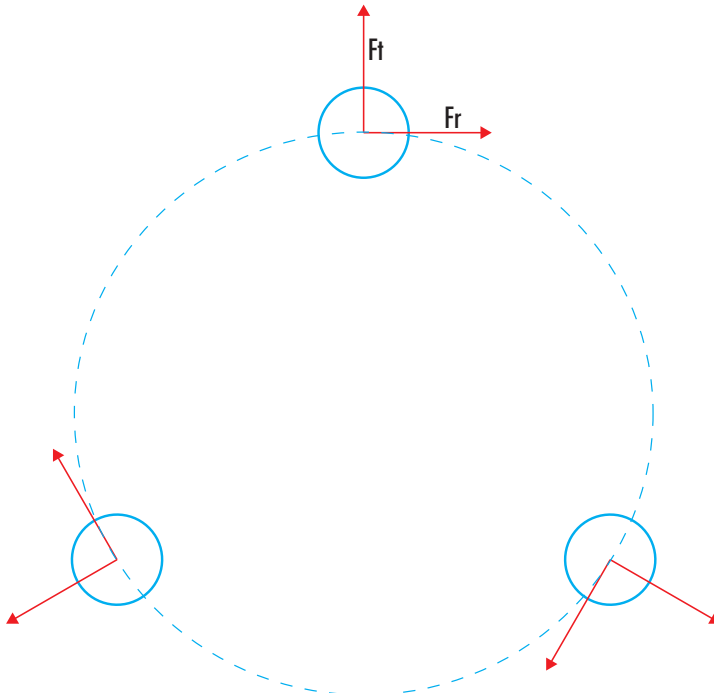
## FEM simulation of planet carrier assembly

The planet carrier assembly was simulated in Hyperworks from Altair. The simulation was run using non-linear contact sets between all interfacing parts. Contact sets were defined with bolt preloads, contact friction and part interference in order to precisely emulate the real world. Quad mesh was used on all the critical areas of the model in order to improve results and reduce simulation time.

The load case was limited to only look at the forces produced by the gears at peak torque. The force from the weight of the car was added,

but additional forces from the tire under turning, accelerating or breaking was neglected. This was done as it was concluded that only torsion would have a significant impact on the axis misalignment. Time constraints and simulation complexity also made it difficult to include these loads.

The results show axis misalignment for both gear stage 1 and gear stage 2. The low misalignment values imply a very stiff planet carrier design with close to no torsional flex.



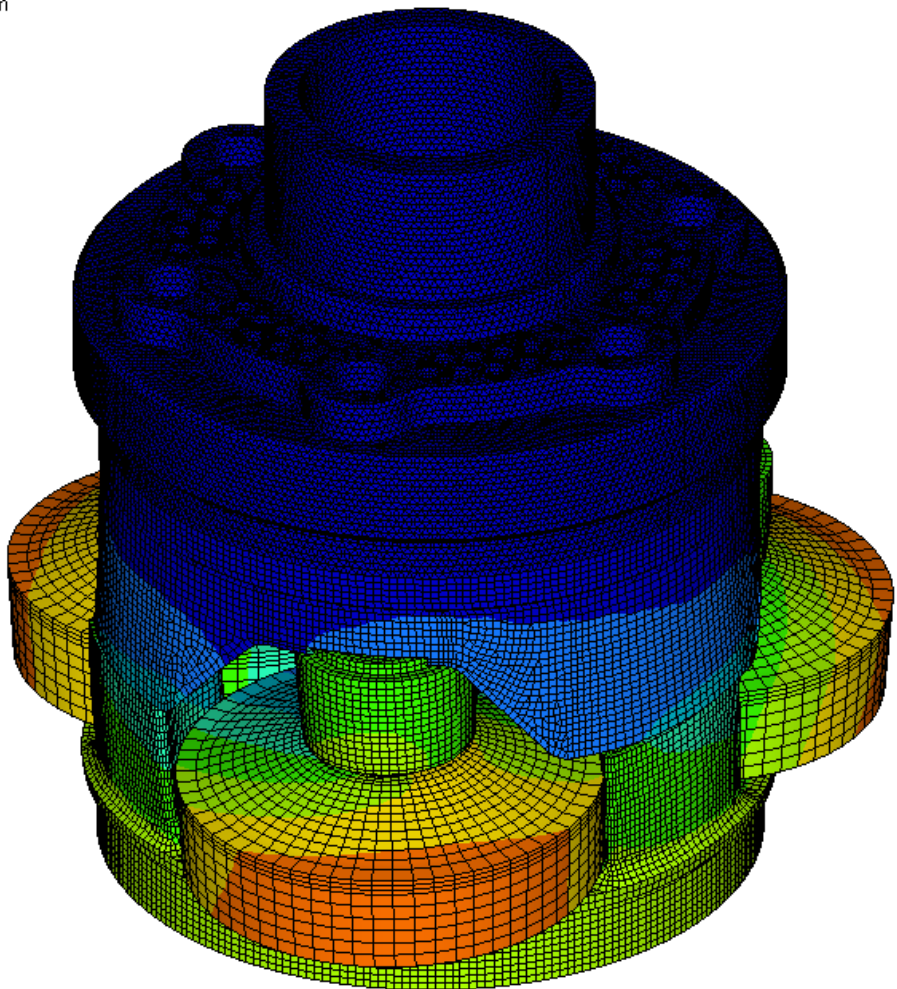
*Load application in tangential and radial direction for each planet set*

Bearing reaction force (N) from planet gears on planet pin shaft		
	Ft:Tangential(positive out of center)	Fr:Radial (positive clockwise)
Roller bearing	-231	942
Needle bearing	830	2433

Contour Plot  
Displacement(Mag)  
Analysis system

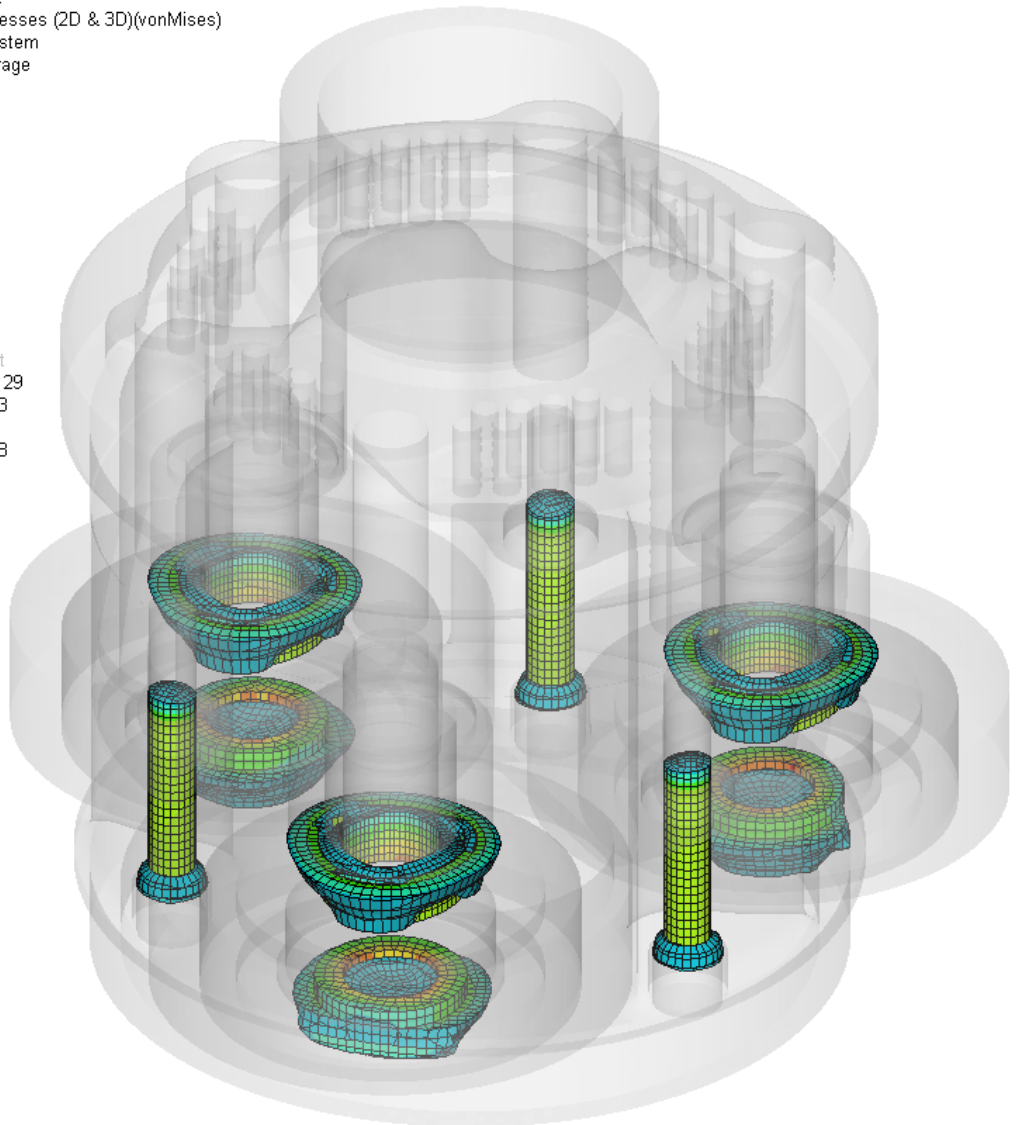


■ No result  
Max = 0.056  
Node 11875  
Min = 0.000  
Node 319276



*Planet carrier assembly displacement plot with visible mesh.*

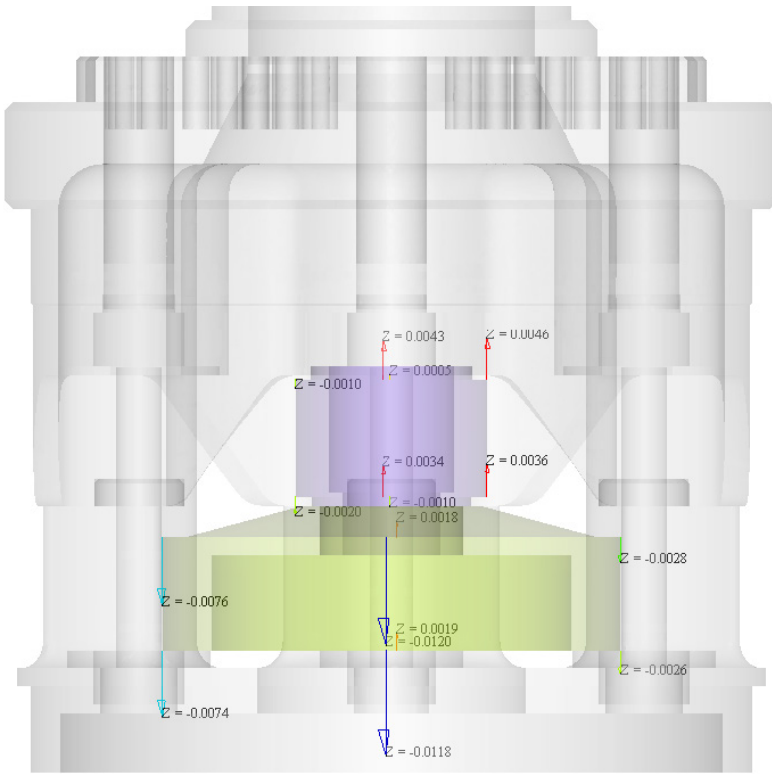
Contour Plot  
 Element Stresses (2D & 3D)(vonMises)  
 Analysis system  
 Simple Average  
 649.129  
 400.000  
 350.003  
 300.006  
 250.008  
 200.011  
 150.014  
 100.017  
 50.019  
 0.022  
 No result  
 Max = 649.129  
 Node 358783  
 Min = 0.022  
 Node 286298



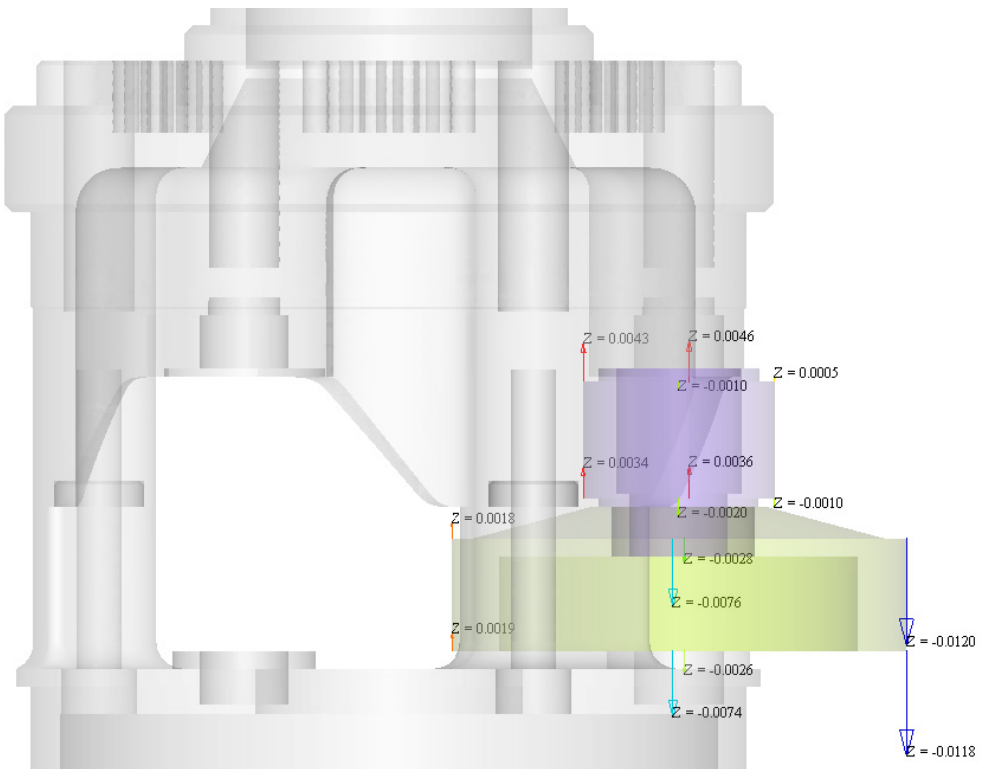
*Stress plot for pretention forces for the non linear contact constraints*

Axis misalignment data from planet carrier FEM analysis (mm)				
	Planet gear 1 radial (delta)	Planet gear 2 radial (delta)	Planet gear 1 tangential (beta)	Planet gear 2 tangential (beta)
Top relative displ.	-1,37E-02	-3,78E-03	5,56E-03	4,81E-03
Bottom relative displ.	-1,37E-02	-4,44E-03	5,67E-03	4,82E-03
theta top (rad)	-0,00027	-0,00018	0,00011	0,00022
theta bottom (rad)	-0,00027	-0,00021	0,00011	0,00023
$f_{\Sigma\delta}/\beta$ (top)	-0,00337	-0,00230	0,00137	0,00292
$f_{\Sigma\delta}/\beta$ (bottom)	-0,00338	-0,00270	0,00139	0,00293

*Table showing relative displacement, theta and the resulting  $f_{\Sigma\delta}$  and  $f_{\Sigma\beta}$  for both top and bottom nodes on each gear, also taking into account the deformation in the gear itself. The worst result for all cases was used for further analysis, taking the conservative approach.*



*Nodal displacement of gears in axis deviation view*



*Nodal displacement of gears in axis inclination view*

## Gear calculation

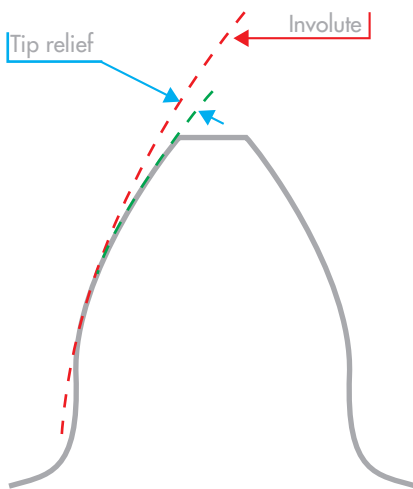
With axis misalignment values established, it was possible to perform an in detail calculation of the gear tooth contact. The KISSys strength calculations for both gear stage 1 and gear stage 2 were done using the load spectrum (previously defined). The contact analysis was performed with peak torque at 9000 RPM for both cases.

Tip relief, tip rounding, helix angle and crowning modifications were then added to improve contact characteristics, reduce tooth on tooth sliding, improve contact load distribution

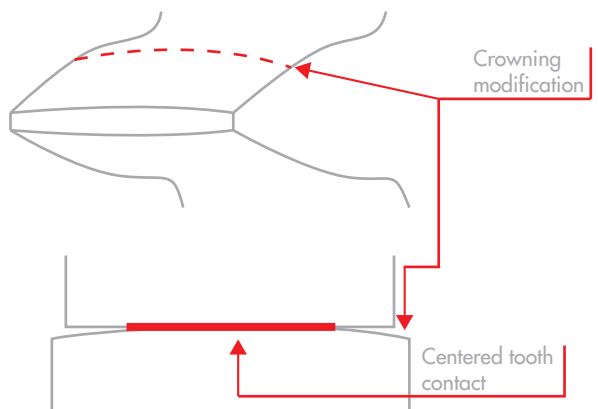
and increase mechanical efficiency. More specifically, tip relief and tip rounding was added to reduce unwanted tooth contact at contact engagement and disengagement between the teeth of two gears. Helix modification and crowning was added to center the tooth contact load on the tooth flank.

The following data shows change in results between non-modified and modified tooth geometry of both gear stage 1 and gear stage 2.

Tooth modifications for gear stage 1 and gear stage 2				
	Gear stage 1		Gear stage 2	
	Sun gear	Planet gear 1	Planet gear 2	Ring gear
Tip relief ( $\mu\text{m}$ )	8 (lin.)	8 (lin.)	16 (arc)	NA
Tip rounding (mm)	NA	NA	0,3	0,3
Helix modification ( $\mu\text{m}$ )	-10.9101 (conical)	NA	4.4873 (conical)	NA
Crowning ( $\mu\text{m}$ )	10	NA	10	NA

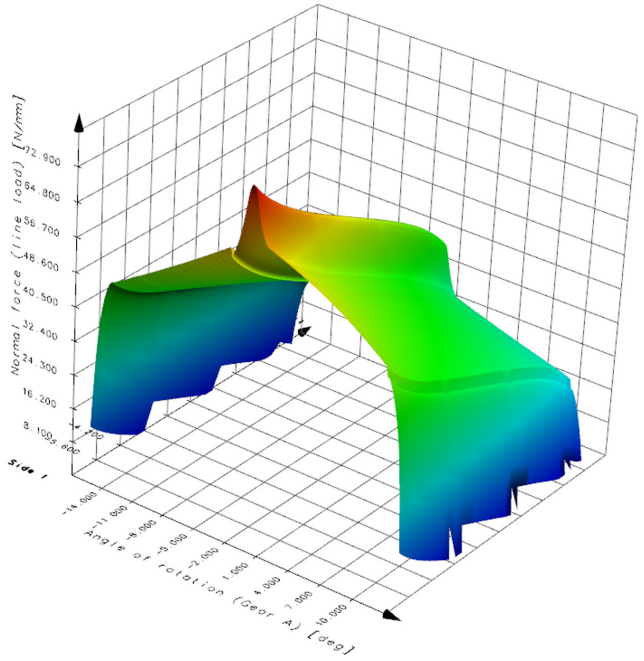
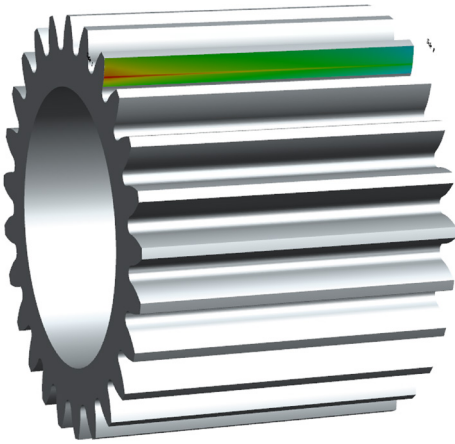


Tip relief modification

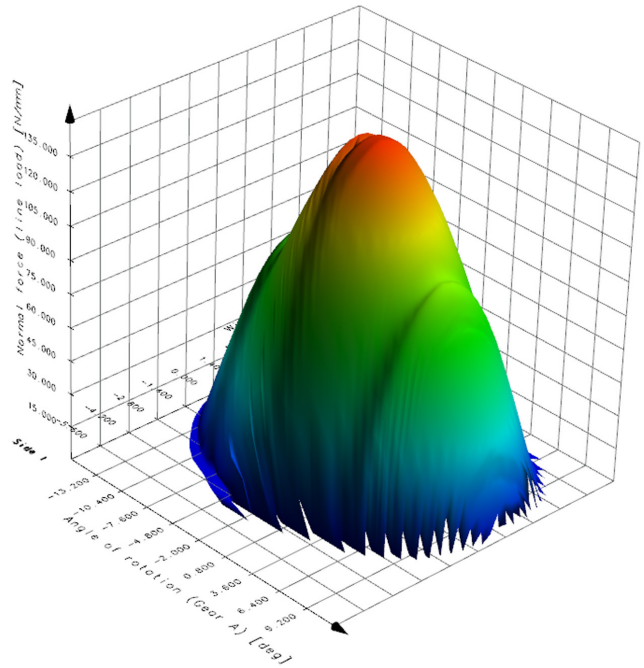
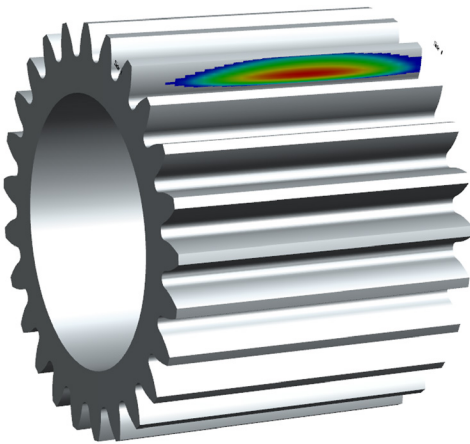


Crowning modification

Normal force (line load) [N/mm]

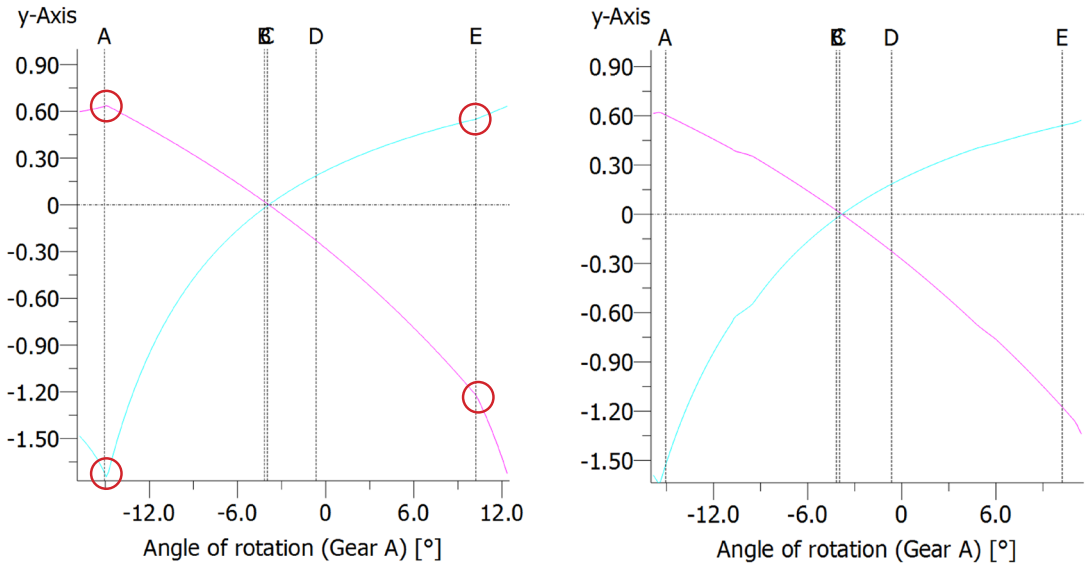


Normal force (line load) [N/mm]



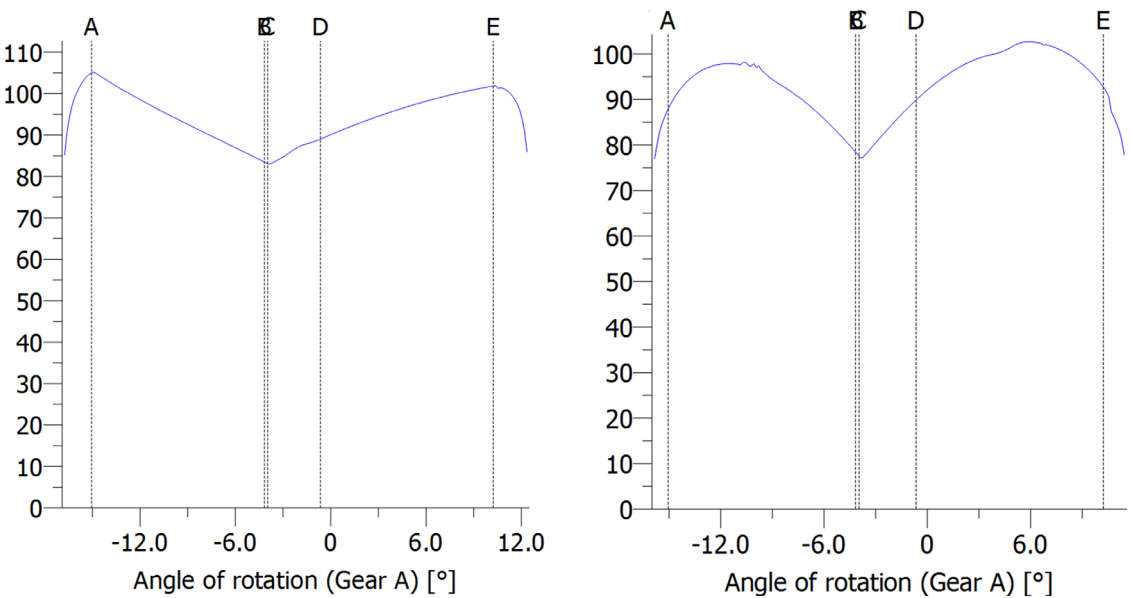
Normal force distribution plot and on tooth representation for unmodified and modified gears in gear stage 1. Notice significant force concentration on the tooth edge before modification.

## Kinematics (specific sliding) gear stage 1 before and after modification



Kinematics plot for specific sliding between the two gears in the gear stage 1 mesh before and after modification. Notice the kinks in sliding speed before modification. This is non load contact where the top of one tooth slides along the surface of the other on the way in or out of the mesh. This effect is almost eliminated with tip relief modification.

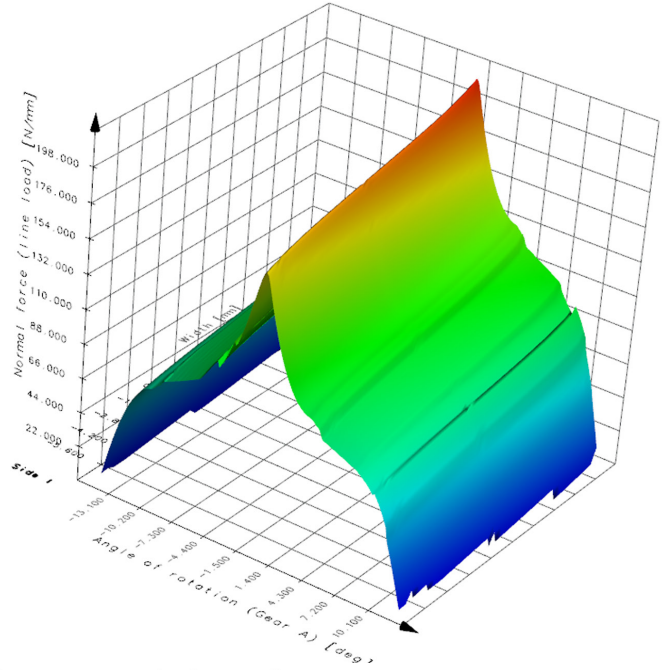
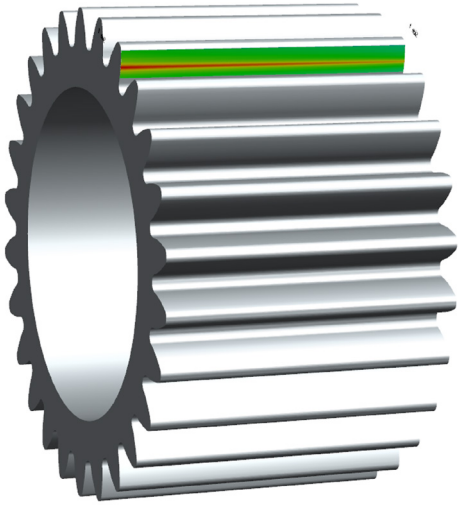
## Contact temperature (Celsius) in gear stage 1 before and after modification



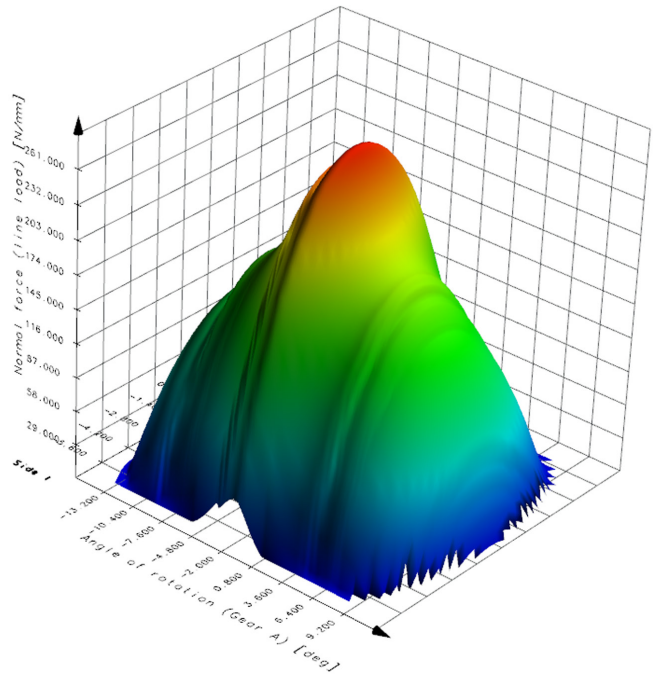
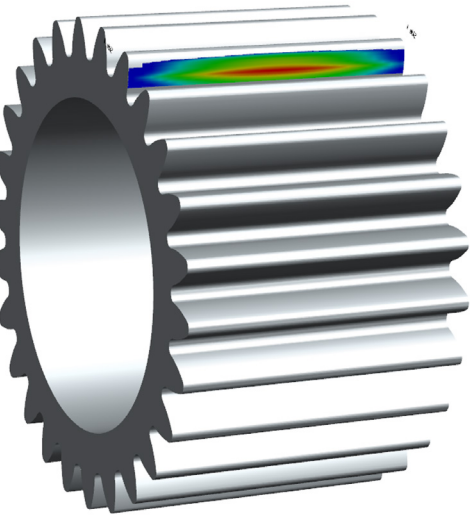
Contact temperature plot for gear stage 1 before and after modification. Notice significant reduction in contact temperature after modification due to less non load sliding and a more optimal force distribution over the tooth flank.



Normal force (line load) [N/mm]

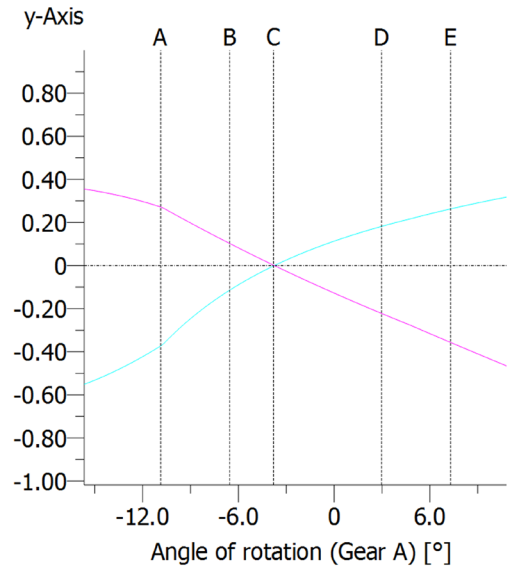
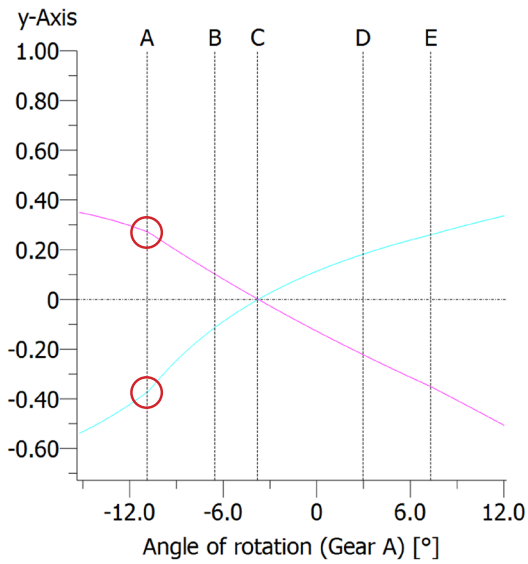


Normal force (line load) [N/mm]



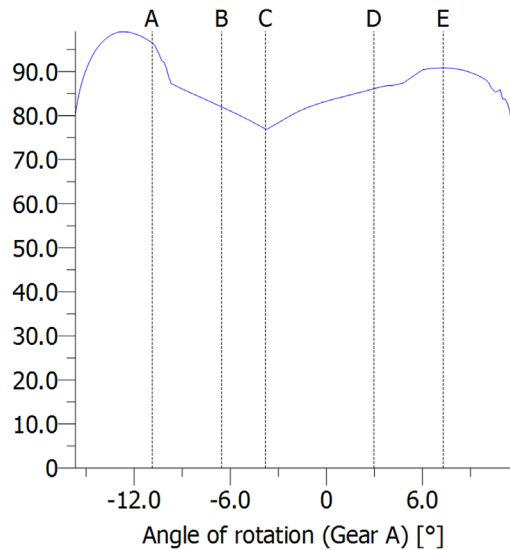
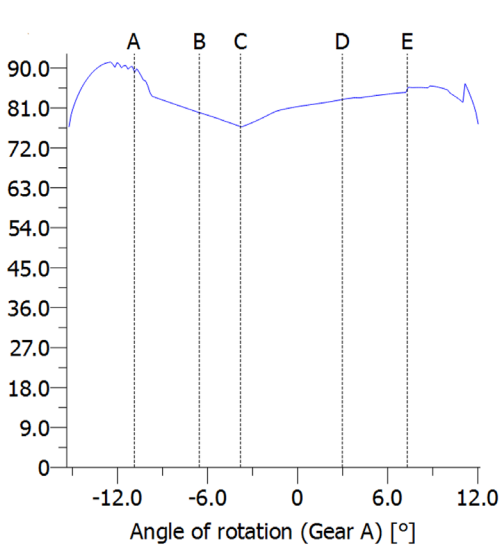
Normal force distribution plot and on tooth representation for unmodified and modified gears in gear stage 2. Notice much better pre modification force distribution than what was the case in gear stage 1. Non the less, the result of modification shows a much more robust contact pattern.

## Kinematics (specific sliding) gear stage 2 before and after modification



Kinematics plot for specific sliding between the two gears in the gear stage 2 mesh before and after modification. Notice the slight kinks in sliding speed before modification. A marginally smoother curve was achieved through tip modification. Due to manufacturing restrictions on the ring gear, tip relief could not be added to both gears in the mesh and only minor improvements were achieved.

## Contact temperature (Celsius) in gear stage 2 before and after modification



Contact temperature plot for gear stage 2 before and after modification. Notice smoother, but higher contact temperature after modification. This is due to a reduction in total contact area from the crowning modification. This higher contact temperature is a trade off in gaining a more reliable gear mesh for gear stage 2.

## Modification result evaluation

Effect of modification on safety factors and efficiency				
	Gear stage 1		Gear stage 2	
	Sun gear	Planet gear 1	Planet gear 2	Ring gear
Required safety root [SFmin] (ISO)	0,72		0,9	
Root safety [SF]	1,495	1,573	1,019	1,336
Root safety [SF] (modified)	1,566	1,798	0,934	1,226
Root safety change (%)	4,75	14,30	8,34	8,23
Required safety flank [SHmin] (ISO)	0,66		0,75	
Flank safety [SH]	0,942	1,203	1,209	1,367
Flank safety [SH] (modified)	1,009	1,275	1,146	1,296
Flank safety change (%)	7,1	5,5	5,21	5,19
Power loss (%)	1,83		0,81	
Power loss modified (%)	1,44		0,76	
Power loss change (%)	21,31		6,17	
Minimum service life [Hatt](h)	>1000		291	

The table shows that the effect of tooth modification on gear stage 1 has resulted in significant improvement in both root and flank safety. Efficiency is also drastically improved, loss of power is reduced by 21.3%. The risk of force concentrations at the tooth edge of the stage 1 gears has been eliminated. The safety factors remain high compared to the ISO requirements for the 0.6 module size, but time constraints put a stop to further optimization.

Gear stage 2 has seen a reduction of both root and flank safety factors from the modifications. The unmodified tooth contact of the gears in

stage 2 was evenly distributed over the entire tooth flank. Helix and crowning modifications reduced the total contact area, thus increasing the contact force. This was considered a worthwhile trade off in order to make the contact between the two gears more robust should unforeseen axis misalignment occur. The resulting root safety factor in planet gear 2 is close to the ISO requirement safety for the 0.75 size tooth module. It was concluded that this still was inside comfortable limits because of the conservative approach in defining the load spectrum and general system limitations.

## Polygon connection

A P3G-Profile DIN 32711-1:2009 polygon connection was used to connect planet gear 1 and planet gear 2 together. The polygon was chosen as it has a fair torque transfer capacity and is very precise compared to the more standard spline type connections. The increased precision is very important in maintaining the tooth mesh timing between the two gears. A large mesh timing deviation results in significant meshing errors in one or both of the gears. This will severely damage the gear teeth.

The polygon connection was first calculated in

KISSSoft using the polygon module to establish a baseline. The calculation was done for 1000000 load cycles at maximum torque with 100000 changes in load direction to emulate breaking torque from KERS. This was done to ensure connection performance throughout the system life span. The connection was then simulated in FEM, again using Hyperworks by Altair. This was done to find the fit interference that would reduce elastic micro sliding to a minimum. This was done to ensure optimal connection stiffness and reduce wear potential and fatigue risk.

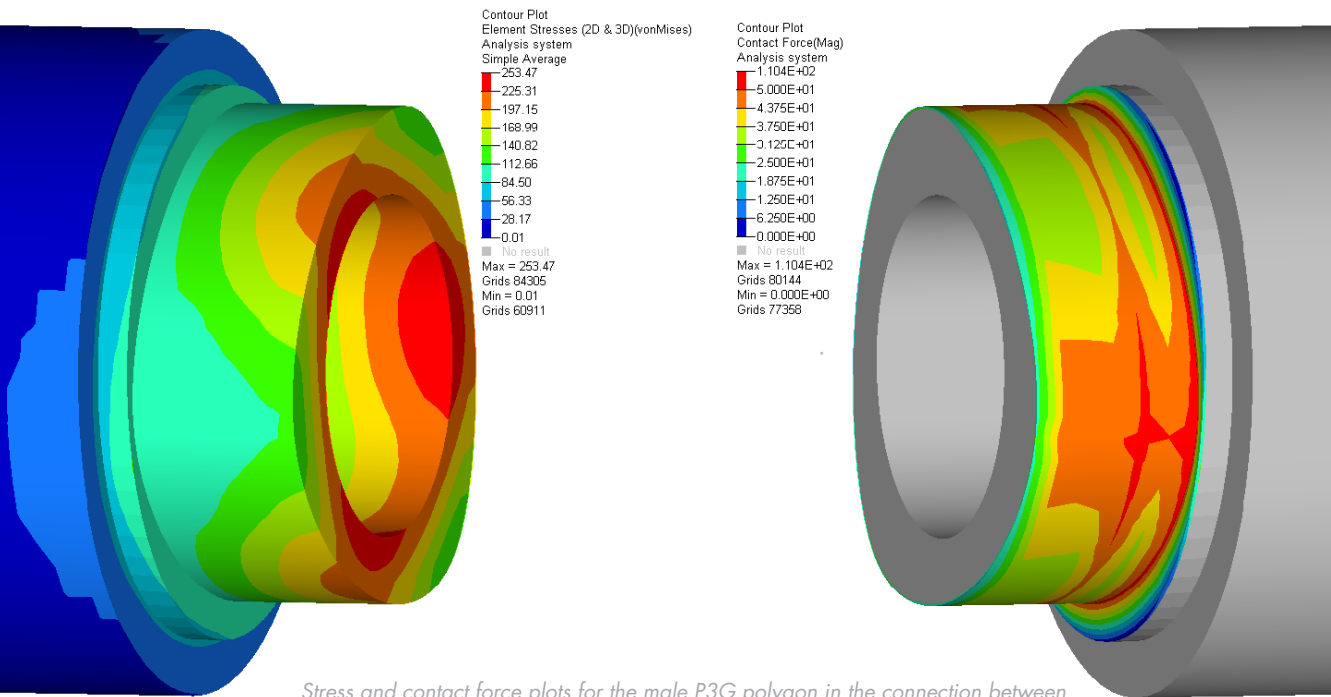
### KISSSoft polygon calculation

Torque $T_{max}$ (Nm)	23
Number of load peaks	1 000 000
Change of load direction	100 000

	Shaft	Hub
Pressure stress at $T_{max}$	181,7	181,7
Safety at $T_{max}$	3,57	4,47

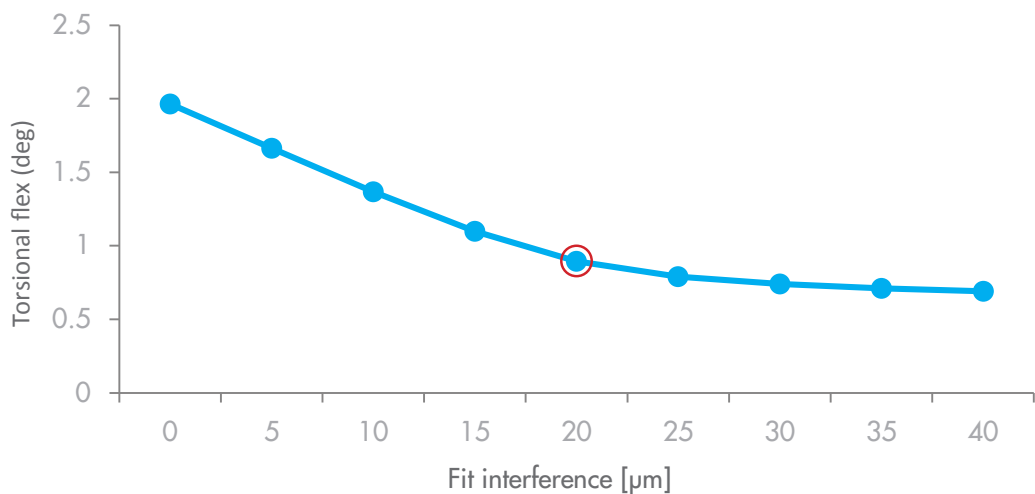


*Male P3G polygon profile used in bike crank shaft and crank arm connection.*



Stress and contact force plots for the male P3G polygon in the connection between planet gear 1 and planet gear 2. Notice the slightly higher stress compared to the KISSSoft results. This is to be expected as KISSSoft does not consider if the male part has an internal hole. It is also easy to see from the peak contact forces how the polygon lobes have more contact stiffness than for the rest of the structure.

### Elastic torsional microsliding vs fit interference in P3G polygon profile



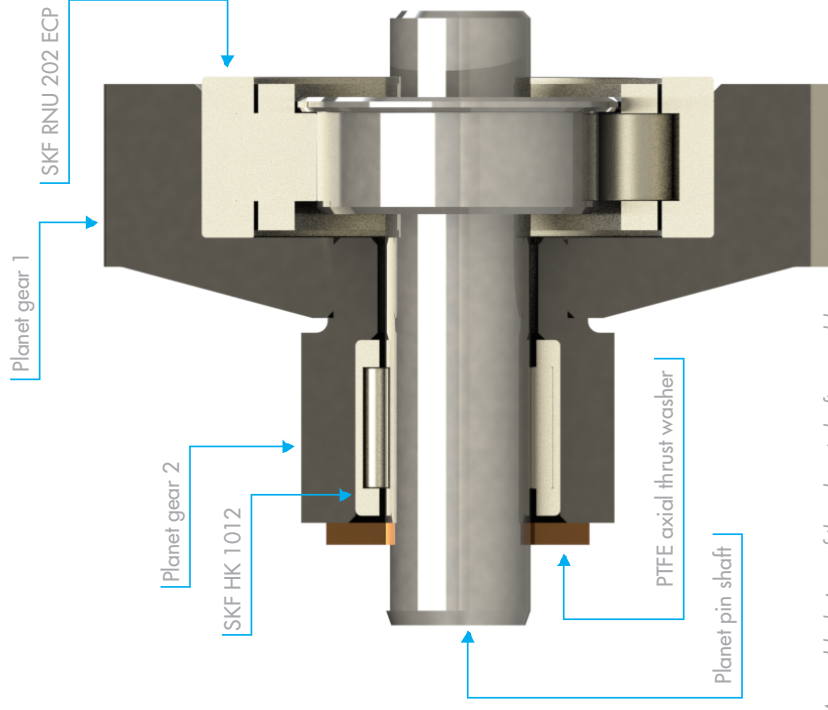
Plot of torsional flex in polygon connection for fit interferences from 0 to 40 µm. Notice convergence of torsional flex after 20µm fit interference. More interference will not significantly reduce performance further, but will increase difficulty of assembly.

# System design

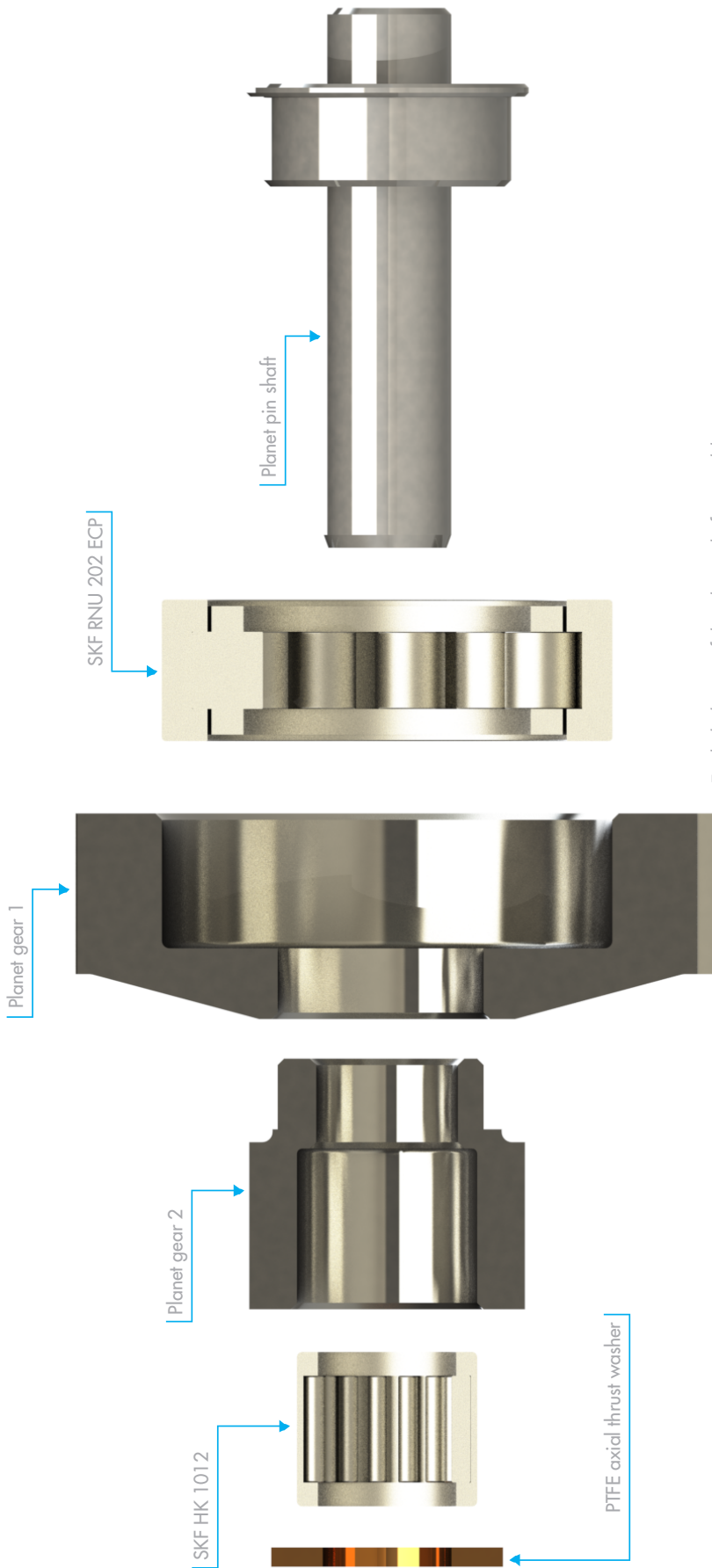
## Planet shaft assembly

The planet shaft assembly is almost identical in design to the KISSsoft model. The planet pin shaft is mounted rigidly in the planet carrier (not shown). Planet gear 1 and planet gear 2 are connected via a P3G polygon connection and rotates on the planet pin shaft using a SKF RNU 202 ECP roller bearing and a SKF HK 1012 needle roller bearing. The small ledge in the planet pin shaft axially locates the roller bearing in one direction while the PTFE axial thrust washer locates the gear shaft in the other direction. This ensures that no axial runaway or rubbing happens during operation.

One compound planetary transmission system includes 3 instances of this subassembly. The difference in tooth timing for each instance means that planet gear 2 has a unique tooth mesh timing in relation to planet gear 1 for each of the 3 assembly positions. This will be elaborated in further in the following pages.



*Assembled view of the planet shaft assembly*



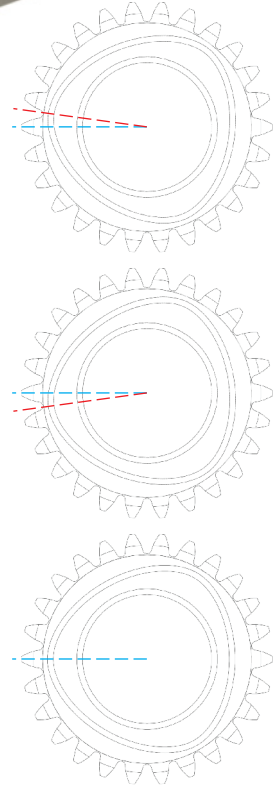
*Exploded view of the planet shaft assembly*

# System design

## Full gear assembly

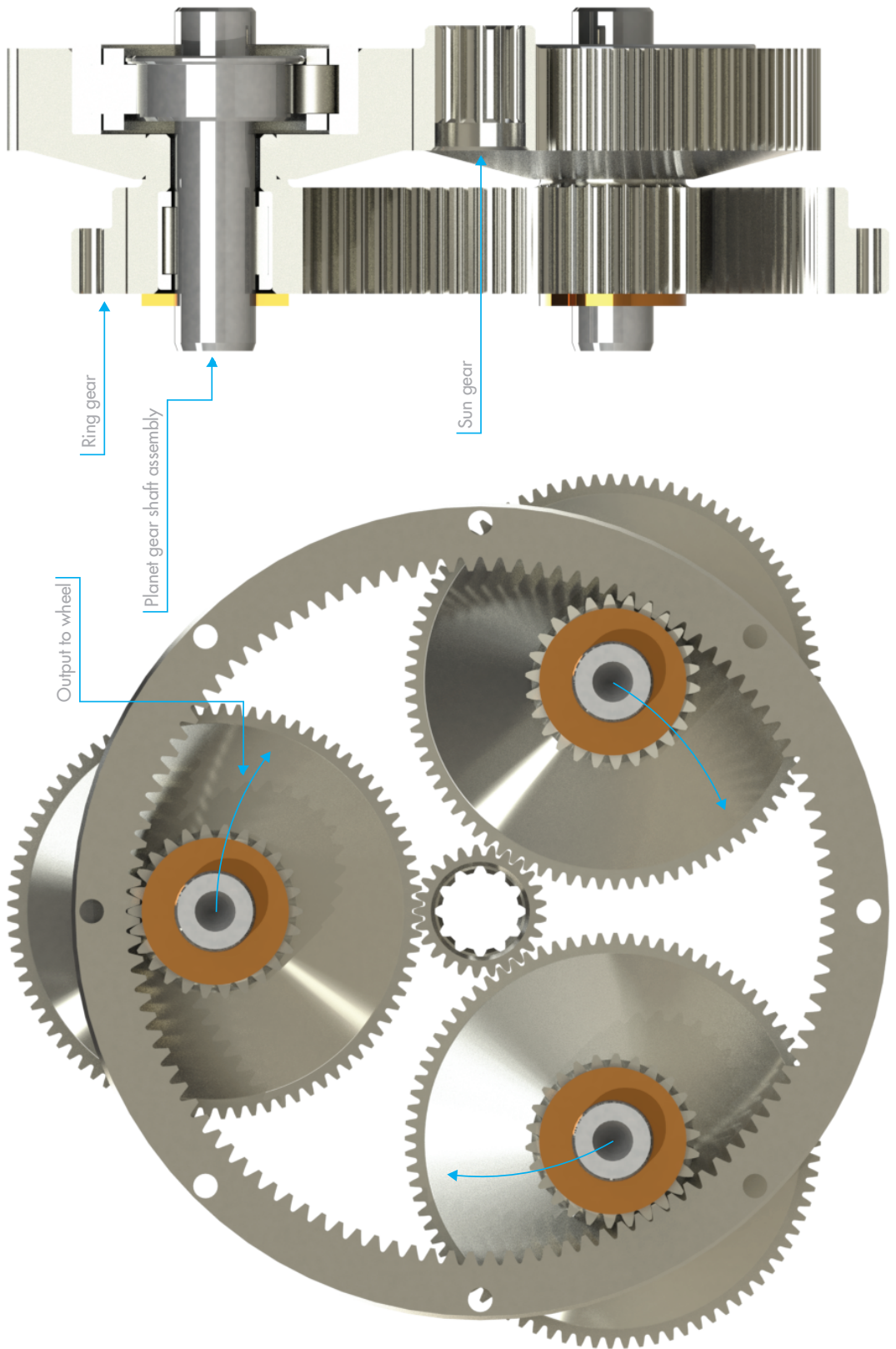
The full gear assembly of the compound planetary system shows how 3 planet shaft assemblies are mounted at each 120 degrees of the circle. It's shown how the sun gear is meshing with the planets in gear stage 1 and how the planets in gear stage 2 is meshing with the ring gear.

As previously mentioned, the 3 positions for planet gear 2 all require a unique instance of this gear where the tooth timing is slightly offset. This is because the number of teeth of the ring gear is 112. 112 divided by 3 is not an integer but rather 37 and one third of a tooth. This means that the tooth mesh timing between planet gear 1 and planet gear 2 needs to be offset by two thirds of a tooth in the 120 and 240 degree positions in order to make the system mesh properly.



*Polygon vs tooth timing for 0, 120 and 240 degree planet gear 2 position*





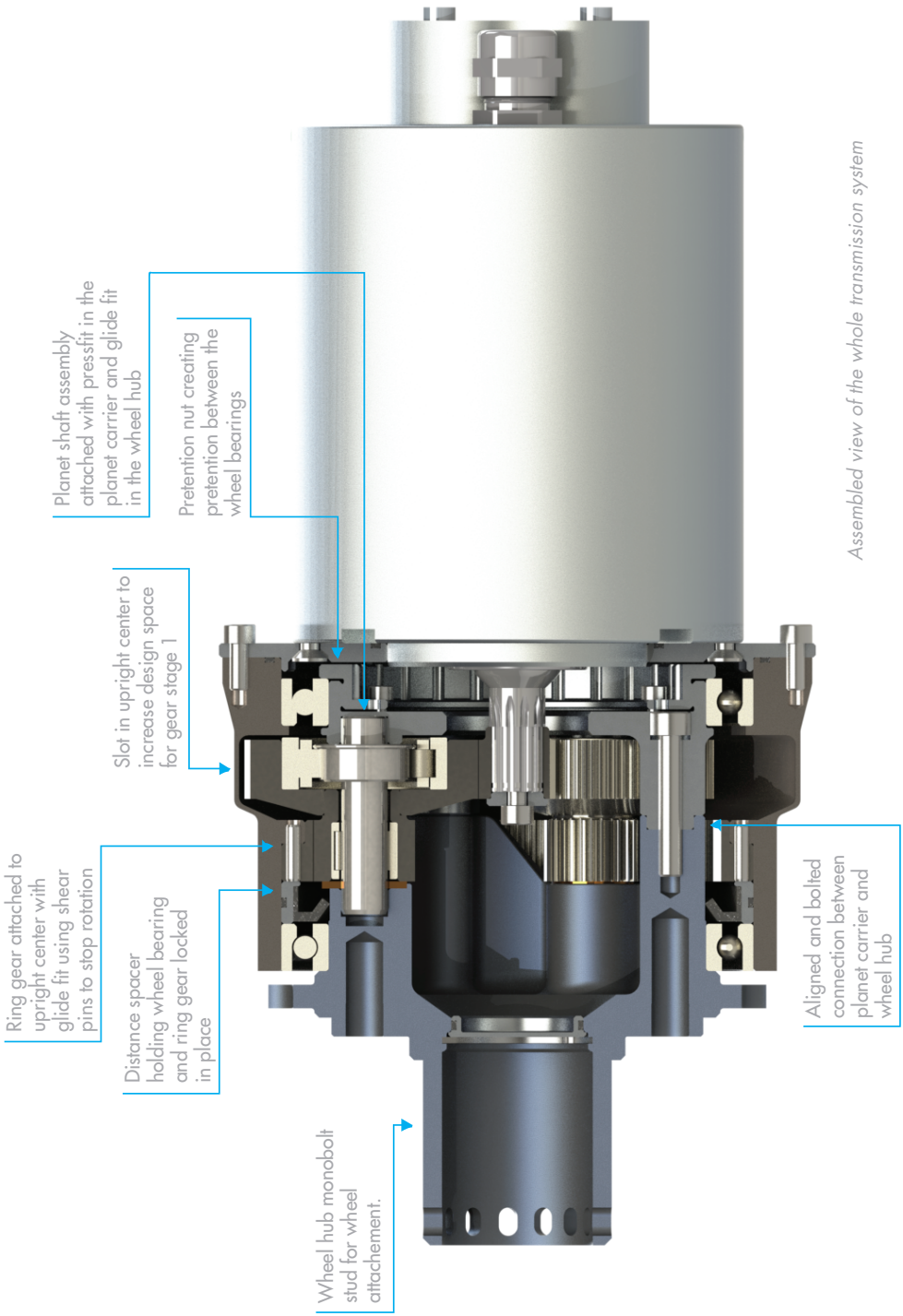
# System design

## Full transmission system assembly

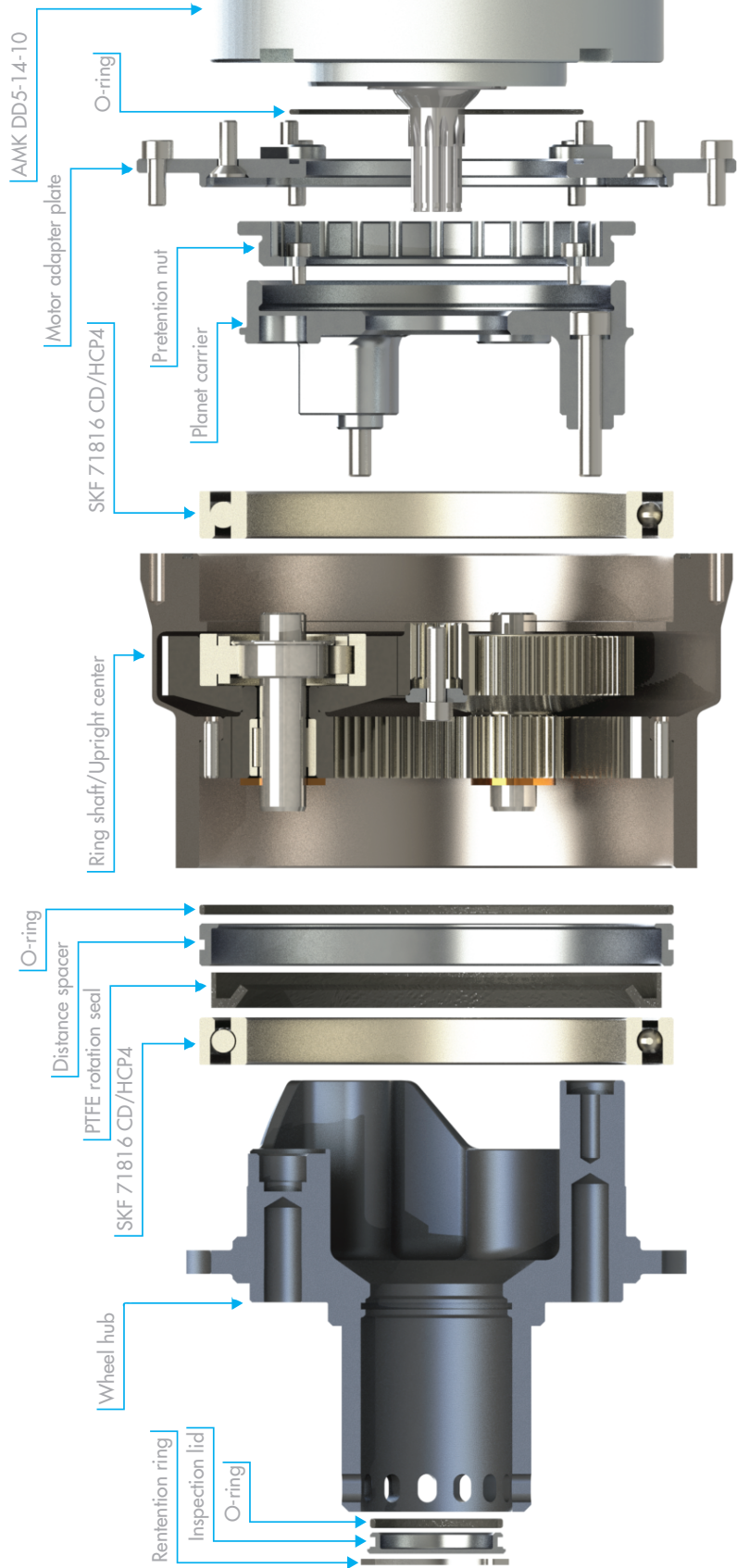
Representation of the full transmission system assembly shows the compound planetary system with all surrounding parts. The planet carrier and wheel hub has been split in order to make assembly possible. The planet pin shaft is attached to the planet carrier using a press fit while it is held in place at the wheel hub side using a glide fit. This bolt less connection was chosen to further simplify the assembly of the system.

The upright center was designed with a slot to increase the radial size of the design space for gear stage 1. Without this slot and the large size of planet gear 1, achieving a final drive ratio of 15.5:1 would be impossible within the limits of the design space.

The final system design has remained very compact despite a high number of parts and very restrictive limitations.



*Assembled view of the whole transmission system*



*Exploded view of the whole transmission system*

# Upright design

## On designing for additive manufacturing

Before designing the upright, a consideration of the most appropriate manufacturing method has to be made. The upright is a complex part, interfacing with the upper and lower wishbone, the tie rod, the break caliper, the motor, the wheel hub and the transmission. In addition to the requirement for proper design of all these interfaces, the upright needs to be sufficiently stiff in order to not produce unwanted compliance under heavy load. The result of significant elastic deformation in the upright structure under high wheel loads is camber gain and loss of tire contact area. The end product is reduced contact friction and turning performance. With so many parameters to optimize for in the design process, the limitations introduced by the manufacturing method can seriously reduce the efficiency of the final design. With this in mind, the manufacturing method that offers the most freedom is 3D printing.

3D printing, or additive manufacturing (AM), was invented in the 1980s as a means to rapidly prototype plastic models for design visualization. The last ten years has seen a rapid acceleration in the development of additive manufacturing methods. We are now starting to see the use of additive manufacturing as a production process for functional products and not just as a rapid prototyping method. This opens up to

totally new and innovative ways of designing products with unconventional shapes. Additive manufacturing is however still mainly used as a cost effective way to produce pre-production representations of parts that are to be injection molded, cast or machined, adhering the design to the limitations these production methods demands. In the few cases where additive manufacturing is used as the production method, the design is seldom optimized to take full advantage of the additive manufacturing capabilities. There are two reasons for this: We as designers have not yet been sufficiently exposed to this new way of designing free form shapes. The concept of restriction less shapes opens up to very non intuitive ways of designing. This brings us to the second reason: That advanced design software has to work in unison with the designers intuition in order to help the designer cope with the non-intuitive nature of this kind of design.

To better explain why designers may struggle to fully utilize the capabilities of 3D printing, it is interesting to evaluate biomechanical examples designed by nature. A cross section of the human femoral bone provides us with a very good example. The outer shape is somewhat intuitively constructed, gradually tapering into a larger cross section in order

to provide sufficient local strength and stiffness at the interfacing articular ends of the bone. The organic shape is however still very hard to intuitively optimize. The internal construction of the bone is far more interesting. The thinner middle part of the bone is hollow, with thick cortical bone almost like a steel tube, providing excellent stiffness and strength at a very low weight. At the tapering ends of the bone, the hollow cortical shell is stabilized by a porous microstructure. The shell thickness is reduced in these areas, but the microstructure stabilization provides excellent buckling resistance, much like a composite sandwich structure. This microstructure is increasing in density towards the interface, providing a smooth force transition over the structural variation in the bone, preventing stress peaks and reducing fatigue risk. The shape and direction of the microstructure is optimized to handle all the load directions sustained under normal use. Evolution has thus provided humans with a minimum weight, minimum material, sufficient strength and sufficient stiffness construction without sacrificing significant functionality. For a human designer to intuitively come up with a similar design within any sort of normal time frame is not to be expected.

From this, it follows that designers have to evolve

their methodology in order to keep up with the ever increasing manufacturing freedom provided by 3D printing. Instead of focusing on the overall form and manufacturability of a part, the focus will shift towards smarter design of system boundaries. The designers job will in large part be to specify the design space of the part, design the connecting interfaces and provide the physical inputs in these connections. When the space and system limitations are set, a finite element topology optimization software will

use this information to run iterations until it finds an optimal solution for the shape of the part. The problem designers currently face is that the existing topology optimization software are few in number and very expert oriented, meaning that they severely lack in user friendliness. They also lack the ability to provide results using both solid and microstructural material compositions without the use of a supercomputer. This means that current attempts at designing parts using these methods are walking the frontier line of

innovation and development.

In the spirit of this innovation, it is the intention to apply as much of the most advanced methods and tools that currently exist and that can be supported inside the project development time frame when designing the uprights. Combining this with creativity and good engineering, the intended goal is to come up with a very efficient and innovative design that pushes the boundaries of current design paradigms for additive manufacturing.



*Cross section of human femoral bone showing evolutionary optimization: The interplay between a variable thickness solid shell and a porous internal microstructure.*

# Upright design

## 3D printing with metallic materials

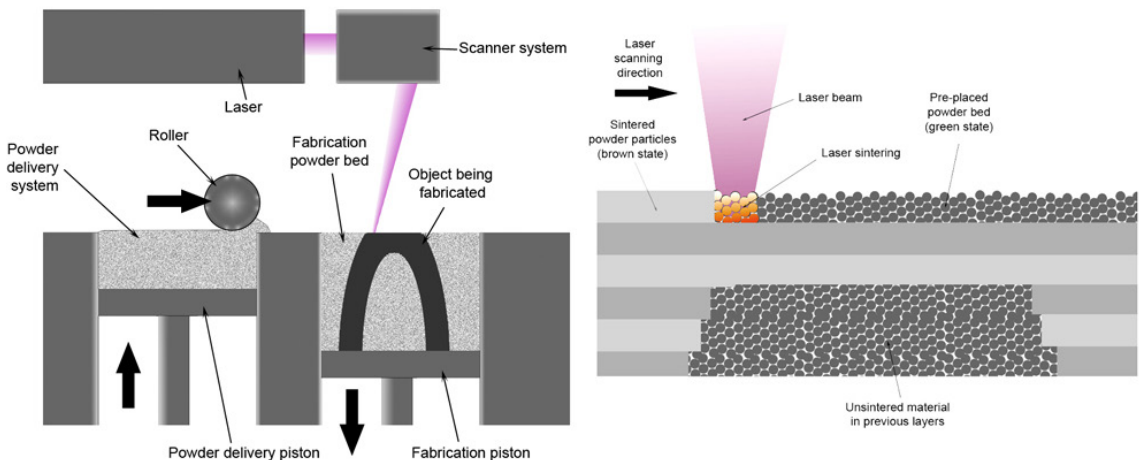
The most popular forms of 3D printing are all based on polymer materials like ABS or nylon. These materials, while cheap and very light weight, do not possess the required mechanical properties required in order to sustain the forces that are subjected to the uprights. These structures have to be printed in metal in order to achieve the strength and stiffness requirements imposed by the gearbox and suspension systems. Using a method called direct metal laser sintering (DMLS), parts with very small details can be printed with fairly high precision in a variety of metallic materials. More specifically, the method uses an Ytterbium (Yb) fiber laser to weld together many thin layers of metallic powder, building parts from the ground up. The powder applicator is able to deliver very thin

powder layers of only 30 microns. This enables a very precise part shape accuracy of  $\pm 50$  microns, equivalent to  $\pm 0.05$ mm. The downside is that the surface roughness is high at Ra 9-12 microns. This means that all high tolerance contact interfaces of the part needs to be post machined or polished if a smoother surface is required. In our case, the upright will require a significant amount of post machining due to the high tolerance requirements of the gearbox.

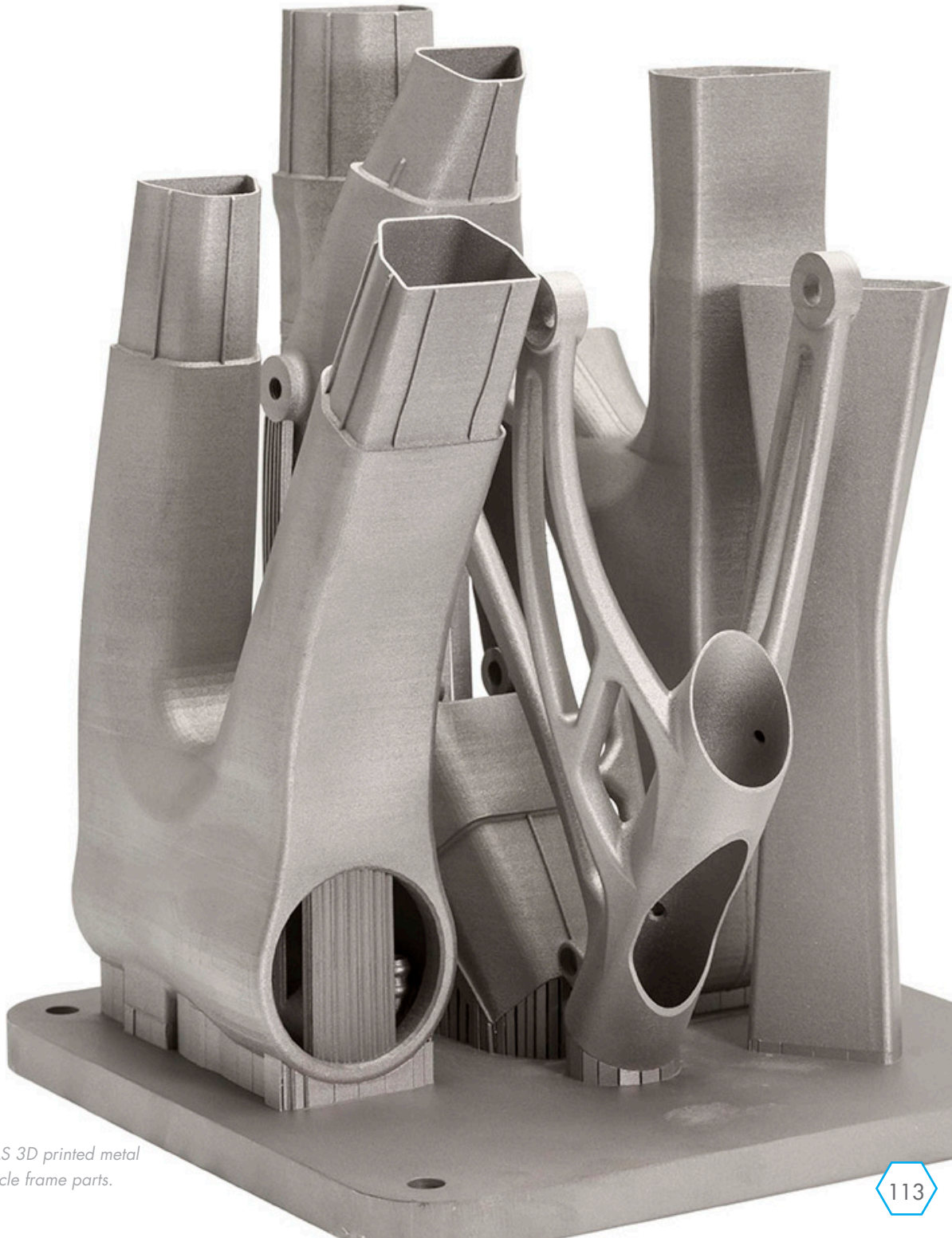
There is more bad news. While it may seem like the DMLS 3D printing method provides restriction less design freedom, significant metallurgical limitations are imposed by the laser welding process. Heat dissipation, thermal expansion and internal stresses are some of

the factors that may limit the manufacturability of a design. That said, the overall form freedom provided by DMLS printing far surpasses what is considered possible using conventional manufacturing methods.

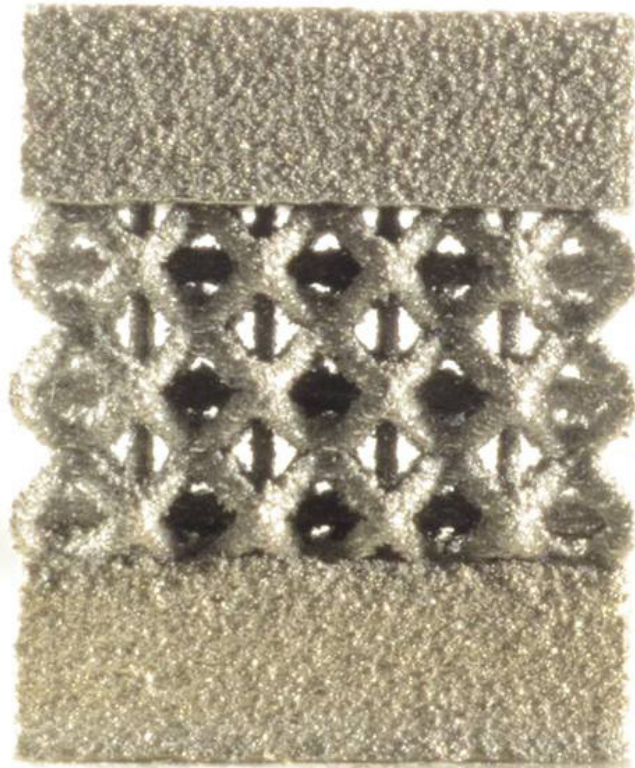
Grade 5 titanium was chosen as the material for the uprights. This material is very strong and moderately stiff at a fairly low density. It is also one of the 3D printing materials that is least challenged by metallurgical limitations. High internal stress is the main negative by product in printed titanium parts. This is however mitigated by argon atmosphere annealing, normalizing the material. Grade 5 titanium is commonly used both in high end aerospace parts and human prosthetics because of its superior characteristics.



*DMLS printing process.*



*DMLS 3D printed metal  
bicycle frame parts.*



*BCC microstructure  
sample printed in grade  
5 titanium with 0.4mm  
beam thickness. Coin for  
reference.*





# Upright design

## Microstructures workflow verification

A prerequisite when designing with the intention of utilizing the capabilities of DMLS printing is the ability to use porous microstructures. As previously mentioned, such structures provide high volume shell parts with buckling stability at an extremely low weight. A buckling stable high volume shell part is significantly stiffer than a low volume solid part. This is due to the fact that the second moment of inertia, the main stiffness contributing factor, is increasing proportionally to the distance between the center of mass and the material volume of the part.

Designing parts with any significant amount of microstructure is not possible using conventional CAD software. Using the 3-matic design software by Materialise, it is possible to efficiently fill 3D volumes of a part with uniform or randomized microstructures.

It is then possible to export the part as a mesh and analyze it using finite element (FEM) software. In the exported part mesh, the microstructure is meshed using 1D FEM elements, significantly reducing the potential calculation time compared to what would be the case if the microstructure would be represented using standard volume mesh. This way, we are able to both design and verify parts that incorporate porous volumes.

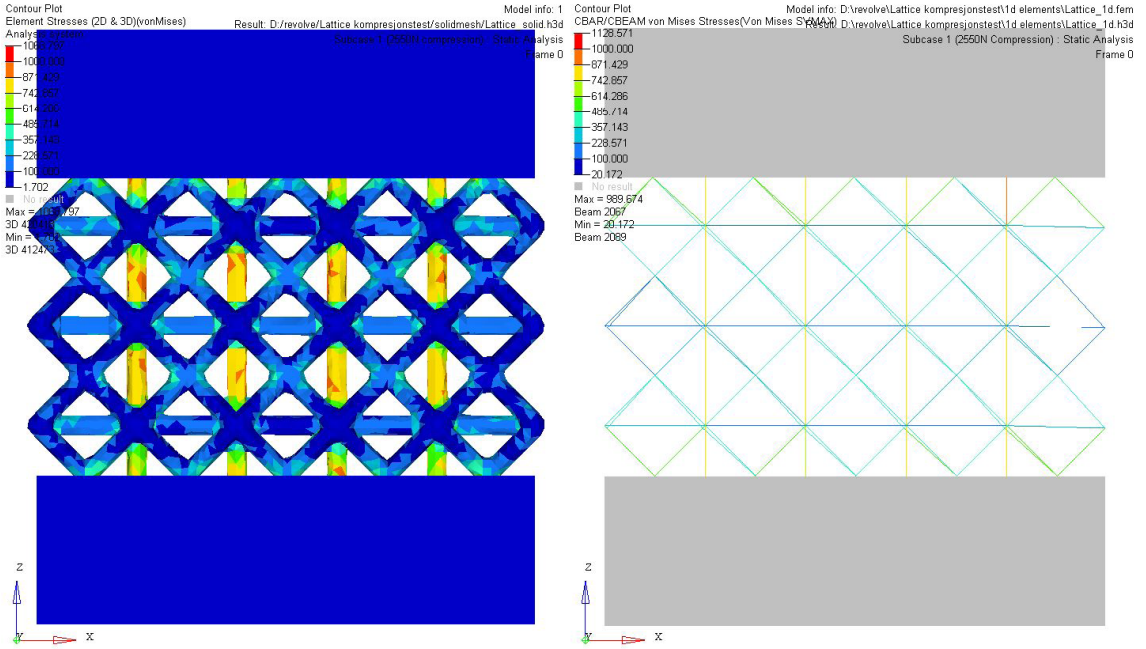
With no previous experience in using the 3-matic software, it was concluded that we needed to do a quality control of the design and simulation workflow, comparing analysis results to real world testing. A 10 by 10 mm grade 5 titanium cube including a segment of body centered cubic structure with a cell size of 2 by 2 by 2mm and a structure thickness of 0.4mm was designed in 3-matic.

Two different instances of the mesh was exported, one with the microstructure as 1D elements, the other with it as standard volume mesh. Both mesh variations were then subjected to a linear elastic compression analysis using Hyperworks FEM software by Altair. Parallel to this, 4 cubes were printed, and subsequently tested to failure in a compression machine. The test and analysis force vs displacement results were then graphed together to reveal any difference between the analysis methods and the real world.

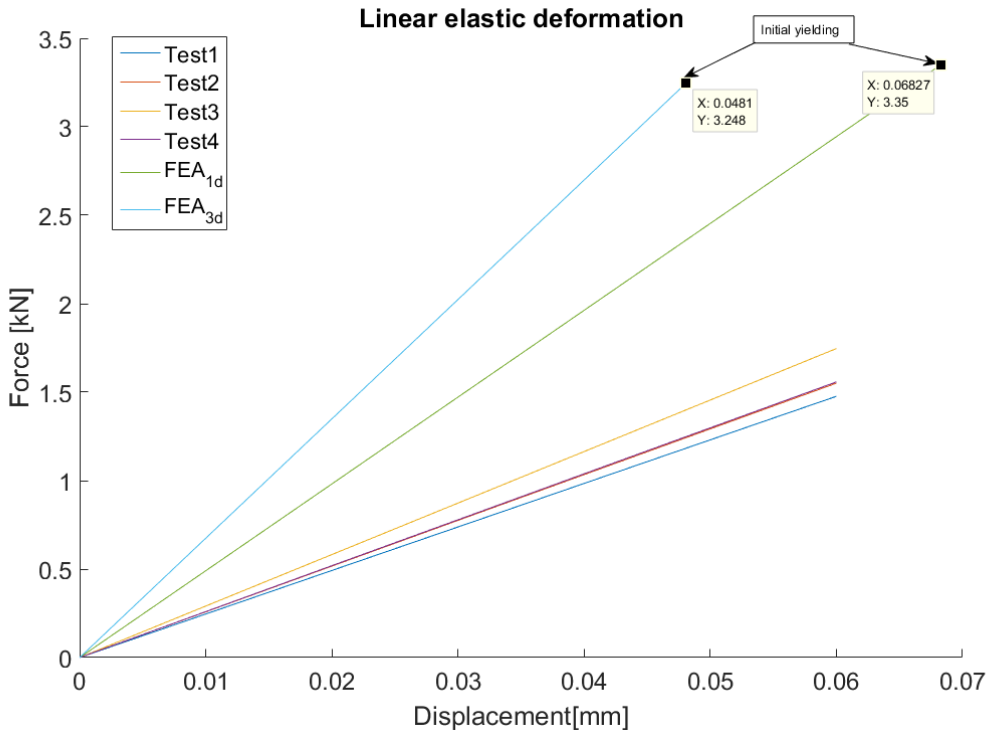
Test results are shown in the graph. It reveals that both FEM methods give results that are up to 50% stiffer than what was measured during real world tests. It is speculated that printing precision at such small beam sizes is too rough to give consistent beam thickness in the test specimen, and



3-matic workflow.



Stress plot from FEM simulation of 3D-mesh on the left and 1D-mesh on the right. Both situations are subjected to the same load.



the result of this is significant loss in stiffness. We are thus unable to precisely simulate the behavior of such structures. 1D elements does however give the most conservative approach.

We will therefore use that mesh type as a best practice approach, making sure all results are conservatively evaluated in order to confirm that sufficient performance is achieved.

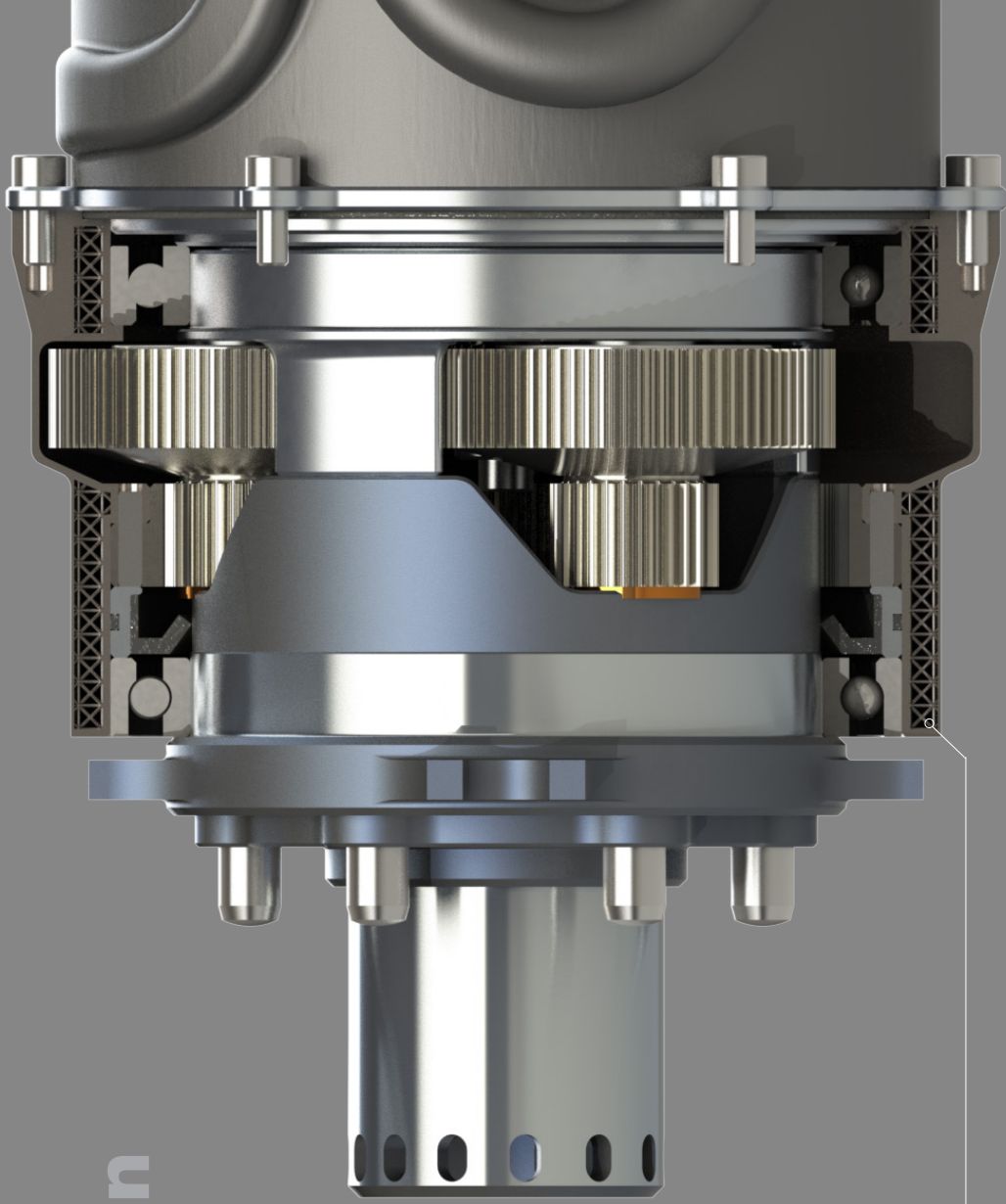
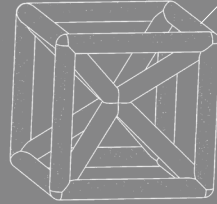
# Upright design

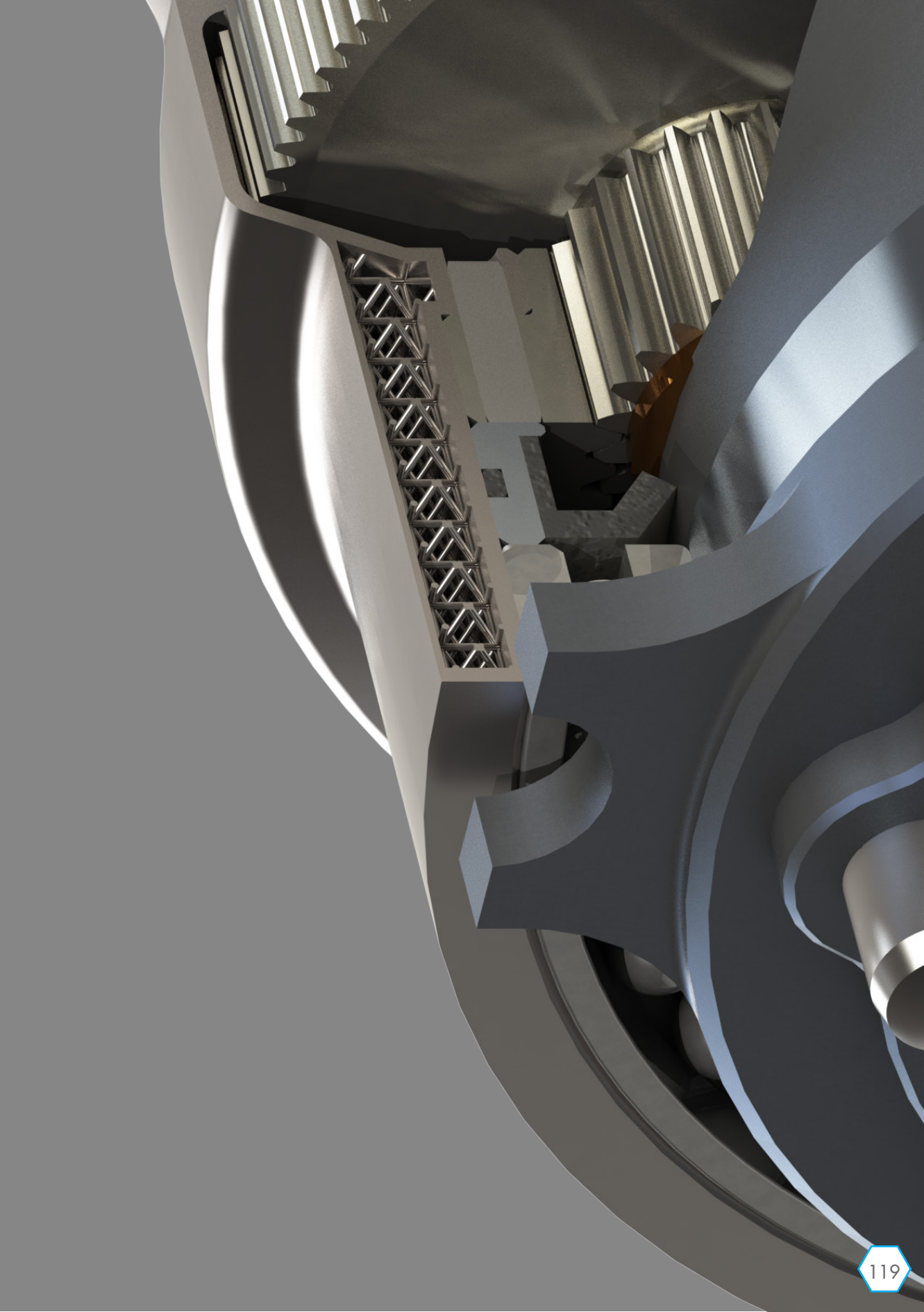
## Microstructure in upright center

The tested BCC microstructure cell has been used to fill the majority of the volume of the wheel bearing contact areas of the upright center. It was thus possible to achieve very high stiffness in these two areas without sacrificing too much weight.

The BCC structure was used as it has a geometry that intuitively behaves similar to an isotropic material for every load direction. This isotropic like behavior would not be achievable using a FCC or a dodecahedral structure. The main reason for this being that the

BCC has axial and shear support rods in all directions while the other two are either shear or axial dominant structures.





# Upright design

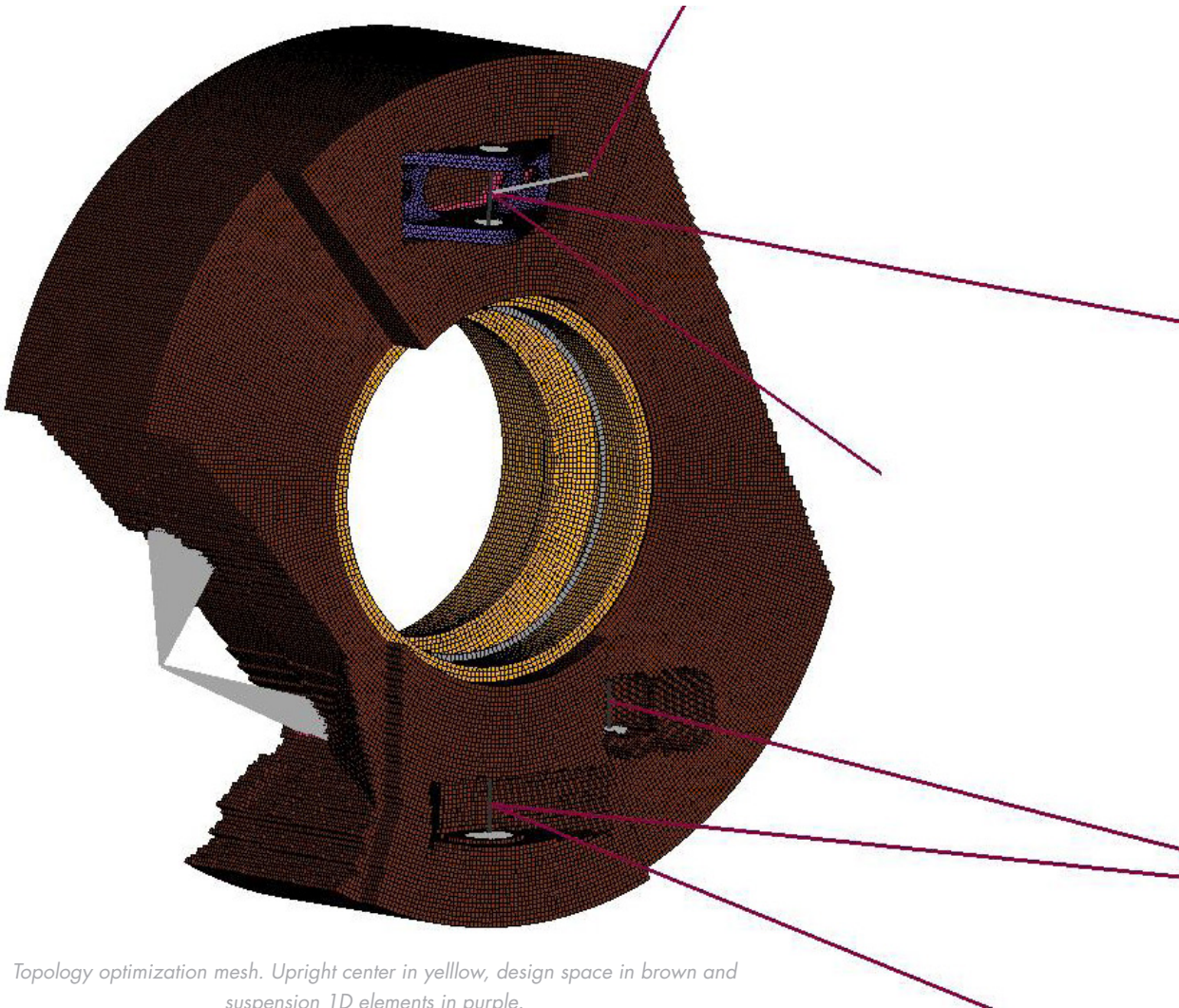
## Topology optimization

The use of OptiStruct topology optimization software from Altair was implemented in the design of the rest of the upright. The upright center was connected to a design space volume also constrained by brake caliper and suspension interfaces. 1D element representation of the suspension with the proper degrees of movement freedom was used to correctly fix the upright in space.

Loads were calculated for all critical load cases. Every relevant load case was then added to the simulation with a 1:1 priority, meaning that all load cases were prioritized equally during the

optimization. Limitations in computing power meant that the model had to be run as a linear static analysis. The non linear contacts were simplified to linear glued contacts. We were thus unable to run the optimization at full detail level.

Optimization was run using minimum global deformation as the success criteria. The upright needs to be very stiff, both to hinder any transmission misalignment and to reduce suspension compliance to a minimum. The weight restriction of the remaining material was set to maximum 250 g.



Topology optimization mesh. Upright center in yellow, design space in brown and suspension 1D elements in purple.

<b>Front upright load case</b>					
Load at tyres	Corner	Inside corner	2g bump	Brake+bump	Acceleration
	High speed 110km/h		High speed 110km/h		
Longitudinal force Px [N]	0	0	0	-2061	447
Transverse force Py [N]	-1846	787	0	0	0
Vertical force Pz [N]	1743	462	1197	2842	440
Brakedisc tangential force				5777,6	

Decomposed Bearingload from FEA	Cell description:			Neglected	Used in sim.
Inner bearing Fx [N]	0	0		-2236	342,6
Outter bearing Fx [N]	0	0		3845	127,4
Inner bearing Fy [N]	1421	946,8		114,3	-56,53
Outter bearing Fy [N]	-3267	-159,8		-114,3	56,53
Inner bearing Fz [N]	11060	-3567		2964	320,7
Outter bearing Fz [N]	-9319	4029		-4585	119,3

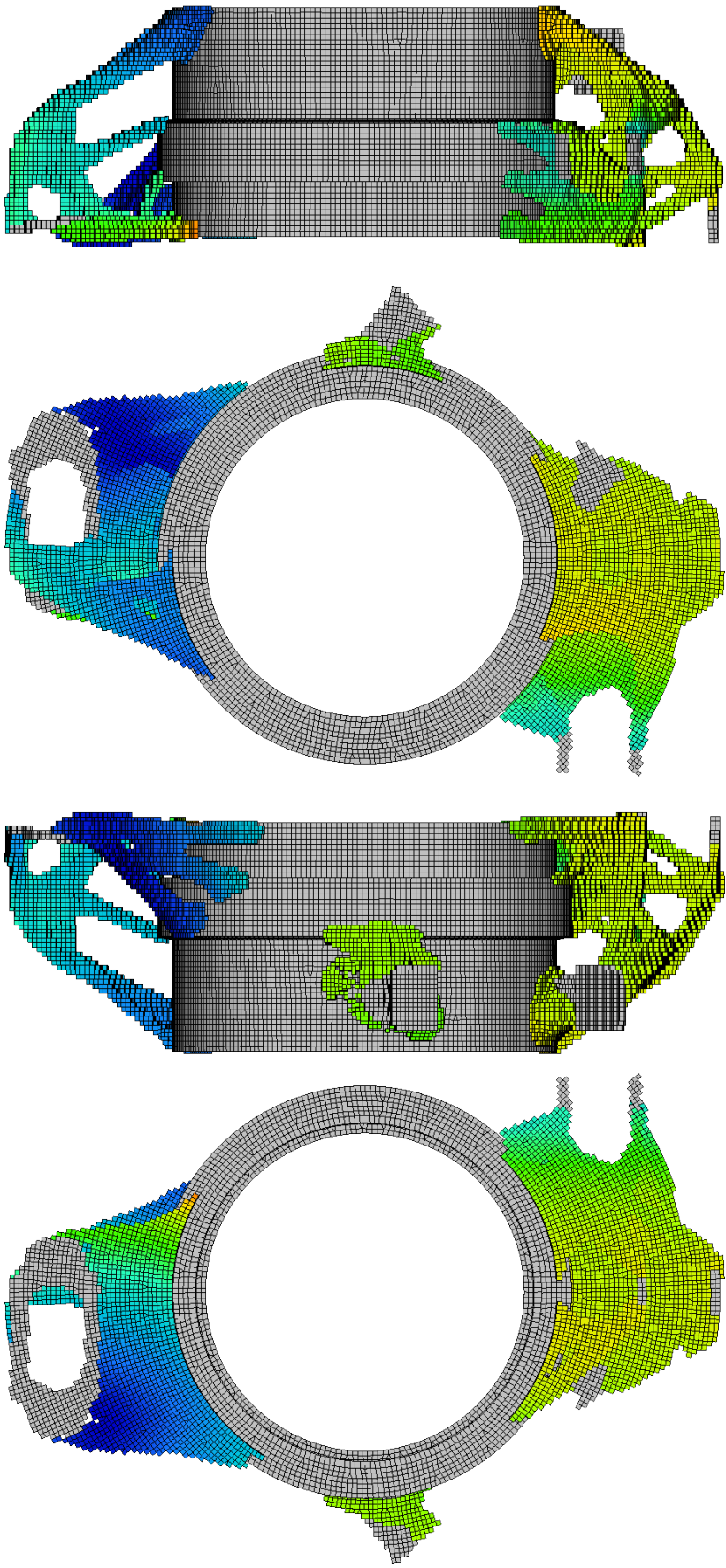
<b>Rear upright load case</b>					
Load at tyre	Corner	Inside corner	2g bump	Brake	Acceleration+bump
	High speed 110 km/h		High speed 110 km/h		
Longitudinal force Px [N]	0	0	0	-860	1413
Transverse force Py [N]	-1850	790	0	0	0
Vertical force Pz [N]	1650	460	1200	560	1765
Brakedisc tangential force				2391	

Decomposed Bearingload from FEA	Cell description:			Neglected	Used in sim.
Inner bearing Fx [N]	0	0		718	-622
Outter bearing Fx [N]	0	0		-1555	-791
Inner bearing Fy [N]	-700	-1209		-22	250
Outter bearing Fy [N]	2550	420		22	-250
Inner bearing Fz [N]	-10450	3713		-586	-1306
Outter bearing Fz [N]	8796	-4173		1723	-1659

Loads calculated based on maximum tire grip for each situation.

# Upright design

## Front upright optimization result



Remaining mass of the front upright after topology optimization. Color map show displacement magnitude.



# Upright design

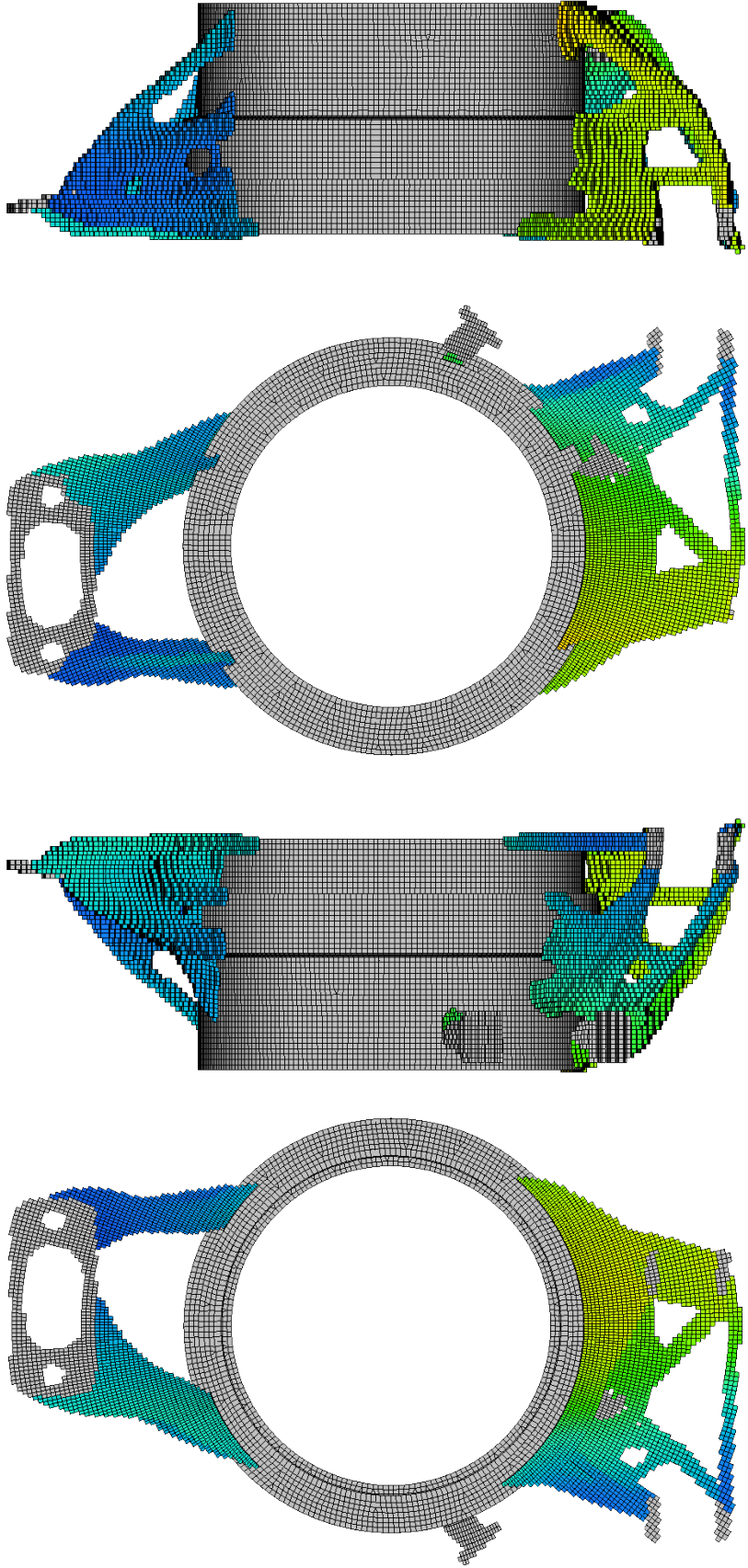
Front upright finished CAD model



*Final 3D model of front upright designed using the topology optimization result as a framework.*

# Upright design

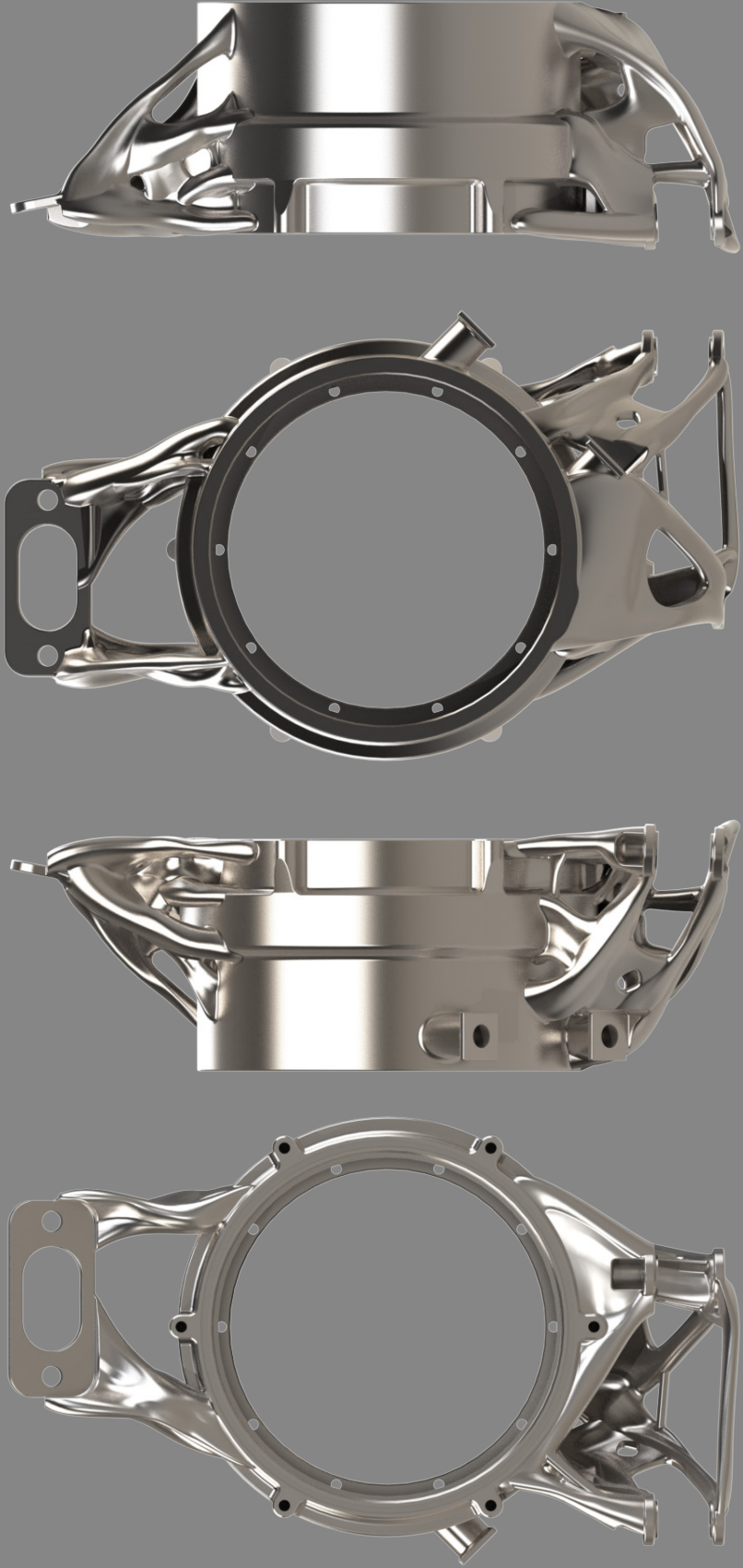
## Rear upright optimization result



Remaining mass of the rear upright after topology optimization. Color map show displacement magnitude.

# Upright design

Rear Upright finished CAD model



*Final 3D model of rear upright designed using the topology optimization result as a framework.*

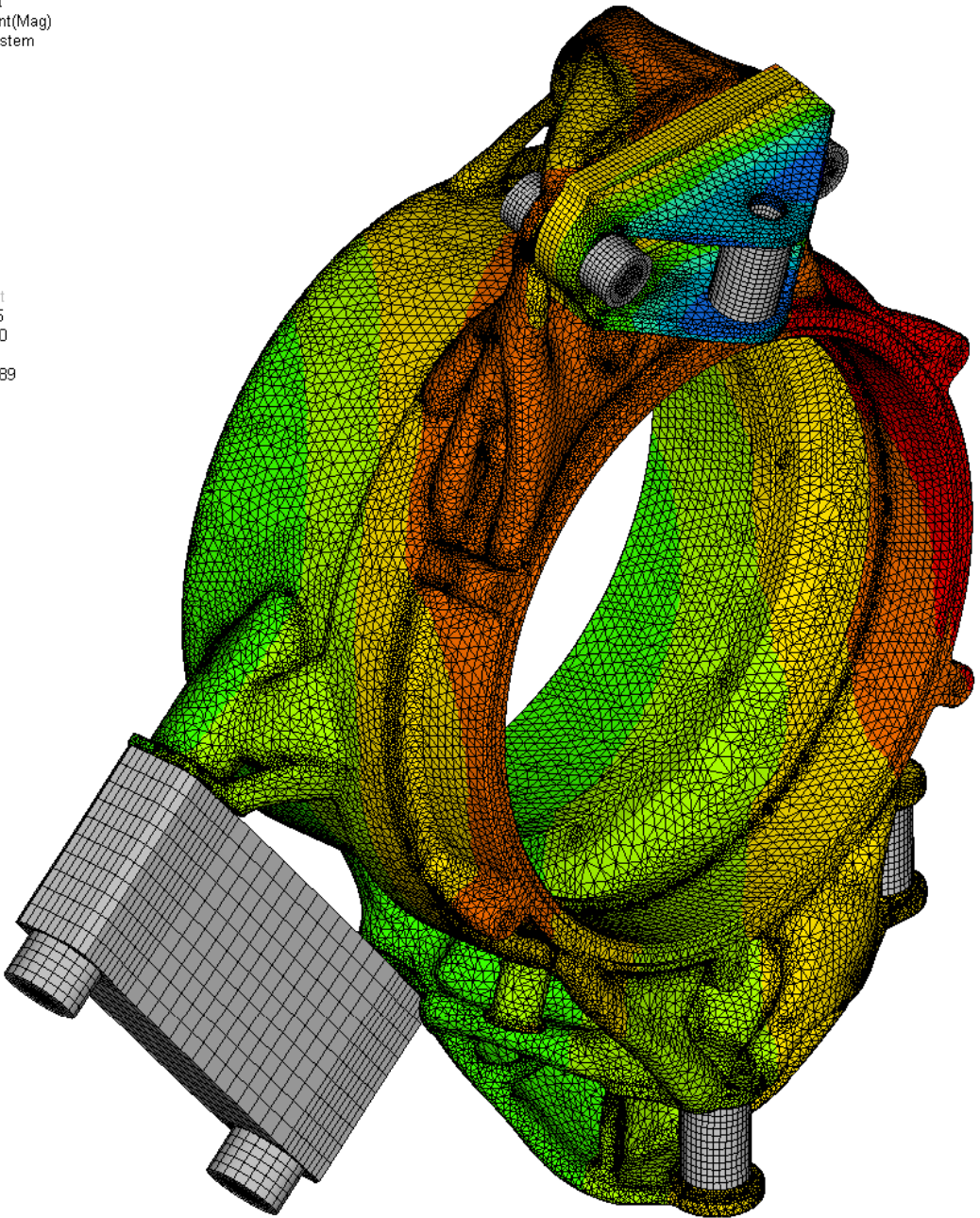
# Upright design

## FEM verification front upright

Contour Plot  
Displacement(Mag)  
Analysis system

0.195
0.176
0.156
0.136
0.117
0.097
0.078
0.058
0.039
0.019

■ No result  
Max = 0.195  
Node 153970  
Min = 0.019  
Node 2044189



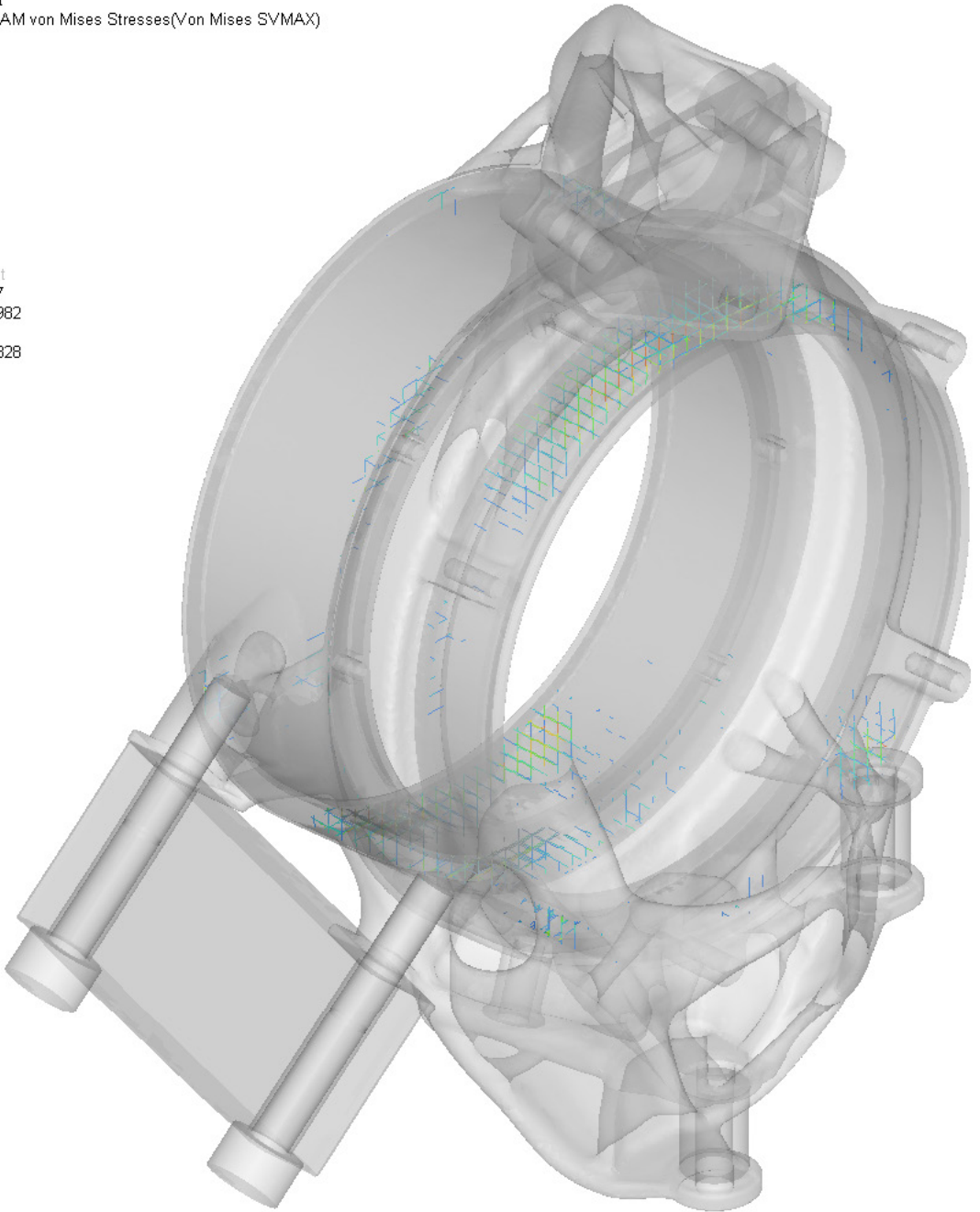
FEM verification of front upright final design using Hyperworks by Altair. All part connections have been fully defined using nonlinear contact constraints in order to better recreate real world

behavior. The analysis was run using the same load cases as during the topology optimization. Both global and local deformations results are within system requirements.

Contour Plot  
CBAR/CBEAM von Mises Stresses(Von Mises SVMAX)



■ No result  
Max = 467.7  
Beam 1268982  
Min = 0.1  
Beam 1272328



The microstructure was modeled as 1D geometry exported from 3-matic and connected to the rest of the model. The stress plot show how stress peaks occur in areas where the topology

optimized structure is connected to the upright center. The peak stress value of over 450 MPa is yielding a safety factor in the microstructure of over 2.

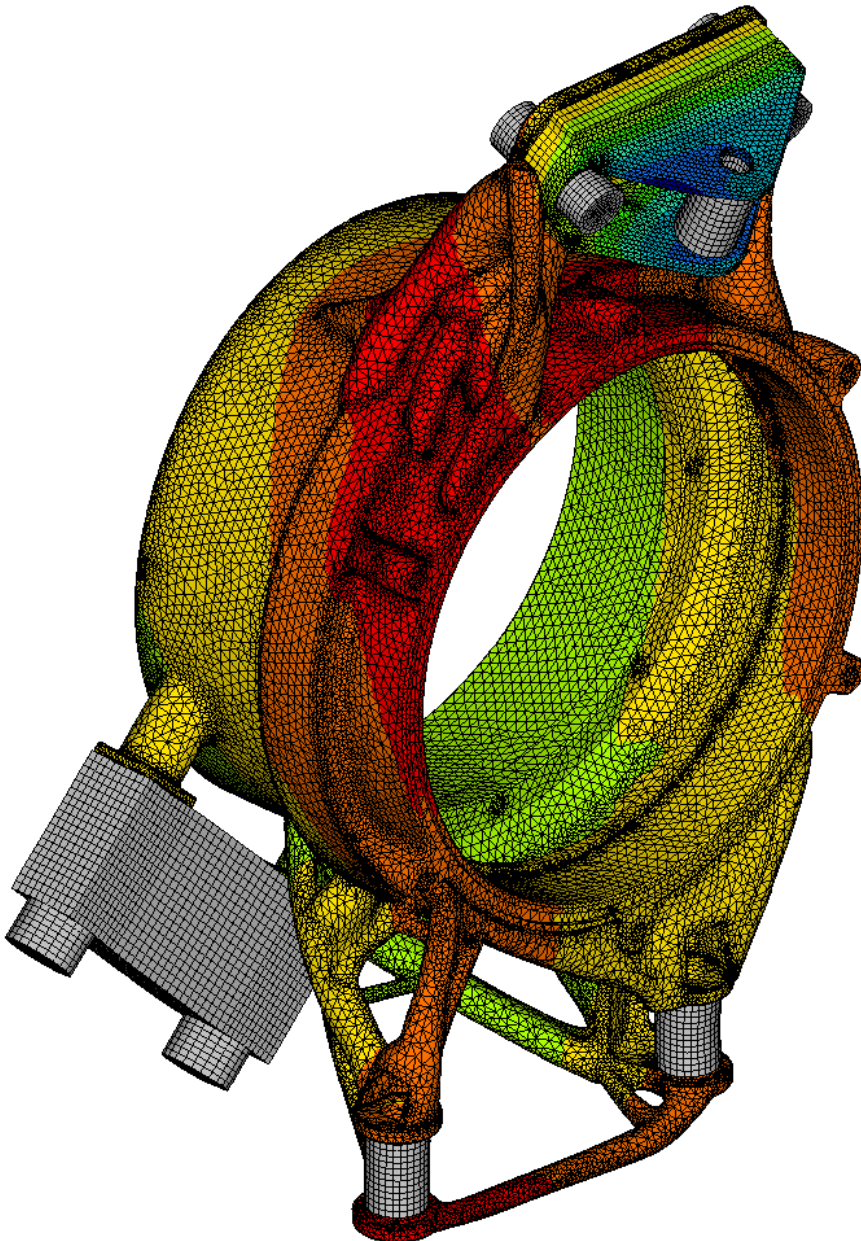
# Upright design

## FEM verification rear upright

Contour Plot  
Displacement(Mag)  
Analysis system

0.279
0.251
0.224
0.196
0.169
0.141
0.114
0.086
0.059
0.031

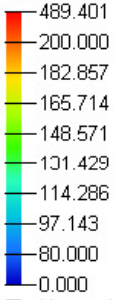
■ No result  
Max = 0.279  
Node 126542  
Min = 0.031  
Node 1181784



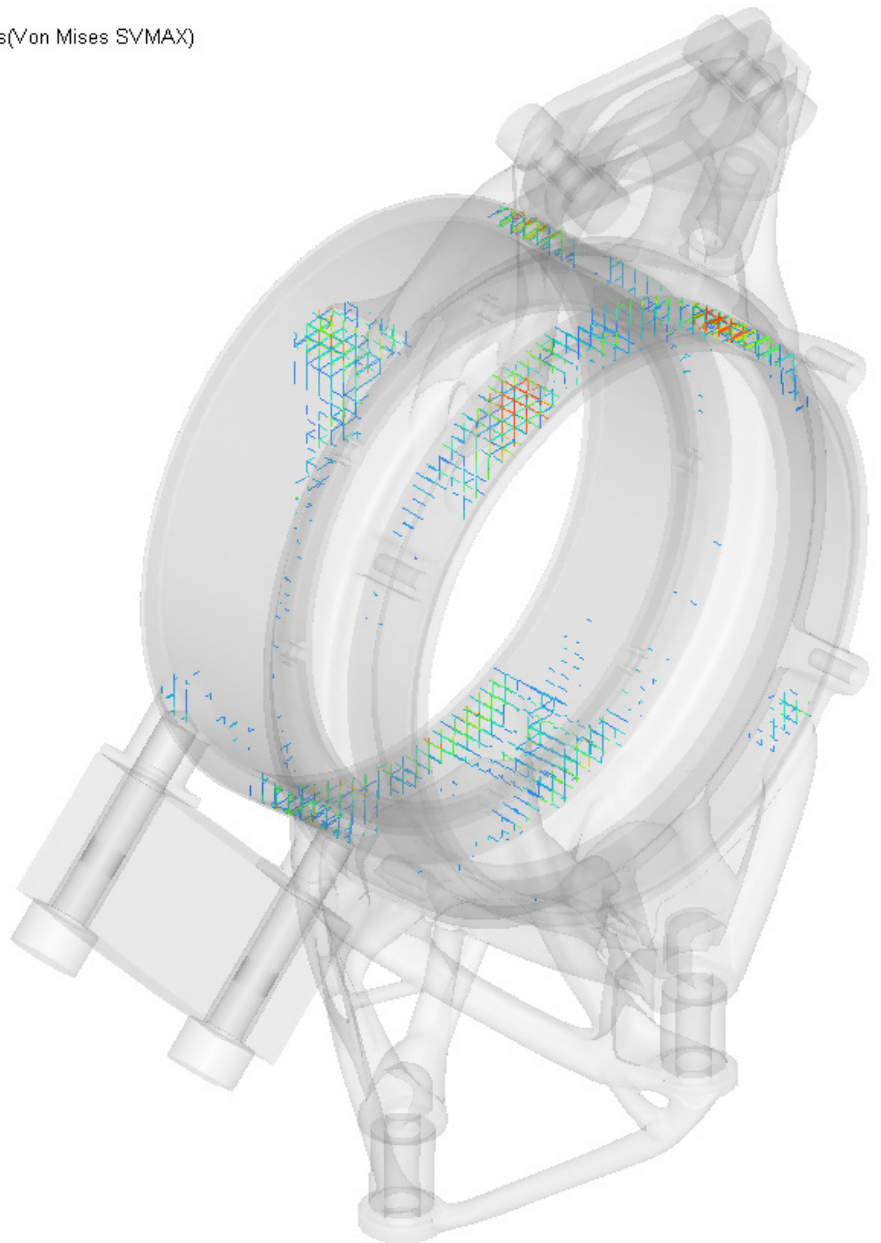
FEM verification of rear upright final design using the same methodology as for the front upright. Global deformation values are higher for the rear upright, but still within maximum allowable values. Topology optimization has

as such resulted in a very high stiffness to weight ratio in both the front and rear upright, minimizing compliance in regard to precise vehicle dynamics performance and smooth transmission operation.

Contour Plot  
CBAR/CBEAM von Mises Stresses(Von Mises SVMAX)



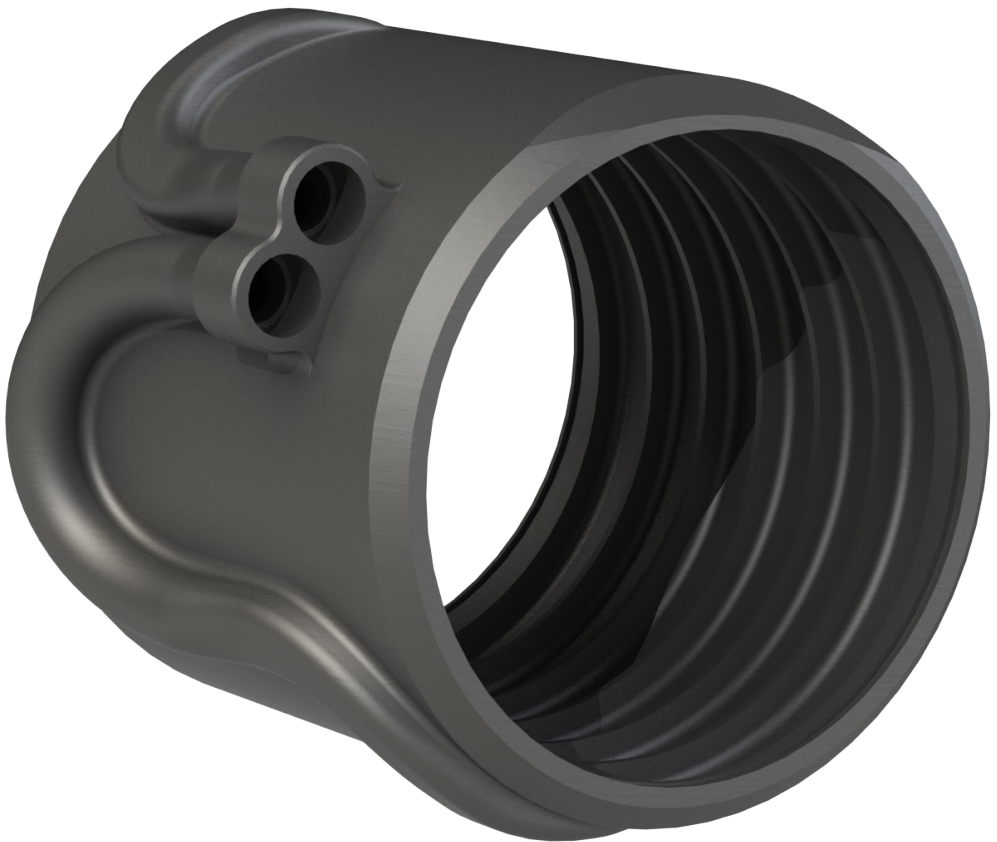
Max = 489.401  
Beam 1237419  
Min = 0.000  
Beam 1243079



*Stress plot for rear upright microstructure.*

# Final design

## Motor cooling block



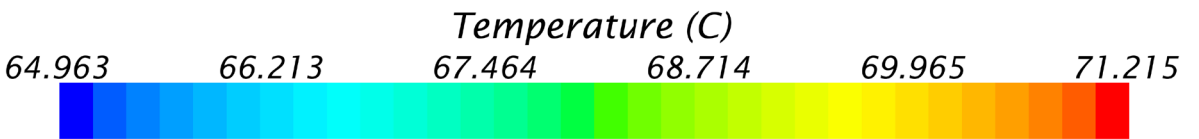
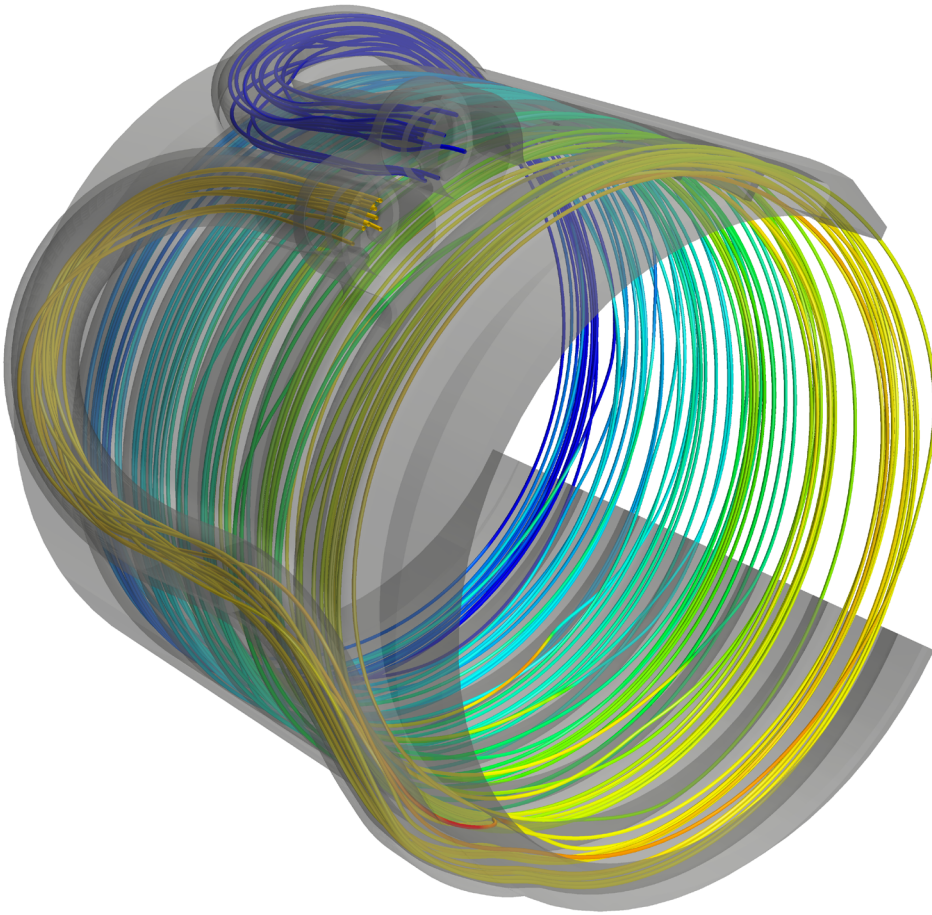
The motor cooling block was designed as 3D printed Nylon sleeve with a flow passage coiling helically around the radial surface of the motor. By using 3D printing in the manufacturing process, it was possible to wrap the inlet and outlet to the outside of the block, creating a common connection point.

The flow passage cross section and helix pitch was optimized by the cooling engineer in order to ensure minimal system pressure loss and

efficient motor cooling. This was done using a computational fluid dynamics (CFD) analysis tool called STAR CCM + supplied by CD Adapco.

The resulting product is a very light weight, easy to manufacture cooling block delivering efficient cooling performance to the four motors of the drivetrain. This will ensure sustained performance throughout the entirety of the endurance race part of the competition.





*Computational fluid dynamic analysis of motor cooling block using STAR CCM+.*

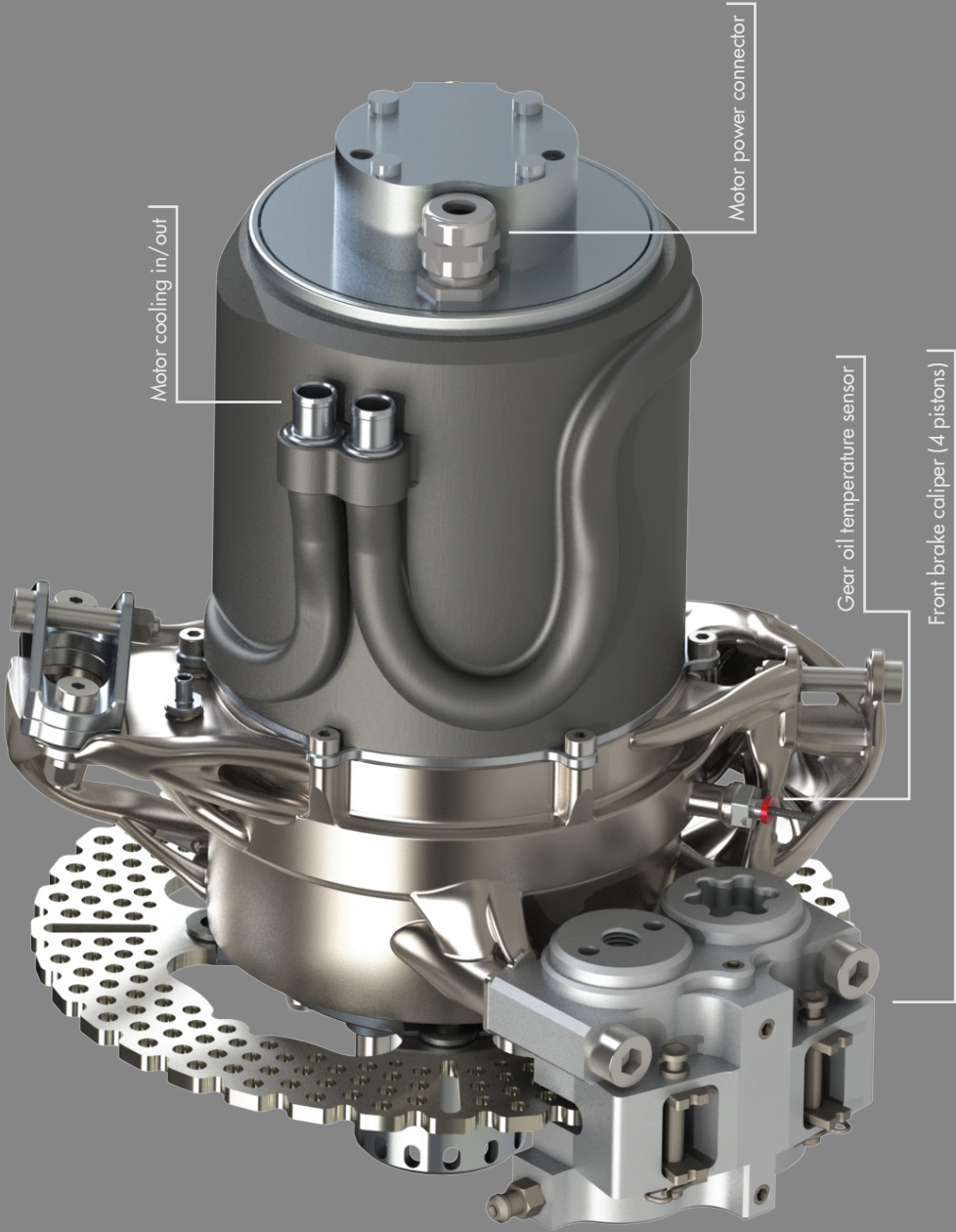
# Final design

## Front assembly



# Final design

## Front assembly



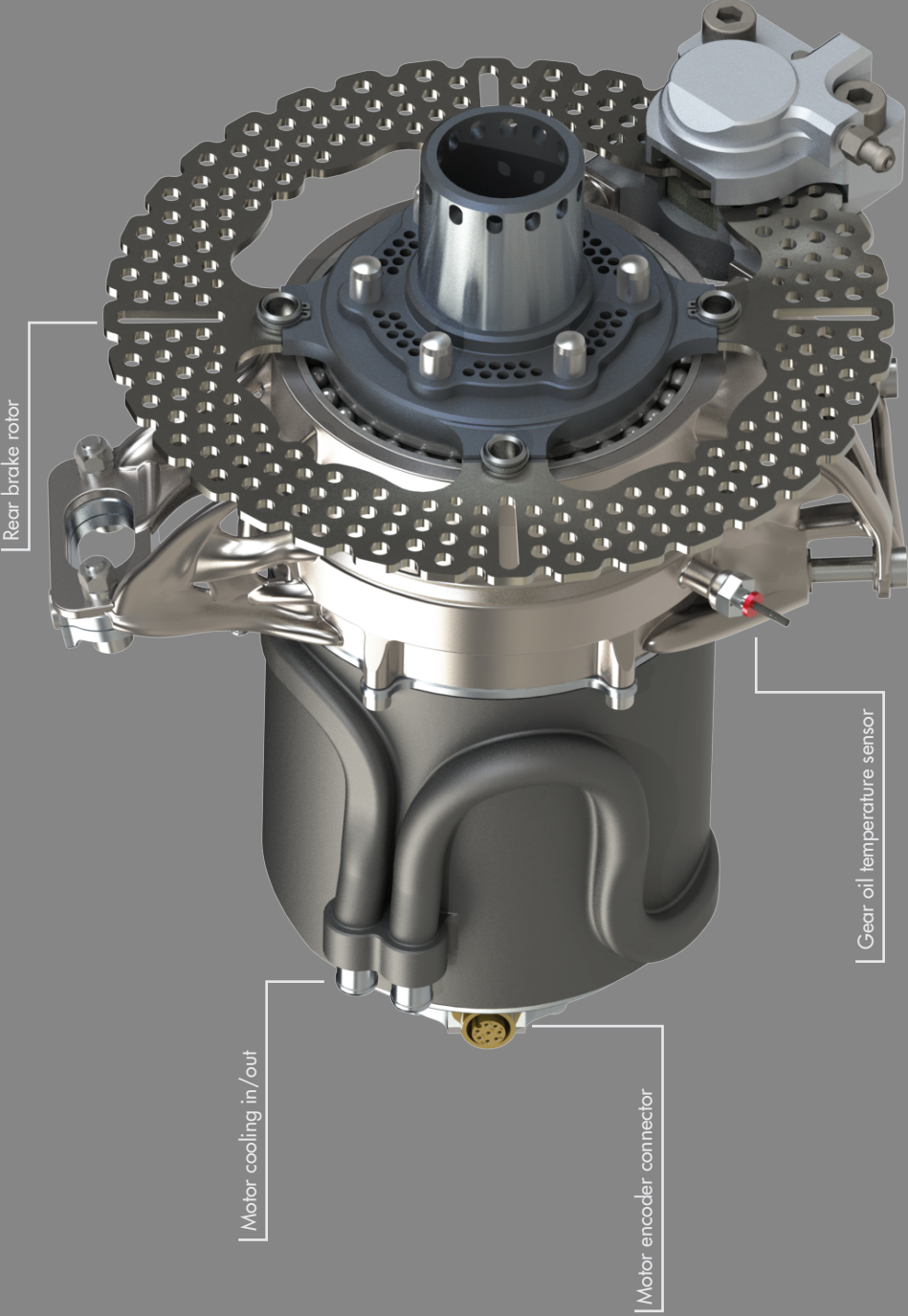
# Final design

## Rear assembly



# Final design

## Rear assembly





Front wheel



# Rear wheel

# Final design

Drivetrain and suspension layout



**148/197.5**

Peak power/Break horse power

**1303 Nm**

Peak torque





**24 kg**  
Total drivetrain weight

**2.2 s**  
0 to 100 kph

# Final design

## Hard data

<b>Moment of inertia 2015 RWD transmission system</b>					
Parts	$I$ [kg*cm <sup>2</sup> ]	$\omega$ [Rad/s]	$t$ [s]	T (local)[Nm]	T @ wheel[Nm]
Emrax 228	421	314	1,75	7,55	35,04
Motor shaft	2,06	314	1,75	0,04	0,17
2nd stage shaft	0,37	104,7	1,75	0,00	0,00
Differential	25	67,7	1,75	0,10	0,10
Tripod housing	5,25	67,7	1,75	0,02	0,02
Gear 1	0,46	314	1,75	0,01	0,04
Gear 2	8,12	104,7	1,75	0,05	0,08
Gear 3	3,82	104,7	1,75	0,02	0,04
Gear 4	18,61	67,7	1,75	0,07	0,07
Driveshaft	5,24	67,7	1,75	0,02	0,02
Hub	17,84	67,7	1,75	0,07	0,07
Total full car					<b>35,64</b>

Full transmission system rotating moment of inertia and torque required to accelerate from 0 to 55kph in 1.75 seconds for the RWD 2015 car.

<b>Moment of inertia 2016 4WD transmission system</b>					
Parts	$I$ [kg*cm <sup>2</sup> ]	$\omega$ [Rad/s]	$t$ [s]	T (local)[Nm]	T @ wheel[Nm]
AMK DD5-14-10	2,74	1047	1,75	0,16	2,54
Sun gear	0,004	1047	1,75	0,00	0,00
Planet gear 1 own	1,458	311,6	1,75	0,03	0,12
Planet gear 1 carrier	5,324	67,7	1,75	0,02	0,02
Planet gear 2 own	0,014	311,6	1,75	0,00	0,00
Planet gear 2 carrier	0,698	67,7	1,75	0,00	0,00
Carrier	1,093	67,7	1,75	0,00	0,00
Hub	3,157	67,7	1,75	0,01	0,01
Planet pin carrier	1,261	67,7	1,75	0,00	0,00
Total					2,70
Total full car					<b>10,82</b>

Full transmission system rotating moment of inertia and torque required to accelerate from 0 to 55kph in 1.75 seconds for the 4WD 2016 car.

<b>Drivetrain and in wheel component weight 2015 vs 2016 (new)</b>			
<b>Part</b>	<b>RWD 2015 (kg)</b>	<b>4WD 2016 (kg)</b>	<b>Change (kg)</b>
Motor	12,5	14,2	1,7
Motor cooling	0	0,52	0,52
Gears	1,721	2,392	0,671
Bearings	0,899	1,772	0,873
Shafts	0,554	0,468	-0,086
Differential	3,395	0	-3,395
Driveshafts	1,488	0	-1,488
Hubs	1,574	1,632	0,058
Uprights	1,34	2,1	0,76
Gearbox	3,529	0	-3,529
Misc.	1,112	0,784	-0,328
<b>Total</b>	<b>28,112</b>	<b>23,868</b>	<b>-4,244</b>

*Difference in weight of drivetrain and in wheel components for the 2WD 2015 system and the new 2016 4WD system.*

<b>General system parameters RWD (2015) vs 4WD (2016)</b>			
	<b>RWD (2015)</b>	<b>4WD (2016)</b>	<b>Change</b>
Peak Torque [Nm]	945	1303	358
Drivetrain efficiency @ peak torque (%)	<95	97,80	2,80
Unsprung mass (kg)	7,5	12,7	5,2
Total battery energy including KERS (kWh)	6,71	7,75	1,04

*Change in general system parameters from RWD in 2015 to the new 4WD system in 2016*

**37.7%**

Increase in peak torque

**17.8%**

System weight reduction

**70.6%**

Reduction in rotating inertia

**69.3%**

Increase in unsprung mass

**2.9%**

Increase in drivetrain efficiency

**15.5%**

Increase in total available energy

# Final design

## Evaluation of data

### **Rotating moment of inertia:**

A significant reduction in rotating moment of inertia was achieved with the new design. It is however apparent that 99% of the total rotational inertia of both systems are located in the motor. One can therefore conclude that the transmission systems can be considered equal in terms of rotating moment of inertia. Furthermore, the total inertia of both systems constitutes a small fraction of the total inertia of the car. The impact of the inertial improvement will therefore not have a large impact on performance.

### **Weight:**

Saving just shy of 18% in total system weight can be considered impressive in every respect. A 4.2kg weight reduction from 2015 at this level of engineering is never an easy task. We see that the predictions made during the conceptual phase has held true. The elimination of differentials, driveshafts and gearboxes is the primary reason for the weight reduction. Saving this amount of weight will result in significant performance improvement, both in acceleration, yaw response and general car handling.

### **Torque:**

The 37,7% increase in peak torque from 945Nm to 1303Nm is major. Paired with a significant improvement in total longitudinal tire grip, this can be seen as a revolution in acceleration performance.

### **Unsprung mass:**

Increasing unsprung mass by almost 70% was a predicted outcome based on the chosen concept. This will slow down the suspension system and thus reduce the tire to road contact performance on uneven surfaces. As we race on smooth tarmac, this may not have significant negative impact on performance. Yaw inertia has also increase as a result of more unsprung mass. This will result in a less yaw responsive vehicle. This will hopefully be counteracted by the torque vectoring yaw controller. Lastly, more unsprung mass will result in a slower steering response in the steering wheel. This may result a less controllable car in quick corners.

### **Drivetrain efficiency:**

Drivetrain efficiency has been increased by at least 2.9%. We say at least because there is no data for the efficiency of the differential or the constant velocity joints of the driveshafts from 2015. We are however very confident that our estimate for the total efficiency of the 2015 system is on the conservative side. A 2.9% improvement in efficiency directly affects total available energy for the endurance race.

### **Available energy:**

Kinetic energy regeneration from four wheel braking has resulted in an increase in available mechanical energy of 15.5%. This will significantly increase the pace in the endurance race, bringing us one step closer to competition victory.

# Final design

## Non quantifiable results

### **4WD:**

We know from lap time simulations that a 4WD car performs better than the 4WD concept performed better than the RWD concept in every respect. It still remains to be seen if the actual system performance is as expected and if the drivers are able to utilize the improvements in increasing their pace.

### **Torque vectoring:**

It remains to be seen how the torque vectoring system will affect overall performance. The key to significant improvements in vehicle dynamics will be if we are able to implement working yaw and traction control algorithms. Real world testing is needed to confirm if we have been successful in this endeavor. These results will therefore not be available before June at the earliest.

### **Education:**

The final result is a testament to the knowledge required to complete this project. From establishing system requirements, via advanced data analysis, creative conceptualization and design, to high level gear and structure simulations, this project has shown the true spirit of the Revolve NTNU slogan: "Theory

to practice". The fact that this is a subproject in a large overall project spanning over 50 participants, all with their own sub projects and performance goals, show the multidisciplinary, collaborative scale in designing the 2016 vehicle.

### **Innovation:**

The grade of innovation shown in this project is twofold. First, by developing, designing and prototyping an unconventional solution to a 4WD driveline using electrical actuators, we have created a product that has significant relevance to the near future of automotive design and engineering. Second, by using the most current design methods, software and manufacturing methods, we have taken small steps towards a future dominated by additive manufacturing.

### **Marketing:**

By designing an innovative and different driveline, we have further improved upon the uniqueness of the vehicle. This will hopefully further increase interest in the Revolve NTNU project, both from future participants and from possible sponsors.

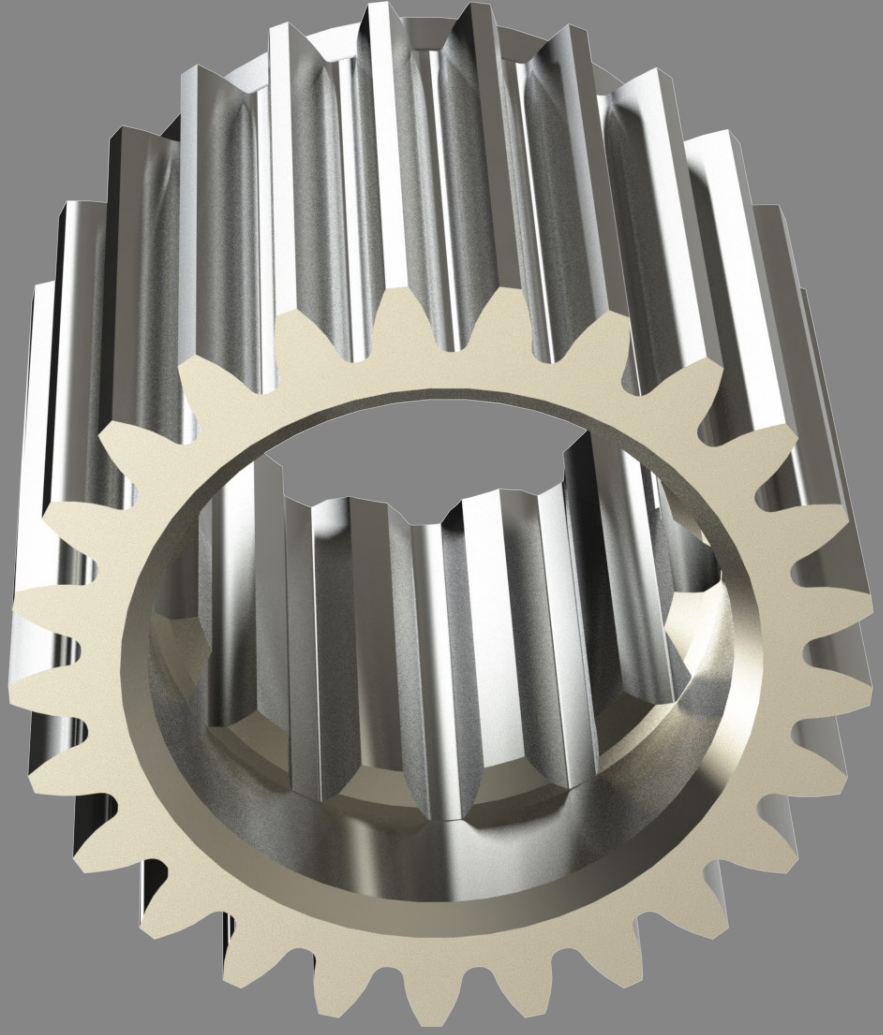
# Manufacturing design





# Sun gear

Manufacturing documentation



**Material:**  
NC310V (steel)

**Weight:**  
9.94 g

**Treatment:**  
Case hardening, carburizing and isotropic superfinishing.

**Machining method:**  
Turning, gear hobbing and gear grinding.

**Manufacturer:**  
PANKL



Gear data	
Reference profile	1.25 / 0.38 / 1.0 ISO 53.2:1997 Profil A
Number of teeth	25
Normal module	0.6
Tip diameter	16.309
Profile shift coef.	0.1094
Facewidth	12.5
Pressure angle	20 deg.
Tooth thickness tolerance	DIN 58405 6e
Quality (DIN 3961)	Q6
Profile and tooth trace modifications (symetric, both flanks)	
Tip relief, linear	Cca=8.000µm
	LCa=1.115mm
	dCa=15.686mm
Crowning	Cp=10.000µm (Crown=1953)
	CHb=-10.910µm
Helix angle modification, tapered or conical	
	Right flank Beta.eff=0.053°-right
	Left flank Beta.eff=0.053°-left

**Treatment:** Case hardened to 59.3 +- 1 HRC. Carburized to thickness 0.1-0.2 after grinding.

\*Carburizing + austenitizing at temperature 925 °C / 940 °C  
Time: 3 hours 30 minutes

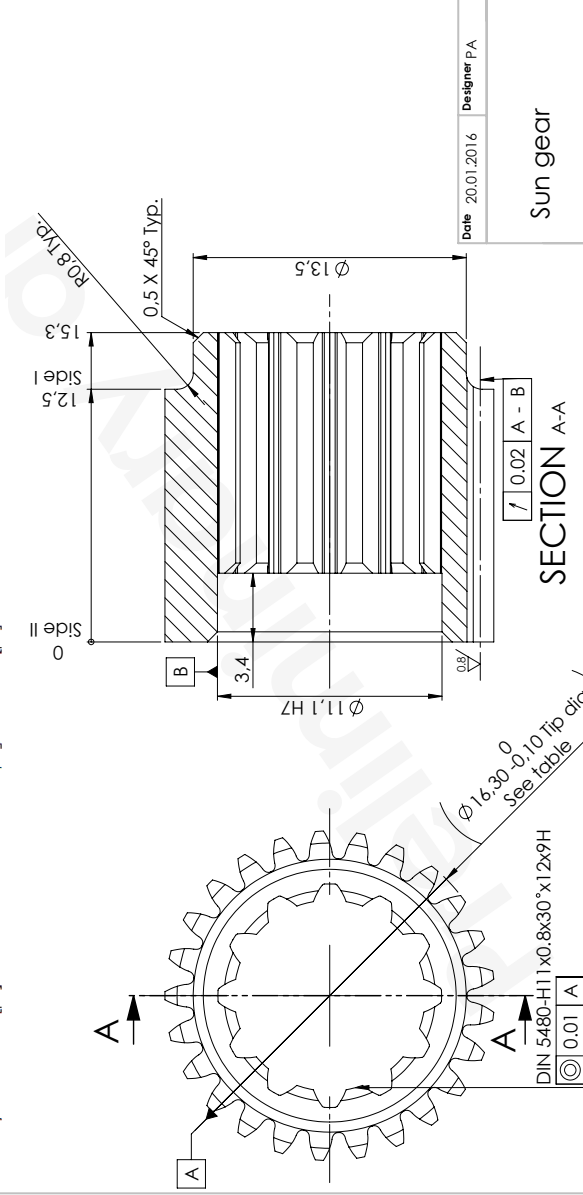
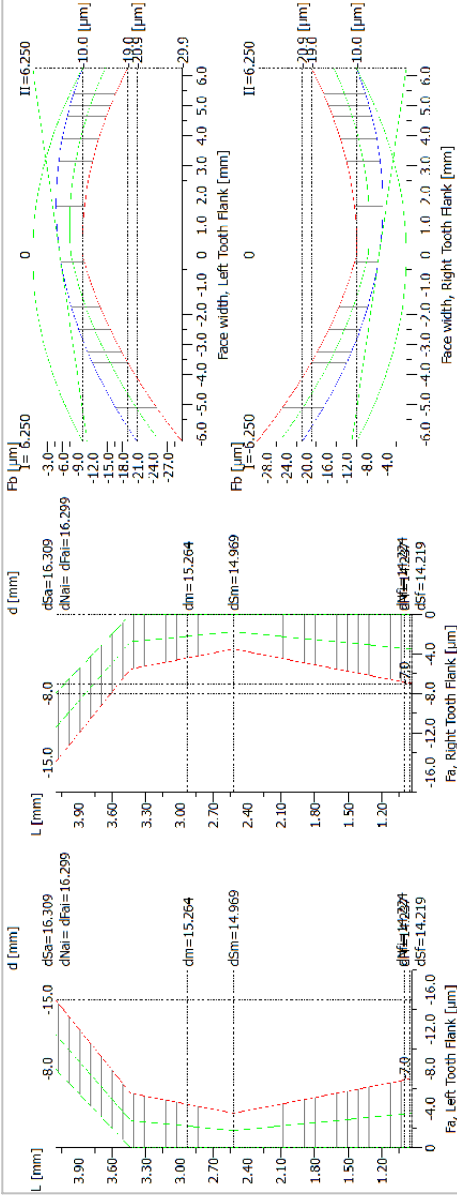
**Direct gas quench**

**Sub-zero at temperature -75 °C**  
Time: 2 hours

**Double tempering at temperature 300 °C**  
Time: 2 hours

\*This grade is containing high level of Si. Low Pressure carburizing is necessary. Else, a pre-oxidation phase is needed to remove the selective oxide passive layer and let the C diffuse.

No sharp edges.



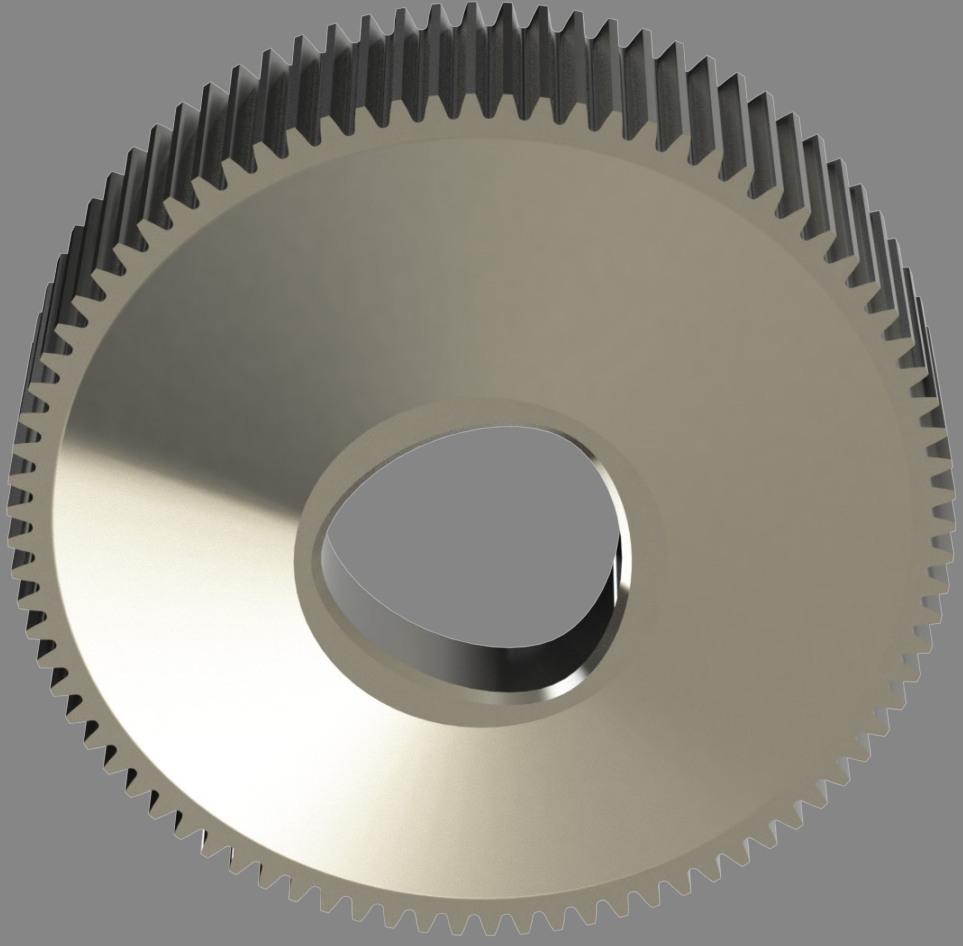
**SOLIDWORKS Student Edition.**  
**For Academic Use Only.**

Date	20.01.2016	Designer	PA	Checked by	TO	Approved by	Not Approved
Sun gear				Material	NC310YW	Weight	9.94g
				SCALE	5:1		
Contact info	Rev no			No of units	revolve		
Revolve Addis +4999459599	01			4			
Drawing N° DRW-0011	Sheet 1			of 1			

This drawing is confidential and it shall not be copied or shown to third party without the written consent of Revolve (INU).  
General tolerances: Mean: ISO 2768-1  
Mean: ISO 2768-2, ISO 286-2  
General surface finish: Ra 3.2

# Planet gear 1

Manufacturing documentation



**Material:**  
NC310V (steel)

**Weight:**  
122.72 g

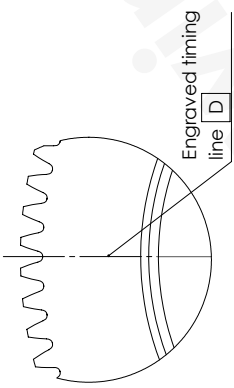
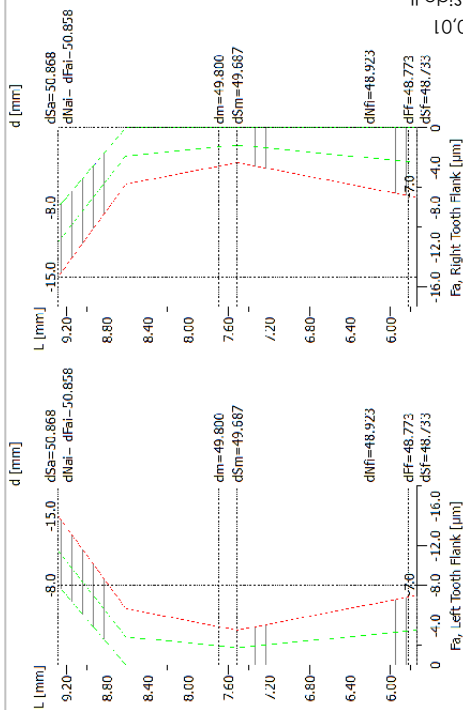
**Treatment:**  
Case hardening, carburizing and isotropic superfinishing.

**Machining method:**  
Turning, gear hobbing and gear grinding.

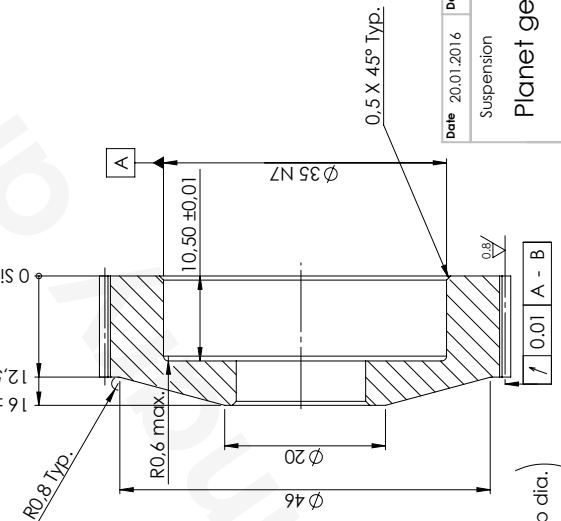
**Manufacturer:**  
PANKL

P3G-Profile DIN 32711-1:2009 H7/p6

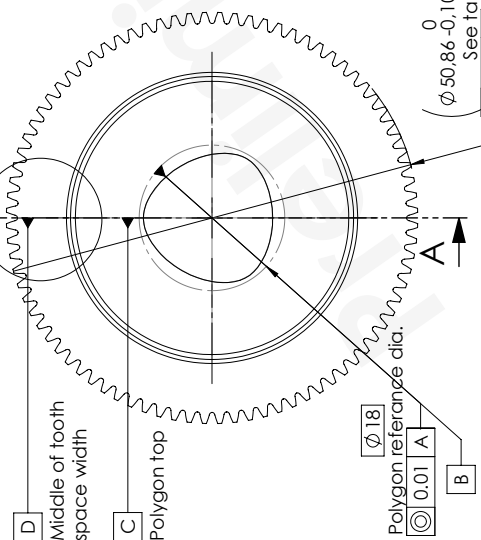
Mean circle	Ø 16 mm
Outer circle	Ø 17 mm
Inner circle	Ø 15 mm
Eccentricity	0.5 mm
Reference profile	1.25 / 0.38 / 1.0 ISO 53.2:1997 Profil A
Number of teeth	84
Normal module	0.6
Tip diameter	50.868
Profile shift coef.	-0.5915
Facewidth	12.5
Pressure angle	20 deg.
Tooth thickness tolerance	DIN 58405 6e
Quality (DIN 3961)	Q6
Profile and tooth trace modifications (symetric, both flanks)	
Tip relief, linear	Coa=8.000µm LCoa=1.115*mm dCa=50.401 mm



DETAIL D  
SCALE 4:1



Timing between polygon top and middle of tooth space width = 0° within 0.05 [C] [D]



SECTION A-A

**SOLIDWORKS Student Edition.**  
**For Academic Use Only.**

No sharp edges.

**Treatment:** Case hardened to 59.3 +- 1 HRC. Carburized to thickness 0.1-0.2 after grinding.  
\*Carburizing + austenitizing at temperature 925 °C / 940 °C  
Time: 3 hours, 30 minutes  
**Direct gas quench**  
Time: 2 hours  
**Sub-zero at temperature -75 °C**  
Time: 2 hours  
**Double tempering at temperature 300 °C**  
Time: 2 hours

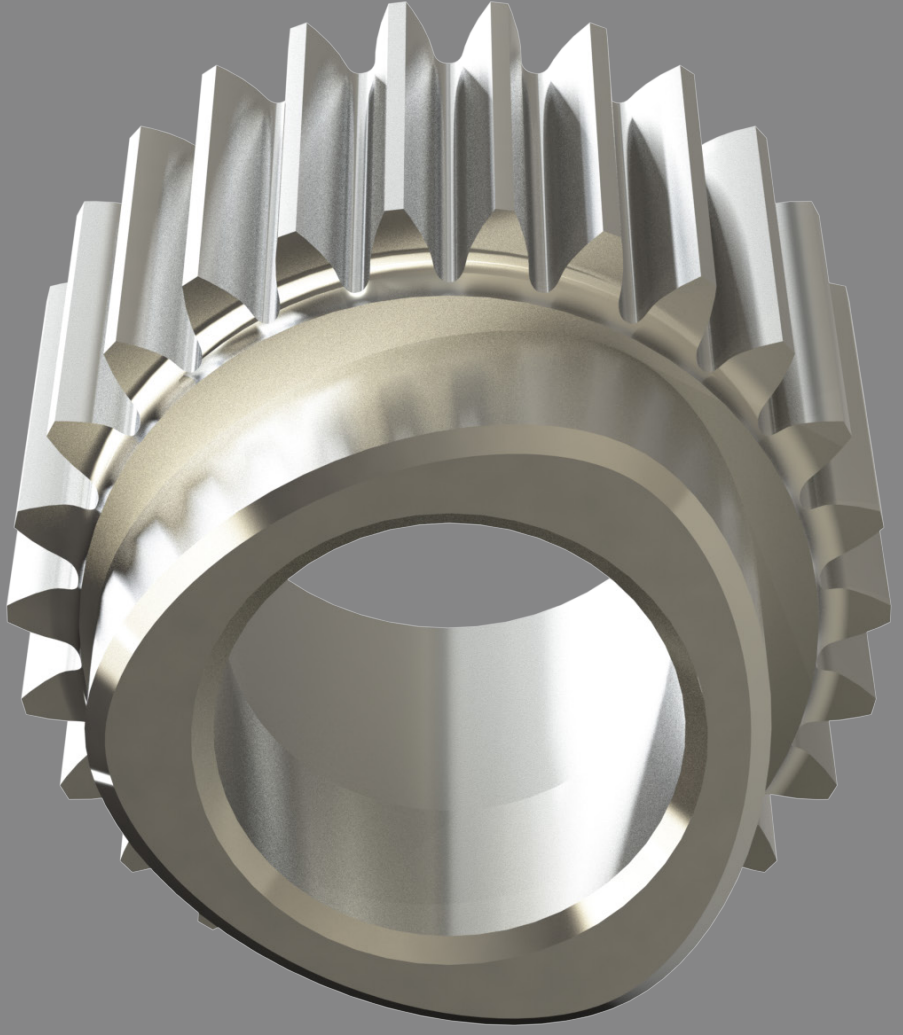
\*This grade is containing high level of Si. Low Pressure carburizing is necessary. Else, a pre-oxidation phase is needed to remove the selective oxide passive layer and let the C diffuse.

Date	20.01.2016	Designer	PA	Checked by	TO	Approved by	Not Approved
Suspension				Material	NC310YW	Weight	122.72g
Planet gear 1				SCALE	2:1		
Contact info	Rev no	No of units					
Phone: +49 799 459599	01	12					
Address: ...	Sheet 1	of 1					
Drawing N°: DRW-0012							

General tolerances: Mean: ISO 2768-1  
Mean: ISO 2768-2, ISO 286-2  
Surface finish: ISO 131, Ra 0.2  
General surface finish: Ra 3.2

# Planet gear 2 (0, 120 and 240 deg.)

## Manufacturing documentation



**Material:**  
NC310V (steel)

**Weight:**  
20.82 g

**Treatment:**  
Case hardening, carburizing and isotropic superfinishing.

**Machining method:**  
Turning, gear hobbing and gear grinding.

**Manufacturer:**  
PANGL

Gear data	
Reference profile	1.25 / 0.38 / 1.0 ISO 53.2:1997 Profil A
Number of teeth	26
Normal module	0.75
Tip diameter	21.418
Profile shift coef.	0.2749
Facewidth	13
Pressure angle	20 deg.
Tooth thickness tolerance	DIN 58405 6e
Quality (DIN 3961)	Q6
Profile and tooth trace modifications (symetric, both flanks)	
Tip relief, arc-like	Caa=16.000µm Lca=0.999*mm dca=20.697mm
Crowning	Cb=10.000µm rcrow=2113mm
Helix angle modification, tapered or conical	Chb=4.487µm Right flank beta.eff=0.021 °-left left flank beta.eff=0.021 °-right
Tip modification, rounding (transverse)	rk=0.3mm

**Treatment:** Case hardened and carburized to 59.3 +- 1 HRC. Hardening depth 0.13-0.25 after grinding.

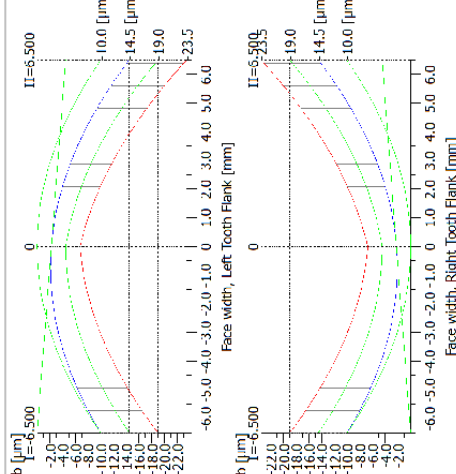
\*Carburizing + austenitizing at temperature 925 °C / 940 °C  
Time: 3 hours 30 minutes

**Direct gas quench**  
Time: 2 hours

**Sub-zero at temperature -75 °C**  
Time: 2 hours

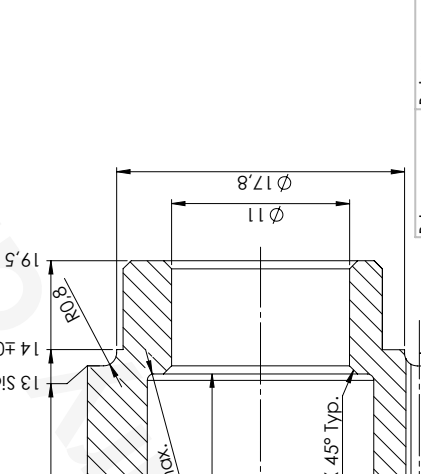
**Double tempering at temperature 300 °C**  
Time: 2 hours

\*This grade is containing high level of Si. Low Pressure carburizing is necessary. Else, a pre-oxidation process is required to create a protective selective oxide passive layer and let the C diffuse.



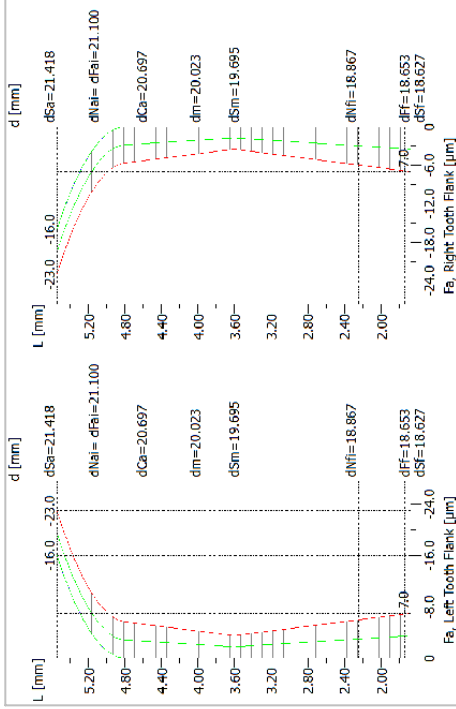
DETAIL C

Timing between polygon top and middle of tooth= 0° within 0.05 | C | D



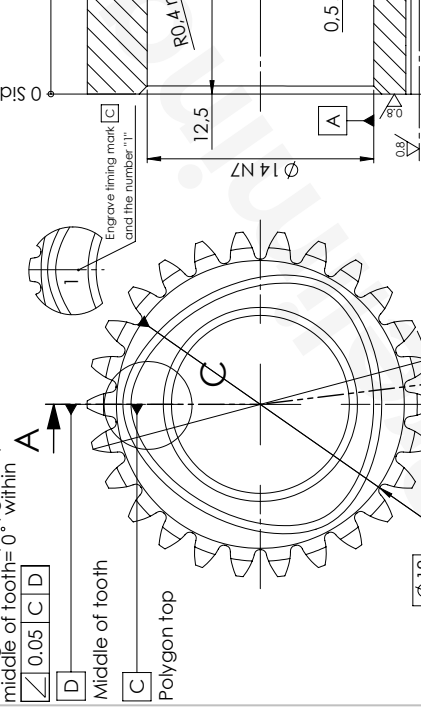
SECTION A-A

SECTION A-A	
P3G-Profile	DIN 32711-1:2009 H7/p6
Mean circle	Ø 16 mm
Outer circle	Ø 17 mm
Inner circle	Ø 15 mm
Eccentricity	0.5 mm
General tolerances:	Mean: ISO 2768-1 Mean: ISO 2768-2, ISO 286-2 Surface finish: ISO 131, Ra 0.2 General surface finish: Ra 3.2



DETAIL C

Timing between polygon top and middle of tooth= 0° within 0.05 | C | D



SECTION A-A

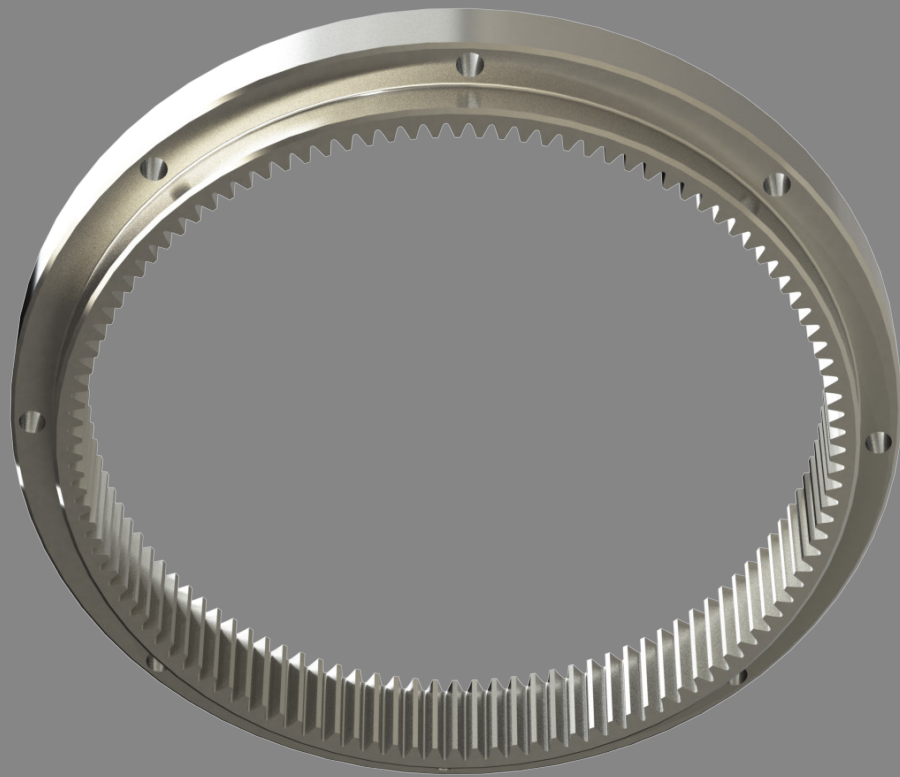
SECTION A-A	
P3G-Profile	DIN 32711-1:2009 H7/p6
Mean circle	Ø 16 mm
Outer circle	Ø 17 mm
Inner circle	Ø 15 mm
Eccentricity	0.5 mm
General tolerances:	Mean: ISO 2768-1 Mean: ISO 2768-2, ISO 286-2 Surface finish: ISO 131, Ra 0.2 General surface finish: Ra 3.2

Date	20.01.2016	Designer	PA	Checked by	TO	Approved by	Not Approved
<b>Planet gear 2 0deg</b>							
Material	NC310YW			Weight	20.629		
SCALE	4:1						
Rev no	01			No of units	4		
Sheet 1	of 1						
Contact info				<b>revolve</b>			
E: sales@revolve.com							
T: +49 794 659599							
Drawing N°				DRW-0013			

**SOLIDWORKS Student Edition.**  
**For Academic Use Only.**

# Ring gear

Manufacturing documentation



**Material:**  
NC310V (steel)

**Weight:**  
157.93 g

**Treatment:**  
Case hardening, carburizing and isotropic superfinishing.

**Machining method:**  
Turning and gear hobbing.

**Manufacturer:**  
PANKL

Gear data	
Reference profile	1.25 / 0.38 / 1.0 ISO 53.2:1997 Profil A
Number of teeth	-112
Normal module	0.75
Tip diameter	-83.218
Profile shift coef.	-0.4784
Facewidth	13
Pressure angle	20 deg.
Tooth thickness tolerance	DIN 58405 7e
Quality (DIN 3961)	Q7
Profile and tooth trace modifications (symetric, both flanks)	
Tip modification, rounding (transverse)	rk=0.3mm

**Treatment:** Case hardened to 59.3 +/- 1 HRC. Carburized to thickness 0.13-0.25 after grinding.

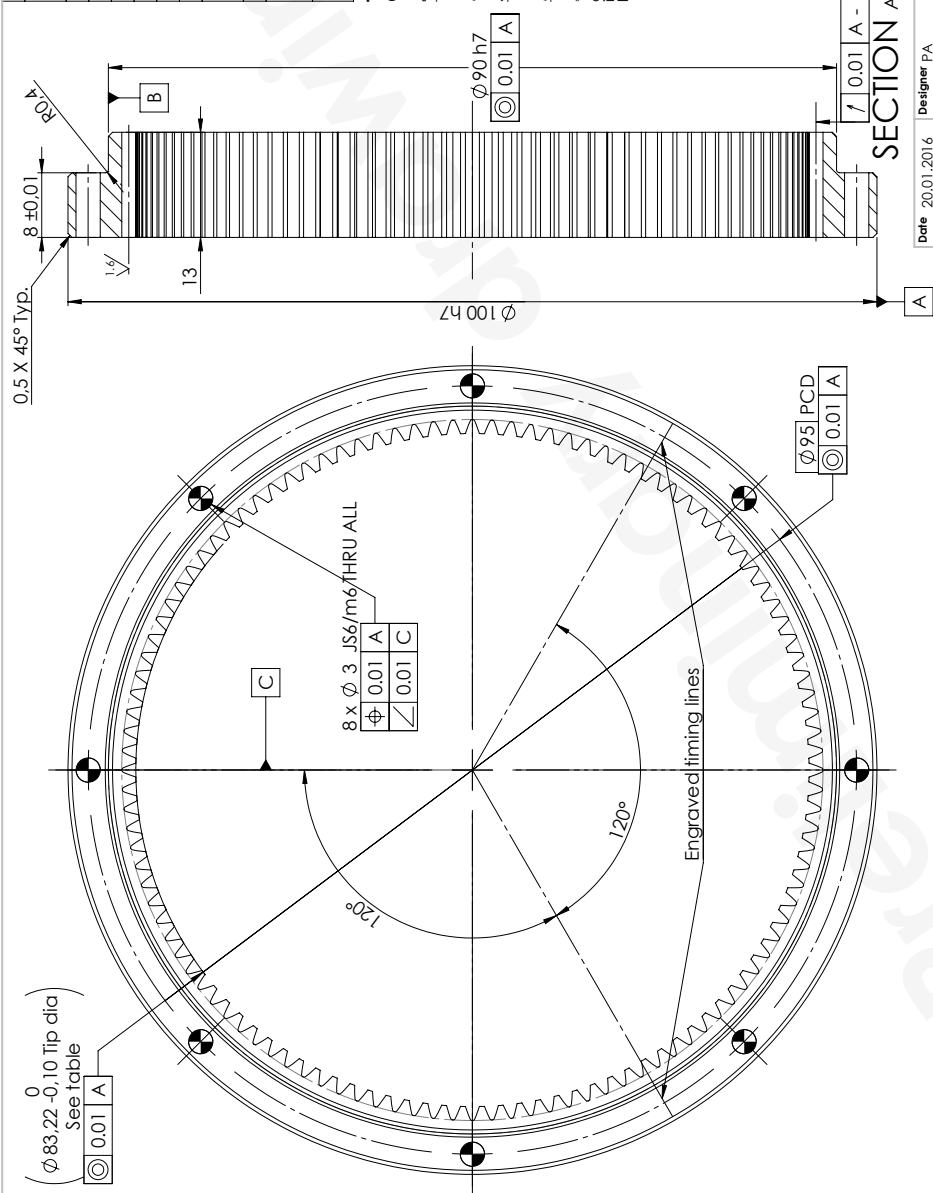
\***Carburizing + austenitizing at temperature 925°C / 940°C**  
Time: 3 hours, 30 minutes

**Direct gas quench**  
Time: 2 hours

**Sub-zero at temperature -75°C**  
Time: 2 hours

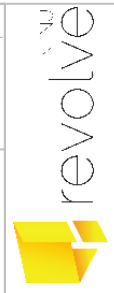
**Double tempering at temperature 300°C**  
Time: 2 hours

\*This grade is containing high level of Si. Low Pressure carburizing is necessary. Else, a pre-oxidation phasis is needed to remove the selective oxide passive layer and let the C diffuse.



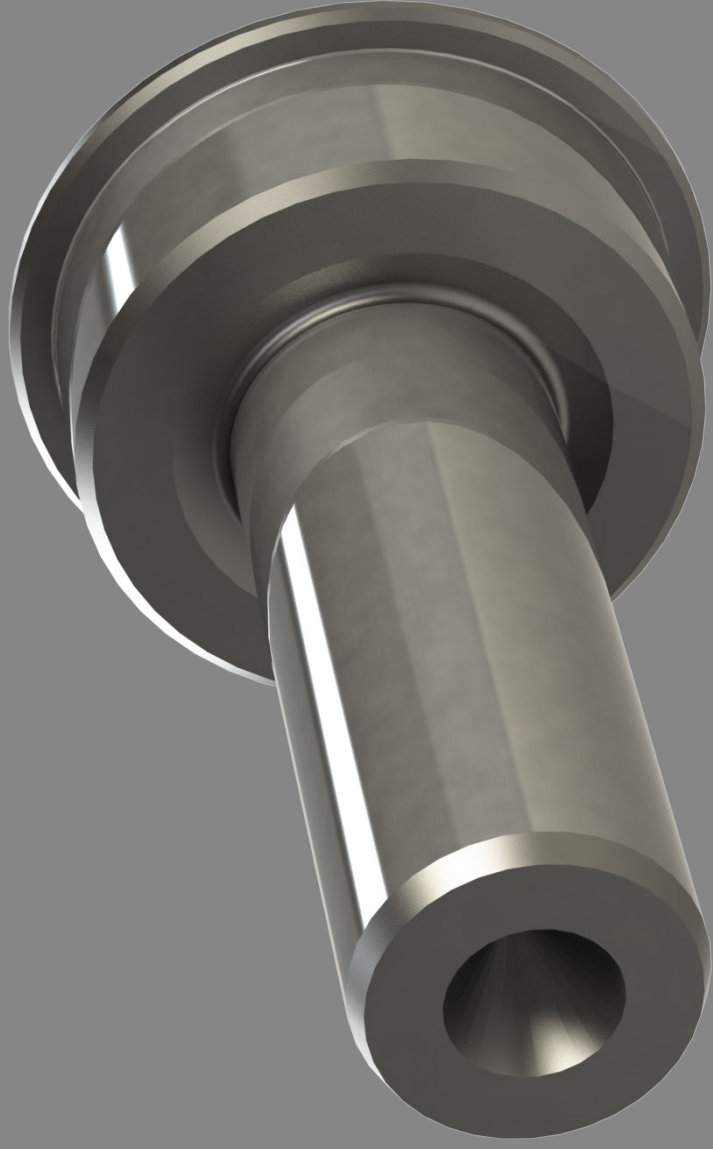
Date	20.01.2016	Designer	PA	Checked by TO	No	Approved by	Not Approved
Suspension Ring gear				Material	NC310YW	Weight	157.93g
Contact info Egeer Adams +4799469599				SCALE	2:1		
Drawing N° DRW-0016				Rev no	01	No of units	4
General tolerances: Mean: ISO 2768-1 Mean : ISO 2768-2, ISO 286-2, 0.2 General surface finish: Ra 3.2				Sheet 1		of 1	

**SOLIDWORKS Student Edition.**  
**For Academic Use Only.**



# Planet pin shaft

Manufacturing documentation



**Material:**  
16NiCr4 (steel)

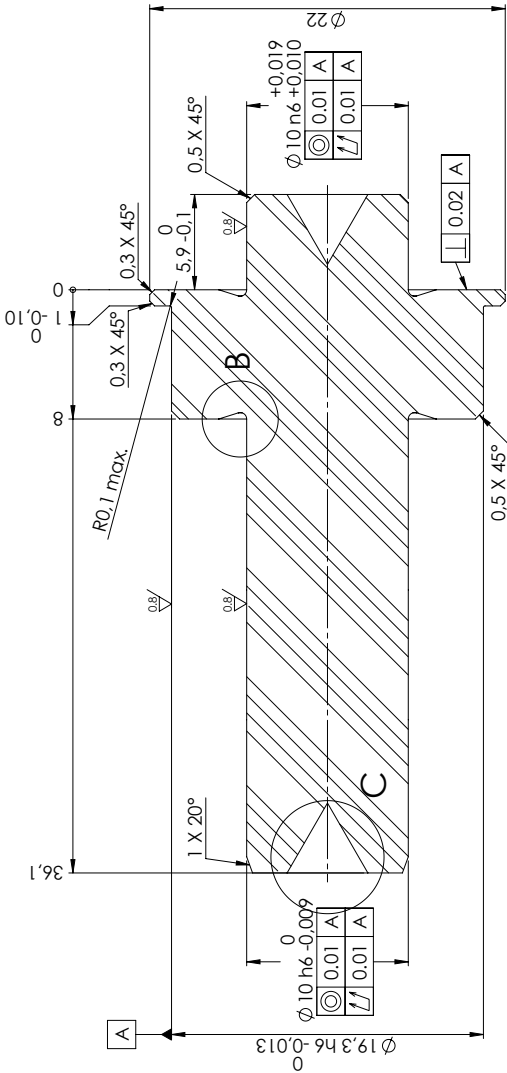
**Weight:**  
38.92 g

**Treatment:**  
Case hardening and carburizing.

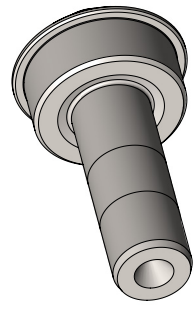
**Machining method:**  
Turning and grinding.

**Manufacturer:**  
Sandvik Teeness

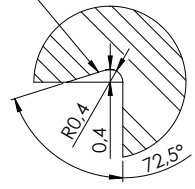




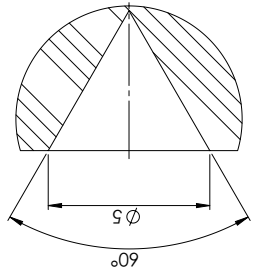
SECTION A-A



DIN 509 Type G  
(Identical on both sides)






DETAIL B  
SCALE 8 : 1



Center tap both sides

DETAIL C  
SCALE 8 : 1

Heat treatment:  
Case hardened to surface hardness of 60 HRC.  
No sharp edges.

Date	03.02.2016	Designer	FA	Checked by	TO	Yes	Approved by	anders.hauglid
Suspension		Planet pin shaft		Material	1.3714 (1.6NiCr4)		Weight	38.729
Contact info		Egil August Aune		SCALE	4:1			
+4799459599		Rev no	01	No of units	12			
DRW-0063		Sheet 1	of		1			

This drawing is confidential and it shall not be copied or shown to third party without the written consent of Revolve NTNU.  
General tolerances: Mean: ISO 2768-1  
Mean: ISO 2768-2, ISO 286-2, ISO 286-3  
General surface finish: Ra 3.2

**SOLIDWORKS Student Edition.**  
**For Academic Use Only.**

# Hub

## Manufacturing documentation



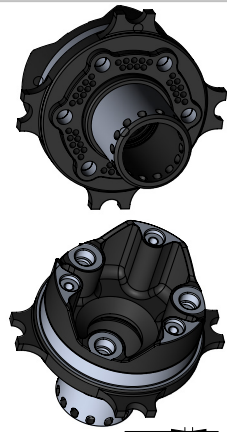
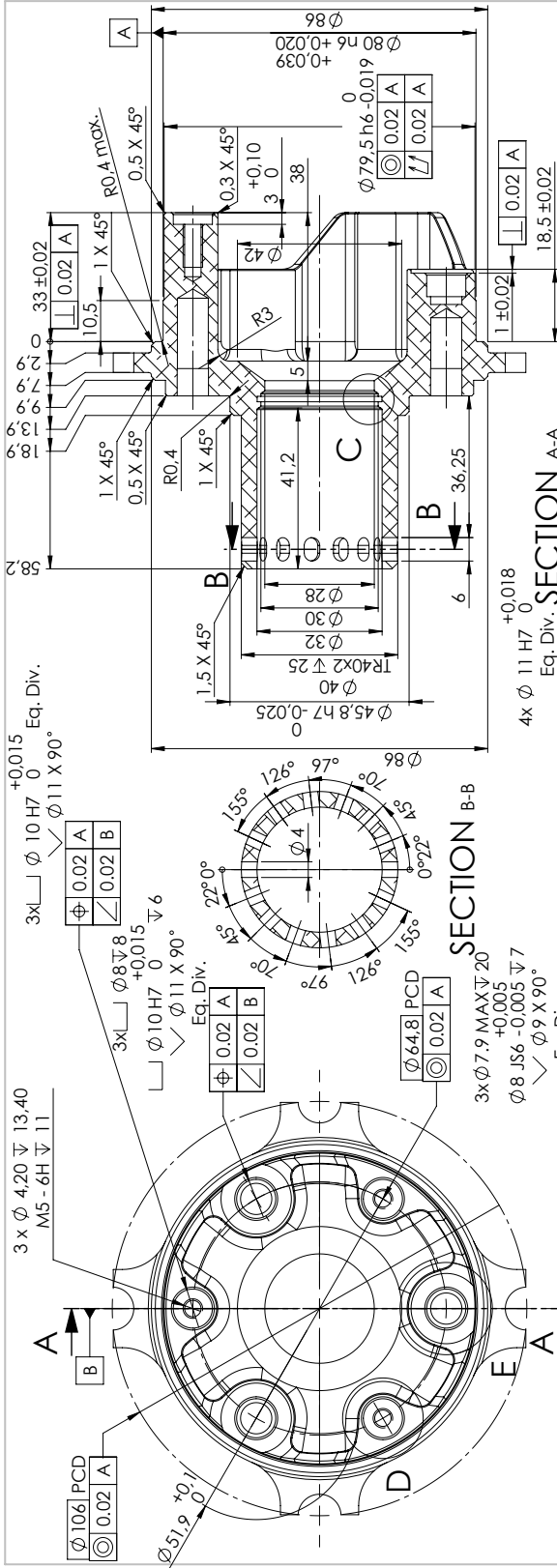
**Material:**  
Uddeholm Alumecc 89

**Weight:**  
307.4 g

**Treatment:**  
Partial hard coat oxide layer.

**Machining method:**  
Turning and milling.

**Manufacturer:**  
Sandvik Teeness and Ahlins (Oxide treatment)



Unspecified parts of the model has to comply with  $\square 0.1 | A | B$ .  
No sharp edges.

Date	03.02.2016	Designer	PA	Checked by	TO	Yes	Approved by	jens.mildestveit
Material		Alumic 89		Weight		307,40g		
Scale		1:1		No of units		2		
Contact info		Ege A/S +4799459599		Sheet 1		of 1		
Drawing N°		DRW-0059		Rev no		01		



Suspension Hub

General tolerances: Mean: SO 27/68-1  
Mean: SO 27/68-2, SO 28/6-2  
Mean: SO 27/68-3, SO 28/6-3  
General surface finish: Ra 3.2

This drawing is confidential and it shall not be copied or shown to third party without the written consent of Revolve NTNU.

**SOLIDWORKS Student Edition.**  
**For Academic Use Only.**

# Planet carrier

Manufacturing documentation



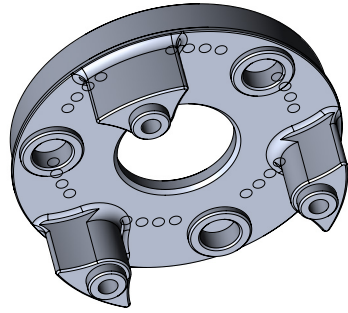
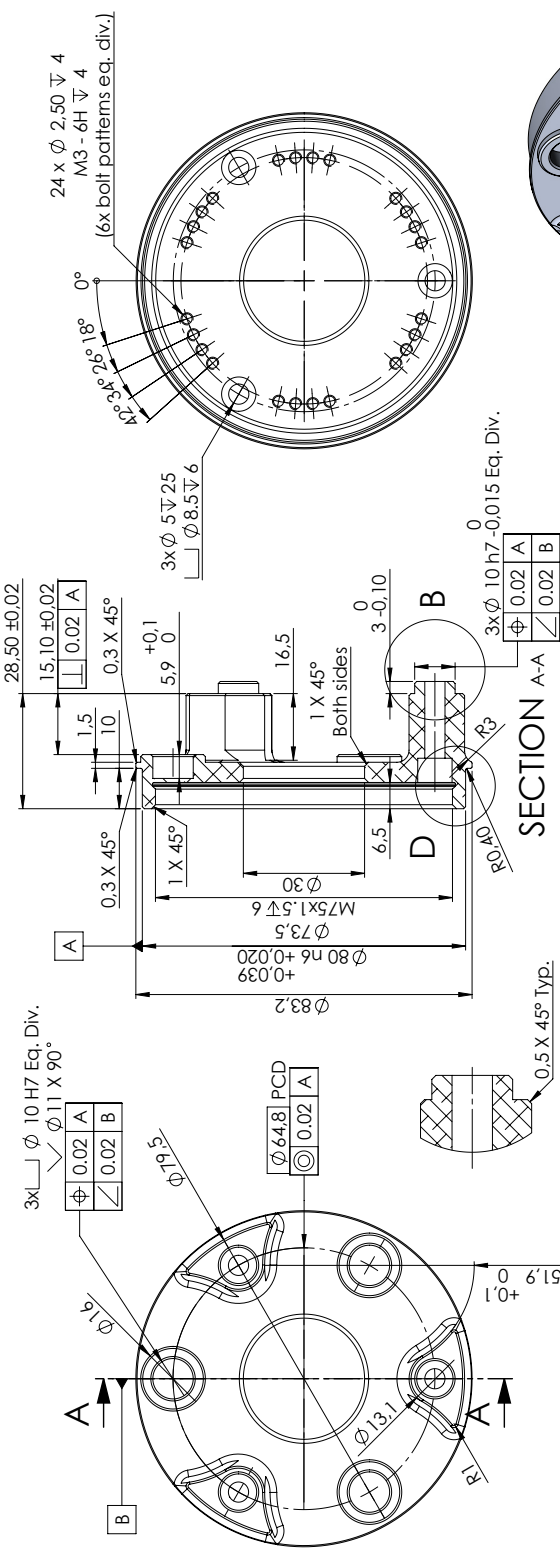
**Material:**  
Uddeholm Alumecc 89

**Weight:**  
100.79 g

**Treatment:**  
None.

**Machining method:**  
Turning and milling.

**Manufacturer:**  
Sandvik Teeness



Unspecified parts of the model has to comply with [0.1 | A | B].  
No sharp edges.

Date	04.02.2016	Designer	PA	Checked by	TO	Y	65	Approved by	jens.mildestveit
Suspension		Planet Carrier		Material	Alumec 89		Weight	100.79g	
Contact info		Ege August Aune +4799469899		SCALE	1:1				
Drawing N°		DRW-0066		No of units	4				
Rev no		01		Sheet 1		of 1			

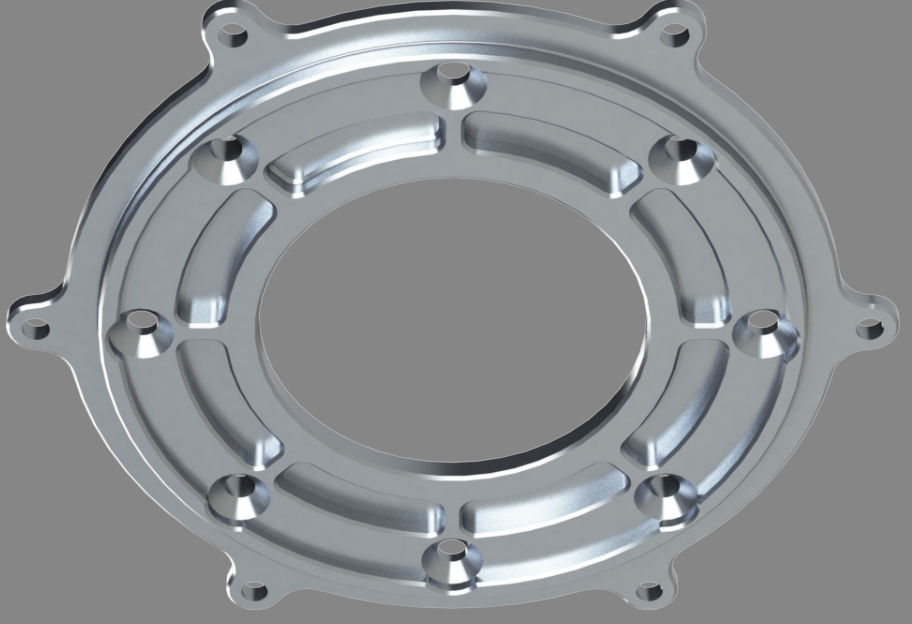
**SOLIDWORKS Student Edition.**  
**For Academic Use Only.**

This drawing is confidential and it shall not be copied or shown to third party without the written consent of Revolve NTNU.

General tolerances: Mean: ISO 2768-1  
Mean : ISO 2768-2, ISO 2865-2, 0.2  
General surface finish: Ra 3.2

# Motor adapter plate

Manufacturing documentation



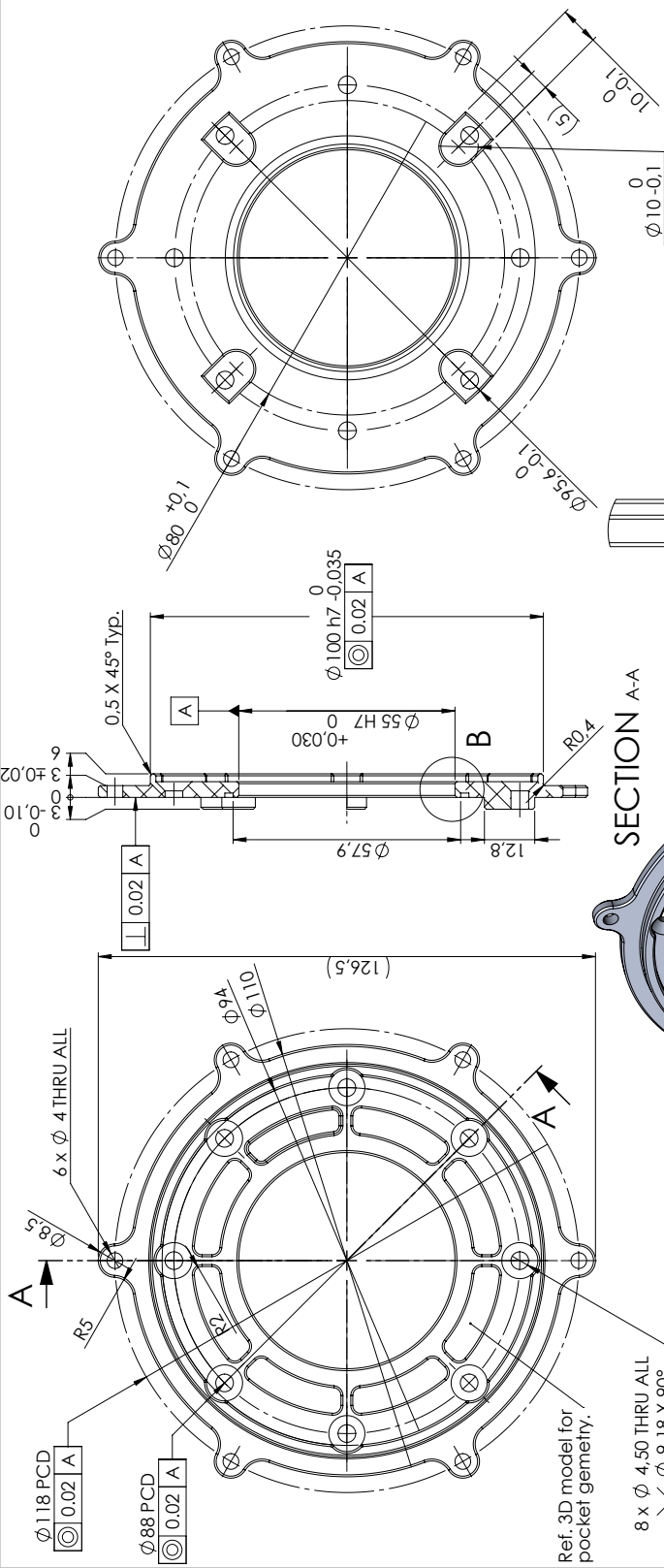
**Material:**  
Uddeholm Alumecc 89

**Weight:**  
71.71 g

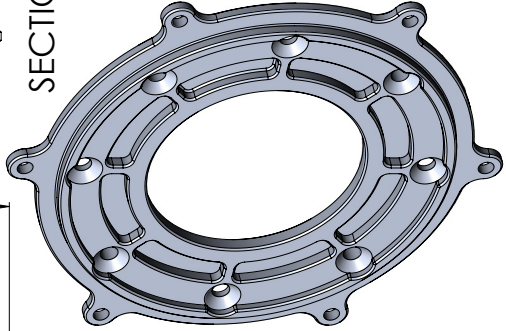
**Treatment:**  
None

**Machining method:**  
Milling

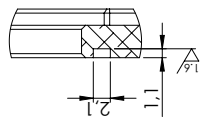
**Manufacturer:**  
Sandvik Teeness



SECTION A-A



DETAIL B  
SCALE 2 : 1



No sharp edges.

Date	03.02.2016	Designer	PA	Checked by	TD	Yes	Approved by	anders.hauglid
Suspension	Motor adapter plate							
Material	Alumec 89							
Weight	71.71g							
SCALE	1:1							
Rev no	01							
No of units	4							
Sheet 1	of 1							
Contact info	Feder August Aune +4779469399							
Drawing N°	DRW-0065							

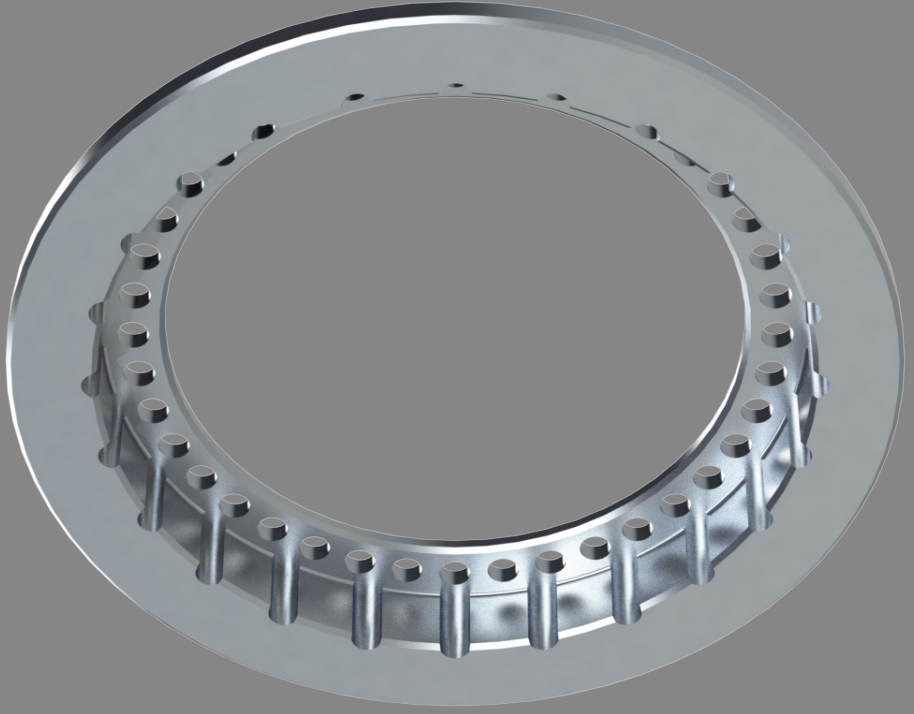
**SOLIDWORKS Student Edition.**  
**For Academic Use Only.**



This drawing is confidential and it shall not be copied or shown to third party persons or companies without the written consent of Revolve NTNU.  
 General tolerances: Mean: ISO 2768-1  
 Mean : ISO 2768-2, ISO 286-2  
 General radius tolerance:  $\sqrt{0.2}$   
 General surface finish: Ra 3.2

# Pretention nut

Manufacturing documentation



**Material:**  
Uddeholm Alumec 89

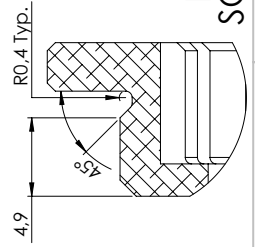
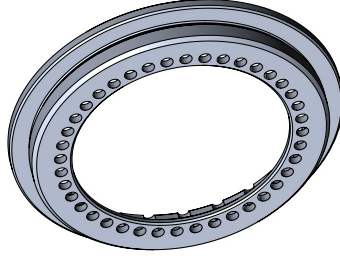
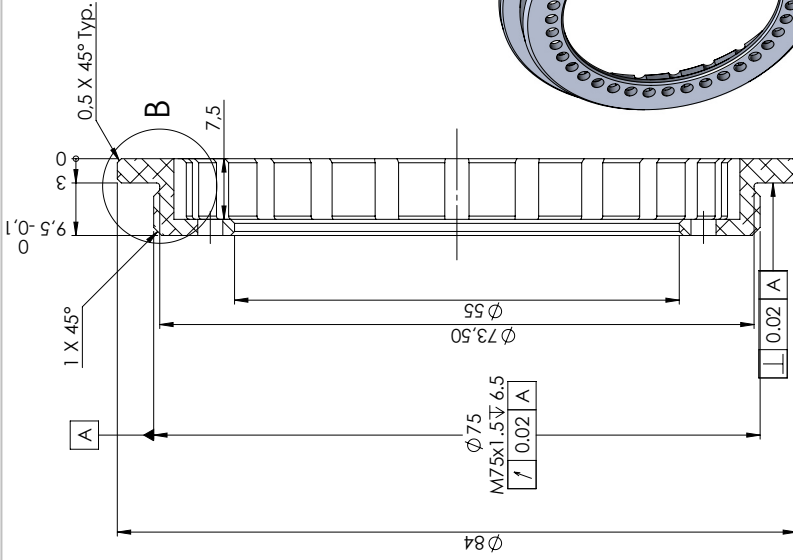
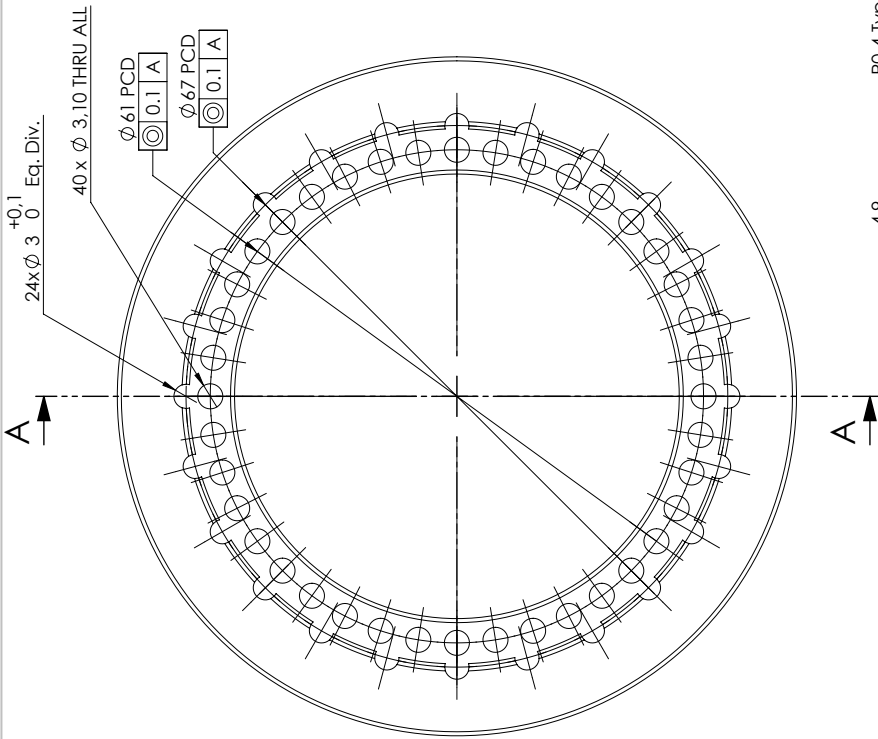
**Weight:**  
36.23 g

**Treatment:**  
None

**Machining method:**  
Turning

**Manufacturer:**  
Sandvik Teeness





**DETAIL B**  
**SCALE 4 : 1**

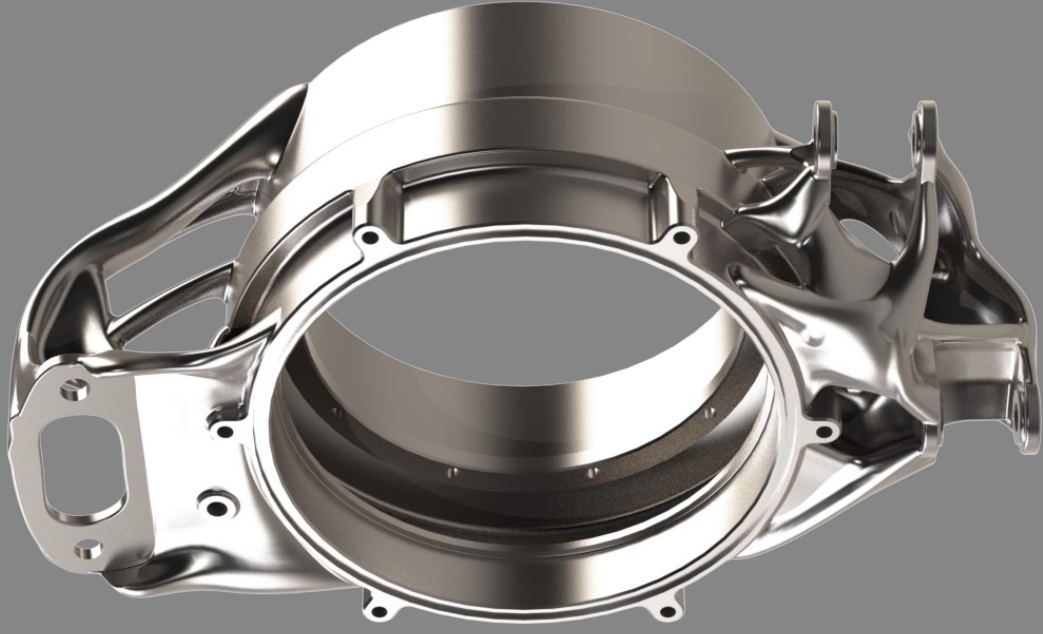
This drawing is confidential and it shall not be copied or shown to third party without the written consent of Revolve NTNU.  
 General tolerances: Mean: ISO 2768-1  
 Mean: ISO 2768-2, ISO 286-2, 0.2  
 General surface finish: Ra 3.2

Date	04.02.2016	Designer	PA	Checked by	TO	Yes	Approved by	jens.mildestveit	
Suspension		Pretension nut		Material		Alumec 89	Weight		35.23g
Contact info		E-post: august@une		SCALE		2:1	NTNU		revolve
Drawing N°		DRW-0068		Rev no		01	No of units		4
				Sheet 1		of		1	

**SOLIDWORKS Student Edition.**  
**For Academic Use Only.**

# Front upright

Manufacturing documentation



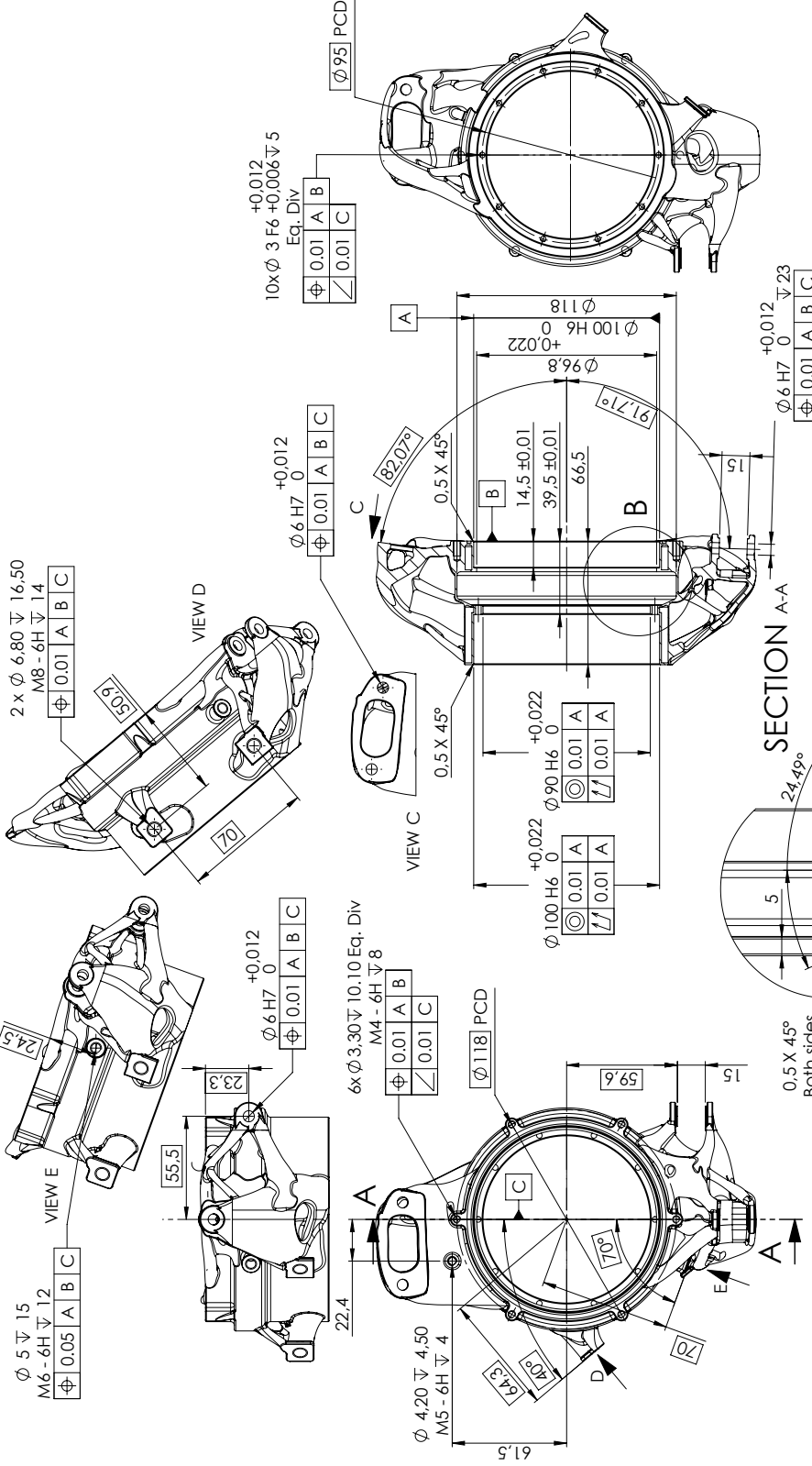
**Material:**  
Ti-6Al-4V

**Weight:**  
515 g

**Treatment:**  
Argon atmosphere annealed.

**Machining method:**  
DMLS (3D-printing), turning and milling.

**Manufacturer:**  
Tronrud Engineering and Sandvik Teeness



Date	11.02.2016	Designer	PA	Checked by	TO	No	Approved by	Not Approved
Suspension				Material		Weight		
FL Upright				Ti-6Al-4V Solution		729.51g		
				Heat treated and aged				
				SCALE		1:2		
Contact info	Feider August Aune			Rev no	01		No of units	1
				Drawing N°		Sheet 1		of 1
				DRW-0570				

**SOLIDWORKS Student Edition.  
 For Academic Use Only.**

This drawing is confidential and it shall not be copied or shown to third party persons or companies without the written consent of Revolve NTNU.

General tolerances: Mean: ISO 2768-1  
 Mean : ISO 2768-2. SO 286-2  
 General radius tolerance: r, 0.2  
 General surface finish: Rd 3.2



# Rear upright

Manufacturing documentation



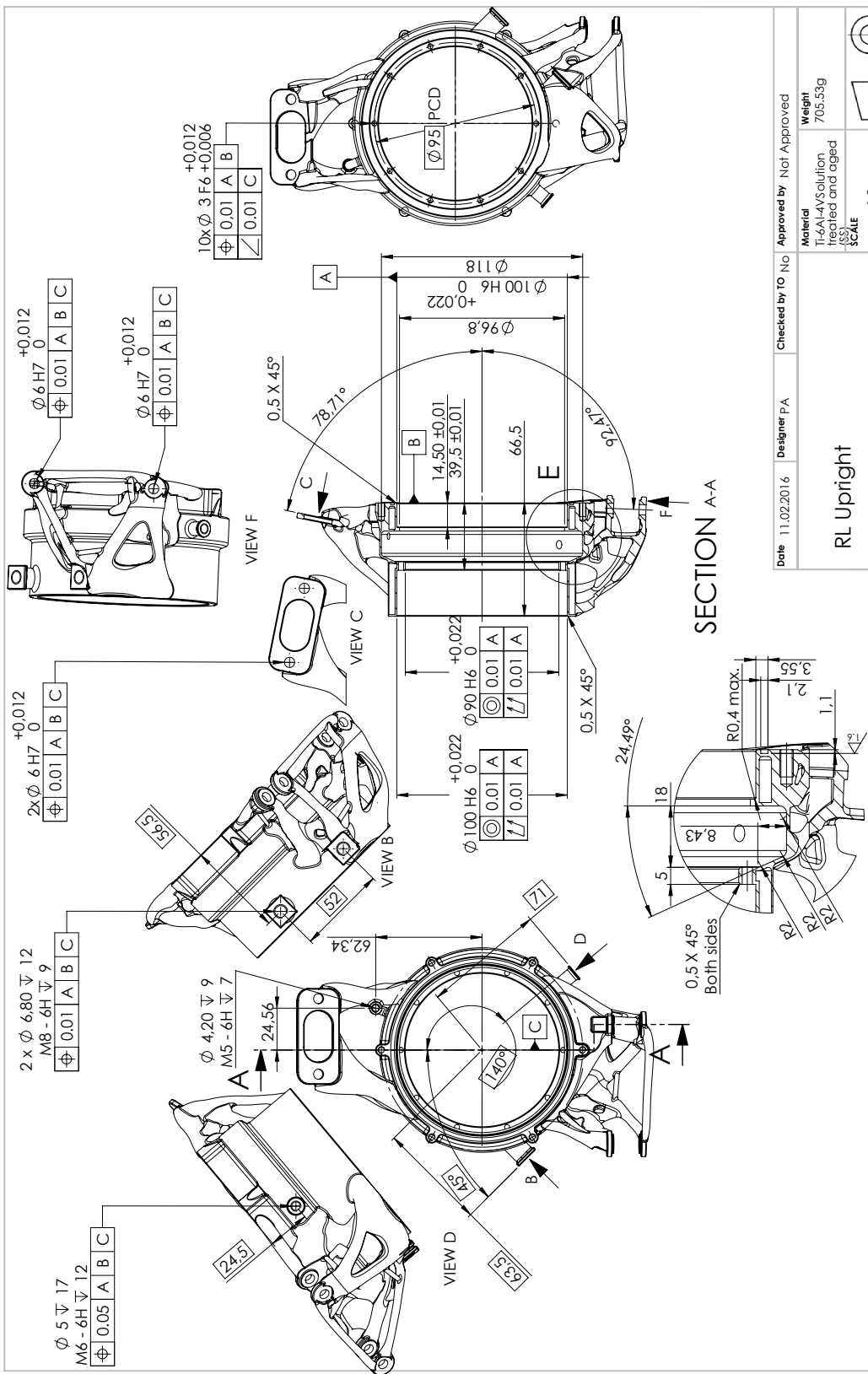
**Material:**  
Ti-6Al-4V

**Weight:**  
495 g

**Treatment:**  
Argon atmosphere annealed.

**Machining method:**  
DMLS (3D-printing), turning and milling.

**Manufacturer:**  
Tronrud Engineering and Sandvik Teeness





**DETAIL E**  
**SCALE 1 : 1**

**SOLIDWORKS Student Edition.**  
**For Academic Use Only.**

This drawing is confidential and it shall not be copied or shown to third party without the prior written consent of Revolve NTNU.

General tolerances: Mean: ISO 2768-1  
Mean : ISO 2768-2, ISO 286-2  
Surface finish: Ra 0.2  
General surface finish: Ra 3.2

Date	11.02.2016	Designer	PA	Checked by	TO	No	Approved by	Not Approved
Contact info		Ege August Aune		Rev no		No of units		 NTNU <b>revolve</b>
+47 994 69 999		01		1		Sheet 1 of 1		
RL Upright				Material Ti-6Al-4V Solution Heat treated and aged		Weight 705.53g		 SCALE 1:2
Drawing N° DRW-0571				Scale		1:2		

# Commercial viability

## Prototype cars

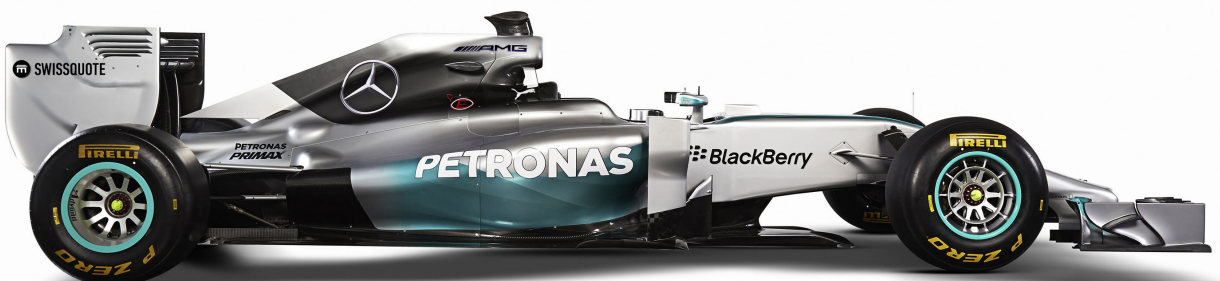
Car racing using prototype sports cars started as far back as before the Second World War. It was however not before the 1960s before prototype cars started to replace homologated sports cars as the top echelon of the sport. Since then, the top prototype classes have seen an extreme progression in vehicle complexity, transforming the crude cars of the 60s into the "perfectly" designed performance beasts of today. Both Le Mans prototype 1 and especially Formula 1, the top endurance (WEC) and grand prix (F1) racing series, are both most commonly associated in two ways. Both of these racing series are associated with a rich tradition and an extreme passion for high performance car racing. They are also associated with the stupendous amount of money and resources that are spent by the teams in development and manufacturing of the cars. Outsiders often question this use of money and resources, claiming that these programs are a marketing ploy and the worlds most expensive boys hobby with no major contribution to society. This may be true to some extent. It is however important to understand that prototype programs are, in large part, used as a research and development department by automotive manufactures. It is they who develop new and innovative technologies that have revolutionized aspects of the automotive industry more than once.:

- Tire technology
- Steel disc brakes
- Active suspension
- Sequential gearbox
- Aerodynamics
- Hybrid systems and kinetic energy recovery
- Vehicle safety (impact absorption etc.)
- Engine technology (Turbochargers etc)

These are just some examples of technologies first developed by prototype racing programs and then later implemented in commercial products.

The liberal budgets and high demand for performance of these projects means that the teams are able to test out new ideas at a much faster pace than any car manufacturer would be able to. This has resulted in a large presence of prototype technology in commercial cars. The reason why this does not seem more apparent is that it usually takes between 5 and 10 years or more to tone down, refine and make prototype technologies cost efficient for the commercial market. The link between the two is therefore in large part invisible to the non initiated.

It is unequivocally proven that prototype racing programs have a significant commercial viability, and that they in fact are leaders of innovation within the industry.



# Commercial viability

## Formula student prototypes

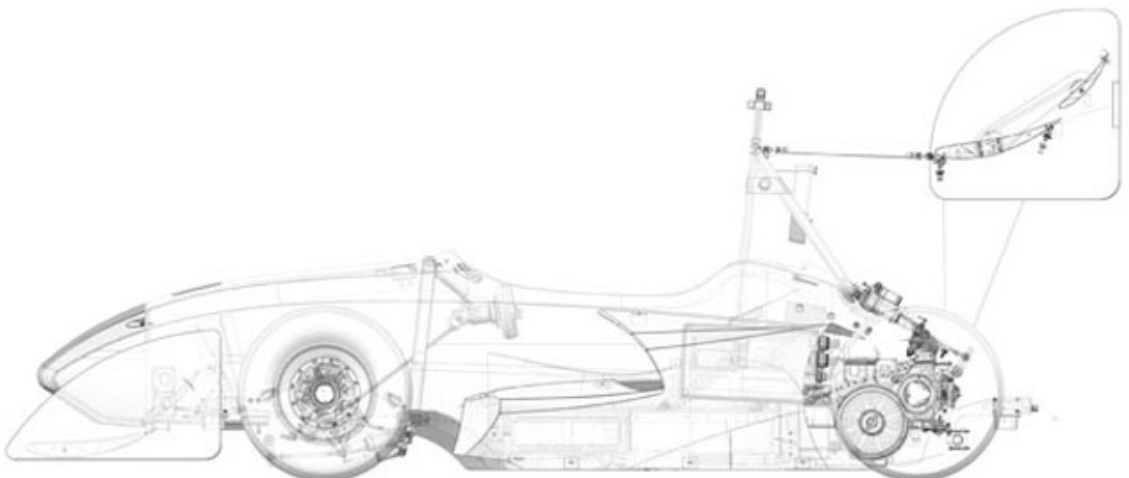
It is a tall order to claim equivalence between GP and WEC prototypes and Formula Student cars. These are similar projects run at entirely different scales of the spectrum in relation to financial and organizational size. It is therefore very difficult for a Formula Student project to have the same potential for commercial adaptation.

The mentality of the designers and engineers of both camps remain very similar despite the glaring difference in money, resources and people. This extremely dedicated and motivated, top athlete like mentality towards improvement and innovation is as much present in a top Formula Student team as in Formula 1. It is this mentality that is the key in creating new and interesting ideas that may find its way to the commercial market.

The GP and WEC series are governed by a very restrictive set of rules that severely limits the attending teams ability to develop truly disruptive solutions. There have been many situations through the years where a team has developed a disruptive solution not covered by the rules, only to see the rules changed and the solution banned. The Formula Student rule set is significantly more liberal in the face of innovation and new ideas. The rule set only restricts areas of the car that are directly related

to driver safety. The potential for disruptive innovation within the Formula Student series may as such be higher than for the prototype racing series.

The cost gap between Formula Student and prototype racing is extreme. But that does in no way mean that Formula Student cars are cheap to manufacture. Top Formula Student teams enjoy sponsorship from world leading companies within a broad spectrum of fields. This opens up to a liberal use of the most expensive materials, technologies and manufacturing methods when designing the cars. This project is a testament to this through the use of the most advanced design and analysis tools and manufacturing methods available today. Topology optimized uprights 3D printed in titanium is the best example of the possibilities available to designers within Formula Student. The price tag of the four complete drivetrain modules developed in this thesis is between 750 000 and 1 000 000 NOK. That is as much as a new, specced out, Tesla model S. While this high price tag is a product of extremely low production volumes, point still stands that this is a serious high end product in line with the same quality and performance that can be found in prototype racers. The format of the design environment within Revolve NTNU is therefore a strong enabler of innovation that may end up having commercial viability.



# Commercial viability

## Performance and implementation

To evaluate the commercial viability of the drivetrain design proposed in this thesis, it is natural to first look at the performance it delivers in relation to what is commonly found in commercial products.

The proposed design is able to deliver 148 kW of power, equivalent to 198.5 break horse power. The output power output is therefore well above the commercial average. We can therefore conclude that a commercial adaptation of the design will easily be able to meet expected power requirement of a normal road car.

The total weight of the system will of course need to increase to fit the mechanical requirement of a much heavier vehicle. At a current weight of just over 23kg, a significant weight increase will still result in a lighter drivetrain compared to current automotive convention. In the time it will take to commercialize the system, manufacturing methods, especially within the field of 3D printing, may have taken steps towards increased efficiency. This may then ensure that the needed increase in weight may be less than what one would initially expect.

The driving experience will be very similar to already existing four wheel drive cars. The added benefit of having torque vectoring and advanced traction control systems will however result in an overall driving experience that far outshines current combustion four wheel drive cars.

In a world increasingly concerned with the environmental consequences of energy consumption, this type of drivetrain will reduce the automotive contribution to global warming. This may seem like a bold claim, but the reduction in efficiency loss in the drivetrain itself, coupled with the ability to absorb kinetic energy during both soft and hard braking situations can only mean a significant reduction in energy vehicle energy consumption.

A total redesign of the system will be required in any respect in order to fulfill the operational requirements of regular car use situations. It is therefore important to consider this prototype as an early concept that can be built upon to finally end up with a system that better fits with a commercial automotive product. As is, the system has little value to the commercial market.





# Commercial viability

## Disruptive effect

Automotive design has seen little change in overall vehicle layout in the past 60 years. The motor sits in the front of the car. Behind the motor sits the driver and front passenger. Behind them is an additional row of passengers. The boot is used as storage for luggage. The drivetrain and exhaust system runs along the underside of the car. This design convention is upheld by the limitations imposed by combustion engine and drivetrain designs. What if these limitations were erased?

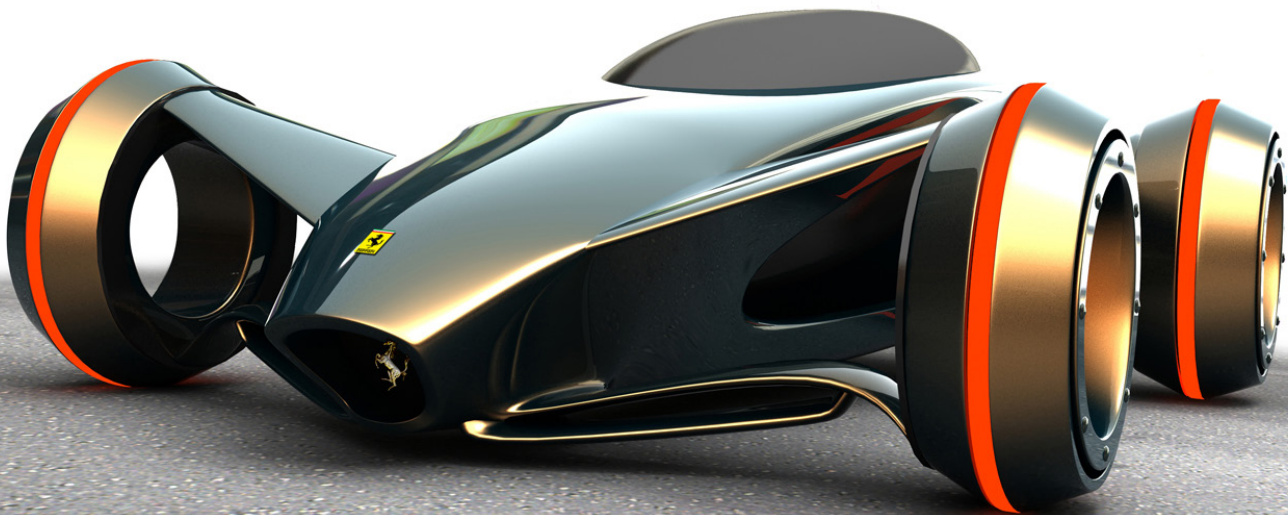
If commercially implemented, the system may have a significant disruptive effect on the future of automotive design. Suddenly no room on the chassis is taken up by engine or drivetrain systems. By moving both motor and drivetrain out into the wheels, the automotive designers are suddenly free to reinvent the chassis layout of a vehicle.

They may be able to significantly improve passenger safety by redesigning the crash absorption area at the front of the car. This is now prevented by an engine bay filled with components. Better crash safety will save lives and can therefore be considered a major improvement compared to current designs.

Form and layout of the overall vehicle may see a complete change from the “normal” of today. Some of the more futuristic car concepts floating around the web may be realizable with this type of drivetrain. The important thing is that increased design freedom opens up to even more innovation. This will further help to improve automotive products at a quicker pace than has been seen in the last decades.

The current number one negative factor of electric cars is the limited range they are able to run between charges. Lack of better battery technology is holding back development in environmental friendly, electric vehicles. By freeing up space on the chassis, these cars can fit more batteries, and as such increase their range. The longer range will make these cars more desirable, resulting in a quicker transition to green transportation technology.

All of these examples are of course only ideas presented in order to better contextualize the kind of impact that may result from implementation of this type of drivetrain. Predicting the future is mostly considered a futile exercise.



# Commercial viability

## Serviceability

Service on engine or drivetrain on the tightly packed vehicles of today is often associated with a very high price tag. The way these cars are designed often means that the mechanic has to perform a significant amount of disassembly before he is able to reach the system he wants to work on. A good example of this is a situation where a change of exhaust system was needed on a four wheel drive car. In order to get to the exhaust system, a complete disassembly of the drivetrain had to be performed. The cost of work hours ended up 3 times higher than the price of a completely new exhaust system. Situations like these are in no way improving the users perception of the product.

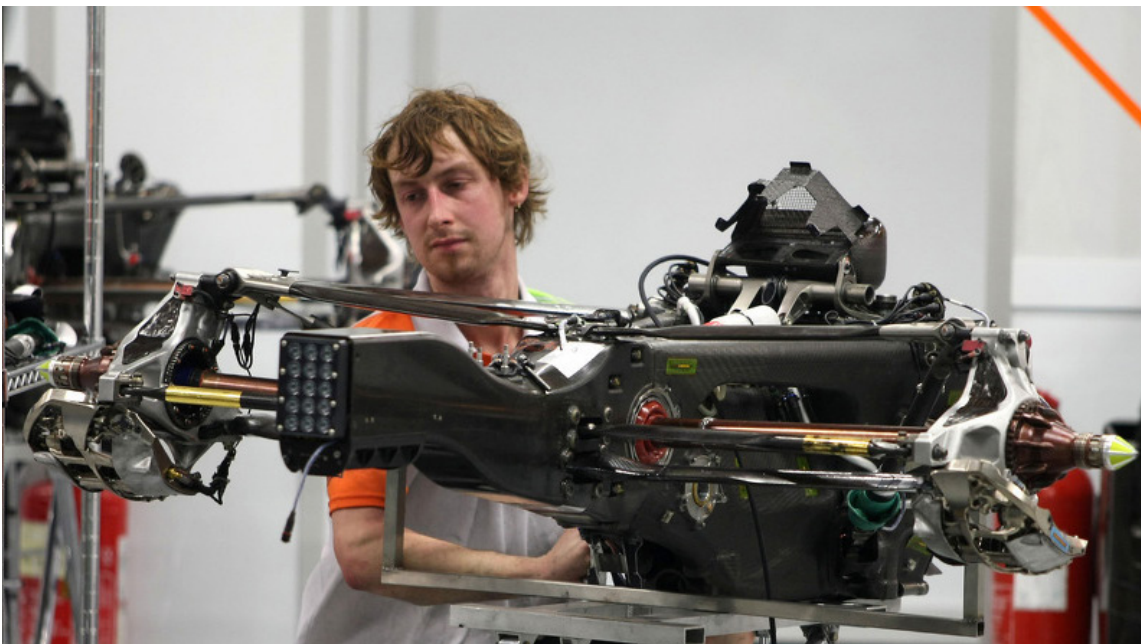
With the motors and drivetrain located in the wheel assembly, removing the wheel leaves the system completely exposed. This significantly simplifies service on the system, reducing

complexity for the mechanic and cost for the owner.

Imagine if instead of doing service on the system while on the car, the mechanic removed the whole wheel unit through loosening the 3 bolts connecting it to the suspension. He would then be able work in a more controlled environment, ensuring better quality of the service.

Imagine again that the removed wheel unit was replaced by a spare unit. This way, the owner of the car would not have to leave his car in the shop for any amount of time. He would just rent the spare unit until service on the damaged unit was performed.

This example is just one of many improvements in serviceability that could be made possible with the proposed drivetrain design.



# Commercial viability

## Torque vectoring and self driving cars

The prospect of self driving cars is no longer just some novelty concept that we dream about. Fully self driving vehicles will most likely be a part of public traffic within the next ten years. This will in itself bring a lot of changes to how we currently perceive a car.

There is no doubt that a smart computer system with the appropriate sensor input is able to react better to unexpected situations than would a human. This is the whole premise of why self driving cars will revolutionize traffic safety. A computers ability to react to input is however based on degree of freedom of its output. With a conventional drivetrain, the only possible reaction is to globally adjust power. Distribution to the wheels is controlled mechanically by a differential and can not be affected. Some output can be generated in the brakes by using the hydraulic system. The overall impression

is that an automated system is significantly restricted in modes of output as a consequence of the mechanical design of the car.

An independent four wheel drive system, like the one proposed in this thesis, will give a self driving car the ability to fully control the output at each wheel. The system will then be able to use this to react much more efficiently to all situations. Self driving cars may then be able to achieve better safety at higher speeds. This will then reduce travel time with no additional risk to the passengers of the car. This will come in addition all the other potential positive benefits related to this type of electric drivetrain design.

The conclusion we can draw is that real commercial viability exist for this type of drivetrain. The future will tell in what direction the automotive industry chose to go.



# Sources

1. Transmission system design for electric formula style race car. Peder Aune 2015
2. Handbook of gear design, second edition. Gitin M. Maitra.
3. <https://en.wikipedia.org/wiki/Gear>
4. [https://en.wikipedia.org/wiki/Epicyclic\\_gearing](https://en.wikipedia.org/wiki/Epicyclic_gearing)
5. Torque Vectoring. Malcolm Burgess-Lotus formula 1
6. Race car vehicle dynamics. William F. Milliken and Douglas L. Milliken
7. KISSSoft manual 2015
8. FSAE Rules 2016



# Appendix

**KISSSoft calculations**

KISSsoft Release 03/2015 F

KISSsoft Academic License - Norwegian University of Science & Technology (NTNU)

File

Name : Unnamed  
 Changed by: Kraftwerk on: 03.02.2016 at: 19:29:01

## Polygon [M02d]

Calculation method: G.Niemann, Maschinenelemente I, 4th Edition, 2005.

Label	Polygon P3G-Profile DIN 32711-1:2009	
Diameter of mean circle (mm)	[d1]	16.00
Diameter of outer circle (mm)	[d2]	17.00
Diameter of inner circle (mm)	[d3]	15.00
Eccentricity (mm)	[e]	0.50
Supporting length (mm)	[ltr]	5.00
Outside diameter, Hub (mm)	[daN]	30.00
Coefficient hub wall	[y]	1.44
Maximal circumferential force (N)	[Ft]	3593.75
Nominal torque (Nm)	[Tnenn]	23.00
Application factor	[KA]	1.25
Service torque (Nm)	[Teq]	28.75
Maximum torque (Nm)	[Tmax]	28.75
Number of load peaks	[NL]	1000000
Torque curve: With alternating torque		
Number of change of load direction	[NW]	100000
Load direction changing coefficient	[fw]	0.63

## Shaft

Material	18CrNiMo7-6	
Type	Case-carburized steel	
Treatment	case-hardened	
Tensile strength (N/mm <sup>2</sup> )	[Rm]	1100.00 (d=16-40mm)
Yield point (N/mm <sup>2</sup> )	[Rp]	745.00 (d=16-40mm)
Surface on shaft (mm <sup>2</sup> )	[Flw]	15.00
Pressure stress (equiv. load) (N/mm <sup>2</sup> )	[peq]	181.68
Pressure stress (maxim. load) (N/mm <sup>2</sup> )	[pmax]	181.68
Support factor	[fs]	1.20
Load peak coefficient	[fL]	1.20
Hardness influence coefficient	[fH]	1.15
Permissible pressure (N/mm <sup>2</sup> )	[pzuleq]	649.13
Permissible pressure (N/mm <sup>2</sup> )	[pzulmax]	1233.72
fw * pzul / peq		3.57
fL * pzul / pmax		6.79
Required safety		1.00
Minimal safety		3.57

## Hub

Material		18CrNiMo7-6
Type		Case-carburized steel
Treatment		case-hardened
Tensile strength (N/mm <sup>2</sup> )	[Rm]	1100.00 (d=16-40mm)
Yield point (N/mm <sup>2</sup> )	[Rp]	745.00 (d=16-40mm)
Surface on hub (mm <sup>2</sup> )	[FIn]	15.00
Outside diameter, Hub (mm)	[D1]	30.00
Smallest hub wall thickness (mm)	[s]	3.29
Pressure stress (equiv. load) (N/mm <sup>2</sup> )	[peq]	181.68
Pressure stress (maxim. load) (N/mm <sup>2</sup> )	[pmax]	181.68
Support factor	[fs]	1.50
Load peak coefficient	[fL]	1.20
Hardness influence coefficient	[fH]	1.15
Permissible pressure (N/mm <sup>2</sup> )	[pzuleq]	811.41
Permissible pressure (N/mm <sup>2</sup> )	[pzulmax]	1542.15
fw * pzul / peq		4.47
fL * pzul / pmax		8.49
Required safety		1.00
Minimal safety		4.47

Remarks:

Contact area according to Niemann  $A = l * n * 2 * e$ ; (n = 3)  
 Smallest hub wall thickness:  $s = y * (T / (Rm * l))^{0.5}$   
 $y = 1.44$  for  $da \leq 35$ ;  $y = 1.2$  for  $da > 35$   
 Pressure load  $T = l * d1 * (0.75 * \pi * e + 0.05 * d1)$   
 Coefficient for load direction changes according to DIN 6892:1998/ fig. 6  
 $pzuleq = fs * fH * fw * (Rm, Rp)$   
 $pzulmax = fs * fH * fL * (Rm, Rp)$   
 (Rm: for brittle material; Rp: for ductile material)

---

End of Report

lines: 92

---

# Wheel bearing calculation

KISSsoft Release 03/2015 F

KISSsoft Academic License - Norwegian University of Science & Technology (NTNU)

File

Name : Wheel bearing calc

Changed by: Kraftwerk on: 11.02.2016 at: 01:56:39

**Important hint: At least one warning has occurred during the calculation:**

1-> Bearing internal geometry data are not correct, an approximation is used instead.

2-> Bearing internal geometry data are not correct, an approximation is used instead.

3-> The required service life of bearing 'Shaft 'Shaft 1', Rolling bearing 'Nondrive' is not achieved!  
The static safety is low (in range 0.5 - 2.0).

Please check whether these values are acceptable or not.

4-> The required service life of bearing 'Shaft 'Shaft 1', Rolling bearing 'Roller bearing' is not achieved!  
The static safety is low (in range 0.5 - 2.0).

Please check whether these values are acceptable or not.

5-> The thermally admissible service speed of bearing 'Shaft 'Shaft 1', Rolling bearing 'Roller bearing' could be critical.  
You can check this by calculating the thermally permissible operating speed in the 'Rolling bearings [W050]' module.

## Analysis of shafts, axle and beams

### Input data

Coordinate system shaft: see picture W-002

Label	Shaft 1
Drawing	
Initial position (mm)	0.000
Length (mm)	82.000
Speed (1/min)	700.00
Sense of rotation: clockwise	
Material	G-AISI9Mg wa
Young's modulus (N/mm <sup>2</sup> )	74000.000
Poisson's ratio nu	0.340
Density (kg/m <sup>3</sup> )	2680.000
Coefficient of thermal expansion (10 <sup>-6</sup> -6/K)	21.000
Temperature (°C)	20.000
Weight of shaft (kg)	0.354
(Notice: Weight stands for the shaft only without considering the gears)	
Weight of shaft, including additional masses (kg)	0.354
Mass moment of inertia (kg*mm <sup>2</sup> )	379.768
Momentum of mass GD2 (Nm <sup>2</sup> )	0.015
Position in space (°)	0.000
Gears mounted with stiffness according to ISO	



Consider deformations due to shearing  
 Shear correction coefficient 1.100  
 Rolling bearing stiffness is calculated from inner bearing geometry  
 Tolerance field: Mean value  
 Reference temperature (°C) 20.000

---

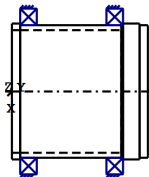
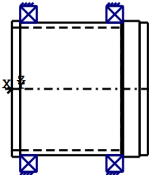


Figure: Load applications

**Shaft definition (Shaft 1)**

**Outer contour**

Cylinder (Cylinder)			0.000mm ...	5.000mm
Diameter (mm)	[d]	82.0000		
Length (mm)	[l]	5.0000		
Surface roughness (µm)	[Rz]	8.0000		
Cylinder (Cylinder)			5.000mm ...	67.000mm
Diameter (mm)	[d]	80.0000		
Length (mm)	[l]	62.0000		
Surface roughness (µm)	[Rz]	8.0000		
Cylinder (Cylinder)			67.000mm ...	77.000mm
Diameter (mm)	[d]	82.0000		
Length (mm)	[l]	10.0000		
Surface roughness (µm)	[Rz]	8.0000		
Cylinder (Cylinder)			77.000mm ...	82.000mm
Diameter (mm)	[d]	80.0000		
Length (mm)	[l]	5.0000		
Surface roughness (µm)	[Rz]	8.0000		

**Inner contour**

Cylinder inside (Cylindrical bore)		0.000mm ...	66.000mm
Diameter (mm)	[d]	74.0000	
Length (mm)	[l]	66.0000	
Surface roughness (µm)	[Rz]	8.0000	

**Forces**

Type of force element

		<b>Eccentric force</b>
Label in the model		Eccentric load
Position on shaft (mm)	[ylocal]	125.8000
Position in global system (mm)	[yglobal]	125.8000
Center point of load application, X-coordinate (mm)		0.0000
Center point of load application, Z -coordinate (mm)		228.6000
Length of load application (mm)		0.0000
Power (kW)		0.0000
Torque (Nm)		0.0000
Axial force (N)		-3088.0000
Shearing force X (N)		0.0000
Shearing force Z (N)		2561.0000
Bending moment X (Nm)		705.9168
Bending moment Z (Nm)		-0.0000

**Bearing**

Label in the model		Nondrive
Bearing type		IBC CB 71816.C.UM
Bearing type		Angular contact ball bearing (single row)
Bearing position (mm)	[ylocal]	10.000
Bearing position (mm)	[yglobal]	10.000
Attachment of external ring		Set fixed bearing right
Inner diameter (mm)	[d]	80.000
External diameter (mm)	[D]	100.000
Width (mm)	[b]	10.000
Corner radius (mm)	[r]	0.300
Number of rolling bodies	[Z]	40
Rolling body reference circle (mm)	[D <sub>pw</sub> ]	90.000
Diameter rolling body (mm)	[D <sub>w</sub> ]	5.324
Distance a (mm)	[a]	17.000
Calculation with approximate bearings internal geometry (*)		
Bearing clearance	0.00 µm	
Tolerance field	Mean value	
Tolerance	DIN 620:1988 PN	
Tolerance shaft	k6, 80.011 mm (min = 80.002 mm , max = 80.021 mm)	
Tolerance hub	H7, 100.018 mm (min = 100.000 mm , max = 100.035 mm)	
Rz1 = 8.00 µm (Roughness shaft/hub in contact with inner ring)		
RzO = 8.00 µm (Roughness shaft/hub in contact with outer ring )		
Change of diametral clearance due to: n = 0 (1/min)		
Interference fit	-4.16 µm	
Temperature	-6.28 µm	
Total bearing clearance change	-4.19 µm, ni = 700 (1/min), no = 0 (1/min)	
The bearing pressure angle will be considered in the calculation		
Position (center of pressure)	(mm)	-2.0000
Basic static load rating	[C <sub>0</sub> ]	16.800

Basic dynamic load rating	[C]	15.000
Fatigue load rating	[C <sub>U</sub> ]	622.000
Values for approximated geometry:		
Basic dynamic load rating (kN)	[C <sub>theo</sub> ]	14.576
Basic static load rating (kN)	[C <sub>0theo</sub> ]	17.350

Label in the model		Roller bearing
Bearing type		IBC CB 71816.C.UM
Bearing type		Angular contact ball bearing (single row)
Bearing position (mm)	[Y <sub>lokal</sub> ]	62.000
Bearing position (mm)	[Y <sub>global</sub> ]	62.000
Attachment of external ring		Set fixed bearing left
Inner diameter (mm)	[d]	80.000
External diameter (mm)	[D]	100.000
Width (mm)	[b]	10.000
Corner radius (mm)	[r]	0.300
Number of rolling bodies	[Z]	40
Rolling body reference circle (mm)	[D <sub>pw</sub> ]	90.000
Diameter rolling body (mm)	[D <sub>w</sub> ]	5.324
Distance a (mm)	[a]	17.000

Calculation with approximate bearings internal geometry (\*)

Bearing clearance	0.00 µm
Tolerance field	Mean value
Tolerance	DIN 620:1988 PN
Tolerance shaft	k6, 80.014 mm (min = 80.003 mm , max = 80.025 mm)
Tolerance hub	H7, 100.018 mm (min = 100.000 mm , max = 100.035 mm)
RzI = 8.00 µm (Roughness shaft/hub in contact with inner ring)	
RzO = 8.00 µm (Roughness shaft/hub in contact with outer ring )	
Change of diametral clearance due to: n = 0 (1/min)	
Interference fit	-4.99 µm
Temperature	-7.10 µm
Total bearing clearance change	-5.01 µm, n <sub>i</sub> = 700 (1/min), n <sub>o</sub> = 0 (1/min)

The bearing pressure angle will be considered in the calculation

Position (center of pressure)	(mm)	74.0000
Basic static load rating	[C <sub>0</sub> ]	16.800
Basic dynamic load rating	[C]	15.000
Fatigue load rating	[C <sub>U</sub> ]	622.000
Values for approximated geometry:		
Basic dynamic load rating (kN)	[C <sub>theo</sub> ]	14.576
Basic static load rating (kN)	[C <sub>0theo</sub> ]	17.350

## Results

### Shaft

Maximum deflection (mm)	0.038
Position of the maximum (mm)	82.000
Mass center of gravity (mm)	58.412
Total axial load (N)	-3088.000
Torsion under torque (°)	0.000

**Bearing**

Probability of failure	[n]	10.00	%
Axial clearance	[u <sub>A</sub> ]	10.00	µm
Rolling bearing service life according to ISO/TS 16281:2008			

**Shaft 'Shaft 1' Rolling bearing 'Nondrive'**

Position (Y-coordinate)	[y]	10.00	mm
Equivalent load	[P]	9.75	kN
Equivalent load	[P <sub>0</sub> ]	9.23	kN
Life modification factor for reliability[a <sub>1</sub> ]		1.000	
Service life	[L <sub>nh</sub> ]	86.73	h
Minimum EHL lubricant film thickness	[h <sub>min</sub> ]	0.120	µm
Spin to roll ratio	[-]	0.037	
Static safety factor	[S <sub>0</sub> ]	1.82	
Calculation with approximate bearings internal geometry			
Reference rating service life	[L <sub>nrh</sub> ]	95.06	h
Effective static safety factor	[S <sub>0w</sub> ]	2.02	
Static safety factor	[S <sub>0ref</sub> ]	1.52	
Equivalent load	[P <sub>0ref</sub> ]	11.04	kN
Bearing reaction force	[F <sub>x</sub> ]	0.000	kN
Bearing reaction force	[F <sub>y</sub> ]	-3.694	kN
Bearing reaction force	[F <sub>z</sub> ]	9.229	kN
Bearing reaction force	[F <sub>r</sub> ]	9.229	kN (90°)
Bearing reaction moment	[M <sub>x</sub> ]	-139.02	Nm
Bearing reaction moment	[M <sub>y</sub> ]	0.00	Nm
Bearing reaction moment	[M <sub>z</sub> ]	0.00	Nm
Bearing reaction moment	[M <sub>r</sub> ]	139.02	Nm (180°)
Oil level	[H]	0.000	mm
Rolling moment of friction	[M <sub>rr</sub> ]	0.315	Nm
Sliding moment of friction	[M <sub>sl</sub> ]	0.401	Nm
Moment of friction, seals	[M <sub>seal</sub> ]	0.000	Nm
Moment of friction for seals determined according to SKF main catalog 10000/1 EN:2013			
Moment of friction flow losses	[M <sub>drag</sub> ]	0.000	Nm
Torque of friction	[M <sub>loss</sub> ]	0.716	Nm
Power loss	[P <sub>loss</sub> ]	52.460	W

The moment of friction is calculated according to the details in SKF Catalog 2013.

The calculation is always performed with a coefficient for additives in the lubricant µbl=0.15.

Displacement of bearing	[u <sub>x</sub> ]	-0.000	µm
Displacement of bearing	[u <sub>y</sub> ]	-9.289	µm
Displacement of bearing	[u <sub>z</sub> ]	-18.653	µm
Displacement of bearing	[u <sub>r</sub> ]	0.019	µm (-90°)
Misalignment of bearing	[r <sub>x</sub> ]	0.839	mrad (2.89°)
Misalignment of bearing	[r <sub>y</sub> ]	-0.000	mrad (0°)
Misalignment of bearing	[r <sub>z</sub> ]	-0.000	mrad (0°)
Misalignment of bearing	[r <sub>r</sub> ]	0.839	mrad (2.89°)

**Shaft 'Shaft 1' Rolling bearing 'Roller bearing'**

Position (Y-coordinate)	[y]	62.00	mm
Equivalent load	[P]	15.63	kN
Equivalent load	[P <sub>0</sub> ]	11.79	kN
Life modification factor for reliability[a <sub>1</sub> ]		1.000	
Service life	[L <sub>nh</sub> ]	21.05	h
Minimum EHL lubricant film thickness	[h <sub>min</sub> ]	0.115	µm

Spin to roll ratio	[-]	0.050	
Static safety factor	[S <sub>0</sub> ]	1.43	
Calculation with approximate bearings internal geometry			
Reference rating service life	[L <sub>nrh</sub> ]	41.15	h
Effective static safety factor	[S <sub>0w</sub> ]	1.54	
Static safety factor	[S <sub>0ref</sub> ]	1.16	
Equivalent load	[P <sub>0ref</sub> ]	14.49	kN
Bearing reaction force	[F <sub>x</sub> ]	-0.000	kN
Bearing reaction force	[F <sub>y</sub> ]	6.782	kN
Bearing reaction force	[F <sub>z</sub> ]	-11.787	kN
Bearing reaction force	[F <sub>r</sub> ]	11.787	kN (-90°)
Bearing reaction moment	[M <sub>x</sub> ]	-250.39	Nm
Bearing reaction moment	[M <sub>y</sub> ]	0.00	Nm
Bearing reaction moment	[M <sub>z</sub> ]	-0.00	Nm
Bearing reaction moment	[M <sub>r</sub> ]	250.39	Nm (-180°)
Oil level	[H]	0.000	mm
Rolling moment of friction	[M <sub>rr</sub> ]	0.395	Nm
Sliding moment of friction	[M <sub>sl</sub> ]	0.612	Nm
Moment of friction, seals	[M <sub>seal</sub> ]	0.000	Nm
Moment of friction for seals determined according to SKF main catalog 10000/1 EN:2013			
Moment of friction flow losses	[M <sub>drag</sub> ]	0.000	Nm
Torque of friction	[M <sub>loss</sub> ]	1.007	Nm
Power loss	[P <sub>loss</sub> ]	73.801	W

The moment of friction is calculated according to the details in SKF Catalog 2013.

The calculation is always performed with a coefficient for additives in the lubricant  $\mu_{bl}=0.15$ .

Displacement of bearing	[u <sub>x</sub> ]	-0.000	µm
Displacement of bearing	[u <sub>y</sub> ]	-5.712	µm
Displacement of bearing	[u <sub>z</sub> ]	8.436	µm
Displacement of bearing	[u <sub>r</sub> ]	0.008	µm (90°)
Misalignment of bearing	[r <sub>x</sub> ]	1.334	mrاد (4.58')
Misalignment of bearing	[r <sub>y</sub> ]	-0.000	mrاد (0')
Misalignment of bearing	[r <sub>z</sub> ]	-0.000	mrاد (0')
Misalignment of bearing	[r <sub>r</sub> ]	1.334	mrاد (4.58')

(\*) Note about roller bearings with an approximated bearing geometry:

The internal geometry of these bearings has not been input in the database.

The geometry is back-calculated as specified in ISO 281, from C and C0 (details in the manufacturer's catalog).

For this reason, the geometry may be different from the actual geometry.

This can lead to differences in the service life calculation and, more importantly, the roller bearing stiffness.

Utilization, with reference to the required service life

[H] ( 20000.000)

B1	B2
5.95	7.86

B1: Nondrive

B2: Roller bearing

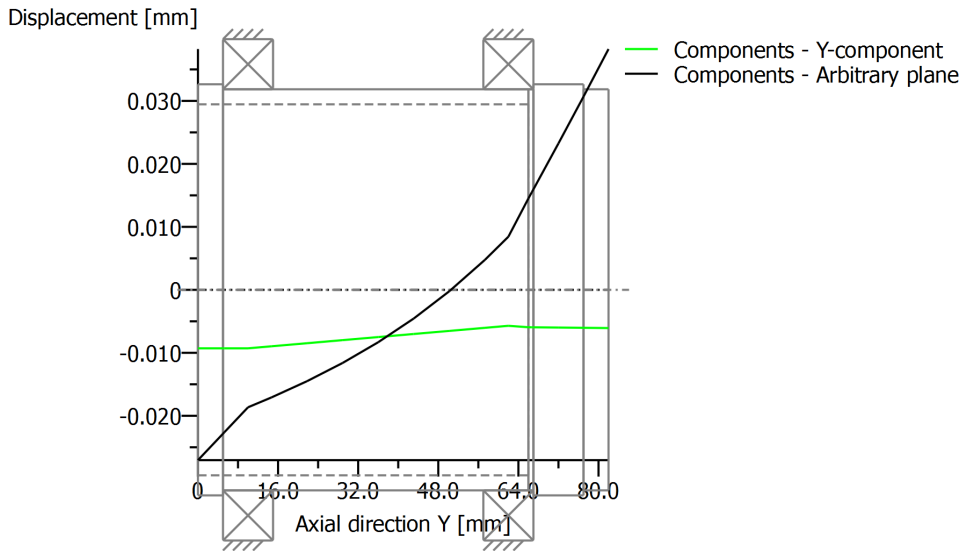
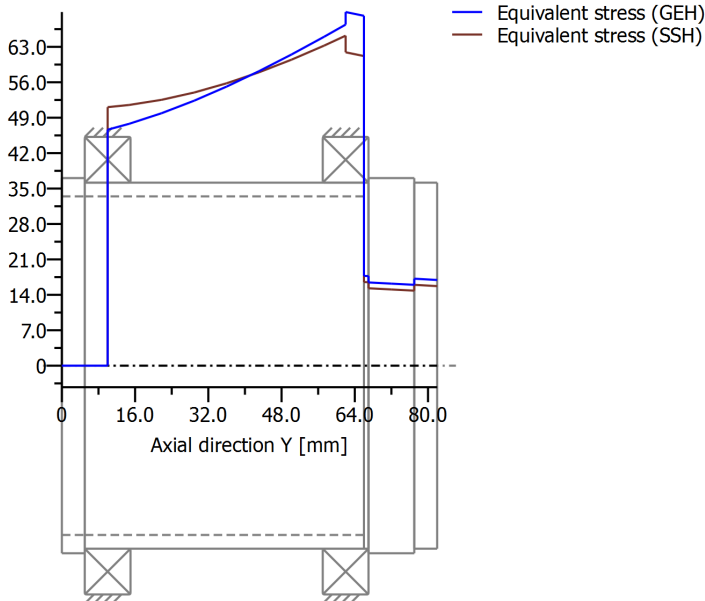


Figure: Deformation (bending etc.) (Arbitrary plane 90 120)  
Stress [N/mm<sup>2</sup>]



GEH(von Mises):  $\text{sigV} = \sqrt{(\text{sigB} + \text{sigZ}, D)^2 + 3 \cdot (\text{tauT} + \text{tauS})^2}$  / 2SSH(Tresca):  $\text{sigV} = \sqrt{(\text{sigB} - \text{sigZ}, D)^2 + 4 \cdot (\text{tauT} + \text{tauS})^2}$  / 2  
Figure: Equivalent stress

# Ring gear shear pin calculation

KISSsoft Release 03/2015 F

KISSsoft Academic License - Norwegian University of Science & Technology (NTNU)

File

Name : Unnamed

Changed by: Kraftwerk

on: 11.02.2016

at: 02:01:40

## Pins [M03a]

### Circular arrangement of bolts (in single shear)

#### Inputs:

Torque (Nm)	[Tn]	303.000
Force per bolt (N)	[Fp]	637.895
Number of bolts	[nb]	10
Bolt diameter (mm)	[d]	3.000
Cross section area (mm <sup>2</sup> )	[A]	7.069
Diameter of arrangement (mm)	[dcirc]	95.000
Thickness component 1 (mm)	[t1]	5.000
Thickness component 2 (mm)	[t2]	8.000
Application factor	[KA]	1.250

Type of load:  
static

Type of pin: Full pin / Bolt

#### Material data:

Dynamic factor	[cd]	1.000
Reduction factor bending/shearing notched pin	[ck]	1.000
Reduction factor pressure notched pin	[ckp]	1.000
Coefficient surface pressure	[faktp]	0.350
Coefficient shearing stress	[fakttau]	0.200
Coefficient bending Stress	[faktsigma]	0.300

#### Pin/ Bolt

Material	C45 (1)	
Tensile strength (N/mm <sup>2</sup> )	[Rm]	700.000
Admissible shear stress (N/mm <sup>2</sup> )	[tauzul]	140.000

#### Component 1

Material	C45 (1)	
Tensile strength (N/mm <sup>2</sup> )	[Rm]	700.000
Permissible surface pressure (N/mm <sup>2</sup> )	[pzul]	245.000

Component 2

Material	C45 (1)		
Tensile strength (N/mm <sup>2</sup> )		[Rm]	700.000
Permissible pressure (N/mm <sup>2</sup> )		[pzul]	245.000

**Results:**

Pin:			
Moment of resistance (mm <sup>3</sup> )		[W]	2.651
Shearing stress (N/mm <sup>2</sup> )		[tau]	112.805
Maximum shear stress (N/mm <sup>2</sup> )		[taumax]	150.406
Component 1:			
Pressure (N/mm <sup>2</sup> )		[pw]	53.158
Component 2:			
Pressure (N/mm <sup>2</sup> )		[pn]	33.224
Safeties:			
Safety shearing (pin):		[SSpin]	1.241
Minimum safety shearing (pin):		[SSpinmin]	0.931
Safety against pressure (component 1):		[SPp1]	4.609
Safety against pressure (component 2):		[SPp2]	7.374

Remarks:

$p = Fp \cdot KA / d \cdot t$

$\tau = Fp \cdot KA / A$

$\tau_{max} = 4/3 \cdot Fp \cdot KA / A$

---

End of Report

lines: 86

---



# Hardening depth gear stage 1

KISSsoft Release 03/2015 F

KISSsoft Academic License - Norwegian University of Science & Technology (NTNU)

File

Name : Unnamed

Changed by: Kraftwerk

on: 11.02.2016

at: 02:03:48

## Proposals for the hardening depth

### Gear pair 1-2

Maximum shear stress	[tauFmax]	443.97	N/mm <sup>2</sup>
tauFmax converted in HV (Si= 1.63)	[HVSi]	452.30	HV
Contact (Flank pressure)	[sigHcont]	1478.51	N/mm <sup>2</sup>
Maximum radius of flank	[rho_r]	1.82	mm
Maximum shear stress depth	[hmax]	0.038	mm
Proposal for hardness-depth EHT	[EHT]	0.076	mm

### Gear 1

Material	NC310YW
Type of treatment	case-hardened
Hardness	59 HRC

#### **Propositions Niemann, Bd.II (p.188)**

Casehardening (2.00 mm <= mn <= 40.00 mm)

Hardening depth EhtHmin...EhtHmax: 0.11 mm...0.21 mm

#### **Propositions AGMA 2101-D04 (p.32-34)**

for carburized and induction hardened external gears

[hemin] 0.12 mm

for tooth-to-tooth induction hardened external gears

[hemin] 0.18 mm

#### **Propositions ISO 6336 part 5 (p.21-23)**

Recommended case depth to avoid pitting

[Ehtmax] 0.60 mm

[EhtHopt] 0.30 mm

Recommended case depth to avoid case-crushing

Quality ML [EhtcML] 0.12 mm

Quality MQ/ME [EhtcMQ] 0.08 mm

### Gear 2

Material	NC310YW
Type of treatment	case-hardened
Hardness	59 HRC

#### **Propositions Niemann, Bd.II (p.188)**

Casehardening (2.00 mm <= mn <= 40.00 mm)

Hardening depth EhtHmin...EhtHmax: 0.11 mm...0.21 mm

#### **Propositions AGMA 2101-D04 (p.32-34)**

for carburized and induction hardened external gears

[hemin] 0.12 mm

for tooth-to-tooth induction hardened external gears

[hemin] 0.18 mm

**Propositions ISO 6336 part 5 (p.21-23)**

Recommended case depth to avoid pitting

[Ehtmax] 0.60 mm

[EhtHopt] 0.30 mm

Recommended case depth to avoid case-crushing

Quality ML [EhtcML] 0.12 mm

Quality MQ/ME [EhtcMQ] 0.08 mm

---

End of Report

lines: 69

---

# Hardening depth gear stage 2

KISSsoft Release 03/2015 F

KISSsoft Academic License - Norwegian University of Science & Technology (NTNU)

File

Name : Unnamed

Changed by: Kraftwerk

on: 11.02.2016

at: 02:05:28

## Proposals for the hardening depth

### Gear pair 1-2

Maximum shear stress	[tauFmax]	443.82	N/mm <sup>2</sup>
tauFmax converted in HV (Si= 1.63)	[HVSij]	452.14	HV
Contact (Flank pressure)	[sigHcont]	1478.03	N/mm <sup>2</sup>
Maximum radius of flank	[rho_r]	4.51	mm
Maximum shear stress depth	[hmax]	0.094	mm
Proposal for hardness-depth EHT	[EHT]	0.188	mm

### Gear 1

Material	NC310YW
Type of treatment	case-hardened
Hardness	59 HRC

### **Propositions Niemann, Bd.II (p.188)**

Casehardening (2.00 mm <= mn <= 40.00 mm)

Hardening depth Ehtmin...Ehtmax: 0.13 mm...0.25 mm

### **Propositions AGMA 2101-D04 (p.32-34)**

for carburized and induction hardened external gears

[hemini] 0.30 mm

for tooth-to-tooth induction hardened external gears

[hemini] 0.44 mm

### **Propositions ISO 6336 part 5 (p.21-23)**

Recommended case depth to avoid pitting

[Ehtmax] 0.60 mm

[EhtHopt] 0.30 mm

Recommended case depth to avoid case-crushing

Quality ML [EhtcML] 0.30 mm

Quality MQ/ME [EhtcMQ] 0.20 mm

### Gear 2

Material	NC310YW
Type of treatment	case-hardened
Hardness	59 HRC

### **Propositions Niemann, Bd.II (p.188)**

Casehardening (2.00 mm <= mn <= 40.00 mm)

Hardening depth Ehtmin...Ehtmax: 0.13 mm...0.25 mm

### **Propositions AGMA 2101-D04 (p.32-34)**

for carburized and induction hardened external gears

[hemini] 0.30 mm

for tooth-to-tooth induction hardened external gears

[hemin] 0.44 mm

**Propositions ISO 6336 part 5 (p.21-23)**

Recommended case depth to avoid pitting

[Ehtmax] 0.60 mm

[EhtHopt] 0.30 mm

Recommended case depth to avoid case-crushing

Quality ML [EhtcML] 0.30 mm

Quality MQ/ME [EhtcMQ] 0.20 mm

---

End of Report

lines: 69

---

# Main line shaft calculation

KISSsoft Release 03/2015 F

KISSsoft Academic License - Norwegian University of Science & Technology (NTNU)

File

Name : Unnamed

Changed by: Kraftwerk on: 02.02.2016 at: 18:54:04

**Important hint: At least one warning has occurred during the calculation:**

1-> Shaft 'CarrierShaft', Rolling bearing 'WheelBearing2':

The minimal load of the bearing is not achieved!

(P = 0.1 kN, Pmind = 0.1 kN, Condition: P/C > 1.000 %)

2-> Shaft 'SunShaft', Rolling bearing 'MotorBearing1':

The minimal load of the bearing is not achieved!

(P = 0.0 kN, Pmind = 0.1 kN, Condition: P/C > 1.000 %)

3-> Shaft 'SunShaft', Rolling bearing 'MotorBearing2':

The minimal load of the bearing is not achieved!

(P = 0.0 kN, Pmind = 0.1 kN, Condition: P/C > 1.000 %)

## Analysis of shafts, axle and beams

### Input data

Coordinate system shaft: see picture W-002

Label	CarrierShaft
Drawing	
Initial position (mm)	120.000
Length (mm)	114.000
Speed (1/min)	100.00
Sense of rotation: clockwise	
Material	G-AISI9Mg wa
Young's modulus (N/mm <sup>2</sup> )	74000.000
Poisson's ratio nu	0.340
Density (kg/m <sup>3</sup> )	2680.000
Coefficient of thermal expansion (10 <sup>-6</sup> /K)	21.000
Temperature (°C)	20.000
Weight of shaft (kg)	0.364
Weight of shaft, including additional masses (kg)	0.364
Mass moment of inertia (kg*mm <sup>2</sup> )	448.588
Momentum of mass GD <sup>2</sup> (Nm <sup>2</sup> )	0.018
Label	RingShaft
Drawing	
Initial position (mm)	120.000
Length (mm)	60.000
Speed (1/min)	100.00
Sense of rotation: clockwise	
Material	C45 (1)

Young's modulus (N/mm <sup>2</sup> )	206000.000
Poisson's ratio nu	0.300
Density (kg/m <sup>3</sup> )	7830.000
Coefficient of thermal expansion (10 <sup>-6</sup> /K)	11.500
Temperature (°C)	20.000
Weight of shaft (kg)	1.708
Weight of shaft, including additional masses (kg)	1.708
Mass moment of inertia (kg*mm <sup>2</sup> )	5562.271
Momentum of mass GD2 (Nm <sup>2</sup> )	0.218
Label	SunShaft
Drawing	
Initial position (mm)	0.000
Length (mm)	143.300
Speed (1/min)	100.00
Sense of rotation: clockwise	
Material	C45 (1)
Young's modulus (N/mm <sup>2</sup> )	206000.000
Poisson's ratio nu	0.300
Density (kg/m <sup>3</sup> )	7830.000
Coefficient of thermal expansion (10 <sup>-6</sup> /K)	11.500
Temperature (°C)	20.000
Weight of shaft (kg)	0.312
Weight of shaft, including additional masses (kg)	0.312
Mass moment of inertia (kg*mm <sup>2</sup> )	18.318
Momentum of mass GD2 (Nm <sup>2</sup> )	0.001
Weight towards ( 0.000, 0.000, -1.000)	
Consider deformations due to shearing	
Shear correction coefficient	1.100
Contact angle of rolling bearings is considered	
Tolerance field: Mean value	
Reference temperature (°C)	20.000

---

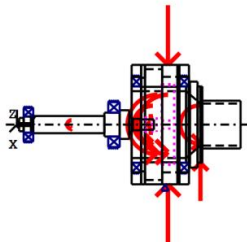
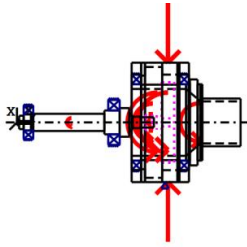


Figure: Load applications

**Shaft definition (CarrierShaft)**

**Outer contour**

<u>Cylinder (Cylinder)</u>			0.000mm ...	10.000mm
Diameter (mm)	[d]	80.0000		
Length (mm)	[l]	10.0000		
Surface roughness (µm)	[Rz]	8.0000		
<u>Cylinder (Cylinder)</u>			10.000mm ...	50.000mm
Diameter (mm)	[d]	79.0000		
Length (mm)	[l]	40.0000		
Surface roughness (µm)	[Rz]	8.0000		
<u>Cylinder (Cylinder)</u>			50.000mm ...	60.000mm
Diameter (mm)	[d]	80.0000		
Length (mm)	[l]	10.0000		
Surface roughness (µm)	[Rz]	8.0000		
<u>Cylinder (Cylinder)</u>			60.000mm ...	61.000mm
Diameter (mm)	[d]	82.0000		
Length (mm)	[l]	1.0000		
Surface roughness (µm)	[Rz]	8.0000		
<u>Cylinder (Cylinder)</u>			61.000mm ...	69.000mm
Diameter (mm)	[d]	90.0000		
Length (mm)	[l]	8.0000		
Surface roughness (µm)	[Rz]	8.0000		
<u>Cylinder (Cylinder)</u>			69.000mm ...	74.000mm
Diameter (mm)	[d]	80.0000		

Length (mm)	[l]	5.0000
Surface roughness (µm)	[Rz]	8.0000

Cylinder (Cylinder) 74.000mm ... 114.000mm

Diameter (mm)	[d]	50.0000
Length (mm)	[l]	40.0000
Surface roughness (µm)	[Rz]	8.0000

**Inner contour**

Cylinder inside (Cylindrical bore) 0.000mm ... 57.000mm

Diameter (mm)	[d]	70.0000
Length (mm)	[l]	57.0000
Surface roughness (µm)	[Rz]	8.0000

Cone inside (Conical bore) 57.000mm ... 72.000mm

Diameter left (mm)	[d <sub>l</sub> ]	70.0000
Diameter right (mm)	[d <sub>r</sub> ]	44.0000
Length (mm)	[l]	15.0000
Surface roughness (µm)	[Rz]	8.0000

Cylinder inside (Cylindrical bore) 72.000mm ... 73.000mm

Diameter (mm)	[d]	0.0000
Length (mm)	[l]	1.0000
Surface roughness (µm)	[Rz]	8.0000

Cylinder inside (Cylindrical bore) 73.000mm ... 114.000mm

Diameter (mm)	[d]	44.0000
Length (mm)	[l]	41.0000
Surface roughness (µm)	[Rz]	8.0000

**Forces**

Type of force element

**Coupling**

Label in the model		CarrierCoupling(Planet2RingConstraint)		
Position on shaft (mm)	[y <sub>local</sub> ]	22.0000		
Position in global system (mm)	[y <sub>global</sub> ]	142.0000		
Effective diameter (mm)		0.0000		
Radial force factor (-)		0.0000		
Direction of the radial force (°)		0.0000		
Axial force factor (-)		0.0000		
Length of load application (mm)		0.0000		
Power (kW)		1.0472		
Torque (Nm)		100.0000		
Axial force (load spectrum) (N)		0.0000 /	0.0000 /	0.0000
Shearing force X (load spectrum) (N)		0.0000 /	0.0000 /	0.0000
Shearing force Z (Load spectrum) (N)		0.0000 /	0.0000 /	0.0000
Mass (kg)		0.0000		
Mass moment of inertia J <sub>p</sub> (kg*m <sup>2</sup> )		0.0000		
Mass moment of inertia J <sub>xx</sub> (kg*m <sup>2</sup> )		0.0000		
Mass moment of inertia J <sub>zz</sub> (kg*m <sup>2</sup> )		0.0000		
Eccentricity (mm)		0.0000		
Load spectrum, driven (input)				

No.	Frequency (%)	Speed (1/min)	Power (kW)	Torque (Nm)
1	4.0000e+001	767.438	6.690	83.249
2	1.0000e+001	1023.251	14.365	134.056



3	6.0000e+000	1151.157	14.365	119.161
4	4.0000e+000	793.019	13.184	158.758
5	3.0000e+001	511.625	12.636	235.844
6	8.0000e+000	1023.251	-8.619	-80.434
7	2.0000e+000	581.627	-11.492	-188.675

Type of force element

		<b>Coupling</b>		
		CarrierCoupling(PlanetCarrierConstraint)		
Label in the model				
Position on shaft (mm)	[Y <sub>local</sub> ]	22.0000		
Position in global system (mm)	[Y <sub>global</sub> ]	142.0000		
Effective diameter (mm)		0.0000		
Radial force factor (-)		0.0000		
Direction of the radial force (°)		0.0000		
Axial force factor (-)		0.0000		
Length of load application (mm)		0.0000		
Power (kW)		1.0472		
Torque (Nm)		100.0000		
Axial force (load spectrum) (N)		0.0000 /	0.0000 /	0.0000
Shearing force X (load spectrum) (N)		0.0000 /	0.0000 /	0.0000
Shearing force Z (Load spectrum) (N)		0.0000 /	0.0000 /	0.0000
Mass (kg)		0.0000		
Mass moment of inertia Jp (kg*m <sup>2</sup> )		0.0000		
Mass moment of inertia Jxx (kg*m <sup>2</sup> )		0.0000		
Mass moment of inertia Jzz (kg*m <sup>2</sup> )		0.0000		
Eccentricity (mm)		0.0000		
Load spectrum, driven (input)				

No.	Frequency (%)	Speed (1/min)	Power (kW)	Torque (Nm)
1	4.0000e+001	767.438	0.000	0.000
2	1.0000e+001	1023.251	0.000	0.000
3	6.0000e+000	1151.157	0.000	0.000
4	4.0000e+000	793.019	0.000	0.000
5	3.0000e+001	511.625	0.000	0.000
6	8.0000e+000	1023.251	0.000	0.000
7	2.0000e+000	581.627	0.000	0.000

Type of force element

		<b>Coupling</b>		
		CarrierCoupling(SunPlanetConstraint)		
Label in the model				
Position on shaft (mm)	[Y <sub>local</sub> ]	22.0000		
Position in global system (mm)	[Y <sub>global</sub> ]	142.0000		
Effective diameter (mm)		0.0000		
Radial force factor (-)		0.0000		
Direction of the radial force (°)		0.0000		
Axial force factor (-)		0.0000		
Length of load application (mm)		0.0000		
Power (kW)		1.0472		
Torque (Nm)		100.0000		
Axial force (load spectrum) (N)		0.0000 /	0.0000 /	0.0000
Shearing force X (load spectrum) (N)		0.0000 /	0.0000 /	0.0000
Shearing force Z (Load spectrum) (N)		0.0000 /	0.0000 /	0.0000
Mass (kg)		0.0000		
Mass moment of inertia Jp (kg*m <sup>2</sup> )		0.0000		
Mass moment of inertia Jxx (kg*m <sup>2</sup> )		0.0000		
Mass moment of inertia Jzz (kg*m <sup>2</sup> )		0.0000		
Eccentricity (mm)		0.0000		
Load spectrum, driven (input)				

No.	Frequency (%)	Speed (1/min)	Power (kW)	Torque (Nm)
1	4.0000e+001	767.438	2.625	32.659
2	1.0000e+001	1023.251	5.635	52.591
3	6.0000e+000	1151.157	5.635	46.747
4	4.0000e+000	793.019	5.172	62.281
5	3.0000e+001	511.625	4.957	92.522
6	8.0000e+000	1023.251	-3.381	-31.554
7	2.0000e+000	581.627	-4.508	-74.018

Type of force element

		Centric force		
Label in the model		CentralLoad1		
Position on shaft (mm)	[y <sub>local</sub> ]	72.0000		
Position in global system (mm)	[y <sub>global</sub> ]	192.0000		
Length of load application (mm)		0.0000		
Power (kW)		0.0000		
Torque (Nm)		0.0000		
Axial force (load spectrum) (N)		0.0000 /	0.0000 /	0.0000
Shearing force X (load spectrum) (N)		0.0000 /	0.0000 /	0.0000
Shearing force Z (Load spectrum) (N)		1000.0000 /	800.0000 /	600.0000
Bending moment X (Load spectrum) (Nm)		0.0000 /	0.0000 /	0.0000
Bending moment Z (Load spectrum) (Nm)		0.0000 /	0.0000 /	0.0000

Load spectrum:

No.	Frequency (%)	Speed (1/min)	Power (%)	Torque (%)	Force (%)
1	4.0000e+001	767.438	7674.382	1000.000	1000.000
2	1.0000e+001	1023.251	8186.007	800.000	800.000
3	6.0000e+000	1151.157	6906.944	600.000	600.000
4	4.0000e+000	793.019	5551.136	700.000	700.000
5	3.0000e+001	511.625	3069.753	600.000	600.000
6	8.0000e+000	1023.251	8186.007	800.000	800.000
7	2.0000e+000	581.627	5816.266	1000.000	1000.000

Type of force element

		Coupling		
Label in the model		Output(WheelOutput)		
Position on shaft (mm)	[y <sub>local</sub> ]	71.0000		
Position in global system (mm)	[y <sub>global</sub> ]	191.0000		
Effective diameter (mm)		0.0000		
Radial force factor (-)		0.0000		
Direction of the radial force (°)		0.0000		
Axial force factor (-)		0.0000		
Length of load application (mm)		0.0000		
Power (kW)		1.0472		
Torque (Nm)		100.0000		
Axial force (load spectrum) (N)		0.0000 /	0.0000 /	0.0000
Shearing force X (load spectrum) (N)		0.0000 /	0.0000 /	0.0000
Shearing force Z (Load spectrum) (N)		0.0000 /	0.0000 /	0.0000
Mass (kg)		0.0000		
Mass moment of inertia J <sub>p</sub> (kg*m <sup>2</sup> )		0.0000		
Mass moment of inertia J <sub>xx</sub> (kg*m <sup>2</sup> )		0.0000		
Mass moment of inertia J <sub>zz</sub> (kg*m <sup>2</sup> )		0.0000		
Eccentricity (mm)		0.0000		

Load spectrum, driven (input)

No.	Frequency (%)	Speed (1/min)	Power (kW)	Torque (Nm)
1	4.0000e+001	767.438	-9.315	-115.908

2	1.0000e+001	1023.251	-20.000	-186.647
3	6.0000e+000	1151.157	-20.000	-165.908
4	4.0000e+000	793.019	-18.356	-221.040
5	3.0000e+001	511.625	-17.593	-328.366
6	8.0000e+000	1023.251	12.000	111.988
7	2.0000e+000	581.627	16.000	262.693

**Bearing**

Label in the model		WheelBearing1
Bearing type		IBC 71816.C.UL
Bearing type		Angular contact ball bearing (single row)
Bearing position (mm)	[Y <sub>lokal</sub> ]	55.000
Bearing position (mm)	[Y <sub>global</sub> ]	175.000
Attachment of external ring		Set fixed bearing left
Inner diameter (mm)	[d]	80.000
External diameter (mm)	[D]	100.000
Width (mm)	[b]	10.000
Corner radius (mm)	[r]	0.300

The bearing pressure angle will be considered in the calculation

Position (center of pressure)	(mm)	67.0000
Radial stiffness (X-direction) (N/μm)		380.000
Radial stiffness (Z-direction) (N/μm)		380.000
Tilting stiffness about X-axis (Nm/°)		0.000
Tilting stiffness about Z-axis (Nm/°)		0.000
Basic static load rating	[C <sub>0</sub> ]	24.000
Basic dynamic load rating	[C]	15.000
Fatigue load rating	[C <sub>U</sub> ]	889.000
Values for approximated geometry:		
Basic dynamic load rating (kN)	[C <sub>theo</sub> ]	0.000
Basic static load rating (kN)	[C <sub>0theo</sub> ]	0.000

Label in the model		WheelBearing2
Bearing type		IBC 71816.C.UX
Bearing type		Angular contact ball bearing (single row)
Bearing position (mm)	[Y <sub>lokal</sub> ]	5.000
Bearing position (mm)	[Y <sub>global</sub> ]	125.000
Attachment of external ring		Set fixed bearing right
Inner diameter (mm)	[d]	80.000
External diameter (mm)	[D]	100.000
Width (mm)	[b]	10.000
Corner radius (mm)	[r]	0.300

The bearing pressure angle will be considered in the calculation

Position (center of pressure)	(mm)	-7.0000
Radial stiffness (X-direction) (N/μm)		320.000
Radial stiffness (Z-direction) (N/μm)		320.000
Tilting stiffness about X-axis (Nm/°)		0.000
Tilting stiffness about Z-axis (Nm/°)		0.000
Basic static load rating	[C <sub>0</sub> ]	24.000
Basic dynamic load rating	[C]	15.000
Fatigue load rating	[C <sub>U</sub> ]	889.000
Values for approximated geometry:		
Basic dynamic load rating (kN)	[C <sub>theo</sub> ]	0.000
Basic static load rating (kN)	[C <sub>0theo</sub> ]	0.000

**Shaft definition (RingShaft)**

**Outer contour**

<u>Cylinder (Cylinder)</u>			0.000mm ...	10.000mm
Diameter (mm)	[d]	125.0000		
Length (mm)	[l]	10.0000		
Surface roughness (µm)	[Rz]	8.0000		
<u>Cylinder (Cylinder)</u>			10.000mm ...	14.000mm
Diameter (mm)	[d]	125.0000		
Length (mm)	[l]	4.0000		
Surface roughness (µm)	[Rz]	8.0000		
<u>Cylinder (Cylinder)</u>			14.000mm ...	32.000mm
Diameter (mm)	[d]	125.0000		
Length (mm)	[l]	18.0000		
Surface roughness (µm)	[Rz]	8.0000		
<u>Cylinder (Cylinder)</u>			32.000mm ...	48.000mm
Diameter (mm)	[d]	125.0000		
Length (mm)	[l]	16.0000		
Surface roughness (µm)	[Rz]	8.0000		
<u>Cylinder (Cylinder)</u>			48.000mm ...	50.000mm
Diameter (mm)	[d]	125.0000		
Length (mm)	[l]	2.0000		
Surface roughness (µm)	[Rz]	8.0000		
<u>Cylinder (Cylinder)</u>			50.000mm ...	60.000mm
Diameter (mm)	[d]	125.0000		
Length (mm)	[l]	10.0000		
Surface roughness (µm)	[Rz]	8.0000		

**Inner contour**

<u>Cylinder inside (Cylindrical bore)</u>			0.000mm ...	10.000mm
Diameter (mm)	[d]	100.0000		
Length (mm)	[l]	10.0000		
Surface roughness (µm)	[Rz]	8.0000		
<u>Cylinder inside (Cylindrical bore)</u>			10.000mm ...	14.000mm
Diameter (mm)	[d]	98.0000		
Length (mm)	[l]	4.0000		
Surface roughness (µm)	[Rz]	8.0000		
<u>Cylinder inside (Cylindrical bore)</u>			14.000mm ...	32.000mm
Diameter (mm)	[d]	116.0000		
Length (mm)	[l]	18.0000		
Surface roughness (µm)	[Rz]	8.0000		
<u>Cylinder inside (Cylindrical bore)</u>			32.000mm ...	48.000mm
Diameter (mm)	[d]	100.0000		
Length (mm)	[l]	16.0000		
Surface roughness (µm)	[Rz]	8.0000		
<u>Cylinder inside (Cylindrical bore)</u>			48.000mm ...	50.000mm
Diameter (mm)	[d]	98.0000		
Length (mm)	[l]	2.0000		

Surface roughness ( $\mu\text{m}$ ) [Rz] 8.0000

<u>Cylinder inside (Cylindrical bore)</u>		50.000mm ...	60.000mm
Diameter (mm)	[d]	100.0000	
Length (mm)	[l]	10.0000	
Surface roughness ( $\mu\text{m}$ )	[Rz]	8.0000	

**Forces**

Type of force element

		<b>Coupling</b>		
		RingCoupling(RingStatic)		
Label in the model		27.0000		
Position on shaft (mm)	[y <sub>local</sub> ]	27.0000		
Position in global system (mm)	[y <sub>global</sub> ]	147.0000		
Effective diameter (mm)		0.0000		
Radial force factor (-)		0.0000		
Direction of the radial force (°)		0.0000		
Axial force factor (-)		0.0000		
Length of load application (mm)		0.0000		
Power (kW)		1.0472		
Torque (Nm)		100.0000		
Axial force (load spectrum) (N)		0.0000 /	0.0000 /	0.0000
Shearing force X (load spectrum) (N)		0.0000 /	0.0000 /	0.0000
Shearing force Z (Load spectrum) (N)		0.0000 /	0.0000 /	0.0000
Mass (kg)		0.0000		
Mass moment of inertia J <sub>p</sub> (kg*m <sup>2</sup> )		0.0000		
Mass moment of inertia J <sub>xx</sub> (kg*m <sup>2</sup> )		0.0000		
Mass moment of inertia J <sub>zz</sub> (kg*m <sup>2</sup> )		0.0000		
Eccentricity (mm)		0.0000		
Load spectrum, driven (input)				

No.	Frequency (%)	Speed (1/min)	Power (kW)	Torque (Nm)
1	4.0000e+001	-820.461	-9.315	108.418
2	1.0000e+001	-1093.947	-20.000	174.585
3	6.0000e+000	-1230.691	-20.000	155.186
4	4.0000e+000	-847.809	-18.356	206.755
5	3.0000e+001	-546.974	-17.593	307.145
6	8.0000e+000	-1093.947	12.000	-104.751
7	2.0000e+000	-621.811	16.000	-245.716

Type of force element

		<b>Cylindrical gear</b>		
		RingGear(Planet2RingConstraint)		
Label in the model		38.0000		
Position on shaft (mm)	[y <sub>local</sub> ]	38.0000		
Position in global system (mm)	[y <sub>global</sub> ]	158.0000		
Operating pitch diameter (mm)		-84.3907		
Spur gear				
Working pressure angle at normal section (°)		20.7165		
Position of contact (°)		-160.0000		
Length of load application (mm)		13.0000		
Power (kW)		1.0472		
Torque (Nm)		100.0000		
Axial force (load spectrum) (N)		0.0000 /	0.0000 /	0.0000
Shearing force X (load spectrum) (N)		-11.4506 /	-18.4389 /	-16.3901
Shearing force Z (Load spectrum) (N)		-915.6094 /	-1474.4004 /	-1310.5781
Bending moment X (Load spectrum) (Nm)		0.0000 /	0.0000 /	0.0000
Bending moment Z (Load spectrum) (Nm)		-0.0000 /	-0.0000 /	-0.0000
Load spectrum, driven (input)				

No.	Frequency (%)	Speed (1/min)	Power (kW)	Torque (Nm)
1	4.0000e+001	-820.461	3.105	-36.139
2	1.0000e+001	-1093.947	6.667	-58.195
3	6.0000e+000	-1230.691	6.667	-51.729
4	4.0000e+000	-847.809	6.119	-68.918
5	3.0000e+001	-546.974	5.864	-102.382
6	8.0000e+000	-1093.947	-4.000	34.917
7	2.0000e+000	-621.811	-5.333	81.905

Type of force element

Type of force element		Cylindrical gear		
Label in the model		RingGear(Planet2RingConstraint)2		
Position on shaft (mm)	[y <sub>local</sub> ]	38.0000		
Position in global system (mm)	[y <sub>global</sub> ]	158.0000		
Operating pitch diameter (mm)		-84.3907		
Spur gear				
Working pressure angle at normal section (°)		20.7165		
Position of contact (°)		-40.0000		
Length of load application (mm)		13.0000		
Power (kW)		1.0472		
Torque (Nm)		100.0000		
Axial force (load spectrum) (N)		0.0000 /	0.0000 /	0.0000
Shearing force X (load spectrum) (N)		798.6663 /	1286.0876 /	1143.1890
Shearing force Z (Load spectrum) (N)		447.8882 /	721.2317 /	641.0948
Bending moment X (Load spectrum) (Nm)		0.0000 /	0.0000 /	0.0000
Bending moment Z (Load spectrum) (Nm)		0.0000 /	0.0000 /	0.0000
Load spectrum, driven (input)				

No.	Frequency (%)	Speed (1/min)	Power (kW)	Torque (Nm)
1	4.0000e+001	-820.461	3.105	-36.139
2	1.0000e+001	-1093.947	6.667	-58.195
3	6.0000e+000	-1230.691	6.667	-51.729
4	4.0000e+000	-847.809	6.119	-68.918
5	3.0000e+001	-546.974	5.864	-102.382
6	8.0000e+000	-1093.947	-4.000	34.917
7	2.0000e+000	-621.811	-5.333	81.905

Type of force element

Type of force element		Cylindrical gear		
Label in the model		RingGear(Planet2RingConstraint)3		
Position on shaft (mm)	[y <sub>local</sub> ]	38.0000		
Position in global system (mm)	[y <sub>global</sub> ]	158.0000		
Operating pitch diameter (mm)		-84.3907		
Spur gear				
Working pressure angle at normal section (°)		20.7165		
Position of contact (°)		80.0000		
Length of load application (mm)		13.0000		
Power (kW)		1.0472		
Torque (Nm)		100.0000		
Axial force (load spectrum) (N)		0.0000 /	0.0000 /	0.0000
Shearing force X (load spectrum) (N)		-787.2157 /	-1267.6488 /	-1126.7989
Shearing force Z (Load spectrum) (N)		467.7212 /	753.1687 /	669.4833
Bending moment X (Load spectrum) (Nm)		-0.0000 /	-0.0000 /	-0.0000
Bending moment Z (Load spectrum) (Nm)		0.0000 /	0.0000 /	0.0000
Load spectrum, driven (input)				

No.	Frequency (%)	Speed (1/min)	Power (kW)	Torque (Nm)
-----	---------------	---------------	------------	-------------

1	4.0000e+001	-820.461	3.105	-36.139
2	1.0000e+001	-1093.947	6.667	-58.195
3	6.0000e+000	-1230.691	6.667	-51.729
4	4.0000e+000	-847.809	6.119	-68.918
5	3.0000e+001	-546.974	5.864	-102.382
6	8.0000e+000	-1093.947	-4.000	34.917
7	2.0000e+000	-621.811	-5.333	81.905

**Bearing**

Label in the model		RingSupport
Bearing type		Own Input
Bearing position (mm)	[Y <sub>lokal</sub> ]	35.000
Bearing position (mm)	[Y <sub>global</sub> ]	155.000
Degrees of freedom		
X: fixedY: fixedZ: fixed		
Rx: fixedRy: freeRz: fixed		

**Shaft definition (SunShaft)**

**Outer contour**

<u>Cylinder (Cylinder)</u>			0.000mm ...	2.300mm
Diameter (mm)	[d]	6.0000		
Length (mm)	[l]	2.3000		
Surface roughness (µm)	[Rz]	8.0000		
<u>Cylinder (Cylinder)</u>			2.300mm ...	7.000mm
Diameter (mm)	[d]	14.0000		
Length (mm)	[l]	4.7000		
Surface roughness (µm)	[Rz]	8.0000		
<u>Cylinder (Cylinder)</u>			7.000mm ...	17.000mm
Diameter (mm)	[d]	17.0000		
Length (mm)	[l]	10.0000		
Surface roughness (µm)	[Rz]	8.0000		
<u>Cylinder (Cylinder)</u>			17.000mm ...	91.500mm
Diameter (mm)	[d]	18.0000		
Length (mm)	[l]	74.5000		
Surface roughness (µm)	[Rz]	8.0000		
<u>Cylinder (Cylinder)</u>			91.500mm ...	107.500mm
Diameter (mm)	[d]	25.0000		
Length (mm)	[l]	16.0000		
Surface roughness (µm)	[Rz]	8.0000		
<u>Cylinder (Cylinder)</u>			107.500mm ...	117.500mm
Diameter (mm)	[d]	30.0000		
Length (mm)	[l]	10.0000		
Surface roughness (µm)	[Rz]	8.0000		
<u>Taper (Cone)</u>			117.500mm ...	121.300mm
Diameter left (mm)	[d <sub>l</sub> ]	20.0000		
Diameter right (mm)	[d <sub>r</sub> ]	12.0000		
Length (mm)	[l]	3.8000		
Surface roughness (µm)	[Rz]	8.0000		

Cylinder (Cylinder)			121.300mm ...	129.500mm
Diameter (mm)	[d]	12.0000		
Length (mm)	[l]	8.2000		
Surface roughness (µm)	[Rz]	8.0000		

Cylinder (Cylinder)			129.500mm ...	143.300mm
Diameter (mm)	[d]	10.8400		
Length (mm)	[l]	13.8000		
Surface roughness (µm)	[Rz]	8.0000		

#### Inner contour

Cylinder inside (Cylindrical bore)			0.000mm ...	14.600mm
Diameter (mm)	[d]	3.0000		
Length (mm)	[l]	14.6000		
Surface roughness (µm)	[Rz]	8.0000		

#### Forces

Type of force element

		Coupling		
		Input(MotorInput)		
Label in the model				
Position on shaft (mm)	[y <sub>local</sub> ]	57.0000		
Position in global system (mm)	[y <sub>global</sub> ]	57.0000		
Effective diameter (mm)		0.0000		
Radial force factor (-)		0.0000		
Direction of the radial force (°)		0.0000		
Axial force factor (-)		0.0000		
Length of load application (mm)		0.0000		
Power (kW)		1.0472		
Torque (Nm)		100.0000		
Axial force (load spectrum) (N)		0.0000 /	0.0000 /	0.0000
Shearing force X (load spectrum) (N)		0.0000 /	0.0000 /	0.0000
Shearing force Z (Load spectrum) (N)		0.0000 /	0.0000 /	0.0000
Mass (kg)		0.0000		
Mass moment of inertia J <sub>p</sub> (kg*m <sup>2</sup> )		0.0000		
Mass moment of inertia J <sub>xx</sub> (kg*m <sup>2</sup> )		0.0000		
Mass moment of inertia J <sub>zz</sub> (kg*m <sup>2</sup> )		0.0000		
Eccentricity (mm)		0.0000		
Load spectrum, driven (input)				

No.	Frequency (%)	Speed (1/min)	Power (kW)	Torque (Nm)
1	4.0000e+001	11875.220	9.315	7.491
2	1.0000e+001	15833.627	20.000	12.062
3	6.0000e+000	17812.830	20.000	10.722
4	4.0000e+000	12271.061	18.356	14.285
5	3.0000e+001	7916.813	17.593	21.221
6	8.0000e+000	15833.627	-12.000	-7.237
7	2.0000e+000	9000.000	-16.000	-16.977

Type of force element

		Cylindrical gear	
		SunGear(SunPlanetConstraint)	
Label in the model			
Position on shaft (mm)	[y <sub>local</sub> ]	140.0000	
Position in global system (mm)	[y <sub>global</sub> ]	140.0000	
Operating pitch diameter (mm)		14.8624	
Spur gear			
Working pressure angle at normal section (°)		18.4874	



Position of contact (°)	-160.0000		
Length of load application (mm)	12.5000		
Power (kW)	1.0472		
Torque (Nm)	100.0000		
Axial force (load spectrum) (N)	0.0000 /	0.0000 /	0.0000
Shearing force X (load spectrum) (N)	220.4843 /	355.0446 /	315.5952
Shearing force Z (Load spectrum) (N)	-277.3120 /	-446.5539 /	-396.9368
Bending moment X (Load spectrum) (Nm)	0.0000 /	0.0000 /	0.0000
Bending moment Z (Load spectrum) (Nm)	-0.0000 /	-0.0000 /	-0.0000
Load spectrum, driven (input)			

No.	Frequency (%)	Speed (1/min)	Power (kW)	Torque (Nm)
1	4.0000e+001	11875.220	-3.105	-2.497
2	1.0000e+001	15833.627	-6.667	-4.021
3	6.0000e+000	17812.830	-6.667	-3.574
4	4.0000e+000	12271.061	-6.119	-4.762
5	3.0000e+001	7916.813	-5.864	-7.074
6	8.0000e+000	15833.627	4.000	2.412
7	2.0000e+000	9000.000	5.333	5.659

Type of force element

**Cylindrical gear**

Label in the model		SunGear(SunPlanetConstraint)2		
Position on shaft (mm)	[Y <sub>local</sub> ]	140.0000		
Position in global system (mm)	[Y <sub>global</sub> ]	140.0000		
Operating pitch diameter (mm)		14.8624		
Spur gear				
Working pressure angle at normal section (°)		18.4874		
Position of contact (°)		-40.0000		
Length of load application (mm)		12.5000		
Power (kW)		1.0472		
Torque (Nm)		100.0000		
Axial force (load spectrum) (N)		0.0000 /	0.0000 /	0.0000
Shearing force X (load spectrum) (N)		129.9171 /	209.2047 /	185.9597
Shearing force Z (Load spectrum) (N)		329.6010 /	530.7545 /	471.7818
Bending moment X (Load spectrum) (Nm)		0.0000 /	0.0000 /	0.0000
Bending moment Z (Load spectrum) (Nm)		0.0000 /	0.0000 /	0.0000
Load spectrum, driven (input)				

No.	Frequency (%)	Speed (1/min)	Power (kW)	Torque (Nm)
1	4.0000e+001	11875.220	-3.105	-2.497
2	1.0000e+001	15833.627	-6.667	-4.021
3	6.0000e+000	17812.830	-6.667	-3.574
4	4.0000e+000	12271.061	-6.119	-4.762
5	3.0000e+001	7916.813	-5.864	-7.074
6	8.0000e+000	15833.627	4.000	2.412
7	2.0000e+000	9000.000	5.333	5.659

Type of force element

**Cylindrical gear**

Label in the model		SunGear(SunPlanetConstraint)3
Position on shaft (mm)	[Y <sub>local</sub> ]	140.0000
Position in global system (mm)	[Y <sub>global</sub> ]	140.0000
Operating pitch diameter (mm)		14.8624
Spur gear		
Working pressure angle at normal section (°)		18.4874
Position of contact (°)		80.0000
Length of load application (mm)		12.5000

Power (kW)	1.0472		
Torque (Nm)	100.0000		
Axial force (load spectrum) (N)	0.0000 /	0.0000 /	0.0000
Shearing force X (load spectrum) (N)	-350.4014 /	-564.2493 /	-501.5549
Shearing force Z (Load spectrum) (N)	-52.2890 /	-84.2007 /	-74.8450
Bending moment X (Load spectrum) (Nm)	-0.0000 /	-0.0000 /	-0.0000
Bending moment Z (Load spectrum) (Nm)	0.0000 /	0.0000 /	0.0000
Load spectrum, driven (input)			

No.	Frequency (%)	Speed (1/min)	Power (kW)	Torque (Nm)
1	4.0000e+001	11875.220	-3.105	-2.497
2	1.0000e+001	15833.627	-6.667	-4.021
3	6.0000e+000	17812.830	-6.667	-3.574
4	4.0000e+000	12271.061	-6.119	-4.762
5	3.0000e+001	7916.813	-5.864	-7.074
6	8.0000e+000	15833.627	4.000	2.412
7	2.0000e+000	9000.000	5.333	5.659

### Bearing

Label in the model	MotorBearing1	
Bearing type	SKF *6003-2RSH	
Bearing type	Deep groove ball bearing (single row)	
Bearing position (mm)	[Y <sub>lokal</sub> ]	12.000
Bearing position (mm)	[Y <sub>global</sub> ]	12.000
Attachment of external ring	Free bearing	
Inner diameter (mm)	[d]	17.000
External diameter (mm)	[D]	35.000
Width (mm)	[b]	10.000
Corner radius (mm)	[r]	0.300
Basic static load rating	[C <sub>0</sub> ]	3.250
Basic dynamic load rating	[C]	6.370
Fatigue load rating	[C <sub>U</sub> ]	0.137
Values for approximated geometry:		
Basic dynamic load rating (kN)	[C <sub>theo</sub> ]	0.000
Basic static load rating (kN)	[C <sub>0theo</sub> ]	0.000

Label in the model	MotorBearing2	
Bearing type	SKF *6005	
Bearing type	Deep groove ball bearing (single row)	
Bearing position (mm)	[Y <sub>lokal</sub> ]	101.500
Bearing position (mm)	[Y <sub>global</sub> ]	101.500
Attachment of external ring	Fixed bearing	
Inner diameter (mm)	[d]	25.000
External diameter (mm)	[D]	47.000
Width (mm)	[b]	12.000
Corner radius (mm)	[r]	0.600
Basic static load rating	[C <sub>0</sub> ]	6.550
Basic dynamic load rating	[C]	11.900
Fatigue load rating	[C <sub>U</sub> ]	0.275
Values for approximated geometry:		
Basic dynamic load rating (kN)	[C <sub>theo</sub> ]	0.000
Basic static load rating (kN)	[C <sub>0theo</sub> ]	0.000

## Results

Note: the maximum deflection and twisting of the shaft under torque, the service life coefficient aISO and the bearing's thinnest lubricant film thickness EHL are predefined for the first load bin.

### Shaft

Maximum deflection	0.007 (SunShaft pos=	143.300)
Mass center of gravity		
CarrierShaft (mm)		52.698
RingShaft (mm)		31.520
SunShaft (mm)		75.797
Total axial load		
CarrierShaft (N)		0.000
RingShaft (N)		0.000
SunShaft (N)		0.000
Torsion under torque		
CarrierShaft (°)		-0.007
RingShaft (°)		-0.000
SunShaft (°)		-0.087

### Bearing

Probability of failure	[n]	10.00	%
Axial clearance	[u <sub>A</sub> ]	10.00	µm

Rolling bearings, classical calculation (contact angle considered)

### Shaft 'CarrierShaft' Rolling bearing 'WheelBearing1'

Position (Y-coordinate)	[y]	55.00	mm
Life modification factor for reliability[a <sub>i</sub> ]		1.000	
Service life	[L <sub>nh</sub> ]	98873.66	h
Static safety factor	[S <sub>0</sub> ]	22.54	

#### Bearing reaction force

	Fx (kN)	Fy (kN)	Fz (kN)	Mx (Nm)	My (Nm)	Mz (Nm)
1	-0.000	0.000	-1.065	-12.776	0.000	0.000
2	-0.000	0.000	-0.851	-10.214	0.000	0.000
3	-0.000	0.000	-0.638	-7.652	0.000	0.000
4	-0.000	0.000	-0.744	-8.933	0.000	0.000
5	-0.000	0.000	-0.638	-7.652	0.000	0.000
6	-0.000	0.000	-0.851	-10.214	0.000	0.000
7	-0.000	0.000	-1.065	-12.776	0.000	0.000

#### Bearing reaction moment

#### Displacement of bearing

	ux (µm)	uy (µm)	uz (µm)	ux (mrad)	uy (mrad)	uz (mrad)
1	0.0000	0.0000	2.2774	0.044	-0.094	-0.000
2	0.0000	0.0000	1.8206	0.035	-0.152	-0.000
3	0.0000	0.0000	1.3638	0.026	-0.135	-0.000
4	0.0000	0.0000	1.5922	0.031	-0.180	-0.000
5	0.0000	0.0000	1.3638	0.026	-0.267	-0.000
6	0.0000	0.0000	1.8206	0.035	0.091	-0.000

#### Misalignment of bearing

7      0.0000      0.0000      2.2774      0.044      0.213      -0.000

**Shaft 'CarrierShaft' Rolling bearing 'WheelBearing2'**

Position (Y-coordinate)                      [y]                      5.00      mm  
 Life modification factor for reliability[a<sub>i</sub>]                      1.000  
 Service life                      [L<sub>nh</sub>]                      > 1000000      h  
 Static safety factor                      [S<sub>0</sub>]                      351.61

**Bearing reaction force**

**Bearing reaction moment**

	Fx (kN)	Fy (kN)	Fz (kN)	Mx (Nm)	My (Nm)	Mz (Nm)
1	-0.000	0.000	0.068	-0.819	0.000	-0.000
2	-0.000	0.000	0.055	-0.657	0.000	-0.000
3	-0.000	0.000	0.041	-0.495	0.000	-0.000
4	-0.000	0.000	0.048	-0.576	0.000	-0.000
5	-0.000	0.000	0.041	-0.495	0.000	-0.000
6	-0.000	0.000	0.055	-0.657	0.000	-0.000
7	-0.000	0.000	0.068	-0.819	0.000	-0.000

**Displacement of bearing**

**Misalignment of bearing**

	ux (µm)	uy (µm)	uz (µm)	ux (mrad)	uy (mrad)	uz (mrad)
1	0.0000	0.0000	0.2847	0.042	0.000	-0.000
2	0.0000	0.0000	0.2271	0.033	0.000	-0.000
3	0.0000	0.0000	0.1696	0.025	0.000	-0.000
4	0.0000	0.0000	0.1983	0.029	0.000	-0.000
5	0.0000	0.0000	0.1696	0.025	0.000	-0.000
6	0.0000	0.0000	0.2271	0.033	0.000	-0.000
7	0.0000	0.0000	0.2847	0.042	0.000	-0.000

**Shaft 'RingShaft' Bearing 'RingSupport'**

Position (Y-coordinate)                      [y]                      35.00      mm

**Bearing reaction force**

**Bearing reaction moment**

	Fx (kN)	Fy (kN)	Fz (kN)	Mx (Nm)	My (Nm)	Mz (Nm)
1	-0.000	0.000	0.017	-0.058	0.000	0.000
2	-0.000	0.000	0.017	-0.058	0.000	0.000
3	-0.000	0.000	0.017	-0.058	0.000	0.000
4	-0.000	0.000	0.017	-0.058	0.000	0.000
5	-0.000	0.000	0.017	-0.058	0.000	-0.000
6	0.000	0.000	0.017	-0.058	0.000	-0.000
7	-0.000	0.000	0.017	-0.058	0.000	-0.000

**Displacement of bearing**

**Misalignment of bearing**

	ux (µm)	uy (µm)	uz (µm)	ux (mrad)	uy (mrad)	uz (mrad)
1	0.0000	0.0000	-0.0000	0.000	-0.001	-0.000
2	0.0000	0.0000	-0.0000	0.000	-0.002	-0.000
3	0.0000	0.0000	-0.0000	0.000	-0.002	-0.000
4	0.0000	0.0000	-0.0000	0.000	-0.003	-0.000
5	0.0000	0.0000	-0.0000	0.000	-0.004	0.000
6	-0.0000	0.0000	-0.0000	0.000	0.001	0.000
7	0.0000	0.0000	-0.0000	0.000	0.003	0.000

**Shaft 'SunShaft' Rolling bearing 'MotorBearing1'**

Position (Y-coordinate)                      [y]                      12.00      mm  
 Life modification factor for reliability[a<sub>i</sub>]                      1.000  
 Service life                      [L<sub>nh</sub>]                      > 1000000      h

Static safety factor [S<sub>0</sub>] 3702.85

	Bearing reaction force			Bearing reaction moment		
	Fx (kN)	Fy (kN)	Fz (kN)	Mx (Nm)	My (Nm)	Mz (Nm)
1	0.000	0.000	0.001	0.000	0.000	0.000
2	0.000	0.000	0.001	0.000	0.000	0.000
3	0.000	0.000	0.001	0.000	0.000	0.000
4	0.000	0.000	0.001	0.000	0.000	0.000
5	0.000	0.000	0.001	0.000	0.000	0.000
6	0.000	0.000	0.001	0.000	0.000	0.000
7	0.000	0.000	0.001	0.000	0.000	0.000

	Displacement of bearing			Misalignment of bearing		
	ux (µm)	uy (µm)	uz (µm)	ux (mrad)	uy (mrad)	uz (mrad)
1	-0.0000	0.0000	-5.2500	-0.012	-0.000	-0.002
2	0.0000	0.0000	-5.2500	-0.012	0.000	-0.002
3	0.0000	0.0000	-5.2500	-0.012	0.000	-0.002
4	-0.0000	0.0000	-5.2500	-0.012	0.000	-0.002
5	-0.0000	0.0000	-5.2500	-0.012	-0.000	-0.002
6	-0.0000	0.0000	-5.2500	-0.012	0.000	-0.002
7	-0.0000	0.0000	-5.2500	-0.012	-0.000	-0.002

**Shaft 'SunShaft' Rolling bearing 'MotorBearing2'**

Position (Y-coordinate) [y] 101.50 mm  
 Life modification factor for reliability[a<sub>1</sub>] 1.000  
 Service life [L<sub>mh</sub>] > 1000000 h  
 Static safety factor [S<sub>0</sub>] 3000.90

	Bearing reaction force			Bearing reaction moment		
	Fx (kN)	Fy (kN)	Fz (kN)	Mx (Nm)	My (Nm)	Mz (Nm)
1	0.000	0.000	0.002	0.000	0.000	0.000
2	0.000	0.000	0.002	0.000	0.000	0.000
3	0.000	0.000	0.002	0.000	0.000	0.000
4	0.000	0.000	0.002	0.000	0.000	0.000
5	0.000	0.000	0.002	0.000	0.000	0.000
6	0.000	0.000	0.002	0.000	0.000	0.000
7	0.000	0.000	0.002	0.000	0.000	0.000

	Displacement of bearing			Misalignment of bearing		
	ux (µm)	uy (µm)	uz (µm)	ux (mrad)	uy (mrad)	uz (mrad)
1	0.1463	0.0000	-6.2483	-0.011	-0.341	-0.002
2	0.1463	0.0000	-6.2483	-0.011	-0.549	-0.002
3	0.1463	0.0000	-6.2483	-0.011	-0.488	-0.002
4	0.1463	0.0000	-6.2483	-0.011	-0.651	-0.002
5	0.1463	0.0000	-6.2483	-0.011	-0.966	-0.002
6	0.1463	0.0000	-6.2483	-0.011	0.330	-0.002
7	0.1463	0.0000	-6.2483	-0.011	0.773	-0.002

Damage (%) [H] ( 50.000)

No.	B1	B2	B3	B4
1	0.03	0.00	0.00	0.00
2	0.01	0.00	0.00	0.00
3	0.00	0.00	0.00	0.00
4	0.00	0.00	0.00	0.00
5	0.00	0.00	0.00	0.00
6	0.00	0.00	0.00	0.00

7	0.00	0.00	0.00	0.00
-----				
$\Sigma$	0.05	0.01	0.01	0.01

Utilization, with reference to the required service life  
[H] ( 50.000)

B1	B2	B3	B4
0.08	0.04	0.04	0.04

- B1: WheelBearing1
- B2: WheelBearing2
- B3: MotorBearing1
- B4: MotorBearing2

Displacement [mm]

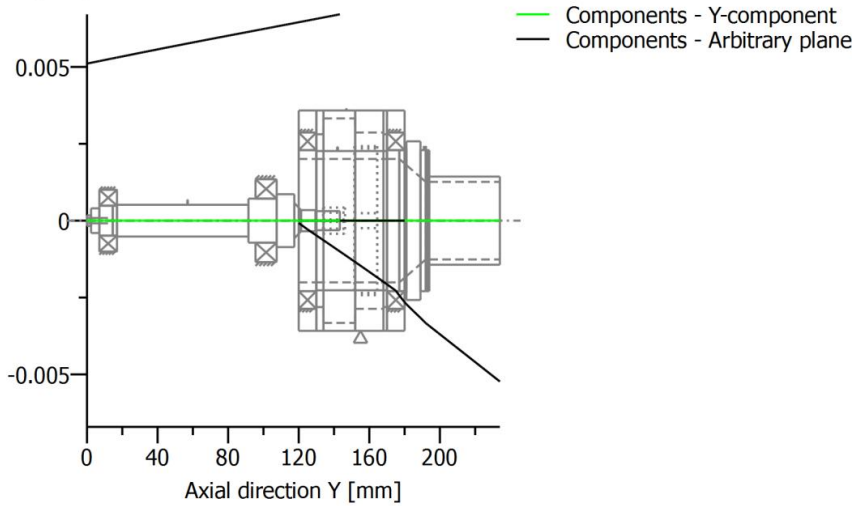
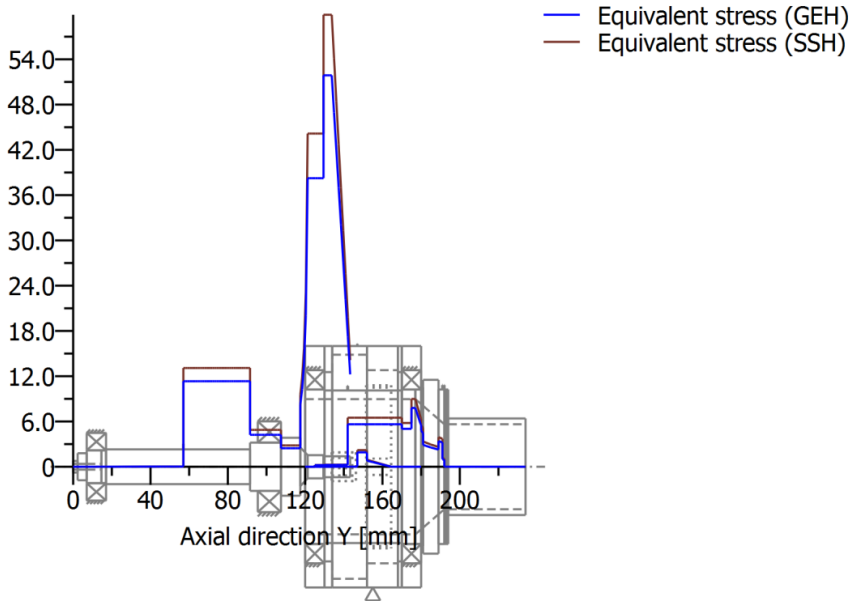


Figure: Deformation (bending etc.) (Arbitrary plane 271.8332482 120)

Stress [N/mm<sup>2</sup>]



GEH(von Mises):  $\text{sigV} = \sqrt{((\text{sigB} + \text{sigZ}, \text{D})^2 + 3 * (\text{tauT} + \text{tauS})^2)^{1/2}}$  SSH(Tresca):  $\text{sigV} = \sqrt{((\text{sigB} - \text{sigZ}, \text{D})^2 + 4 * (\text{tauT} + \text{tauS})^2)^{1/2}}$   
Figure: Equivalent stress

# Planet shaft calculation

KISSsoft Release 03/2015 F

KISSsoft Academic License - Norwegian University of Science & Technology (NTNU)

File

Name : Unnamed

Changed by: Kraftwerk on: 02.02.2016 at: 18:54:00

**Important hint: At least one warning has occurred during the calculation:**

1-> Shaft 'PlanetPinShaft', bearing 'SKF NU 202 ECP': This type of bearing is not recommended to support axial forces. Please check the result carefully!

2-> The speed is 0! ('SKF NU 202 ECP')

3-> Rolling bearing 'ConnectionRollerBearing1':  
Cylindrical roller bearings:

The axial force should be at most 0.0 N (at full complement roller bearings 0.0 N), in order that a hydro-dynamical lubricant film may be formed.

More detailed input about the lubricant may be entered in the tab 'Basic Data', under 'Additional Data' and 'Modified rating life'.

4-> The required service life of bearing 'Rolling bearing 'ConnectionRollerBearing1' is not achieved!

5-> The speed is 0! ('INA HK1012')

6-> The required service life of bearing 'Rolling bearing 'ConnectionRollerBearing2' is not achieved!

## Analysis of shafts, axle and beams

### Input data

Coordinate system shaft: see picture W-002

Label	PlanetGearShaft
Drawing	
Initial position (mm)	14.000
Length (mm)	31.000
Speed (1/min)	100.00
Sense of rotation: clockwise	
Material	C45 (1)
Young's modulus (N/mm <sup>2</sup> )	206000.000
Poisson's ratio nu	0.300
Density (kg/m <sup>3</sup> )	7830.000
Coefficient of thermal expansion (10 <sup>-6</sup> /K)	11.500
Temperature (°C)	20.000
Weight of shaft (kg)	0.137
(Notice: Weight stands for the shaft only without considering the gears)	
Weight of shaft, including additional masses (kg)	0.171
Mass moment of inertia (kg*mm <sup>2</sup> )	60.827
Momentum of mass GD2 (Nm <sup>2</sup> )	0.002



Label	PlanetPinShaft
Drawing	
Initial position (mm)	0.000
Length (mm)	53.000
Speed (1/min)	100.00
Sense of rotation: clockwise	
Material	C45 (1)
Young's modulus (N/mm <sup>2</sup> )	206000.000
Poisson's ratio nu	0.300
Density (kg/m <sup>3</sup> )	7830.000
Coefficient of thermal expansion (10 <sup>-6</sup> /K)	11.500
Temperature (°C)	20.000
Weight of shaft (kg)	0.040
(Notice: Weight stands for the shaft only without considering the gears)	
Weight of shaft, including additional masses (kg)	0.040
Mass moment of inertia (kg*mm <sup>2</sup> )	0.688
Momentum of mass GD2 (Nm <sup>2</sup> )	0.000
Weight towards ( 0.000, 0.000, -1.000)	
Regard gears as masses and stiffness	
Consider deformations due to shearing	
Shear correction coefficient	1.100
A non-linear shaft model is used	
Rolling bearing stiffness is calculated from inner bearing geometry	
Tolerance field: Mean value	
Reference temperature (°C)	20.000

---

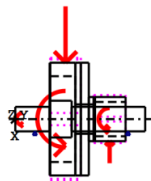
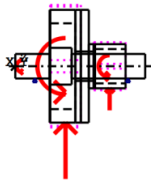


Figure: Load applications

**Shaft definition (PlanetGearShaft)**

**Outer contour**

Cylinder (Cylinder)			0.000mm ...	16.000mm
Diameter (mm)	[d]	46.0000		
Length (mm)	[l]	16.0000		
Surface roughness (µm)	[Rz]	8.0000		

Chamfer right (Chamfer right)  
l=3.50 (mm), alpha=75.00 (°)

Cylinder (Cylinder)			16.000mm ...	31.000mm
Diameter (mm)	[d]	18.0000		
Length (mm)	[l]	15.0000		
Surface roughness (µm)	[Rz]	8.0000		

**Inner contour**

Cylinder inside (Cylindrical bore)			0.000mm ...	10.500mm
Diameter (mm)	[d]	35.0000		
Length (mm)	[l]	10.5000		
Surface roughness (µm)	[Rz]	8.0000		

Cylinder inside (Cylindrical bore)			10.500mm ...	18.500mm
Diameter (mm)	[d]	12.0000		
Length (mm)	[l]	8.0000		
Surface roughness (µm)	[Rz]	8.0000		

Cylinder inside (Cylindrical bore)			18.500mm ...	31.000mm
Diameter (mm)	[d]	14.0000		
Length (mm)	[l]	12.5000		
Surface roughness (µm)	[Rz]	8.0000		

**Forces**

Type of force element

		Cylindrical gear		
		Planet1(SunPlanetConstraint)		
Label in the model		Planet1(SunPlanetConstraint)		
Position on shaft (mm)	[y <sub>local</sub> ]	6.5000		
Position in global system (mm)	[y <sub>global</sub> ]	20.5000		
Operating pitch diameter (mm)		49.9376		
Spur gear				
Working pressure angle at normal section (°)		18.4874		
Position of contact (°)		20.0000		
Length of load application (mm)		12.5000		
Power (kW)		1.0472		
Torque (Nm)		100.0000		
Axial force (load spectrum) (N)		0.0000 /	0.0000 /	0.0000
Shearing force X (load spectrum) (N)		-220.4843 /	-355.0446 /	-315.5952
Shearing force Z (Load spectrum) (N)		277.3120 /	446.5539 /	396.9368
Bending moment X (Load spectrum) (Nm)		-0.0000 /	-0.0000 /	-0.0000
Bending moment Z (Load spectrum) (Nm)		0.0000 /	0.0000 /	0.0000
Load spectrum, driven (input)				

No.	Frequency (%)	Speed (1/min)	Power (kW)	Torque (Nm)
1	4.0000e+001	-3534.292	3.105	-8.389

2	1.0000e+001	-4712.389	6.667	-13.510
3	6.0000e+000	-5301.438	6.667	-12.008
4	4.0000e+000	-3652.101	6.119	-15.999
5	3.0000e+001	-2356.194	5.864	-23.767
6	8.0000e+000	-4712.389	-4.000	8.106
7	2.0000e+000	-2678.571	-5.333	19.014

Type of force element

		<b>Cylindrical gear</b>		
Label in the model		Planet2(Planet2RingConstraint)		
Position on shaft (mm)	[Y <sub>local</sub> ]	24.5000		
Position in global system (mm)	[Y <sub>global</sub> ]	38.5000		
Operating pitch diameter (mm)		19.5907		
Spur gear				
Working pressure angle at normal section (°)		20.7165		
Position of contact (°)		-160.0000		
Length of load application (mm)		13.0000		
Power (kW)		1.0472		
Torque (Nm)		100.0000		
Axial force (load spectrum) (N)		-0.0000 /	-0.0000 /	-0.0000
Shearing force X (load spectrum) (N)		11.4506 /	18.4389 /	16.3901
Shearing force Z (Load spectrum) (N)		915.6094 /	1474.4004 /	1310.5781
Bending moment X (Load spectrum) (Nm)		-0.0000 /	-0.0000 /	-0.0000
Bending moment Z (Load spectrum) (Nm)		0.0000 /	0.0000 /	0.0000
Load spectrum, driven (input)				

No.	Frequency (%)	Speed (1/min)	Power (kW)	Torque (Nm)
1	4.0000e+001	-3534.292	-3.105	8.389
2	1.0000e+001	-4712.389	-6.667	13.510
3	6.0000e+000	-5301.438	-6.667	12.008
4	4.0000e+000	-3652.101	-6.119	15.999
5	3.0000e+001	-2356.194	-5.864	23.767
6	8.0000e+000	-4712.389	4.000	-8.106
7	2.0000e+000	-2678.571	5.333	-19.014

**Shaft definition (PlanetPinShaft)**

**Outer contour**

<u>Cylinder (Cylinder)</u>		0.000mm ...	<u>14.000mm</u>
Diameter (mm)	[d]	10.0000	
Length (mm)	[l]	14.0000	
Surface roughness (µm)	[Rz]	8.0000	
<u>Cylinder (Cylinder)</u>		14.000mm ...	<u>23.000mm</u>
Diameter (mm)	[d]	15.0000	
Length (mm)	[l]	9.0000	
Surface roughness (µm)	[Rz]	8.0000	
<u>Cylinder (Cylinder)</u>		23.000mm ...	<u>53.000mm</u>
Diameter (mm)	[d]	10.0000	
Length (mm)	[l]	30.0000	
Surface roughness (µm)	[Rz]	8.0000	

**Forces**

Type of force element

		<b>Coupling</b>		
		CarrierCoupling(PlanetCarrierConstraint)		
Label in the model				
Position on shaft (mm)	[Y <sub>local</sub> ]	3.0000		
Position in global system (mm)	[Y <sub>global</sub> ]	3.0000		
Effective diameter (mm)		0.0000		
Radial force factor (-)		0.0000		
Direction of the radial force (°)		0.0000		
Axial force factor (-)		0.0000		
Length of load application (mm)		0.0000		
Power (kW)		1.0472		
Torque (Nm)		100.0000		
Axial force (load spectrum) (N)		0.0000 /	0.0000 /	0.0000
Shearing force X (load spectrum) (N)		0.0000 /	0.0000 /	0.0000
Shearing force Z (Load spectrum) (N)		0.0000 /	0.0000 /	0.0000
Mass (kg)		0.0000		
Mass moment of inertia J <sub>p</sub> (kg*m <sup>2</sup> )		0.0000		
Mass moment of inertia J <sub>xx</sub> (kg*m <sup>2</sup> )		0.0000		
Mass moment of inertia J <sub>zz</sub> (kg*m <sup>2</sup> )		0.0000		
Eccentricity (mm)		0.0000		
Load spectrum, driven (input)				

No.	Frequency (%)	Speed (1/min)	Power (kW)	Torque (Nm)
1	4.0000e+001	-228.404	-0.000	0.000
2	1.0000e+001	-304.539	-0.000	0.000
3	6.0000e+000	-342.606	-0.000	0.000
4	4.0000e+000	-236.018	-0.000	0.000
5	3.0000e+001	-152.269	-0.000	0.000
6	8.0000e+000	-304.539	-0.000	0.000
7	2.0000e+000	-173.103	-0.000	0.000

**Bearing**

Label in the model		PinSupport1
Bearing type		Own Input
Bearing position (mm)	[Y <sub>local</sub> ]	8.000
Bearing position (mm)	[Y <sub>global</sub> ]	8.000
Degrees of freedom		
X: fixedY: fixedZ: fixed		
Rx: freeRy: freeRz: free		

Label in the model		PinSupport2
Bearing type		Own Input
Bearing position (mm)	[Y <sub>local</sub> ]	46.000
Bearing position (mm)	[Y <sub>global</sub> ]	46.000
Degrees of freedom		
X: fixedY: freeZ: fixed		
Rx: freeRy: freeRz: free		

**CONNECTIONS**

SKF NU 202 ECP (ConnectionRollerBearing1) 19.000mm

Set fixed bearing left  
d = 15.000 (mm), D = 35.000 (mm), b = 11.000 (mm), r = 0.600 (mm)  
C = 12.500 (kN), C<sub>0</sub> = 10.200 (kN), C<sub>u</sub> = 1.220 (kN)  
C<sub>theo</sub> = 12.501 (kN), C<sub>0theo</sub> = 10.200 (kN)  
Calculation with approximate bearings internal geometry (\*)  
Z =9, D<sub>pw</sub> = 24.180 (mm), D<sub>w</sub> = 5.266 (mm)

Lwe = 6.253 (mm)  
 Diameter, external race (mm) [d<sub>e</sub>] 29.446  
 Diameter, internal race (mm) [d<sub>i</sub>] 18.914  
 Bearing clearance 0.00 μm

INA HK1012 (ConnectionRollerBearing2) 38.500mm

Free bearing  
 d = 10.000 (mm), D = 14.000 (mm), b = 12.000 (mm), r = 0.000 (mm)  
 C = 5.500 (kN), C<sub>0</sub> = 6.800 (kN), C<sub>u</sub> = 0.930 (kN)  
 C<sub>theo</sub> = 5.501 (kN), C<sub>0theo</sub> = 6.800 (kN)  
 Calculation with approximate bearings internal geometry (\*)  
 Z=17, Dpw = 11.689 (mm), Dw = 1.451 (mm)  
 Lwe = 7.155 (mm)

Diameter, external race (mm) [d<sub>e</sub>] 13.140  
 Diameter, internal race (mm) [d<sub>i</sub>] 10.239  
 Bearing clearance 0.00 μm

-----  
 Shaft 'PlanetGearShaft': Cylindrical gear 'Planet1(SunPlanetConstraint)' (y= 5.3750 (mm)) is taken into account as component of the shaft.

El (y= 0.2500 (mm)): 30101.7191 (Nm<sup>2</sup>), El (y= 10.5000 (mm)): 30101.7191 (Nm<sup>2</sup>), m (yS= 5.3750 (mm)): 0.0238 (kg)  
 Jp: 0.0000 (kg\*m<sup>2</sup>), Jxx: 0.0000 (kg\*m<sup>2</sup>), Jzz: 0.0000 (kg\*m<sup>2</sup>)

-----  
 Shaft 'PlanetGearShaft': Cylindrical gear 'Planet1(SunPlanetConstraint)' (y= 11.6250 (mm)) is taken into account as component of the shaft.

El (y= 10.5000 (mm)): 45066.3587 (Nm<sup>2</sup>), El (y= 12.7500 (mm)): 45066.3587 (Nm<sup>2</sup>), m (yS= 11.6250 (mm)): 0.0052 (kg)  
 Jp: 0.0000 (kg\*m<sup>2</sup>), Jxx: 0.0000 (kg\*m<sup>2</sup>), Jzz: 0.0000 (kg\*m<sup>2</sup>)

-----  
 Shaft 'PlanetGearShaft': Cylindrical gear 'Planet2(Planet2RingConstraint)' (y= 18.2500 (mm)) is taken into account as component of the shaft.

El (y= 18.0000 (mm)): 851.8350 (Nm<sup>2</sup>), El (y= 18.5000 (mm)): 851.8350 (Nm<sup>2</sup>), m (yS= 18.2500 (mm)): 0.0002 (kg)  
 Jp: 0.0000 (kg\*m<sup>2</sup>), Jxx: 0.0000 (kg\*m<sup>2</sup>), Jzz: 0.0000 (kg\*m<sup>2</sup>)

-----  
 Shaft 'PlanetGearShaft': Cylindrical gear 'Planet2(Planet2RingConstraint)' (y= 24.7500 (mm)) is taken into account as component of the shaft.

El (y= 18.5000 (mm)): 673.0548 (Nm<sup>2</sup>), El (y= 31.0000 (mm)): 673.0548 (Nm<sup>2</sup>), m (yS= 24.7500 (mm)): 0.0046 (kg)  
 Jp: 0.0000 (kg\*m<sup>2</sup>), Jxx: 0.0000 (kg\*m<sup>2</sup>), Jzz: 0.0000 (kg\*m<sup>2</sup>)

**Results**

Note: the maximum deflection and twisting of the shaft under torque, <br>the service life coefficient aISO and the bearing's thinnest lubricant film thickness EHL are<br>predefined for the first load bin.

**Shaft**

Maximum deflection 0.008 (PlanetGearShaft pos= 45.000)

Mass center of gravity	
PlanetGearShaft (mm)	10.794
PlanetPinShaft (mm)	25.099
Total axial load	
PlanetGearShaft (N)	0.000
PlanetPinShaft (N)	0.000
Torsion under torque	
PlanetGearShaft (°)	0.005
PlanetPinShaft (°)	0.000

### Bearing

Probability of failure	[n]	10.00	%
Axial clearance	[u <sub>A</sub> ]	10.00	µm
Rolling bearing service life according to ISO/TS 16281:2008			

### Shaft 'PlanetPinShaft' Bearing 'PinSupport1'

Position (Y-coordinate) [y] 8.00 mm

#### Bearing reaction force

	Fx (kN)	Fy (kN)	Fz (kN)	Mx (Nm)	My (Nm)	Mz (Nm)
1	0.146	-0.000	-0.366	0.000	0.000	0.000
2	0.235	-0.000	-0.589	0.000	0.000	0.000
3	0.209	-0.000	-0.524	0.000	0.000	0.000
4	0.278	-0.000	-0.698	0.000	0.000	0.000
5	0.413	-0.000	-1.038	0.000	0.000	0.000
6	-0.120	0.000	0.363	0.000	0.000	0.000
7	-0.281	-0.000	0.850	0.000	0.000	0.000

#### Bearing reaction moment

#### Displacement of bearing

	ux (µm)	uy (µm)	uz (µm)	ux (mrad)	uy (mrad)	uz (mrad)
1	-0.0000	0.0000	0.0000	0.434	0.000	0.104
2	-0.0000	0.0000	0.0000	0.692	0.000	0.166
3	-0.0000	0.0000	0.0000	0.617	0.000	0.148
4	-0.0000	0.0000	0.0000	0.817	0.000	0.196
5	-0.0000	0.0000	0.0000	1.206	0.000	0.289
6	0.0000	-0.0000	-0.0000	-0.388	-0.000	-0.193
7	0.0000	0.0000	-0.0000	-0.893	-0.000	-0.445

#### Misalignment of bearing

### Shaft 'PlanetPinShaft' Bearing 'PinSupport2'

Position (Y-coordinate) [y] 46.00 mm

#### Bearing reaction force

	Fx (kN)	Fy (kN)	Fz (kN)	Mx (Nm)	My (Nm)	Mz (Nm)
1	0.063	0.000	-0.825	0.000	0.000	0.000
2	0.102	0.000	-1.329	0.000	0.000	0.000
3	0.091	0.000	-1.182	0.000	0.000	0.000
4	0.121	0.000	-1.575	0.000	0.000	0.000
5	0.179	0.000	-2.339	0.000	0.000	0.000
6	-0.466	0.000	0.652	0.000	0.000	0.000
7	-1.094	0.000	1.527	0.000	0.000	0.000

#### Bearing reaction moment

	Displacement of bearing			Misalignment of bearing		
	ux (µm)	uy (µm)	uz (µm)	ux (mrad)	uy (mrad)	uz (mrad)
1	-0.0000	-0.0038	0.0000	-0.668	0.000	-0.103
2	-0.0000	-0.0097	0.0000	-1.063	0.000	-0.165
3	-0.0000	-0.0077	0.0000	-0.947	0.000	-0.147
4	-0.0000	-0.0135	0.0000	-1.254	0.000	-0.194
5	-0.0000	-0.0293	0.0000	-1.847	0.000	-0.286
6	0.0000	-0.0036	-0.0000	0.560	-0.000	0.339
7	0.0000	-0.0190	-0.0000	1.287	-0.000	0.779

**Rolling bearing 'ConnectionRollerBearing1'**

Position (Y-coordinate)	[y]	19.00	mm
Life modification factor for reliability[a <sub>r</sub> ]		1.000	
Service life	[L <sub>nh</sub> ]	0.00	h
Minimum EHL lubricant film thickness	[h <sub>min</sub> ]	0.000	µm
Static safety factor	[S <sub>0</sub> ]	10.05	
Calculation with approximate bearings internal geometry			
Reference rating service life	[L <sub>nrh</sub> ]	301084.49	h

	Bearing reaction force			Bearing reaction moment		
	Fx (kN)	Fy (kN)	Fz (kN)	Mx (Nm)	My (Nm)	Mz (Nm)
1	-0.200	0.000	0.288	-0.077	-0.000	-0.050
2	-0.322	0.000	0.472	-0.165	-0.000	-0.103
3	-0.286	0.000	0.418	-0.137	-0.000	-0.086
4	-0.381	0.000	0.562	-0.216	-0.000	-0.132
5	-0.565	0.000	0.843	-0.387	-0.000	-0.230
6	0.032	-0.000	-0.339	0.086	0.000	0.011
7	0.085	0.000	-0.807	0.324	0.000	0.050

	Displacement of bearing			Misalignment of bearing		
	ux (µm)	uy (µm)	uz (µm)	ux (mrad)	uy (mrad)	uz (mrad)
1	1.8517	-0.4305	-2.6369	0.304	-0.000	0.175
2	2.5286	-0.0951	-3.6607	0.473	-0.000	0.257
3	2.3395	-0.5154	-3.3734	0.424	-0.000	0.234
4	2.8308	-0.1452	-4.1131	0.554	-0.000	0.296
5	3.7060	4.3160	-5.4290	0.801	-0.001	0.412
6	-0.2757	-0.5742	3.1498	-0.337	0.000	-0.060
7	-0.5520	-1.2169	5.6108	-0.720	0.000	-0.157

**Rolling bearing 'ConnectionRollerBearing2'**

Position (Y-coordinate)	[y]	38.50	mm
Life modification factor for reliability[a <sub>r</sub> ]		1.000	
Service life	[L <sub>nh</sub> ]	0.00	h
Minimum EHL lubricant film thickness	[h <sub>min</sub> ]	0.000	µm
Static safety factor	[S <sub>0</sub> ]	2.68	
Calculation with approximate bearings internal geometry			
Reference rating service life	[L <sub>nrh</sub> ]	179.99	h

	Bearing reaction force			Bearing reaction moment		
	Fx (kN)	Fy (kN)	Fz (kN)	Mx (Nm)	My (Nm)	Mz (Nm)
1	-0.009	0.000	0.903	0.732	-0.000	-0.021
2	-0.015	0.000	1.447	1.360	-0.000	-0.016
3	-0.013	0.000	1.288	1.171	-0.000	-0.019
4	-0.018	0.000	1.711	1.679	-0.000	-0.010
5	-0.027	0.000	2.535	2.711	-0.000	0.009
6	0.554	-0.000	-0.675	-0.522	0.000	-0.466

7            1.289            0.000            -1.571            -1.583            0.000            -1.335

	Displacement of bearing			Misalignment of bearing		
	ux (µm)	uy (µm)	uz (µm)	ux (mrad)	uy (mrad)	uz (mrad)
1	0.0451	-0.4312	-2.4229	-0.470	-0.075	0.024
2	0.0633	-0.0970	-3.5336	-0.753	-0.121	0.017
3	0.0595	-0.5169	-3.2160	-0.670	-0.108	0.020
4	0.0707	-0.1478	-4.0506	-0.890	-0.144	0.013
5	0.0962	4.3103	-5.6048	-1.318	-0.213	-0.003
6	-1.4876	-0.5749	1.8338	0.333	0.073	0.311
7	-2.9451	-1.2206	3.6210	0.805	0.171	0.686

(\*) Note about roller bearings with an approximated bearing geometry:  
The internal geometry of these bearings has not been input in the database.  
The geometry is back-calculated as specified in ISO 281, from C and C0 (details in the manufacturer's catalog).  
For this reason, the geometry may be different from the actual geometry.  
This can lead to differences in the service life calculation and, more importantly, the roller bearing stiffness.

Damage (%)			[H] ( 50.000)
No.	B1	B2	
1	0.00	0.43	
2	0.00	1.04	
3	0.00	0.42	
4	0.00	0.71	
5	0.01	24.48	
6	0.00	0.10	
7	0.00	0.61	
-----			
Σ	0.02	27.78	

Utilization, with reference to the required service life

		[H] ( 50.000)
B1	B2	
0.07	0.68	

B1: ConnectionRollerBearing1 (Connecting rolling bearing)  
B2: ConnectionRollerBearing2 (Connecting rolling bearing)

---



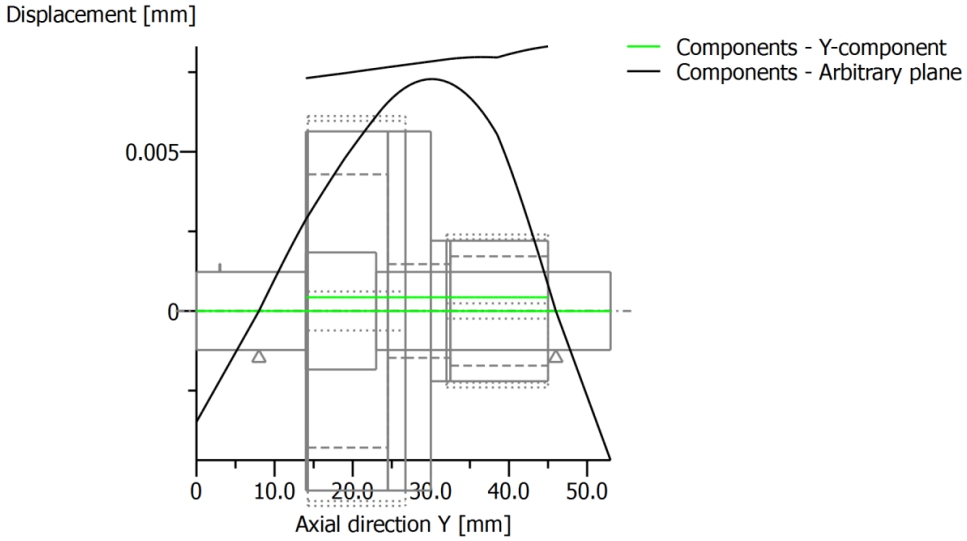
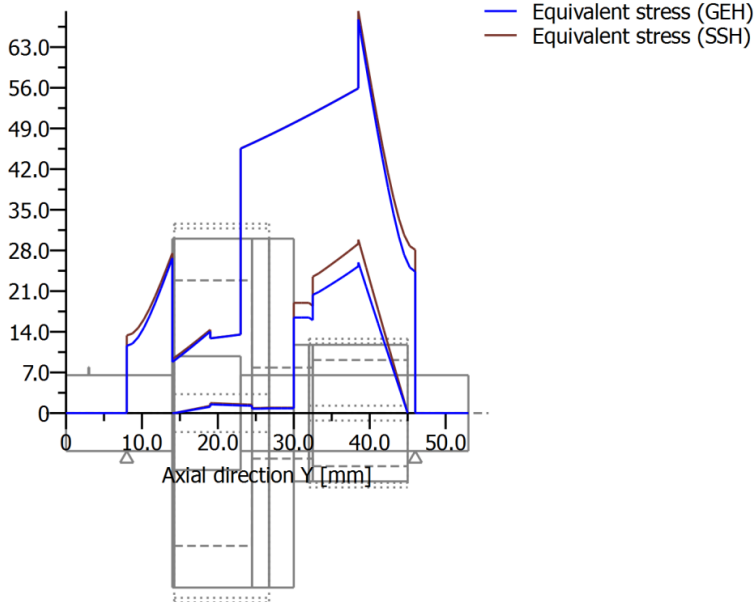


Figure: Deformation (bending etc.) (Arbitrary plane 91.00822717 120)  
Stress [N/mm<sup>2</sup>]



GEH(von Mises):  $\sigma_V = \sqrt{(\sigma_B + \sigma_{Z,D})^2 + 3 \cdot (\tau_T + \tau_S)^2} / 2$  SSH(Tresca):  $\sigma_V = \sqrt{(\sigma_B - \sigma_{Z,D})^2 + 4 \cdot (\tau_T + \tau_S)^2} / 2$   
Figure: Equivalent stress

# Gear stage 1 calculation

KISSsoft Release 03/2015 F

KISSsoft Academic License - Norwegian University of Science & Technology (NTNU)

File

Name : Unnamed  
 Changed by: Kraftwerk on: 02.02.2016 at: 18:54:06

**Important hint: At least one warning has occurred during the calculation:**

1-> Gear 1:  
 Equivalent tip relief Ceq: 8.0 µm

According to ISO15144, the tip relief is not in the optimum range.  
 Recommended:  
 Delete optimal tip relief [CaOpt].

(In the 'Pair/Gear data' tab, in the 'Strength details' window.)

2-> Gear 2:  
 Equivalent tip relief Ceq: 8.0 µm

According to ISO15144, the tip relief is not in the optimum range.  
 Recommended:  
 Delete optimal tip relief [CaOpt].

(In the 'Pair/Gear data' tab, in the 'Strength details' window.)

3-> Calculation for load spectra:  
 The application factor should be set to 1.0!  
 (according ISO6336-6 or DIN3990-6)

4-> Some elements of the Load spectrum are unusually big.  
 Check the Load spectrum.  
 (Element no. 1)

## CALCULATION OF A CYLINDRICAL SPUR GEAR PAIR

Drawing or article number:  
 Gear 1: SunGear(SunPlanetConstraint)  
 Gear 2: Planet1(SunPlanetConstraint)

### Load spectrum

load\_spectrum\_100  
 Number of bins in the load spectrum: 7  
 Reference gear: 1

No.	[%]	[kW]	[1/min]	[Nm]	KV	KHβ	KHα	Ky	YM1	YM2	OilTemp
1	40.00000	3.1050	11875.2	2.4969	1.1189	1.4914	1.0000	1.0000	1.0000	1.0000	70
2	10.00000	6.6667	15833.6	4.0207	1.1250	1.4587	1.0000	1.0000	1.0000	1.0000	70
3	6.00000	6.6667	17812.8	3.5739	1.1491	1.4597	1.0000	1.0000	1.0000	1.0000	70
4	4.00000	6.1187	12271.1	4.7616	1.0890	1.4549	1.0000	1.0000	1.0000	1.0000	70
5	30.00000	5.8643	7916.8	7.0736	1.0471	1.4228	1.0000	1.0000	1.0000	1.0000	70

6	8.00000	-4.0000	15833.6	-2.4124	1.1613	1.4513	1.0000	1.0000	0.7000	0.7000	70
7	2.00000	-5.3333	9000.0	-5.6589	1.0599	1.4278	1.0000	1.0000	0.7000	0.7000	70

**Notice:**

Tooth flank with load spectrum: Consider all negative load spectrum bins as positive

Tooth root with load spectrum: Consider all negative load spectrum bins as positive

Is only applied on load spectrum bins, where the alternating bending factor (mean stress influence factor) YM=1.0.

Woehler line (S-N curve) in the endurance domain according: according to standard

**Results**

Root safety	1.566	1.789
Flank safety	1.009	1.275

Scuffing safety (integral temperature) 6.821

Scuffing safety (flash temperature) 13.608

(Safety against scuffing/micropitting/EHT is indicated for the most critical element of the load spectrum.)

Analysis of critical elements in load spectrum: See section 10

**ONLY AS INFORMATION: CALCULATION WITH REFERENCE POWER**

Calculation method DIN 3990:1987 Method B (YF Method C)

		----- GEAR 1 -----	----- GEAR 2 --
Power (kW)	[P]		1.047
Speed (1/min)	[n]	100.0	29.8
Torque (Nm)	[T]	100.0	336.0
Application factor	[KA]		1.25
Required service life (h)	[H]		50.00
Gear driving (+) / driven (-)		+	-
Working flank gear 1: Left flank			

**1. TOOTH GEOMETRY AND MATERIAL**

(geometry calculation according to

DIN 3960:1987)

		----- GEAR 1 -----	----- GEAR 2 --
Center distance (mm)	[a]		32.400
Centre distance tolerance	ISO 286:2010 Measure js7		
Normal module (mm)	[mn]		0.6000
Pressure angle at normal section (°)	[alfn]		20.0000
Helix angle at reference circle (°)	[beta]		0.0000
Number of teeth	[z]	25	84
Facewidth (mm)	[b]	12.50	12.50
Hand of gear			Spur gear
Accuracy grade	[Q-DIN 3961:1978]	6	6
Inner diameter (mm)	[di]	10.80	40.00
Inner diameter of gear rim (mm)	[dbi]	10.80	40.00

Material

Gear 1: (Own input) NC310YW, Case-carburized steel, case-hardened

Gear 2: (Own input) NC310YW, Case-carburized steel, case-hardened

		----- GEAR 1 -----	GEAR 2 --
Surface hardness		HRC 59	HRC 59
Fatigue strength. tooth root stress (N/mm <sup>2</sup> )	[sigFlim]	525.00	525.00
Fatigue strength for Hertzian pressure (N/mm <sup>2</sup> )	[sigHlim]	1650.00	1650.00
Tensile strength (N/mm <sup>2</sup> )	[Rm]	2150.00	2150.00
Yield point (N/mm <sup>2</sup> )	[Rp]	1790.00	1790.00
Young's modulus (N/mm <sup>2</sup> )	[E]	202000	202000
Poisson's ratio	[ny]	0.300	0.300
Roughness average value DS, flank (µm)	[RAH]	0.80	0.80
Roughness average value DS, root (µm)	[RAF]	0.80	0.80
Mean roughness height, Rz, flank (µm)	[RZH]	6.30	6.30
Mean roughness height, Rz, root (µm)	[RZF]	6.30	6.30

Gear reference profile 1 :

Reference profile 1.25 / 0.38 / 1.0 ISO 53.2:1997 Profil A

Dedendum coefficient	[hfP*]	1.250
Root radius factor	[rhofP*]	0.380 (rhofPmax*=0.472)
Addendum coefficient	[haP*]	1.000
Tip radius factor	[rhoaP*]	0.000
Protuberance height factor	[hprP*]	0.000
Protuberance angle	[alfprP]	0.000
Tip form height coefficient	[hFaP*]	0.000
Ramp angle	[alfKP]	0.000

not topping

Gear reference profile 2 :

Reference profile 1.25 / 0.38 / 1.0 ISO 53.2:1997 Profil A

Dedendum coefficient	[hfP*]	1.250
Root radius factor	[rhofP*]	0.380 (rhofPmax*=0.472)
Addendum coefficient	[haP*]	1.000
Tip radius factor	[rhoaP*]	0.000
Protuberance height factor	[hprP*]	0.000
Protuberance angle	[alfprP]	0.000
Tip form height coefficient	[hFaP*]	0.000
Ramp angle	[alfKP]	0.000

not topping

Summary of reference profile gears:

Dedendum reference profile	[hfP*]	1.250	1.250
Tooth root radius Refer. profile	[rofP*]	0.380	0.380
Addendum Reference profile	[haP*]	1.000	1.000
Protuberance height factor	[hprP*]	0.000	0.000
Protuberance angle (°)	[alfprP]	0.000	0.000
Tip form height coefficient	[hFaP*]	0.000	0.000
Ramp angle (°)	[alfKP]	0.000	0.000

Type of profile modification:

for high load capacity gearbox

Tip relief (µm)	[Ca]	8.0	8.0
-----------------	------	-----	-----

Lubrication type oil bath lubrication

Type of oil	Oil: Klübersynth GH 6-22		
Lubricant base	Synthetic oil based on Polyglycol		
Kinem. viscosity oil at 40 °C (mm <sup>2</sup> /s)	[nu40]	22.00	
Kinem. viscosity oil at 100 °C (mm <sup>2</sup> /s)	[nu100]	5.30	
FZG test A/8.3/90 ( ISO 14635-1:2006)	[FZGtestA]	14	
Specific density at 15 °C (kg/dm <sup>3</sup> )	[roOil]	1.025	
Oil temperature (°C)	[TS]	70.000	

		----- GEAR 1 -----	GEAR 2 --	
Overall transmission ratio	[itot]			-3.360
Gear ratio	[u]			3.360
Transverse module (mm)	[mt]			0.600
Pressure angle at pitch circle (°)	[alfit]			20.000
Working transverse pressure angle (°)	[alfwt]			18.487
	[alfwt.e/i]	18.553 /	18.421	
Working pressure angle at normal section (°)	[alfwn]			18.487
Helix angle at operating pitch circle (°)	[betaw]			0.000
Base helix angle (°)	[betab]			0.000
Reference centre distance (mm)	[ad]			32.700
Sum of profile shift coefficients	[Summexi]			-0.4821
Profile shift coefficient	[x]	0.1094		-0.5915
Tooth thickness (Arc) (module) (module)	[sn*]	1.6504		1.1402
Tip alteration (mm)	[k*mn]	-0.011		-0.011
Reference diameter (mm)	[d]	15.000		50.400
Base diameter (mm)	[db]	14.095		47.361
Tip diameter (mm)	[da]	16.309		50.868
(mm)	[da.e/i]	16.309 /	16.299	50.868 / 50.858
Tip diameter allowances (mm)	[Ada.e/i]	0.000 /	-0.010	0.000 / -0.010
Tip form diameter (mm)	[dFa]			50.868
(mm)	[dFa.e/i]	16.309 /	16.299	50.868 / 50.858
Active tip diameter (mm)	[dNa]			50.868
Active tip diameter (mm)	[dNa.e/i]	16.309 /	16.299	50.868 / 50.858
Operating pitch diameter (mm)	[dw]			49.938
(mm)	[dw.e/i]	14.868 /	14.857	49.957 / 49.918
Root diameter (mm)	[df]			48.190
Generating Profile shift coefficient	[xE.e/i]	0.0704/	0.0461	-0.6402/ -0.6719
Manufactured root diameter with xE (mm)	[df.e/i]	13.584 /	13.555	48.132 / 48.094
Theoretical tip clearance (mm)	[c]			0.150
Effective tip clearance (mm)	[c.e/i]	0.216 /	0.167	0.206 / 0.161
Active root diameter (mm)	[dNf]			48.943
(mm)	[dNf.e/i]	14.250 /	14.224	48.968 / 48.923
Root form diameter (mm)	[dFf]			48.773
(mm)	[dFf.e/i]	14.219 /	14.208	48.733 / 48.707
Reserve (dNf-dFf)/2 (mm)	[cF.e/i]	0.021 /	0.003	0.130 / 0.095
Addendum (mm)	[ha=mn*(haP*+x)]			0.655 0.234
(mm)	[ha.e/i]	0.655 /	0.650	0.234 / 0.229
Dedendum (mm)	[hf=mn*(hfP*-x)]			0.684 1.105
(mm)	[hf.e/i]	0.708 /	0.722	1.134 / 1.153
Roll angle at dFa (°)	[xsi_dFa.e/i]	33.350 /	33.269	22.456 / 22.423
Roll angle to dNa (°)	[xsi_dNa.e/i]	33.350 /	33.269	22.456 / 22.423
Roll angle to dNf (°)	[xsi_dNf.e/i]	8.503 /	7.750	15.052 / 14.837
Roll angle at dFf (°)	[xsi_dFf.e/i]	7.597 /	7.250	13.892 / 13.758
Tooth height (mm)	[H]			1.339
Virtual gear no. of teeth	[zn]			84.000
Normal-tooth thickness at tip circle (mm)	[san]			0.513
(mm)	[san.e/i]	0.411 /	0.394	0.495 / 0.477
Normal-tooth thickness on tip form circle (mm)	[sFan]			0.513

	(mm)	[sFan.e/i]	0.411 /	0.394	0.495 /	0.477
Normal space width at root circle (mm)		[efn]		0.000		0.534
	(mm)	[efn.e/i]	0.000 /	0.000	0.543 /	0.549
Max. sliding velocity at tip (m/s)		[vga]		0.024		0.019
Specific sliding at the tip		[zetaaa]		0.552		0.641
Specific sliding at the root		[zetaaf]		-1.782		-1.233
Mean specific sliding		[zetam]			0.591	
Sliding factor on tip		[Kga]		0.305		0.238
Sliding factor on root		[Kgf]		-0.238		-0.305
Pitch on reference circle (mm)		[pt]			1.885	
Base pitch (mm)		[pbt]			1.771	
Transverse pitch on contact-path (mm)		[pet]			1.771	
Length of path of contact (mm)		[ga, e/i]		3.109 (	3.149 /	3.046)
Length T1-A, T2-A (mm)		[T1A, T2A]	0.993(	0.953/	1.046)	9.281( 9.281/ 9.267)
Length T1-B (mm)		[T1B, T2B]	2.331(	2.331/	2.321)	7.943( 7.903/ 7.992)
Length T1-C (mm)		[T1C, T2C]	2.356(	2.347/	2.365)	7.918( 7.887/ 7.948)
Length T1-D (mm)		[T1D, T2D]	2.764(	2.725/	2.817)	7.510( 7.510/ 7.496)
Length T1-E (mm)		[T1E, T2E]	4.102(	4.102/	4.092)	6.172( 6.132/ 6.221)
Length T1-T2 (mm)		[T1T2]		10.274 (	10.234 /	10.313)
Diameter of single contact point B (mm)		[d-B]	14.846(	14.846/	14.840)	49.954( 49.929/ 49.985)
Diameter of single contact point D (mm)		[d-D]	15.141(	15.112/	15.180)	49.685( 49.685/ 49.677)
Addendum contact ratio		[eps]	0.986(	0.991/	0.975)	0.770( 0.787/ 0.745)
Minimal length of contact line (mm)		[Lmin]				12.500
Transverse contact ratio		[eps_a]				1.755
Transverse contact ratio with allowances		[eps_a.e/m/i]		1.778 /	1.749 /	1.720
Overlap ratio		[eps_b]				0.000
Total contact ratio		[eps_g]				1.755
Total contact ratio with allowances		[eps_g.e/m/i]		1.778 /	1.749 /	1.720

## **2. FACTORS OF GENERAL INFLUENCE**

		----- GEAR 1 -----	GEAR 2 --
Nominal circum. force at pitch circle (N)	[Ft]		13333.3
Axial force (N)	[Fa]		0.0
Radial force (N)	[Fr]		4852.9
Normal force (N)	[Fnorm]		14189.0
Nominal circumferential force per mm (N/mm)	[w]		1066.67
Only as information: Forces at operating pitch circle:			
Nominal circumferential force (N)	[Ftw]		13456.8
Axial force (N)	[Faw]		0.0
Radial force (N)	[Frw]		4499.3
Circumferential speed reference circle (m/s)	[v]		0.08
Circumferential speed operating pitch circle (m/s)	[v(dw)]		0.08
Running-in value (µm)	[yp]		0.5
Running-in value (µm)	[yf]		0.3
Correction coefficient	[CM]		0.800
Gear body coefficient	[CR, bs/b, sr/mn]		0.827 (0.250, 2.359)
Reference profile coefficient	[CBS]		0.975
Material coefficient	[E/Est]		0.981
Singular tooth stiffness (N/mm/µm)	[c]		10.747
Meshing stiffness (N/mm/µm)	[cg]		16.836
Reduced mass (kg/mm)	[mRed]		0.00050
Resonance speed (min-1)	[nE1]		70428
Resonance ratio (-)	[N]		0.001

Subcritical range			
Running-in value ( $\mu\text{m}$ )	[ya]	0.5	
Dynamic factor	[KV]	1.000	
User specified factor KHb:			
Face load factor - flank	[KHb]	1.368	
- Tooth root	[KFb]	1.322	
- Scuffing	[KBb]	1.368	
Transverse load factor - flank	[KH <sub>a</sub> ]	1.000	
- Tooth root	[KF <sub>a</sub> ]	1.000	
- Scuffing	[KB <sub>a</sub> ]	1.000	
Helical load factor scuffing	[K <sub>bg</sub> ]	1.000	
Number of load cycles (in mio.)	[NL]	0.900	0.089

### 3. TOOTH ROOT STRENGTH

Calculation of Tooth form coefficients according method: C

Calculation of tooth form coefficients with graphical method

(Determination of biggest value for  $Y_F * Y_S$  on the effective tooth shape)

		----- GEAR 1 -----	----- GEAR 2 --
Tooth form factor	[YF]	2.56	2.40
Stress correction factor	[YS]	1.62	1.66
Working angle (°)	[alfFen]	29.82	22.52
Diameter of application of force (mm)	[dan]	16.31	50.87
Bending lever arm (mm)	[hF]	1.16	1.17
Tooth thickness at root (mm)	[sFn]	1.23	1.31
Tooth root radius (mm)	[roF]	0.32	0.33
(hF* = 1.928/ 1.943 sFn* = 2.042/ 2.186 roF* = 0.530/ 0.549 dsFn = 13.789/ 48.319 alfsFn = 31.62/ 37.96)			

Contact ratio factor	[Yeps]	0.677	
Helix angle factor	[Ybet]	1.000	
Effective facewidth (mm)	[beff]	12.50	12.50
Nominal stress at tooth root (N/mm <sup>2</sup> )	[sigF0]	5009.53	4803.06
Tooth root stress (N/mm <sup>2</sup> )	[sigF]	8283.44	7942.02

Permissible bending stress at root of Test-gear

Notch sensitivity factor	[YdrelT]	1.002	1.025
Surface factor	[YRrelT]	1.024	1.016
size factor (Tooth root)	[YX]	1.000	1.000
Finite life factor	[YNT]	1.148	1.495
	[YdrelT*YRrelT*YX*YNT]	1.178	1.557

Alternating bending factor (mean stress influence coefficient)

	[YM]	0.700	0.700
Stress correction factor	[Yst]	2.00	
Yst*sigFlim (N/mm <sup>2</sup> )	[sigFE]	1050.00	1050.00
Permissible tooth root stress (N/mm <sup>2</sup> )	[sigFP=sigFG/SFmin]	1202.19	1589.73
Limit strength tooth root (N/mm <sup>2</sup> )	[sigFG]	865.58	1144.61
Required safety	[SFmin]	0.72	0.72

### 4. SAFETY AGAINST PITTING (TOOTH FLANK)

		----- GEAR 1 -----	GEAR 2 --
Zone factor	[ZH]		2.603
Elasticity coefficient ( $\sqrt{N/mm}$ )	[ZE]		187.960
Contact ratio factor	[Zeps]		0.865
Helix angle factor	[Zbet]		1.000
Effective facewidth (mm)	[beff]		12.50
Nominal flank pressure (N/mm <sup>2</sup> )	[sigH0]		4064.79
Surface pressure at operating pitch circle (N/mm <sup>2</sup> )	[sigHw]		5316.85
Single tooth contact factor	[ZB,ZD]	1.00	1.00
Flank pressure (N/mm <sup>2</sup> )	[sigHB, sigHD]	5337.24	5316.85
Lubrication coefficient at NL	[ZL]	0.970	1.000
Speed coefficient at NL	[ZV]	0.977	1.000
Roughness coefficient at NL	[ZR]	0.969	1.000
Work hardening factor at NL	[ZW]	1.000	1.000
Finite life factor	[ZNT]	1.355	1.600
	[ZL*ZV*ZR*ZNT]	1.244	1.600
Small no. of pittings permissible:	no		
Size factor (flank)	[ZX]	1.000	1.000
Permissible surface pressure (N/mm <sup>2</sup> )	[sigHP=sigHG/SHmin]	3110.38	4000.00
Limit strength pitting (N/mm <sup>2</sup> )	[sigHG]	2052.85	2640.00
Required safety	[SHmin]	0.66	0.66

#### **4b. MICROPITTING ACCORDING TO ISO/TR 15144-1:2014**

Calculation did not run. (Lubricant: Load stage micropitting test is unknown.)

#### **5. STRENGTH AGAINST SCUFFING**

Calculation method according to

DIN 3990:1987

Lubrication coefficient (for lubrication type)	[XS]		1.000
Relative structure coefficient (Scuffing)	[XWrelT]		1.000
Thermal contact factor (N/mm/s <sup>0.5</sup> /K)	[BM]	13.629	13.629
Relevant tip relief ( $\mu\text{m}$ )	[Ca]	8.00	8.00
Optimal tip relief ( $\mu\text{m}$ )	[Ceff]		124.07
Ca taken as optimal in the calculation (0=no, 1=yes)		0	0
Effective facewidth (mm)	[beff]		12.500
Applicable circumferential force/facewidth (N/mm)	[wBt]		1824.998
Angle factor ( $\epsilon_1:0.986, \epsilon_2:0.770$ )	[Xalfbet]		0.955
Flash temperature-criteria			
Tooth mass temperature ( $^{\circ}\text{C}$ )	[theM-B]		159.44
theM-B = theoil + XS*0.47*theflamax	[theflamax]		190.30
Scuffing temperature ( $^{\circ}\text{C}$ )	[theS]		739.42
Coordinate gamma (point of highest temp.)	[Gamma]		0.376
[Gamma.A]=0.579 [Gamma.E]=0.741			
Highest contact temp. ( $^{\circ}\text{C}$ )	[theB]		349.74
Flash factor ( $^{\circ}\text{K}^{\circ}\text{N}^{\wedge-.75}\text{s}^{\wedge.5}\text{m}^{\wedge-.5}\text{mm}$ )	[XM]		50.362
Geometry factor	[XB]		0.173



Load sharing factor	[XGam]	0.694
Dynamic viscosity (mPa*s)	[etaM]	2.34 ( 159.4 °C)
Coefficient of friction	[mym]	1.008
Integral temperature-criteria		
Tooth mass temperature (°C)	[theM-C]	124.11
theM-C = theoil + XS*0.70*theflaint	[theflaint]	77.30
Integral scuffing temperature (°C)	[theSint]	739.42
Flash factor (°K*N <sup>-1</sup> .75*s <sup>0.5</sup> *m <sup>-0.5</sup> *mm)	[XM]	50.362
Contact ratio factor	[Xeps]	0.223
Dynamic viscosity (mPa*s)	[etaOil]	9.52 ( 70.0 °C)
Mean coefficient of friction	[mym]	0.770
Geometry factor	[XBE]	0.318
Meshing factor	[XQ]	1.000
Tip relief factor	[XCa]	1.117
Integral tooth flank temperature (°C)	[theint]	240.05

## 6. MEASUREMENTS FOR TOOTH THICKNESS

		----- GEAR 1 -----	----- GEAR 2 --
		DIN 58405 6e	DIN 58405 6e
Tooth thickness deviation			
Tooth thickness allowance (normal section) (mm)	[As.e/i]	-0.017 / -0.028	-0.021 / -0.035
Number of teeth spanned	[k]	3.000	9.000
Base tangent length (no backlash) (mm)	[Wk]	4.683	15.519
Actual base tangent length ("span") (mm)	[Wk.e/i]	4.667 / 4.657	15.499 / 15.486
(mm)	[ΔWk.e/i]	-0.016 / -0.026	-0.020 / -0.033
Diameter of contact point (mm)	[dMWk.m]	14.846	49.830
Theoretical diameter of ball/pin (mm)	[DM]	1.049	0.996
Eff. Diameter of ball/pin (mm)	[DMeff]	1.100	1.000
Theor. dim. centre to ball (mm)	[MrK]	8.381	25.507
Actual dimension centre to ball (mm)	[MrK.e/i]	8.362 / 8.351	25.475 / 25.455
Diameter of contact point (mm)	[dMMr.m]	15.173	49.622
Diametral measurement over two balls without clearance (mm)	[MdK]	16.731	51.013
Actual dimension over balls (mm)	[MdK.e/i]	16.694 / 16.671	50.950 / 50.909
Diametral measurement over rolls without clearance (mm)	[MdR]	16.731	51.013
Actual dimension over rolls (mm)	[MdR.e/i]	16.694 / 16.671	50.950 / 50.909
Dimensions over 3 rolls without clearance (mm)	[Md3R]	16.700	0.000
Actual dimensions over 3 rolls (mm)	[Md3R.e/i]	16.663 / 16.640	0.000 / 0.000
Chordal tooth thickness (no backlash) (mm)	[sn]	0.990	0.684
Actual chordal tooth thickness (mm)	[sn.e/i]	0.973 / 0.962	0.663 / 0.649
Reference chordal height from da.m (mm)	[ha]	0.668	0.234
Tooth thickness (Arc) (mm)	[sn]	0.990	0.684
(mm)	[sn.e/i]	0.973 / 0.963	0.663 / 0.649
Backlash free center distance (mm)	[aControl.e/i]	32.343 / 32.306	
Backlash free center distance, allowances (mm)	[jta]	-0.057 / -0.094	
dNf.i with aControl (mm)	[dNf0.i]	14.163	48.794
Reserve (dNf0.i-dFf.e)/2 (mm)	[cF0.i]	-0.028	0.031
Tip clearance	[c0.i(aControl)]	0.085	0.079
Centre distance allowances (mm)	[Aa.e/i]	0.013 / -0.013	
Circumferential backlash from Aa (mm)	[jtw_Aa.e/i]	0.008 / -0.008	

Radial clearance (mm)	[jrw]	0.107 /	0.045
Circumferential backlash (transverse section) (mm)	[jtw]	0.071 /	0.030
Rotation angle when gear 1 is fixed (°)		0.1619 /	0.0679
Normal backlash (mm)	[jnw]	0.066 /	0.028

## 7. GEAR ACCURACY

----- GEAR 1 ----- GEAR 2 --

According to DIN 3961:1978

One or several gear data (mn, b or d) lay beyond the limits covered by the standard.

The tolerances are calculated on the basis of the formulae in the standard.

However, their values are outside the official range of validity!

Accuracy grade	[Q-DIN3961]	6	6
Profile form deviation (µm)	[ff]	4.50	4.50
Profile slope deviation (µm)	[fHa]	4.50	4.50
Total profile deviation (µm)	[Ff]	7.00	7.00
Helix form deviation (µm)	[fbf]	4.00	4.00
Helix slope deviation (µm)	[fHb]	8.00	8.00
Total helix deviation (µm)	[Fb]	9.00	9.00
Normal base pitch deviation (µm)	[fpe]	6.00	7.00
Single pitch deviation (µm)	[fp]	6.00	7.00
Adjacent pitch difference (µm)	[fu]	8.00	9.00
Total cumulative pitch deviation (µm)	[Fp]	17.00	22.00
Sector pitch deviation over z/8 pitches (µm)	[Fpz/8]	11.00	14.00
Runout (µm)	[Fr]	11.00	13.00
Tooth Thickness Variation (µm)	[Rs]	6.00	8.00
Single flank composite, total (µm)	[Fi']	19.00	23.00
Single flank composite, tooth-to-tooth (µm)	[fi']	9.00	9.00
Radial composite, total (µm)	[Fi'']	15.00	18.00
Radial composite, tooth-to-tooth (µm)	[fi'']	5.50	7.00

According to DIN 58405:1972 (Feinwerktechnik):

Tooth-to-tooth composite error (µm)	[fi'']	5.50	7.00
Composite error (µm)	[Fi'']	16.00	20.00
Axis alignment error (µm)	[fp]	5.51	5.51
Flank direction error (µm)	[fbeta]	5.00	5.00
Runout (µm)	[Trk, Fr]	18.00	24.00

## 8. ADDITIONAL DATA

Maximal possible centre distance (eps_a=1.0)	[aMAX]	32.849	
Weight - calculated with da (g)	[Mass]	11.23	74.27
Total weight (g)	[Mass]	85.50	
Moment of inertia (System referenced to wheel 1): calculation without consideration of the exact tooth shape			
single gears ((da+df)/2...di) (kg*m²)	[TraeghMom]	3.401e-007	3.232e-005
System ((da+df)/2...di) (kg*m²)	[TraeghMom]	3.203e-006	
Torsional stiffness (MNm/rad)	[cr]	0.0	0.1
Mean coeff. of friction (acc. Niemann)	[mum]	0.200	
Wear sliding coef. by Niemann	[zetw]	1.037	
Gear power loss (kW)	[PVZ]	0.028	
(Meshing efficiency (%))	[etaz]	97.363)	

## 9. DETERMINATION OF TOOTH FORM

Profile and tooth trace modifications for gear 1

**Symmetric (both flanks)**

- Tip relief, linear Caa = 8.000µm LCa = 1.115\*mn dCa = 15.686mm
  - Crowning Cb = 10.000µm (rcrown= 1953 mm)
  - Helix angle modification, tapered or conical CHb = -10.910µm
- CHb=-10.9101 -> Right Tooth Flank beta.eff = 0.053°-right Left Tooth Flank beta.eff = 0.053°-left

Profile and tooth trace modifications for gear 2

**Symmetric (both flanks)**

- Tip relief, linear Caa = 8.000µm LCa = 1.115\*mn dCa = 50.401mm

Data for the tooth form calculation :

**Calculation of Gear 1**

Tooth form, Gear 1, Step 1: Automatic (final machining)  
haP\*= 1.029, hfP\*= 1.250, rofP\*= 0.380

**Calculation of Gear 2**

Tooth form, Gear 2, Step 1: Automatic (final machining)  
haP\*= 1.042, hfP\*= 1.250, rofP\*= 0.380

**10. SERVICE LIFE, DAMAGE**

Required safety for tooth root	[SFmin]	0.72
Required safety for tooth flank	[SHmin]	0.66

Service life (calculated with required safeties):

System service life (h) [Hatt] > 1000000

Tooth root service life (h)	[HFatt]	1e+006	1e+006
Tooth flank service life (h)	[HHatt]	1e+006	1e+006

Note: The entry 1e+006 h means that the Service life > 1,000,000 h.

Damage calculated on basis of required service life

No.	F1%	F2%	H1%	H2%	
					[H] ( 50.0 h)
1	0.00	0.00	0.00	0.00	
2	0.00	0.00	0.00	0.00	
3	0.00	0.00	0.00	0.00	
4	0.00	0.00	0.00	0.00	
5	0.00	0.00	0.00	0.00	
6	0.00	0.00	0.00	0.00	
7	0.00	0.00	0.00	0.00	
Σ	0.00	0.00	0.00	0.00	

**REMARKS:**

- Specifications with [e/i] imply: Maximum [e] and Minimal value [i] with consideration of all tolerances

# Contact analysis gear stage 1

KISSsoft Release 03/2015 F

KISSsoft Academic License - Norwegian University of Science & Technology (NTNU)

File

Name : Unnamed

Changed by: Kraftwerk

on: 02.02.2016

at: 18:51:46

## Contact Analysis

Meshing gear 1 - gear 2

Accuracy of calculation

Medium

**Partial load for calculation** [w<sub>t</sub>] **100.0000 (%)**

Note: In order to obtain contact analysis results for scuffing, micropitting and tooth flank fracture according to method A of ISO the calculation would have to be performed with  $w_t = 100 \cdot K_{gam} \cdot K_A \cdot K_V \dots$

(w<sub>t</sub>\*K<sub>gam</sub>\*K<sub>A</sub>\*K<sub>V</sub> = 131.69 %)

Working flank

Right tooth flank

Center distance	[a]	32.4000	(mm)
Single pitch deviation	[f <sub>p</sub> ]	0.0000	(μm)
Coefficient. of friction	[μ]	0.1237	
Deviation error of axis	[f <sub>Σβ</sub> ]	1.3942	(μm)
Inclination error of axis	[f <sub>Σδ</sub> ]	3.3720	(μm)
Torque	[T <sub>1</sub> ]	7.0736	(Nm)

Torsion

Gear A:-, B:-

		min	max	Δ	μ	σ
Transmission error	(μm)	-9.8570	-6.6537	3.2033	-8.5006	1.0758
Tangent Stiffness curve	(N/μm)	138.1343	214.6276	76.4933	192.1524	21.9077
Secant stiffness curve	(N/μm)	101.5753	147.7384	46.1630	118.4544	15.2211
Line load	(N/mm)	0.0000	142.6563	142.6563	59.3978	42.8024
Torque Gear 1	(Nm)	7.0729	7.0740	0.0011	7.0736	0.0002
Torque Gear 2	(Nm)	23.1626	23.7255	0.5628	23.4594	0.1651
Power loss	(W)	20.2050	145.1334	124.9284	96.0524	43.2565
Contact temperature	(°C)	76.9429	104.2973	27.3544	87.8492	8.0317
Thickness of lubrication film	(μm)	0.0278	0.1342	0.1064	0.0518	0.0300
Hertzian pressure	(N/mm <sup>2</sup> )		1655.0364		759.4899	
Tooth root stress gear 1	(N/mm <sup>2</sup> )		446.9217		66.0854	
Tooth root stress gear 2	(N/mm <sup>2</sup> )		489.6851		72.5210	

Safety against micropitting (ISO/TR 15144 Method A) 0.0000

Safety against scuffing 19.5182

Transverse contact ratio under load [ε<sub>α</sub>] 1.9158

min 0.0000

μ 1.5639

max 1.9158

Overlap ratio under load [ε<sub>β</sub>] 0.0000

Total contact ratio under load [ε<sub>γ</sub>] 1.9158

Efficiency [η] 98.5600

Face load factor (ISO6336-1 Annex E, takes into account K<sub>A</sub>\*K<sub>V</sub>)

[K<sub>Hβ</sub>]

1.5384

Note: The resulting safeties do not correspond with Method A according ISO because K<sub>γ</sub>, K<sub>A</sub> and K<sub>V</sub> are not taken into account.

Amplitude spectrum of the transmission error

Harmonics	Amplitude (μm)
1	1.502
2	0.258

3	0.075
4	0.037
5	0.023
6	0.026
7	0.020
8	0.015
9	0.012
10	0.015

**K<sub>Hβ</sub> Calculation - Gear 1 - Gear 2**

Right flank

Load distribution calculated with:  $T_{nom} * K_v * K_A * K_y$ ; Axis alignment calculated with:  $T_{nom}$   
(Partial load for calculation: Load distribution calculated with: 131.69 %; Axis alignment calculated with: 100.00 %)

$f_{\Sigma\beta} = 1.394 \mu\text{m}$  ,  $f_{\Sigma\delta} = 3.372 \mu\text{m}$

$f_{ma} = 0.000 \mu\text{m}$  ,  $f_{H\beta} = 0.000 \mu\text{m}$

Result after i = 1 iterations of load distribution

Gear 1

Point in polar co-ordinates:

$R = 7.431 \text{ mm}$  ,  $\varphi = 0.000^\circ$

Displacement calculated in direction 108.487 °

	y	φ1.t	f1.t	f1.b	f1.tot	f1.C	f1.tot+f1.C
1	-6.127 mm	0.0000°	-0.0000 μm	0.0000 μm	0.0000 μm	0.0000 μm	0.0000 μm
2	-5.882 mm	0.0000°	0.0000 μm	0.0000 μm	0.0000 μm	-0.9476 μm	-0.9476 μm
3	-5.637 mm	0.0000°	0.0000 μm	0.0000 μm	0.0000 μm	-1.8936 μm	-1.8936 μm
4	-5.392 mm	0.0000°	0.0000 μm	0.0000 μm	0.0000 μm	-2.7907 μm	-2.7907 μm
5	-5.147 mm	0.0000°	0.0000 μm	0.0000 μm	0.0000 μm	-3.6681 μm	-3.6681 μm
6	-4.902 mm	0.0000°	0.0000 μm	0.0000 μm	0.0000 μm	-4.5146 μm	-4.5146 μm
7	-4.657 mm	0.0000°	0.0000 μm	0.0000 μm	0.0000 μm	-5.3235 μm	-5.3235 μm
8	-4.412 mm	0.0000°	0.0000 μm	0.0000 μm	0.0000 μm	-6.1144 μm	-6.1144 μm
9	-4.167 mm	0.0000°	0.0000 μm	0.0000 μm	0.0000 μm	-6.8596 μm	-6.8596 μm
10	-3.922 mm	0.0000°	0.0000 μm	0.0000 μm	0.0000 μm	-7.5820 μm	-7.5820 μm
11	-3.676 mm	0.0000°	0.0000 μm	0.0000 μm	0.0000 μm	-8.2766 μm	-8.2766 μm
12	-3.431 mm	0.0000°	0.0000 μm	0.0000 μm	0.0000 μm	-8.9305 μm	-8.9305 μm
13	-3.186 mm	0.0000°	0.0000 μm	0.0000 μm	0.0000 μm	-9.5663 μm	-9.5663 μm
14	-2.941 mm	0.0000°	0.0000 μm	0.0000 μm	0.0000 μm	-10.1598 μm	-10.1598 μm
15	-2.696 mm	0.0000°	0.0000 μm	0.0000 μm	0.0000 μm	-10.7271 μm	-10.7271 μm
16	-2.451 mm	0.0000°	0.0000 μm	0.0000 μm	0.0000 μm	-11.2699 μm	-11.2699 μm
17	-2.206 mm	0.0000°	0.0000 μm	0.0000 μm	0.0000 μm	-11.7687 μm	-11.7687 μm
18	-1.961 mm	0.0000°	0.0000 μm	0.0000 μm	0.0000 μm	-12.2495 μm	-12.2495 μm
19	-1.716 mm	0.0000°	0.0000 μm	0.0000 μm	0.0000 μm	-12.6911 μm	-12.6911 μm
20	-1.471 mm	0.0000°	0.0000 μm	0.0000 μm	0.0000 μm	-13.1033 μm	-13.1033 μm
21	-1.225 mm	0.0000°	0.0000 μm	0.0000 μm	0.0000 μm	-13.4944 μm	-13.4944 μm
22	-0.980 mm	0.0000°	0.0000 μm	0.0000 μm	0.0000 μm	-13.8381 μm	-13.8381 μm
23	-0.735 mm	0.0000°	0.0000 μm	0.0000 μm	0.0000 μm	-14.1638 μm	-14.1638 μm
24	-0.490 mm	0.0000°	0.0000 μm	0.0000 μm	0.0000 μm	-14.4536 μm	-14.4536 μm
25	-0.245 mm	0.0000°	0.0000 μm	0.0000 μm	0.0000 μm	-14.7108 μm	-14.7108 μm
26	0.000 mm	0.0000°	0.0000 μm	0.0000 μm	0.0000 μm	-14.9500 μm	-14.9500 μm
27	0.245 mm	0.0000°	0.0000 μm	0.0000 μm	0.0000 μm	-15.1386 μm	-15.1386 μm
28	0.490 mm	0.0000°	0.0000 μm	0.0000 μm	0.0000 μm	-15.3093 μm	-15.3093 μm
29	0.735 mm	0.0000°	0.0000 μm	0.0000 μm	0.0000 μm	-15.4473 μm	-15.4473 μm
30	0.980 mm	0.0000°	0.0000 μm	0.0000 μm	0.0000 μm	-15.5495 μm	-15.5495 μm
31	1.225 mm	0.0000°	0.0000 μm	0.0000 μm	0.0000 μm	-15.6336 μm	-15.6336 μm
32	1.471 mm	0.0000°	0.0000 μm	0.0000 μm	0.0000 μm	-15.6704 μm	-15.6704 μm
33	1.716 mm	0.0000°	0.0000 μm	0.0000 μm	0.0000 μm	-15.6860 μm	-15.6860 μm

34	1.961 mm	0.0000°	0.0000 μm	0.0000 μm	0.0000 μm	-15.6723 μm	-15.6723 μm
35	2.206 mm	0.0000°	0.0000 μm	0.0000 μm	0.0000 μm	-15.6193 μm	-15.6193 μm
36	2.451 mm	0.0000°	0.0000 μm	0.0000 μm	0.0000 μm	-15.5484 μm	-15.5484 μm
37	2.696 mm	0.0000°	0.0000 μm	0.0000 μm	0.0000 μm	-15.4334 μm	-15.4334 μm
38	2.941 mm	0.0000°	0.0000 μm	0.0000 μm	0.0000 μm	-15.2939 μm	-15.2939 μm
39	3.186 mm	0.0000°	0.0000 μm	0.0000 μm	0.0000 μm	-15.1284 μm	-15.1284 μm
40	3.431 mm	0.0000°	0.0000 μm	0.0000 μm	0.0000 μm	-14.9203 μm	-14.9203 μm
41	3.676 mm	0.0000°	0.0000 μm	0.0000 μm	0.0000 μm	-14.6944 μm	-14.6944 μm
42	3.922 mm	0.0000°	0.0000 μm	0.0000 μm	0.0000 μm	-14.4276 μm	-14.4276 μm
43	4.167 mm	0.0000°	0.0000 μm	0.0000 μm	0.0000 μm	-14.1330 μm	-14.1330 μm
44	4.412 mm	0.0000°	0.0000 μm	0.0000 μm	0.0000 μm	-13.8157 μm	-13.8157 μm
45	4.657 mm	0.0000°	0.0000 μm	0.0000 μm	0.0000 μm	-13.4526 μm	-13.4526 μm
46	4.902 mm	0.0000°	0.0000 μm	0.0000 μm	0.0000 μm	-13.0715 μm	-13.0715 μm
47	5.147 mm	0.0000°	0.0000 μm	0.0000 μm	0.0000 μm	-12.6529 μm	-12.6529 μm
48	5.392 mm	0.0000°	0.0000 μm	0.0000 μm	0.0000 μm	-12.2033 μm	-12.2033 μm
49	5.637 mm	0.0000°	0.0000 μm	0.0000 μm	0.0000 μm	-11.7341 μm	-11.7341 μm
50	5.882 mm	0.0000°	0.0000 μm	0.0000 μm	0.0000 μm	-11.2160 μm	-11.2160 μm
51	6.127 mm	0.0000°	0.0000 μm	0.0000 μm	0.0000 μm	-10.6962 μm	-10.6962 μm

Gear 2

Point in polar co-ordinates:

R = 24.969 mm , φ = 180.000 °

Displacement calculated in direction 108.487 °

	y	φ2.t	f2.t	f2.b	f2.tot	f2.C	f2.tot+f2.C
1	-6.127 mm	0.0000°	0.0000 μm	0.0156 μm	0.0156 μm	0.0000 μm	0.0156 μm
2	-5.882 mm	0.0000°	0.0000 μm	-0.0328 μm	-0.0328 μm	-0.0000 μm	-0.0328 μm
3	-5.637 mm	0.0000°	0.0000 μm	-0.0813 μm	-0.0813 μm	-0.0000 μm	-0.0813 μm
4	-5.392 mm	0.0000°	0.0000 μm	-0.1297 μm	-0.1297 μm	-0.0000 μm	-0.1297 μm
5	-5.147 mm	0.0000°	0.0000 μm	-0.1782 μm	-0.1782 μm	-0.0000 μm	-0.1782 μm
6	-4.902 mm	0.0000°	0.0000 μm	-0.2266 μm	-0.2266 μm	-0.0000 μm	-0.2266 μm
7	-4.657 mm	0.0000°	0.0000 μm	-0.2751 μm	-0.2751 μm	-0.0000 μm	-0.2751 μm
8	-4.412 mm	0.0000°	0.0000 μm	-0.3236 μm	-0.3236 μm	-0.0000 μm	-0.3236 μm
9	-4.167 mm	0.0000°	0.0000 μm	-0.3720 μm	-0.3720 μm	-0.0000 μm	-0.3720 μm
10	-3.922 mm	0.0000°	0.0000 μm	-0.4205 μm	-0.4205 μm	-0.0000 μm	-0.4205 μm
11	-3.676 mm	0.0000°	0.0000 μm	-0.4689 μm	-0.4689 μm	-0.0000 μm	-0.4689 μm
12	-3.431 mm	0.0000°	0.0000 μm	-0.5174 μm	-0.5174 μm	-0.0000 μm	-0.5174 μm
13	-3.186 mm	0.0000°	0.0000 μm	-0.5658 μm	-0.5658 μm	-0.0000 μm	-0.5658 μm
14	-2.941 mm	0.0000°	0.0000 μm	-0.6143 μm	-0.6143 μm	-0.0000 μm	-0.6143 μm
15	-2.696 mm	0.0000°	0.0000 μm	-0.6627 μm	-0.6627 μm	-0.0000 μm	-0.6627 μm
16	-2.451 mm	0.0000°	0.0000 μm	-0.7112 μm	-0.7112 μm	-0.0000 μm	-0.7112 μm
17	-2.206 mm	0.0000°	0.0000 μm	-0.7597 μm	-0.7597 μm	-0.0000 μm	-0.7597 μm
18	-1.961 mm	0.0000°	0.0000 μm	-0.8081 μm	-0.8081 μm	-0.0000 μm	-0.8081 μm
19	-1.716 mm	0.0000°	0.0000 μm	-0.8566 μm	-0.8566 μm	-0.0000 μm	-0.8566 μm
20	-1.471 mm	0.0000°	0.0000 μm	-0.9050 μm	-0.9050 μm	-0.0000 μm	-0.9050 μm
21	-1.225 mm	0.0000°	0.0000 μm	-0.9535 μm	-0.9535 μm	-0.0000 μm	-0.9535 μm
22	-0.980 mm	0.0000°	0.0000 μm	-1.0019 μm	-1.0019 μm	-0.0000 μm	-1.0019 μm
23	-0.735 mm	0.0000°	0.0000 μm	-1.0504 μm	-1.0504 μm	-0.0000 μm	-1.0504 μm
24	-0.490 mm	0.0000°	0.0000 μm	-1.0988 μm	-1.0988 μm	-0.0000 μm	-1.0988 μm
25	-0.245 mm	0.0000°	0.0000 μm	-1.1473 μm	-1.1473 μm	-0.0000 μm	-1.1473 μm
26	0.000 mm	0.0000°	0.0000 μm	-1.1957 μm	-1.1957 μm	-0.0000 μm	-1.1957 μm
27	0.245 mm	0.0000°	0.0000 μm	-1.2442 μm	-1.2442 μm	-0.0000 μm	-1.2442 μm
28	0.490 mm	0.0000°	0.0000 μm	-1.2927 μm	-1.2927 μm	-0.0000 μm	-1.2927 μm
29	0.735 mm	0.0000°	0.0000 μm	-1.3411 μm	-1.3411 μm	-0.0000 μm	-1.3411 μm
30	0.980 mm	0.0000°	0.0000 μm	-1.3896 μm	-1.3896 μm	-0.0000 μm	-1.3896 μm
31	1.225 mm	0.0000°	0.0000 μm	-1.4380 μm	-1.4380 μm	-0.0000 μm	-1.4380 μm
32	1.471 mm	0.0000°	0.0000 μm	-1.4865 μm	-1.4865 μm	-0.0000 μm	-1.4865 μm

33	1.716 mm	0.0000°	0.0000 μm	-1.5349 μm	-1.5349 μm	-0.0000 μm	-1.5349 μm
34	1.961 mm	0.0000°	0.0000 μm	-1.5834 μm	-1.5834 μm	-0.0000 μm	-1.5834 μm
35	2.206 mm	0.0000°	0.0000 μm	-1.6318 μm	-1.6318 μm	-0.0000 μm	-1.6318 μm
36	2.451 mm	0.0000°	0.0000 μm	-1.6803 μm	-1.6803 μm	-0.0000 μm	-1.6803 μm
37	2.696 mm	0.0000°	0.0000 μm	-1.7288 μm	-1.7288 μm	-0.0000 μm	-1.7288 μm
38	2.941 mm	0.0000°	0.0000 μm	-1.7772 μm	-1.7772 μm	-0.0000 μm	-1.7772 μm
39	3.186 mm	0.0000°	0.0000 μm	-1.8257 μm	-1.8257 μm	-0.0000 μm	-1.8257 μm
40	3.431 mm	0.0000°	0.0000 μm	-1.8741 μm	-1.8741 μm	-0.0000 μm	-1.8741 μm
41	3.676 mm	0.0000°	0.0000 μm	-1.9226 μm	-1.9226 μm	-0.0000 μm	-1.9226 μm
42	3.922 mm	0.0000°	0.0000 μm	-1.9710 μm	-1.9710 μm	-0.0000 μm	-1.9710 μm
43	4.167 mm	0.0000°	0.0000 μm	-2.0195 μm	-2.0195 μm	-0.0000 μm	-2.0195 μm
44	4.412 mm	0.0000°	0.0000 μm	-2.0679 μm	-2.0679 μm	-0.0000 μm	-2.0679 μm
45	4.657 mm	0.0000°	0.0000 μm	-2.1164 μm	-2.1164 μm	-0.0000 μm	-2.1164 μm
46	4.902 mm	0.0000°	0.0000 μm	-2.1649 μm	-2.1649 μm	-0.0000 μm	-2.1649 μm
47	5.147 mm	0.0000°	0.0000 μm	-2.2133 μm	-2.2133 μm	-0.0000 μm	-2.2133 μm
48	5.392 mm	0.0000°	0.0000 μm	-2.2618 μm	-2.2618 μm	-0.0000 μm	-2.2618 μm
49	5.637 mm	0.0000°	0.0000 μm	-2.3102 μm	-2.3102 μm	-0.0000 μm	-2.3102 μm
50	5.882 mm	0.0000°	0.0000 μm	-2.3587 μm	-2.3587 μm	-0.0000 μm	-2.3587 μm
51	6.127 mm	0.0000°	0.0000 μm	-2.4071 μm	-2.4071 μm	-0.0000 μm	-2.4071 μm

Explanations:

- y : Width
- φ.t : Static torsion
- f.t : Displacement due to torsion
- f.b : Displacement due to bending
- f.tot : Total displacement (f.b+f.t)
- f.C : Change due to flank line modification

Load distribution

Contact stiffness = 15.879 N/mm/μm

Young's modulus = 202000.0/202000.0 N/mm<sup>2</sup>

	y	δ	g	w
1.	-6.1275 mm	14.1800 μm	0.0000 μm	0.0000 N/mm
2.	-5.8824 mm	13.2808 μm	0.0000 μm	0.0000 N/mm
3.	-5.6373 mm	12.3832 μm	0.0000 μm	0.0000 N/mm
4.	-5.3922 mm	11.5346 μm	0.0000 μm	0.0000 N/mm
5.	-5.1471 mm	10.7056 μm	0.0000 μm	0.0000 N/mm
6.	-4.9020 mm	9.9077 μm	0.2431 μm	3.8599 N/mm
7.	-4.6569 mm	9.1472 μm	1.0035 μm	15.9346 N/mm
8.	-4.4118 mm	8.4047 μm	1.7460 μm	27.7242 N/mm
9.	-4.1667 mm	7.7080 μm	2.4428 μm	38.7880 N/mm
10.	-3.9216 mm	7.0340 μm	3.1167 μm	49.4890 N/mm
11.	-3.6765 mm	6.3879 μm	3.7629 μm	59.7494 N/mm
12.	-3.4314 mm	5.7825 μm	4.3683 μm	69.3619 N/mm
13.	-3.1863 mm	5.1951 μm	4.9557 μm	78.6892 N/mm
14.	-2.9412 mm	4.6501 μm	5.5006 μm	87.3426 N/mm
15.	-2.6961 mm	4.1312 μm	6.0195 μm	95.5814 N/mm
16.	-2.4510 mm	3.6369 μm	6.5139 μm	103.4314 N/mm
17.	-2.2059 mm	3.1866 μm	6.9642 μm	110.5815 N/mm
18.	-1.9608 mm	2.7542 μm	7.3965 μm	117.4466 N/mm
19.	-1.7157 mm	2.3611 μm	7.7897 μm	123.6896 N/mm
20.	-1.4706 mm	1.9973 μm	8.1535 μm	129.4661 N/mm
21.	-1.2255 mm	1.6547 μm	8.4961 μm	134.9057 N/mm
22.	-0.9804 mm	1.3595 μm	8.7913 μm	139.5936 N/mm
23.	-0.7353 mm	1.0822 μm	9.0686 μm	143.9964 N/mm
24.	-0.4902 mm	0.8408 μm	9.3099 μm	147.8291 N/mm
25.	-0.2451 mm	0.6321 μm	9.5187 μm	151.1433 N/mm

26.	0.0000 mm	0.4413 μm	9.7094 μm	154.1725 N/mm
27.	0.2451 mm	0.3011 μm	9.8496 μm	156.3982 N/mm
28.	0.4902 mm	0.1789 μm	9.9718 μm	158.3387 N/mm
29.	0.7353 mm	0.0894 μm	10.0614 μm	159.7609 N/mm
30.	0.9804 mm	0.0357 μm	10.1150 μm	160.6129 N/mm
31.	1.2255 mm	0.0000 μm	10.1508 μm	161.1798 N/mm
32.	1.4706 mm	0.0116 μm	10.1391 μm	160.9951 N/mm
33.	1.7157 mm	0.0445 μm	10.1063 μm	160.4735 N/mm
34.	1.9608 mm	0.1067 μm	10.0440 μm	159.4852 N/mm
35.	2.2059 mm	0.2081 μm	9.9426 μm	157.8750 N/mm
36.	2.4510 mm	0.3275 μm	9.8233 μm	155.9797 N/mm
37.	2.6961 mm	0.4909 μm	9.6598 μm	153.3845 N/mm
38.	2.9412 mm	0.6789 μm	9.4719 μm	150.4006 N/mm
39.	3.1863 mm	0.8929 μm	9.2579 μm	147.0020 N/mm
40.	3.4314 mm	1.1494 μm	9.0014 μm	142.9295 N/mm
41.	3.6765 mm	1.4238 μm	8.7270 μm	138.5719 N/mm
42.	3.9216 mm	1.7390 μm	8.4117 μm	133.5663 N/mm
43.	4.1667 mm	2.0820 μm	8.0687 μm	128.1201 N/mm
44.	4.4118 mm	2.4479 μm	7.7029 μm	122.3111 N/mm
45.	4.6569 mm	2.8594 μm	7.2913 μm	115.7764 N/mm
46.	4.9020 mm	3.2889 μm	6.8618 μm	108.9565 N/mm
47.	5.1471 mm	3.7560 μm	6.3948 μm	101.5405 N/mm
48.	5.3922 mm	4.2540 μm	5.8967 μm	93.6321 N/mm
49.	5.6373 mm	4.7717 μm	5.3791 μm	85.4126 N/mm
50.	5.8824 mm	5.3383 μm	4.8125 μm	76.4156 N/mm
51.	6.1275 mm	5.9065 μm	4.2442 μm	67.3926 N/mm

Explanations:

δ : Gap

g : Flank overlap

w : Line load

Force application point, Y direction:  $y = 1.185 \text{ mm}$  ( $F = 1309.7 \text{ N}$ )

To take into account the load distribution in the shaft calculation: Force center point offset:  $\Delta y = 1.185 \text{ mm}$

$w_{\max} = 161.180 \text{ N/mm}$ ,  $w_m = 104.773 \text{ N/mm}$

$w_m = K_V * K_A * K_Y * (F_t/b) / \cos(\alpha_{wt})$

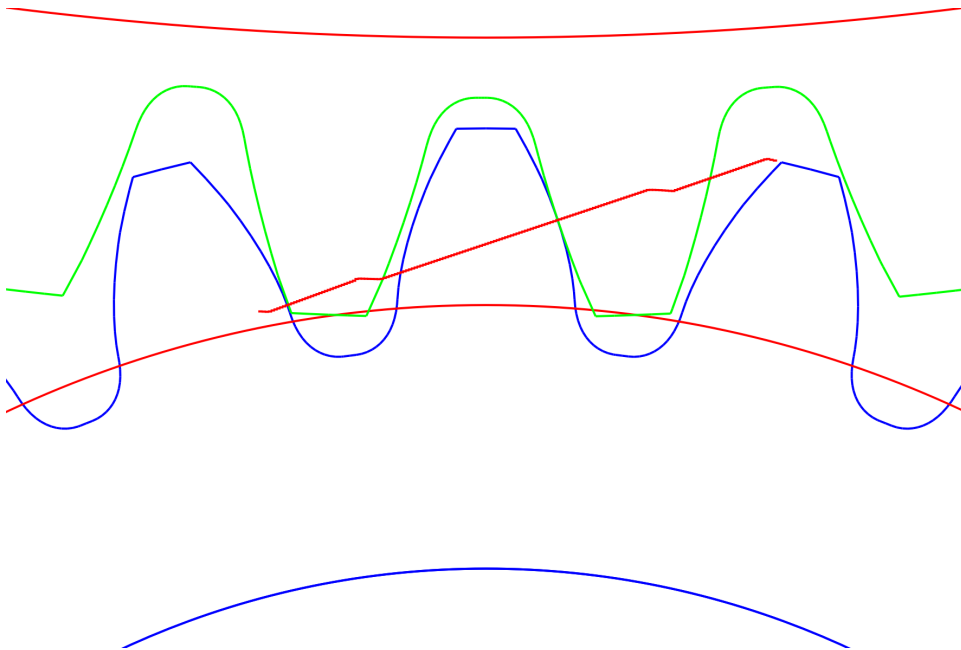
$K_V = 1.0536$ ,  $K_A = 1.250$ ,  $K_Y = 1.000$

$K_{H\beta} = w_{\max}/w_m = 1.5384$  (Calculation according to ISO 6336-1, Appendix E)

Side I, II:  $w_I / w_m = 0.0000$   $w_{II} / w_m = 0.6432$

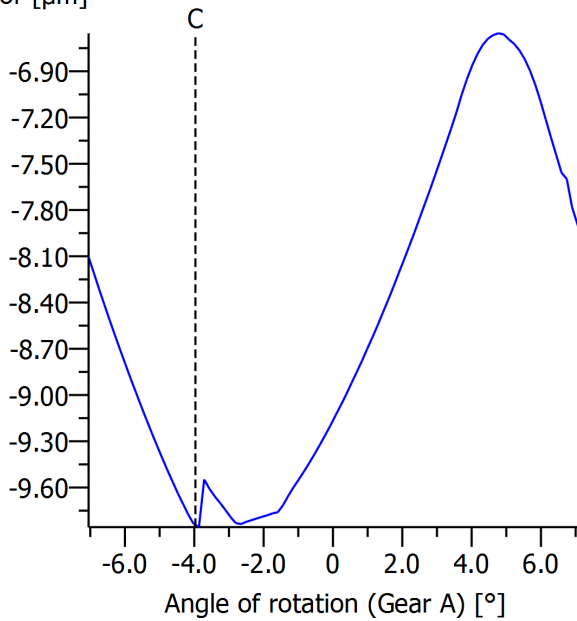
Notice: The influence of the exceeding facewidth is not taken into account in the calculation of  $K_{H\beta}$ .





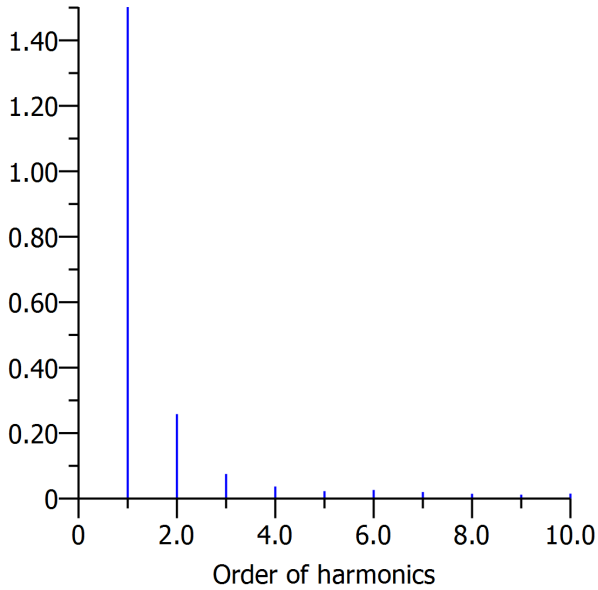
da1 = 16.3043 mm, df1 = 13.5699 mm, As1 = -0.0223 mm da2 = 50.8632 mm, df2 = 48.1127 mm, As2 = -0.0282 mm  
Figure: Meshing Gear 1 - Gear 2

Transmission error [ $\mu\text{m}$ ]



wt = 100 %, a = 32.400 mm, fpt = 0.000  $\mu\text{m}$ ,  $\mu = 0.124$  Working flank: Right flank The transmission error contains the backlash  
Figure: Transmission error

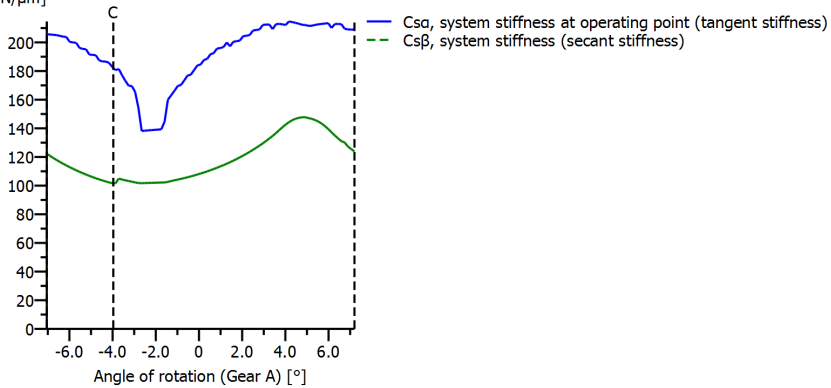
Amplitude [ $\mu\text{m}$ ]



Order of harmonics	Amplitude [ $\mu\text{m}$ ]	1.	1.5018072.	0.2580413.	0.0751214.	0.0368405.	0.0226726.
0.0262687.	0.0199808.	0.0146229.	0.01186810.	0.015047	wt = 100 %, a = 32.400 mm, fpt = 0.000 $\mu\text{m}$ , $\mu = 0.124$		

Figure: Amplitude spectrum of transmission error

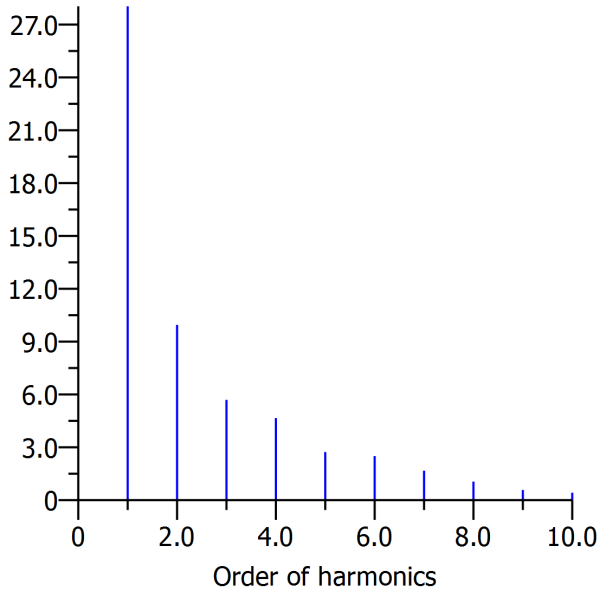
System stiffness [ $\text{N}/\mu\text{m}$ ]



wt = 100 %, a = 32.400 mm, fpt = 0.000  $\mu\text{m}$ ,  $\mu = 0.124$  Working flank: Right flank  $C_{sa\_mean} = 191.9913819 \text{ N}/\mu\text{m}$   $C_{s\beta\_mean} = 118.4052696 \text{ N}/\mu\text{m}$   
 $C_{s\alpha} = C_{y\alpha} * b$   $C_{s\beta} = C_{y\beta} * b$

Figure: Stiffness curve

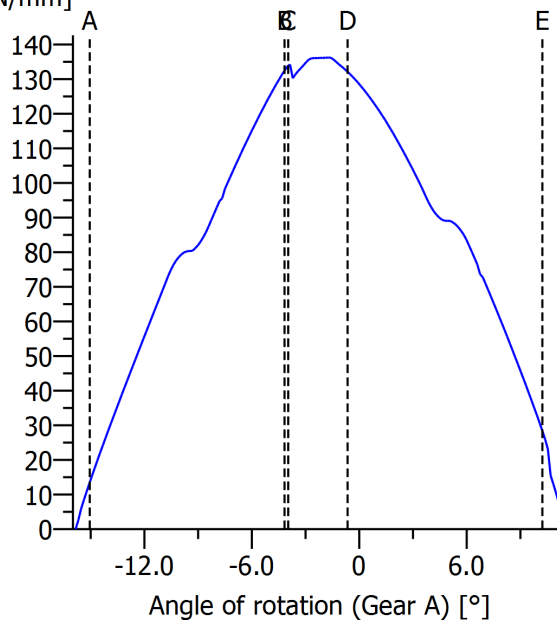
Amplitude [ $\mu\text{m}$ ]



Order of harmonics Amplitude [N/mm/ $\mu\text{m}$ ]1. 28.0369392. 9.9485933. 5.6928404. 4.6566715.  
2.7296766. 2.5011147. 1.6724608. 1.0522129. 0.57786310. 0.421905wt = 100 %, a = 32.400  
mm, fpt = 0.000  $\mu\text{m}$ ,  $\mu$  = 0.124Working flank: Right flank

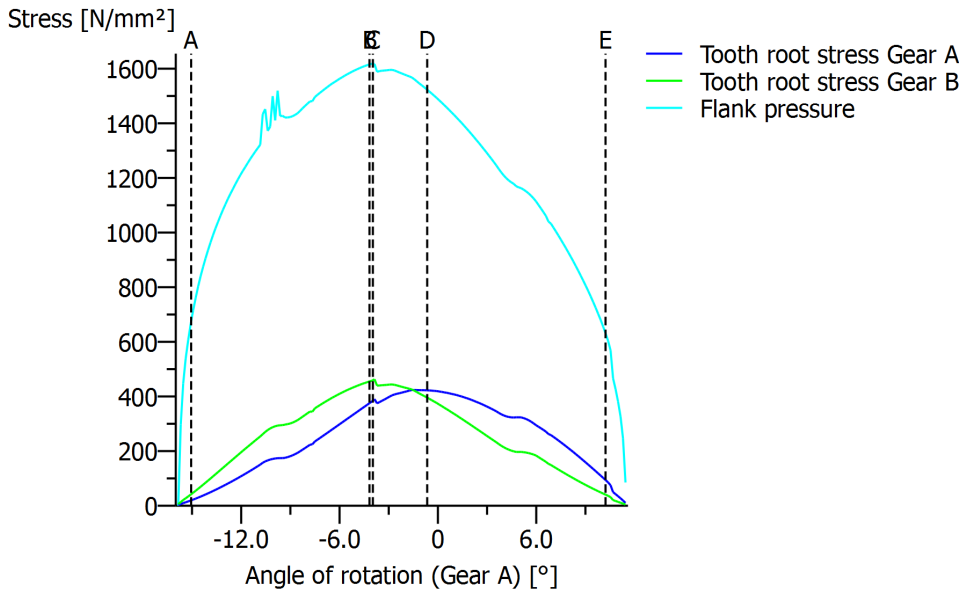
Figure: Amplitude spectrum of contact stiffness

Normal force (line load) [N/mm]

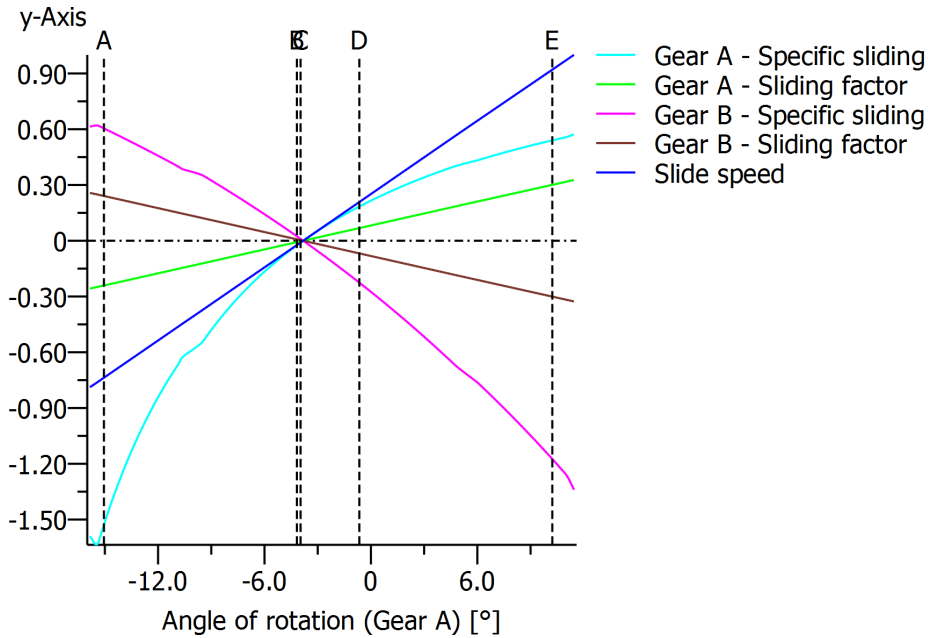


wt = 100 %, a = 32.400 mm, fpt = 0.000  $\mu\text{m}$ ,  $\mu$  = 0.124Working flank: Right flank

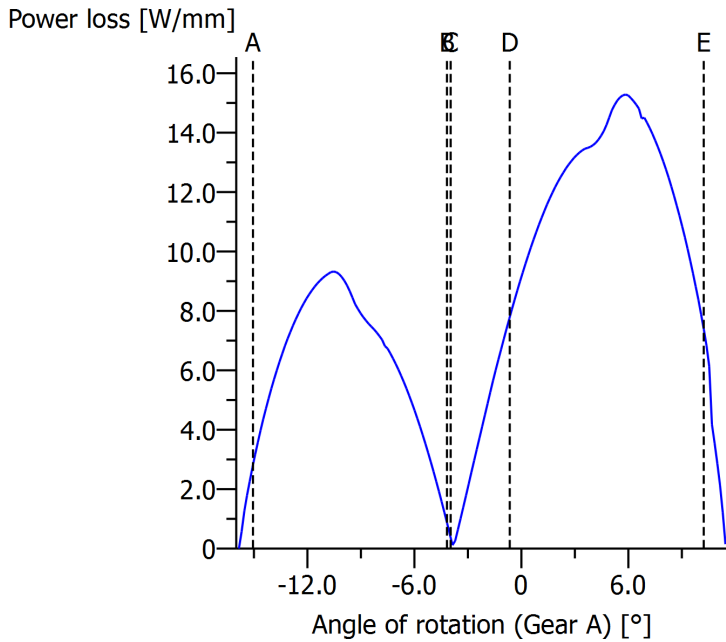
Figure: Normal force curve (Line load)



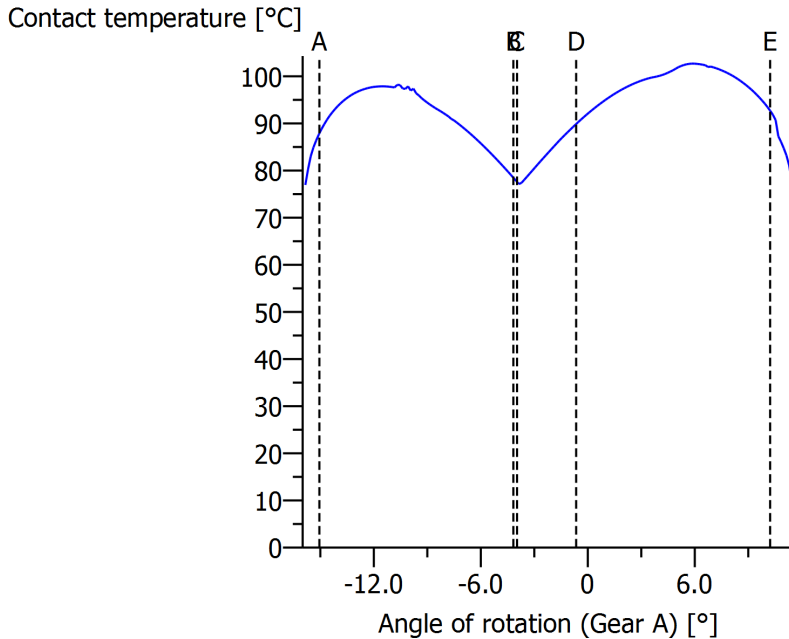
wt = 100 %, a = 32.400 mm, f<sub>pt</sub> = 0.000 μm, μ = 0.124 Working flank: Right flank  
Figure: Stress curve



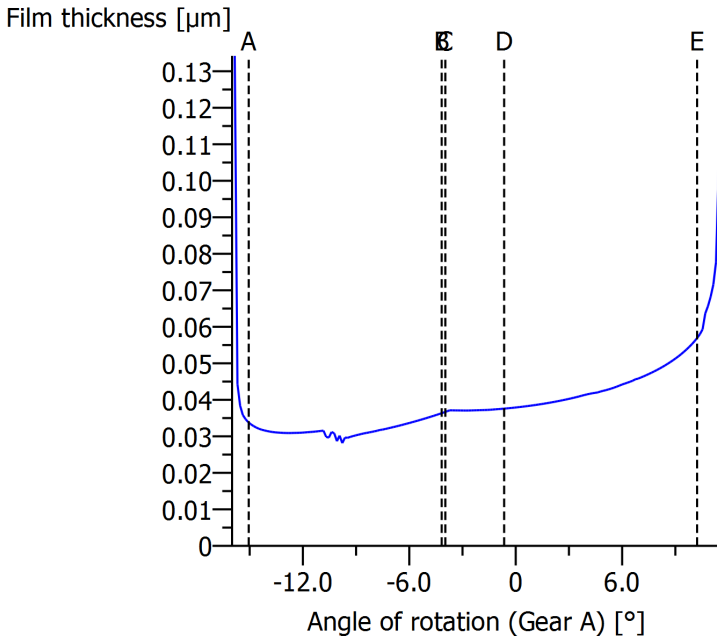
wt = 100 %, a = 32.400 mm, f<sub>pt</sub> = 0.000 μm, μ = 0.124 Working flank: Right flank Maximum sliding velocity: 1.000 m/s  
Figure: Kinematics



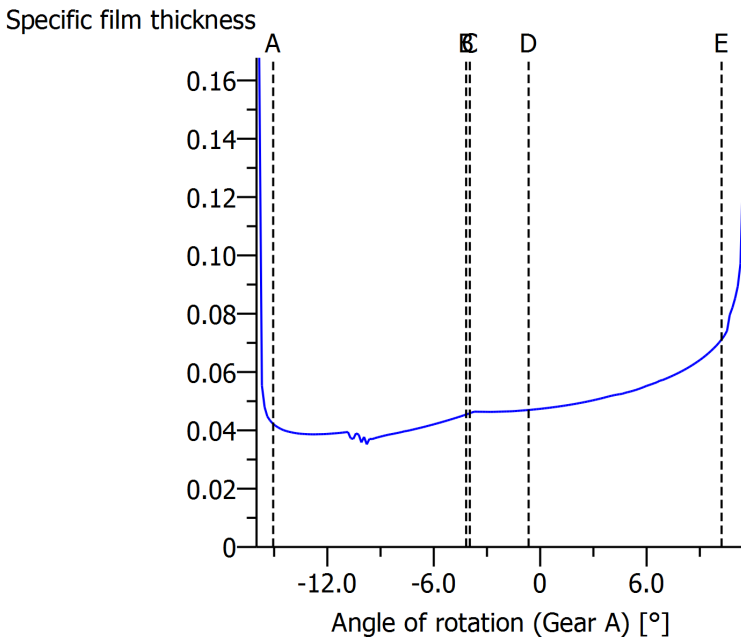
wt = 100 %, a = 32.400 mm, fpt = 0.000  $\mu\text{m}$ ,  $\mu = 0.124$  Displaying power losses per mm facewidth Working flank: Right flank  
Figure: Specific Power Loss



wt = 100 %, a = 32.400 mm, fpt = 0.000  $\mu\text{m}$ ,  $\mu = 0.092$  the Oil = 70.0 °C, the M = 76.9 °C, etaM = 8.12 mPa\*s Working flank: Right flank  
Figure: Contact temperature



wt = 100 %, a = 32.400 mm, fpt = 0.000  $\mu\text{m}$ ,  $\mu = 0.092$  the oil = 70.0  $^\circ\text{C}$ , the M = 76.9  $^\circ\text{C}$ , etaM = 8.12 mPa\*shMini(ISO) = 0.028  $\mu\text{m}$ , Ra = 0.800  $\mu\text{m}$  Working flank: Right flank  
Figure: Lubricating film (ISO TR 15144)



wt = 100 %, a = 32.400 mm, fpt = 0.000  $\mu\text{m}$ ,  $\mu = 0.092$  the oil = 70.0  $^\circ\text{C}$ , the M = 76.9  $^\circ\text{C}$ , etaM = 8.12 mPa\*shMini(ISO) = 0.028  $\mu\text{m}$ , Ra = 0.800  $\mu\text{m}$ , lamGFmin = 0.035 Working flank: Right flank  
Figure: Specific film thickness (ISO TR 15144)

# Gear stage 2 calculation

KISSsoft Release 03/2015 F

KISSsoft Academic License - Norwegian University of Science & Technology (NTNU)

File

Name : Unnamed  
 Changed by: Kraftwerk on: 02.02.2016 at: 18:54:07

**Important hint: At least one warning has occurred during the calculation:**

1-> Gear 1:  
 Equivalent tip relief Ceq: 16.0 µm

According to ISO15144, the tip relief is not in the optimum range.  
 Recommended:  
 Delete optimal tip relief [CaOpt].

(In the 'Pair/Gear data' tab, in the 'Strength details' window.)

2-> Gear 2:  
 Equivalent tip relief Ceq: 16.0 µm

According to ISO15144, the tip relief is not in the optimum range.  
 Recommended:  
 Delete optimal tip relief [CaOpt].

(In the 'Pair/Gear data' tab, in the 'Strength details' window.)

3-> Calculation for load spectra:  
 The application factor should be set to 1.0!  
 (according ISO6336-6 or DIN3990-6)

4-> Some elements of the Load spectrum are unusually big.  
 Check the Load spectrum.  
 (Element no. 1)

## CALCULATION OF A CYLINDRICAL SPUR GEAR PAIR

Drawing or article number:

Gear 1: Planet2(Planet2RingConstraint)  
 Gear 2: RingGear(Planet2RingConstraint)

### Load spectrum

load\_spectrum\_100  
 Number of bins in the load spectrum: 7  
 Reference gear: 1

No.	[%]	[kW]	[1/min]	[Nm]	KV	KHβ	KHα	Kγ	YM1	YM2	OilTemp
1	40.00000	3.1050	-3534.3	-8.3895	1.0712	1.4529	1.0000	1.0000	1.0000	1.0000	70
2	10.00000	6.6667	-4712.4	-13.5095	1.0705	1.3460	1.0000	1.0000	1.0000	1.0000	70
3	6.00000	6.6667	-5301.4	-12.0085	1.0860	1.3823	1.0000	1.0000	1.0000	1.0000	70
4	4.00000	6.1187	-3652.1	-15.9989	1.0490	1.3010	1.0000	1.0000	1.0000	1.0000	70
5	30.00000	5.8643	-2356.2	-23.7672	1.0250	1.2149	1.0000	1.0000	1.0000	1.0000	70

6	8.00000	-4.0000	-4712.4	8.1057	1.0965	1.4437	1.0000	1.0000	0.7000	0.7000	70
7	2.00000	-5.3333	-2678.6	19.0137	1.0323	1.2596	1.0000	1.0000	0.7000	0.7000	70

Notice:

Tooth flank with load spectrum: Consider all negative load spectrum bins as positive

Tooth root with load spectrum: Consider all negative load spectrum bins as positive

Is only applied on load spectrum bins, where the alternating bending factor (mean stress influence factor) YM=1.0.

Woehler line (S-N curve) in the endurance domain according: according to standard

## Results

Root safety	0.934	1.226
Flank safety	1.146	1.296

Scuffing safety (integral temperature) 7.981

Scuffing safety (flash temperature) 18.441

(Safety against scuffing/micropitting/EHT is indicated for the most critical element of the load spectrum.)

Analysis of critical elements in load spectrum: See section 10

## ONLY AS INFORMATION: CALCULATION WITH REFERENCE POWER

Calculation method DIN 3990:1987 Method B (YF Method C)

		----- GEAR 1 -----	----- GEAR 2 --
Power (kW)	[P]		1.047
Speed (1/min)	[n]	100.0	23.2
Torque (Nm)	[T]	100.0	430.8
Application factor	[KA]		1.25
Required service life (h)	[H]		50.00
Gear driving (+) / driven (-)		+	-
Working flank gear 1: Right flank			

### 1. TOOTH GEOMETRY AND MATERIAL

(geometry calculation according to

DIN 3960:1987)

		----- GEAR 1 -----	----- GEAR 2 --
Center distance (mm)	[a]		-32.400
Centre distance tolerance	ISO 286:2010 Measure js9		
Normal module (mm)	[mn]		0.7500
Pressure angle at normal section (°)	[alfn]		20.0000
Helix angle at reference circle (°)	[beta]		0.0000
Number of teeth	[z]	26	-112
Facewidth (mm)	[b]	13.00	13.00
Hand of gear			Spur gear
Accuracy grade	[Q-DIN 3961:1978]	6	7
Inner diameter (mm)	[di]	14.50	
External diameter (mm)	[dj]		100.00



Inner diameter of gear rim (mm) [dbi] 14.50  
Outer diameter of gear rim (mm) [dbi] 100.00

Material

Gear 1: (Own input) NC310YW, Case-carburized steel, case-hardened

Gear 2: (Own input) NC310YW, Case-carburized steel, case-hardened

		----- GEAR 1 -----	GEAR 2 --
Surface hardness		HRC 59	HRC 59
Fatigue strength. tooth root stress (N/mm <sup>2</sup> )	[sigFlim]	525.00	525.00
Fatigue strength for Hertzian pressure (N/mm <sup>2</sup> )	[sigHlim]	1650.00	1650.00
Tensile strength (N/mm <sup>2</sup> )	[Rm]	2150.00	2150.00
Yield point (N/mm <sup>2</sup> )	[Rp]	1790.00	1790.00
Young's modulus (N/mm <sup>2</sup> )	[E]	202000	202000
Poisson's ratio	[ny]	0.300	0.300
Roughness average value DS, flank (µm)	[RAH]	0.80	1.60
Roughness average value DS, root (µm)	[RAF]	0.80	1.60
Mean roughness height, Rz, flank (µm)	[RZH]	6.30	11.25
Mean roughness height, Rz, root (µm)	[RZF]	6.30	11.25

Gear reference profile 1 :

Reference profile	1.25 / 0.38 / 1.0 ISO 53.2:1997 Profil A		
Dedendum coefficient	[hfP*]	1.250	
Root radius factor	[rhofP*]	0.380 (rhofPmax*=0.472)	
Addendum coefficient	[haP*]	1.000	
Tip radius factor	[rhoaP*]	0.000	
Protuberance height factor	[hprP*]	0.000	
Protuberance angle	[alfprP]	0.000	
Tip form height coefficient	[hFaP*]	0.000	
Ramp angle	[alfKP]	0.000	
		not topping	

Gear reference profile 2 :

Reference profile	1.25 / 0.38 / 1.0 ISO 53.2:1997 Profil A		
Dedendum coefficient	[hfP*]	1.250	
Root radius factor	[rhofP*]	0.380 (rhofPmax*=0.472)	
Addendum coefficient	[haP*]	1.000	
Tip radius factor	[rhoaP*]	0.000	
Protuberance height factor	[hprP*]	0.000	
Protuberance angle	[alfprP]	0.000	
Tip form height coefficient	[hFaP*]	0.000	
Ramp angle	[alfKP]	0.000	
		not topping	

Summary of reference profile gears:

Dedendum reference profile	[hfP*]	1.250	1.250
Tooth root radius Refer. profile	[rofpP*]	0.380	0.380
Addendum Reference profile	[haP*]	1.000	1.000
Protuberance height factor	[hprP*]	0.000	0.000
Protuberance angle (°)	[alfprP]	0.000	0.000
Tip form height coefficient	[hFaP*]	0.000	0.000
Ramp angle (°)	[alfKP]	0.000	0.000

Type of profile modification:

for high load capacity gearboxes

Tip relief (µm)	[Ca]	16.0	0.0
-----------------	------	------	-----

Lubrication type	oil bath lubrication		
Type of oil	Oil: Klübersynth GH 6-22		
Lubricant base	Synthetic oil based on Polyglycol		
Kinem. viscosity oil at 40 °C (mm <sup>2</sup> /s)	[nu40]	22.00	
Kinem. viscosity oil at 100 °C (mm <sup>2</sup> /s)	[nu100]	5.30	
FZG test A/8.3/90 ( ISO 14635-1:2006)	[FZGtestA]	14	
Specific density at 15 °C (kg/dm <sup>3</sup> )	[roOil]	1.025	
Oil temperature (°C)	[TS]	70.000	
----- GEAR 1 ----- GEAR 2 --			
Overall transmission ratio	[itot]	4.308	
Gear ratio	[u]	-4.308	
Transverse module (mm)	[mt]	0.750	
Pressure angle at pitch circle (°)	[alfit]	20.000	
Working transverse pressure angle (°)	[alfwt]	20.717	
	[alfwt.e/i]	20.571 /	20.861
Working pressure angle at normal section (°)	[alfwn]	20.717	
Helix angle at operating pitch circle (°)	[betaw]	0.000	
Base helix angle (°)	[betab]	0.000	
Reference centre distance (mm)	[ad]	-32.250	
Sum of profile shift coefficients	[Summexi]	-0.2035	
Profile shift coefficient	[x]	0.2749	-0.4784
Tooth thickness (Arc) (module) (module)	[sn*]	1.7709	1.2226
Tip alteration (mm)	[k*mn]	0.003	0.000
Reference diameter (mm)	[d]	19.500	-84.000
Base diameter (mm)	[db]	18.324	-78.934
Tip diameter (mm)	[da]	21.418	-83.218
(mm)	[da.e/i]	21.418 /	21.408 -83.218 / -83.228
Tip diameter allowances (mm)	[Ada.e/i]	0.000 /	-0.010 0.000 / -0.010
Chamfer (1) / tip rounding (2)		2	2
Tip rounding (mm)	[rK]	0.300	0.300
Tip form diameter (mm)	[dFa]	21.110	-83.618
(mm)	[dFa.e/i]	21.110 /	21.100 -83.618 / -83.628
Active tip diameter (mm)	[dNa]	21.110	-83.618
Active tip diameter (mm)	[dNa.e/i]	21.110 /	21.100 -83.618 / -83.628
Operating pitch diameter (mm)	[dw]	19.591	-84.391
(mm)	[dw.e/i]	19.572 /	19.609 -84.310 / -84.471
Root diameter (mm)	[df]	18.037	-86.593
Generating Profile shift coefficient	[xE.e/i]	0.2418/	0.2204 -0.5388/ -0.5797
Manufactured root diameter with xE (mm)	[df.e/i]	17.988 /	17.956 -86.683 / -86.745
Theoretical tip clearance (mm)	[c]	0.187	0.190
Effective tip clearance (mm)	[c.e/i]	0.299 /	0.201 0.267 / 0.184
Active root diameter (mm)	[dNf]	18.910	-85.711
(mm)	[dNf.e/i]	18.962 /	18.867 -85.635 / -85.779
Root form diameter (mm)	[dFf]	18.653	-86.188
(mm)	[dFf.e/i]	18.627 /	18.610 -86.277 / -86.337
Internal toothing: Calculation dFf with pinion type cutter (z0=	36, x0=	0.000)	
Reserve (dNf-dFf)/2 (mm)	[cF.e/i]	0.176 /	0.120 0.351 / 0.249
Addendum (mm)	[ha=mn*(haP*+x)]	0.959	
(mm)	[ha.e/i]	0.959 /	0.954 0.391 / 0.386
Dedendum (mm)	[hf=mn*(hfP*-x)]	0.731	
(mm)	[hf.e/i]	0.756 /	0.772 1.342 / 1.372
Roll angle at dFa (°)	[xsi_dFa.e/i]	32.773 /	32.710 20.028 / 20.050
Roll angle to dNa (°)	[xsi_dNa.e/i]	32.773 /	32.710 20.028 / 20.050
Roll angle to dNf (°)	[xsi_dNf.e/i]	15.245 /	14.054 24.104 / 24.373

Roll angle at dFf (°)	[xsi_dFf.e/i]	10.457 / 10.163	25.282 / 25.390
Tooth height (mm)	[H]	1.691	1.688
Virtual gear no. of teeth	[zn]	26.000	-112.000
Normal-tooth thickness at tip circle (mm)	[san]	0.472	0.637
(mm)	[san.e/i]	0.458 / 0.440	0.607 / 0.582
(without consideration of tip chamfer/ tip rounding)			
Normal-tooth thickness on tip form circle (mm)	[sFan]	0.646	0.777
(mm)	[sFan.e/i]	0.632 / 0.614	0.747 / 0.722
Normal space width at root circle (mm)	[efn]	0.000	0.408
(mm)	[efn.e/i]	0.000 / 0.000	0.402 / 0.397
Max. sliding velocity at tip (m/s)	[vga]	0.014	0.009
Specific sliding at the tip	[zetaa]	0.260	0.271
Specific sliding at the root	[zetaf]	-0.372	-0.352
Mean specific sliding	[zetam]		0.264
Sliding factor on tip	[Kga]	0.139	0.089
Sliding factor on root	[Kgf]	-0.089	-0.139
Pitch on reference circle (mm)	[pt]		2.356
Base pitch (mm)	[pbt]		2.214
Transverse pitch on contact-path (mm)	[pet]		2.214
Length of path of contact (mm)	[ga, e/i]	2.906 ( 2.993 / 2.793)	
Length T1-A, T2-A (mm)	[T1A, T2A]	2.335( 2.247/ 2.438)	-13.796( -13.796/ -13.811)
Length T1-B (mm)	[T1B, T2B]	3.026( 3.026/ 3.016)	-14.488( -14.575/ -14.390)
Length T1-C (mm)	[T1C, T2C]	3.465( 3.491/ 3.438)	-14.926( -15.040/ -14.812)
Length T1-D (mm)	[T1D, T2D]	4.549( 4.461/ 4.652)	-16.010( -16.010/ -16.025)
Length T1-E (mm)	[T1E, T2E]	5.241( 5.241/ 5.230)	-16.702( -16.789/ -16.604)
Length T1-T2 (mm)	[T1T2]		-11.461 ( -11.549 / -11.373)
Diameter of single contact point B (mm)	[d-B]	19.298( 19.298/ 19.292)	-84.084( -84.145/ -84.017)
Diameter of single contact point D (mm)	[d-D]	20.458( 20.381/ 20.551)	-85.182( -85.182/ -85.193)
Addendum contact ratio	[eps]	0.802( 0.790/ 0.809)	0.511( 0.562/ 0.452)
Minimal length of contact line (mm)	[Lmin]		13.000
Transverse contact ratio	[eps_a]		1.312
Transverse contact ratio with allowances	[eps_a.e/m/i]	1.352 / 1.307 / 1.261	
Overlap ratio	[eps_b]		0.000
Total contact ratio	[eps_g]		1.312
Total contact ratio with allowances	[eps_g.e/m/i]	1.352 / 1.307 / 1.261	

## **2. FACTORS OF GENERAL INFLUENCE**

		----- GEAR 1 -----	----- GEAR 2 --
Nominal circum. force at pitch circle (N)	[Ft]		10256.4
Axial force (N)	[Fa]		0.0
Radial force (N)	[Fr]		3733.0
Normal force (N)	[Fnorm]		10914.6
Nominal circumferential force per mm (N/mm)	[w]		788.95
Only as information: Forces at operating pitch circle:			
Nominal circumferential force (N)	[Ftw]		10208.9
Axial force (N)	[Faw]		0.0
Radial force (N)	[Frw]		3861.0
Circumferential speed reference circle (m/s)	[v]		0.10
Circumferential speed operating pitch circle (m/s)	[v(dw)]		0.10
Running-in value (µm)	[yp]		0.8
Running-in value (µm)	[yf]		0.5
Correction coefficient	[CM]		0.800
Gear body coefficient	[CR, bs/b, sr/mn]		0.827 (0.250, 2.358)

Reference profile coefficient	[CBS]	0.975	
Material coefficient	[E/Est]	0.981	
Singular tooth stiffness (N/mm/μm)	[c]	12.171	
Meshing stiffness (N/mm/μm)	[cg]	15.023	
Reduced mass (kg/mm)	[mRed]	0.00092	
Resonance speed (min-1)	[nE1]	46864	
Resonance ratio (-)	[N]	0.002	
Subcritical range			
Running-in value (μm)	[ya]	0.8	
Dynamic factor	[KV]	1.001	
User specified factor KHb:			
Face load factor - flank	[KHb]	1.150	
- Tooth root	[KFb]	1.129	
- Scuffing	[KBb]	1.150	
Transverse load factor - flank	[KHα]	1.000	
- Tooth root	[KFα]	1.000	
- Scuffing	[KBα]	1.000	
Helical load factor scuffing	[Kβg]	1.000	
Number of load cycles (in mio.)	[NL]	0.300	0.209

### **3. TOOTH ROOT STRENGTH**

Calculation of Tooth form coefficients according method: C

		----- GEAR 1 -----	GEAR 2 --
Calculated with manufacturing profile shift	[xE.e]	0.24	-0.54
Tooth form factor	[YF]	2.12	1.27
Stress correction factor	[YS]	1.77	2.36
Working angle (°)	[alfFen]	28.07	20.00
Bending lever arm (mm)	[hF]	1.29	1.16
Tooth thickness at root (mm)	[sFn]	1.60	2.03
Tooth root radius (mm)	[roF]	0.36	0.29
(hF* = 1.719/ 1.541 sFn* = 2.138/ 2.703 roF* = 0.483/ 0.380 dsFn = 18.259/ 0.000 alfsFn = 30.00/ 30.00)			
Contact ratio factor	[Yeps]	0.821	
Helix angle factor	[Ybet]	1.000	
Effective facewidth (mm)	[beff]	13.00	13.00
Nominal stress at tooth root (N/mm²)	[sigF0]	3233.72	2583.22
Tooth root stress (N/mm²)	[sigF]	4565.06	3646.75
Permissible bending stress at root of Test-gear			
Notch sensitivity factor	[YdrelT]	1.031	1.133
Surface factor	[YRrelT]	1.020	0.996
size factor (Tooth root)	[YX]	1.000	1.000
Finite life factor	[YNT]	1.302	1.357
	[YdrelT*YRrelT*YX*YNT]	1.369	1.531
Alternating bending factor (mean stress influence coefficient)	[YM]	0.700	0.700
Stress correction factor	[Yst]	2.00	
Yst*sigFlim (N/mm²)	[sigFE]	1050.00	1050.00
Permissible tooth root stress (N/mm²)	[sigFP=sigFG/SFmin]	1117.71	1250.28
Limit strength tooth root (N/mm²)	[sigFG]	1005.94	1125.25
Required safety	[SFmin]	0.90	0.90

**4. SAFETY AGAINST PITTING (TOOTH FLANK)**

		----- GEAR 1 -----	----- GEAR 2 -----
Zone factor	[ZH]		2.447
Elasticity coefficient ( $\sqrt{N/mm}$ )	[ZE]		187.960
Contact ratio factor	[Zeps]		0.946
Helix angle factor	[Zbet]		1.000
Effective facewidth (mm)	[beff]		13.00
Nominal flank pressure (N/mm <sup>2</sup> )	[sigH0]		2426.61
Surface pressure at operating pitch circle (N/mm <sup>2</sup> )	[sigHw]		2909.88
Single tooth contact factor	[ZB,ZD]	1.09	1.00
Flank pressure (N/mm <sup>2</sup> )	[sigHB, sigHD]	3160.38	2909.88
Lubrication coefficient at NL	[ZL]	0.985	0.990
Speed coefficient at NL	[ZV]	0.989	0.992
Roughness coefficient at NL	[ZR]	0.982	0.988
Work hardening factor at NL	[ZW]	1.000	1.000
Finite life factor	[ZNT]	1.472	1.513
	[ZL*ZV*ZR*ZNT]	1.408	1.468
Small no. of pittings permissible:	no		
Size factor (flank)	[ZX]	1.000	1.000
Permissible surface pressure (N/mm <sup>2</sup> )	[sigHP=sigHG/SHmin]	3096.93	3230.32
Limit strength pitting (N/mm <sup>2</sup> )	[sigHG]	2322.70	2422.74
Required safety	[SHmin]	0.75	0.75

**4b. MICROPITTING ACCORDING TO ISO/TR 15144-1:2014**

Calculation did not run. (Lubricant: Load stage micropitting test is unknown.)

**5. STRENGTH AGAINST SCUFFING**

Calculation method according to

DIN 3990:1987

Lubrication coefficient (for lubrication type)	[XS]		1.000
Relative structure coefficient (Scuffing)	[XWrelT]		1.000
Thermal contact factor (N/mm/s <sup>0.5</sup> /K)	[BM]	13.629	13.629
Relevant tip relief ( $\mu\text{m}$ )	[Ca]	16.00	0.00
Optimal tip relief ( $\mu\text{m}$ )	[Ceff]		81.03
Ca taken as optimal in the calculation (0=no, 1=yes)		0	0
Effective facewidth (mm)	[beff]		13.000
Applicable circumferential force/facewidth (N/mm)	[wBt]		1134.495
Angle factor	[Xalfbet]		0.988
( $\epsilon_1:0.802, \epsilon_2:0.511$ )			
Flash temperature-criteria			
Tooth mass temperature (°C)	[theM-B]		91.49
theM-B = theoil + XS*0.47*theflamax	[theflamax]		45.71
Scuffing temperature (°C)	[theS]		739.42

Coordinate gamma (point of highest temp.) [Gamma.A]=0.326 [Gamma.E]=0.512	[Gamma]	0.313
Highest contact temp. (°C)	[theB]	137.20
Flash factor (°K*N <sup>-1</sup> .75*s <sup>1.5</sup> *m <sup>-1.5</sup> *mm)	[XM]	50.362
Geometry factor	[XB]	0.065
Load sharing factor	[XGam]	1.000
Dynamic viscosity (mPa*s)	[etaM]	6.10 ( 91.5 °C)
Coefficient of friction	[mym]	0.539

Integral temperature-criteria		
Tooth mass temperature (°C)	[theM-C]	82.95
theM-C = theoil + XS*0.70*theffaint	[theffaint]	18.50
Integral scuffing temperature (°C)	[theSint]	739.42
Flash factor (°K*N <sup>-1</sup> .75*s <sup>1.5</sup> *m <sup>-1.5</sup> *mm)	[XM]	50.362
Contact ratio factor	[Xeps]	0.294
Dynamic viscosity (mPa*s)	[etaOil]	9.52 ( 70.0 °C)
Mean coefficient of friction	[mym]	0.549
Geometry factor	[XBE]	0.097
Meshing factor	[XQ]	1.000
Tip relief factor	[XCa]	1.103
Integral tooth flank temperature (°C)	[theint]	110.71

## 6. MEASUREMENTS FOR TOOTH THICKNESS

		----- GEAR 1 -----	----- GEAR 2 --
		DIN 58405 6e	DIN 58405 7e
Tooth thickness deviation			
Tooth thickness allowance (normal section) (mm)	[As.e/i]	-0.018 /	-0.030 -0.033 / -0.055
Number of teeth spanned	[k]	4.000	-14.000
(Internal toothing: k = (Measurement gap number)			
Base tangent length (no backlash) (mm)	[Wk]	8.164	-31.312
Actual base tangent length ('span') (mm)	[Wk.e/i]	8.147 /	8.136 -31.343 / -31.364
(mm)	[ΔWk.e/i]	-0.017 /	-0.028 -0.031 / -0.052
Diameter of contact point (mm)	[dMWk.m]	20.051	-84.933
Theoretical diameter of ball/pin (mm)	[DM]	1.357	1.260
Eff. Diameter of ball/pin (mm)	[DMeff]	1.400	1.400
Theor. dim. centre to ball (mm)	[MrK]	10.989	-41.230
Actual dimension centre to ball (mm)	[MrK.e/i]	10.970 /	10.958 -41.276 / -41.307
Diameter of contact point (mm)	[dMMr.m]	19.936	-84.471
Diametral measurement over two balls without clearance (mm)	[MdK]	21.978	-82.460
Actual dimension over balls (mm)	[MdK.e/i]	21.940 /	21.916 -82.552 / -82.613
Diametral measurement over rolls without clearance (mm)	[MdR]	21.978	-82.460
Actual dimension over rolls (mm)	[MdR.e/i]	21.940 /	21.916 -82.552 / -82.613
Chordal tooth thickness (no backlash) (mm)	[sn]	1.327	0.917
Actual chordal tooth thickness (mm)	[sn.e/i]	1.309 /	1.297 0.884 / 0.862
Reference chordal height from da.m (mm)	[ha]	0.979	0.386
Tooth thickness (Arc) (mm)	[sn]	1.328	0.917
(mm)	[sn.e/i]	1.310 /	1.298 0.884 / 0.862
Backlash free center distance (mm)	[aControl.e/i]	-32.467	/ -32.512
Backlash free center distance, allowances (mm)	[jta]	-0.067	/ -0.112
dNf.i with aControl (mm)	[dNf0.i]	18.765	-85.956
Reserve (dNf0.i-dFf.e)/2 (mm)	[cF0.i]	0.069	0.160

Tip clearance	[c0.i(aControl)]	0.121	0.103
Centre distance allowances (mm)	[Aa.e/i]	0.031 /	-0.031
Circumferential backlash from Aa (mm)	[jtw_Aa.e/i]	0.023 /	-0.023
Radial clearance (mm)	[jrw]	0.143 /	0.036
Circumferential backlash (transverse section) (mm)	[jtw]	0.109 /	0.028
Rotation angle when gear 1 is fixed (°)		0.1480 /	0.0378
Normal backlash (mm)	[jnw]	0.102 /	0.026

## 7. GEAR ACCURACY

----- GEAR 1 ----- GEAR 2 --

According to DIN 3961:1978

One or several gear data (mn, b or d) lay beyond the limits covered by the standard.

The tolerances are calculated on the basis of the formulae in the standard.

However, their values are outside the official range of validity!

Accuracy grade	[Q-DIN3961]	6	7
Profile form deviation (µm)	[ff]	5.00	7.00
Profile slope deviation (µm)	[fHa]	4.50	7.00
Total profile deviation (µm)	[Ff]	7.00	10.00
Helix form deviation (µm)	[fbf]	4.00	5.50
Helix slope deviation (µm)	[fHb]	8.00	11.00
Total helix deviation (µm)	[Fb]	9.00	13.00
Normal base pitch deviation (µm)	[fpe]	6.00	10.00
Single pitch deviation (µm)	[fp]	6.00	10.00
Adjacent pitch difference (µm)	[fu]	8.00	12.00
Total cumulative pitch deviation (µm)	[Fp]	18.00	31.00
Sector pitch deviation over z/8 pitches (µm)	[Fpz/8]	11.00	20.00
Runout (µm)	[Fr]	12.00	20.00
Tooth Thickness Variation (µm)	[Rs]	7.00	11.00
Single flank composite, total (µm)	[Fi']	20.00	33.00
Single flank composite, tooth-to-tooth (µm)	[fi']	9.00	14.00
Radial composite, total (µm)	[Fi'']	15.00	26.00
Radial composite, tooth-to-tooth (µm)	[fi'']	5.50	10.00

According to DIN 58405:1972 (Feinwerktechnik):

Tooth-to-tooth composite error (µm)	[fi'']	6.00	11.00
Composite error (µm)	[Fi'']	18.00	32.00
Axis alignment error (µm)	[fp]	5.51	7.13
Flank direction error (µm)	[fbeta]	5.00	7.00
Runout (µm)	[Trk, Fr]	18.00	44.00

## 8. ADDITIONAL DATA

Maximal possible centre distance (eps_a=1.0)	[aMAX]	-32.162	
Weight - calculated with da (g)	[Mass]	19.43	240.48
Total weight (g)	[Mass]	259.92	
Moment of inertia (System referenced to wheel 1): calculation without consideration of the exact tooth shape			
single gears ((da+df)/2...di) (kg*m <sup>2</sup> )	[TraeghMom]	1.038e-006	0.0004681
System ((da+df)/2...di) (kg*m <sup>2</sup> )	[TraeghMom]	2.626e-005	
Torsional stiffness (MNm/rad)	[cr]	0.0	0.3
Mean coeff. of friction (acc. Niemann)	[mum]	0.170	
Wear sliding coef. by Niemann	[zetw]	0.347	
Gear power loss (kW)	[PVZ]	0.010	

(Meshing efficiency (%)) [etaz] 99.069)

**9. DETERMINATION OF TOOTH FORM**

Profile and tooth trace modifications for gear \_\_\_\_\_ 1

**Symmetric (both flanks)**

- Tip relief, arc-like Caa = 16.000µm LCa = 0.999\*mn dCa = 20.697mm  
 - Crowning Cb = 10.000µm (rcrown= 2113 mm)  
 - Helix angle modification, tapered or conical CHb = 4.487µm  
 CHb=4.4873 -> Right Tooth Flank beta.eff = 0.021°-left Left Tooth Flank beta.eff = 0.021°-right

Data for the tooth form calculation :  
 Data not available.

**10. SERVICE LIFE, DAMAGE**

Required safety for tooth root [SFmin] 0.90  
 Required safety for tooth flank [SHmin] 0.75

Service life (calculated with required safeties):

System service life (h) [Hatt] 291

Tooth root service life (h) [HFatt] 291.2 1e+006

Tooth flank service life (h) [HHatt] 1e+006 1e+006

Note: The entry 1e+006 h means that the Service life > 1,000,000 h.

Damage calculated on basis of required service life

[H] ( 50.0 h)

No.	F1%	F2%	H1%	H2%
1	0.00	0.00	0.00	0.00
2	0.00	0.00	0.00	0.00
3	0.00	0.00	0.00	0.00
4	0.00	0.00	0.00	0.00
5	0.00	0.00	0.00	0.00
6	0.00	0.00	0.00	0.00
7	17.17	0.00	0.00	0.00
-----				
Σ	17.17	0.00	0.00	0.00

Damage calculated on basis of system service life

[Hatt] ( 291.2 h)

No.	F1%	F2%	H1%	H2%
1	0.00	0.00	0.00	0.00
2	0.00	0.00	0.00	0.00
3	0.00	0.00	0.00	0.00
4	0.00	0.00	0.00	0.00
5	0.00	0.00	0.00	0.00
6	0.00	0.00	0.00	0.00
7	100.00	0.00	0.00	0.00
-----				
Σ	100.00	0.00	0.00	0.00

Damage calculated on basis of individual service life

HFatt & HHatt



	HFatt1	HFatt2	HHatt1	HHatt2
(h)	291.2	1e+006	1e+006	1e+006
No.	F1%	F2%	H1%	H2%
1	0.00	0.00	0.00	0.00
2	0.00	0.00	0.00	0.00
3	0.00	0.00	0.00	0.00
4	0.00	0.00	0.00	0.00
5	0.00	0.00	0.00	0.00
6	0.00	0.00	0.00	0.00
7	100.00	0.00	0.00	0.00
-----				
Σ	100.00	0.00	0.00	0.00

**REMARKS:**

- Specifications with [e/i] imply: Maximum [e] and Minimal value [i] with consideration of all tolerances
- Specifications with [m] imply: Mean value within tolerance
- For the backlash tolerance, the center distance tolerances and the tooth thickness deviation are taken into account. Shown is the maximal and the minimal backlash corresponding the largest resp. the smallest allowances
- The calculation is done for the Operating pitch circle..
- Details of calculation method:
  - cg according to method B
  - KV according to method B

---

End of Report

lines: 570

---

# Contact analysis gear stage 2

KISSsoft Release 03/2015 F

KISSsoft Academic License - Norwegian University of Science & Technology (NTNU)

File

Name : Unnamed

Changed by: Kraftwerk

on: 02.02.2016

at: 18:27:41

## Contact Analysis

Meshing gear 1 - gear 2

Accuracy of calculation

Medium

**Partial load for calculation**  $[w_t]$  **100.0000** (%)

Note: In order to obtain contact analysis results for scuffing, micropitting and tooth flank fracture according to method A of ISO the calculation would have to be performed with  $w_t = 100 * K_{gam} * K_A * K_V ..$

$(w_t * K_{gam} * K_A * K_V = 128.56 \%)$

Working flank		Left tooth flank	
Center distance	[a]	-32.4000	(mm)
Single pitch deviation	[f <sub>pt</sub> ]	0.0000	(μm)
Coefficient. of friction	[μ]	0.1105	
Deviation error of axis	[f <sub>Σβ</sub> ]	2.9260	(μm)
Inclination error of axis	[f <sub>Σδ</sub> ]	2.7000	(μm)
Torque	[T <sub>1</sub> ]	23.7672	(Nm)

Torsion

Gear A:-, B:-

		min	max	Δ	μ	σ
Transmission error	(μm)	-15.3422	-10.5955	4.7467	-12.4905	1.5476
Tangent Stiffness curve	(N/μm)	211.2722	332.1165	120.8443	311.0535	26.2917
Secant stiffness curve	(N/μm)	168.7158	242.3469	73.6311	209.1987	24.1936
Line load	(N/mm)	0.0000	281.3218	281.3218	109.6061	75.2120
Torque Gear 1	(Nm)	23.7649	23.7695	0.0046	23.7671	0.0008
Torque Gear 2	(Nm)	-102.4056	-100.9869	1.4187	-101.6563	0.4580
Power loss	(W)	13.9614	69.5249	55.5635	50.8996	18.8285
Contact temperature	(°C)	76.8355	99.1069	22.2714	83.4033	5.5193
Thickness of lubrication film	(μm)	0.0074	0.1003	0.0929	0.0344	0.0231
Hertzian pressure	(N/mm <sup>2</sup> )		4011.2429		1163.7201	
Tooth root stress gear 1	(N/mm <sup>2</sup> )		731.7794		96.2374	
Tooth root stress gear 2	(N/mm <sup>2</sup> )		666.3910		124.4914	

Safety against micropitting (ISO/TR 15144 Method A) 0.0000

Safety against scuffing 22.9987

Transverse contact ratio under load  $[\epsilon\alpha]$  1.9684  
 min 1.1158  
 μ 1.8187  
 max 1.9684

Overlap ratio under load  $[\epsilon\beta]$  0.0000

Total contact ratio under load  $[\epsilon\gamma]$  1.9684

Efficiency  $[\eta]$  99.2400

Face load factor (ISO6336-1 Annex E, takes into account  $K_A * K_V$ )

$[K_{H\beta}]$

1.1966

Note: The resulting safeties do not correspond with Method A according ISO because  $K_\gamma$ ,  $K_A$  and  $K_V$  are not taken into account.

Amplitude spectrum of the transmission error

Harmonics	Amplitude (μm)
1	2.135
2	0.450

3	0.193
4	0.042
5	0.090
6	0.048
7	0.050
8	0.020
9	0.020
10	0.008

**K<sub>Hβ</sub> Calculation - Gear 1 - Gear 2**

Left flank

Load distribution calculated with:  $T_{nom} * K_v * K_A * K_y$ ; Axis alignment calculated with:  $T_{nom}$   
(Partial load for calculation: Load distribution calculated with: 128.56 %; Axis alignment calculated with: 100.00 %)

$f_{\Sigma\beta} = 2.926 \mu\text{m}$  ,  $f_{\Sigma\delta} = 2.700 \mu\text{m}$

$f_{ma} = 0.000 \mu\text{m}$  ,  $f_{H\beta} = 0.000 \mu\text{m}$

Result after i = 1 iterations of load distribution

Gear 1

Point in polar co-ordinates:

R = 9.795 mm ,  $\varphi = 0.000^\circ$

Displacement calculated in direction 249.283 °

	y	$\varphi_{1.t}$	f1.t	f1.b	f1.tot	f1.C	f1.tot+f1.C
1	-6.373 mm	0.0000°	0.0000 $\mu\text{m}$	0.0000 $\mu\text{m}$	0.0000 $\mu\text{m}$	0.0000 $\mu\text{m}$	0.0000 $\mu\text{m}$
2	-6.118 mm	0.0000°	0.0000 $\mu\text{m}$	0.0000 $\mu\text{m}$	0.0000 $\mu\text{m}$	-0.6457 $\mu\text{m}$	-0.6457 $\mu\text{m}$
3	-5.863 mm	0.0000°	0.0000 $\mu\text{m}$	0.0000 $\mu\text{m}$	0.0000 $\mu\text{m}$	-1.2898 $\mu\text{m}$	-1.2898 $\mu\text{m}$
4	-5.608 mm	0.0000°	0.0000 $\mu\text{m}$	0.0000 $\mu\text{m}$	0.0000 $\mu\text{m}$	-1.8849 $\mu\text{m}$	-1.8849 $\mu\text{m}$
5	-5.353 mm	0.0000°	0.0000 $\mu\text{m}$	0.0000 $\mu\text{m}$	0.0000 $\mu\text{m}$	-2.4605 $\mu\text{m}$	-2.4605 $\mu\text{m}$
6	-5.098 mm	0.0000°	0.0000 $\mu\text{m}$	0.0000 $\mu\text{m}$	0.0000 $\mu\text{m}$	-3.0050 $\mu\text{m}$	-3.0050 $\mu\text{m}$
7	-4.843 mm	0.0000°	0.0000 $\mu\text{m}$	0.0000 $\mu\text{m}$	0.0000 $\mu\text{m}$	-3.5120 $\mu\text{m}$	-3.5120 $\mu\text{m}$
8	-4.588 mm	0.0000°	0.0000 $\mu\text{m}$	0.0000 $\mu\text{m}$	0.0000 $\mu\text{m}$	-4.0010 $\mu\text{m}$	-4.0010 $\mu\text{m}$
9	-4.333 mm	0.0000°	0.0000 $\mu\text{m}$	0.0000 $\mu\text{m}$	0.0000 $\mu\text{m}$	-4.4443 $\mu\text{m}$	-4.4443 $\mu\text{m}$
10	-4.078 mm	0.0000°	0.0000 $\mu\text{m}$	0.0000 $\mu\text{m}$	0.0000 $\mu\text{m}$	-4.8648 $\mu\text{m}$	-4.8648 $\mu\text{m}$
11	-3.824 mm	0.0000°	0.0000 $\mu\text{m}$	0.0000 $\mu\text{m}$	0.0000 $\mu\text{m}$	-5.2575 $\mu\text{m}$	-5.2575 $\mu\text{m}$
12	-3.569 mm	0.0000°	0.0000 $\mu\text{m}$	0.0000 $\mu\text{m}$	0.0000 $\mu\text{m}$	-5.6094 $\mu\text{m}$	-5.6094 $\mu\text{m}$
13	-3.314 mm	0.0000°	0.0000 $\mu\text{m}$	0.0000 $\mu\text{m}$	0.0000 $\mu\text{m}$	-5.9434 $\mu\text{m}$	-5.9434 $\mu\text{m}$
14	-3.059 mm	0.0000°	0.0000 $\mu\text{m}$	0.0000 $\mu\text{m}$	0.0000 $\mu\text{m}$	-6.2349 $\mu\text{m}$	-6.2349 $\mu\text{m}$
15	-2.804 mm	0.0000°	0.0000 $\mu\text{m}$	0.0000 $\mu\text{m}$	0.0000 $\mu\text{m}$	-6.5003 $\mu\text{m}$	-6.5003 $\mu\text{m}$
16	-2.549 mm	0.0000°	0.0000 $\mu\text{m}$	0.0000 $\mu\text{m}$	0.0000 $\mu\text{m}$	-6.7412 $\mu\text{m}$	-6.7412 $\mu\text{m}$
17	-2.294 mm	0.0000°	0.0000 $\mu\text{m}$	0.0000 $\mu\text{m}$	0.0000 $\mu\text{m}$	-6.9381 $\mu\text{m}$	-6.9381 $\mu\text{m}$
18	-2.039 mm	0.0000°	0.0000 $\mu\text{m}$	0.0000 $\mu\text{m}$	0.0000 $\mu\text{m}$	-7.1170 $\mu\text{m}$	-7.1170 $\mu\text{m}$
19	-1.784 mm	0.0000°	0.0000 $\mu\text{m}$	0.0000 $\mu\text{m}$	0.0000 $\mu\text{m}$	-7.2567 $\mu\text{m}$	-7.2567 $\mu\text{m}$
20	-1.529 mm	0.0000°	0.0000 $\mu\text{m}$	0.0000 $\mu\text{m}$	0.0000 $\mu\text{m}$	-7.3670 $\mu\text{m}$	-7.3670 $\mu\text{m}$
21	-1.275 mm	0.0000°	0.0000 $\mu\text{m}$	0.0000 $\mu\text{m}$	0.0000 $\mu\text{m}$	-7.4561 $\mu\text{m}$	-7.4561 $\mu\text{m}$
22	-1.020 mm	0.0000°	0.0000 $\mu\text{m}$	0.0000 $\mu\text{m}$	0.0000 $\mu\text{m}$	-7.4979 $\mu\text{m}$	-7.4979 $\mu\text{m}$
23	-0.765 mm	0.0000°	0.0000 $\mu\text{m}$	0.0000 $\mu\text{m}$	0.0000 $\mu\text{m}$	-7.5218 $\mu\text{m}$	-7.5218 $\mu\text{m}$
24	-0.510 mm	0.0000°	0.0000 $\mu\text{m}$	0.0000 $\mu\text{m}$	0.0000 $\mu\text{m}$	-7.5097 $\mu\text{m}$	-7.5097 $\mu\text{m}$
25	-0.255 mm	0.0000°	0.0000 $\mu\text{m}$	0.0000 $\mu\text{m}$	0.0000 $\mu\text{m}$	-7.4649 $\mu\text{m}$	-7.4649 $\mu\text{m}$
26	-0.000 mm	0.0000°	0.0000 $\mu\text{m}$	0.0000 $\mu\text{m}$	0.0000 $\mu\text{m}$	-7.4022 $\mu\text{m}$	-7.4022 $\mu\text{m}$
27	0.255 mm	0.0000°	0.0000 $\mu\text{m}$	0.0000 $\mu\text{m}$	0.0000 $\mu\text{m}$	-7.2890 $\mu\text{m}$	-7.2890 $\mu\text{m}$
28	0.510 mm	0.0000°	0.0000 $\mu\text{m}$	0.0000 $\mu\text{m}$	0.0000 $\mu\text{m}$	-7.1577 $\mu\text{m}$	-7.1577 $\mu\text{m}$
29	0.765 mm	0.0000°	0.0000 $\mu\text{m}$	0.0000 $\mu\text{m}$	0.0000 $\mu\text{m}$	-6.9938 $\mu\text{m}$	-6.9938 $\mu\text{m}$
30	1.020 mm	0.0000°	0.0000 $\mu\text{m}$	0.0000 $\mu\text{m}$	0.0000 $\mu\text{m}$	-6.7940 $\mu\text{m}$	-6.7940 $\mu\text{m}$
31	1.275 mm	0.0000°	0.0000 $\mu\text{m}$	0.0000 $\mu\text{m}$	0.0000 $\mu\text{m}$	-6.5763 $\mu\text{m}$	-6.5763 $\mu\text{m}$
32	1.529 mm	0.0000°	0.0000 $\mu\text{m}$	0.0000 $\mu\text{m}$	0.0000 $\mu\text{m}$	-6.3112 $\mu\text{m}$	-6.3112 $\mu\text{m}$
33	1.784 mm	0.0000°	0.0000 $\mu\text{m}$	0.0000 $\mu\text{m}$	0.0000 $\mu\text{m}$	-6.0249 $\mu\text{m}$	-6.0249 $\mu\text{m}$

34	2.039 mm	0.0000°	0.0000 μm	0.0000 μm	0.0000 μm	-5.7092 μm	-5.7092 μm
35	2.294 mm	0.0000°	0.0000 μm	0.0000 μm	0.0000 μm	-5.3543 μm	-5.3543 μm
36	2.549 mm	0.0000°	0.0000 μm	0.0000 μm	0.0000 μm	-4.9815 μm	-4.9815 μm
37	2.804 mm	0.0000°	0.0000 μm	0.0000 μm	0.0000 μm	-4.5646 μm	-4.5646 μm
38	3.059 mm	0.0000°	0.0000 μm	0.0000 μm	0.0000 μm	-4.1232 μm	-4.1232 μm
39	3.314 mm	0.0000°	0.0000 μm	0.0000 μm	0.0000 μm	-3.6557 μm	-3.6557 μm
40	3.569 mm	0.0000°	0.0000 μm	0.0000 μm	0.0000 μm	-3.1458 μm	-3.1458 μm
41	3.824 mm	0.0000°	0.0000 μm	0.0000 μm	0.0000 μm	-2.6179 μm	-2.6179 μm
42	4.078 mm	0.0000°	0.0000 μm	0.0000 μm	0.0000 μm	-2.0492 μm	-2.0492 μm
43	4.333 mm	0.0000°	0.0000 μm	0.0000 μm	0.0000 μm	-1.4528 μm	-1.4528 μm
44	4.588 mm	0.0000°	0.0000 μm	0.0000 μm	0.0000 μm	-0.8335 μm	-0.8335 μm
45	4.843 mm	0.0000°	0.0000 μm	0.0000 μm	0.0000 μm	-0.1685 μm	-0.1685 μm
46	5.098 mm	0.0000°	0.0000 μm	0.0000 μm	0.0000 μm	0.5145 μm	0.5145 μm
47	5.353 mm	0.0000°	0.0000 μm	0.0000 μm	0.0000 μm	1.2350 μm	1.2350 μm
48	5.608 mm	0.0000°	0.0000 μm	0.0000 μm	0.0000 μm	1.9865 μm	1.9865 μm
49	5.863 mm	0.0000°	0.0000 μm	0.0000 μm	0.0000 μm	2.7576 μm	2.7576 μm
50	6.118 mm	0.0000°	0.0000 μm	0.0000 μm	0.0000 μm	3.5777 μm	3.5777 μm
51	6.373 mm	0.0000°	0.0000 μm	0.0000 μm	0.0000 μm	4.3994 μm	4.3994 μm

Gear 2

Point in polar co-ordinates:

R = -42.195 mm , φ = 0.000 °

Displacement calculated in direction 249.283 °

	y	φ2.t	f2.t	f2.b	f2.tot	f2.C	f2.tot+f2.C
1	-6.373 mm	0.0000°	0.0000 μm	-0.0116 μm	-0.0116 μm	0.0000 μm	-0.0116 μm
2	-6.118 mm	0.0000°	0.0000 μm	0.0245 μm	0.0245 μm	-0.0000 μm	0.0245 μm
3	-5.863 mm	0.0000°	0.0000 μm	0.0606 μm	0.0606 μm	-0.0000 μm	0.0606 μm
4	-5.608 mm	0.0000°	0.0000 μm	0.0967 μm	0.0967 μm	-0.0000 μm	0.0967 μm
5	-5.353 mm	0.0000°	0.0000 μm	0.1328 μm	0.1328 μm	-0.0000 μm	0.1328 μm
6	-5.098 mm	0.0000°	0.0000 μm	0.1689 μm	0.1689 μm	-0.0000 μm	0.1689 μm
7	-4.843 mm	0.0000°	0.0000 μm	0.2050 μm	0.2050 μm	-0.0000 μm	0.2050 μm
8	-4.588 mm	0.0000°	0.0000 μm	0.2411 μm	0.2411 μm	-0.0000 μm	0.2411 μm
9	-4.333 mm	0.0000°	0.0000 μm	0.2772 μm	0.2772 μm	-0.0000 μm	0.2772 μm
10	-4.078 mm	0.0000°	0.0000 μm	0.3133 μm	0.3133 μm	-0.0000 μm	0.3133 μm
11	-3.824 mm	0.0000°	0.0000 μm	0.3494 μm	0.3494 μm	-0.0000 μm	0.3494 μm
12	-3.569 mm	0.0000°	0.0000 μm	0.3855 μm	0.3855 μm	-0.0000 μm	0.3855 μm
13	-3.314 mm	0.0000°	0.0000 μm	0.4216 μm	0.4216 μm	-0.0000 μm	0.4216 μm
14	-3.059 mm	0.0000°	0.0000 μm	0.4577 μm	0.4577 μm	-0.0000 μm	0.4577 μm
15	-2.804 mm	0.0000°	0.0000 μm	0.4938 μm	0.4938 μm	-0.0000 μm	0.4938 μm
16	-2.549 mm	0.0000°	0.0000 μm	0.5299 μm	0.5299 μm	-0.0000 μm	0.5299 μm
17	-2.294 mm	0.0000°	0.0000 μm	0.5660 μm	0.5660 μm	-0.0000 μm	0.5660 μm
18	-2.039 mm	0.0000°	0.0000 μm	0.6021 μm	0.6021 μm	-0.0000 μm	0.6021 μm
19	-1.784 mm	0.0000°	0.0000 μm	0.6382 μm	0.6382 μm	-0.0000 μm	0.6382 μm
20	-1.529 mm	0.0000°	0.0000 μm	0.6743 μm	0.6743 μm	-0.0000 μm	0.6743 μm
21	-1.275 mm	0.0000°	0.0000 μm	0.7104 μm	0.7104 μm	-0.0000 μm	0.7104 μm
22	-1.020 mm	0.0000°	0.0000 μm	0.7465 μm	0.7465 μm	-0.0000 μm	0.7465 μm
23	-0.765 mm	0.0000°	0.0000 μm	0.7826 μm	0.7826 μm	-0.0000 μm	0.7826 μm
24	-0.510 mm	0.0000°	0.0000 μm	0.8187 μm	0.8187 μm	-0.0000 μm	0.8187 μm
25	-0.255 mm	0.0000°	0.0000 μm	0.8548 μm	0.8548 μm	-0.0000 μm	0.8548 μm
26	-0.000 mm	0.0000°	0.0000 μm	0.8909 μm	0.8909 μm	-0.0000 μm	0.8909 μm
27	0.255 mm	0.0000°	0.0000 μm	0.9270 μm	0.9270 μm	-0.0000 μm	0.9270 μm
28	0.510 mm	0.0000°	0.0000 μm	0.9631 μm	0.9631 μm	-0.0000 μm	0.9631 μm
29	0.765 mm	0.0000°	0.0000 μm	0.9992 μm	0.9992 μm	-0.0000 μm	0.9992 μm
30	1.020 mm	0.0000°	0.0000 μm	1.0353 μm	1.0353 μm	-0.0000 μm	1.0353 μm
31	1.275 mm	0.0000°	0.0000 μm	1.0714 μm	1.0714 μm	-0.0000 μm	1.0714 μm
32	1.529 mm	0.0000°	0.0000 μm	1.1074 μm	1.1074 μm	-0.0000 μm	1.1074 μm

33	1.784 mm	0.0000°	0.0000 μm	1.1435 μm	1.1435 μm	-0.0000 μm	1.1435 μm
34	2.039 mm	0.0000°	0.0000 μm	1.1796 μm	1.1796 μm	-0.0000 μm	1.1796 μm
35	2.294 mm	0.0000°	0.0000 μm	1.2157 μm	1.2157 μm	-0.0000 μm	1.2157 μm
36	2.549 mm	0.0000°	0.0000 μm	1.2518 μm	1.2518 μm	-0.0000 μm	1.2518 μm
37	2.804 mm	0.0000°	0.0000 μm	1.2879 μm	1.2879 μm	-0.0000 μm	1.2879 μm
38	3.059 mm	0.0000°	0.0000 μm	1.3240 μm	1.3240 μm	-0.0000 μm	1.3240 μm
39	3.314 mm	0.0000°	0.0000 μm	1.3601 μm	1.3601 μm	-0.0000 μm	1.3601 μm
40	3.569 mm	0.0000°	0.0000 μm	1.3962 μm	1.3962 μm	-0.0000 μm	1.3962 μm
41	3.824 mm	0.0000°	0.0000 μm	1.4323 μm	1.4323 μm	-0.0000 μm	1.4323 μm
42	4.078 mm	0.0000°	0.0000 μm	1.4684 μm	1.4684 μm	-0.0000 μm	1.4684 μm
43	4.333 mm	0.0000°	0.0000 μm	1.5045 μm	1.5045 μm	-0.0000 μm	1.5045 μm
44	4.588 mm	0.0000°	0.0000 μm	1.5406 μm	1.5406 μm	-0.0000 μm	1.5406 μm
45	4.843 mm	0.0000°	0.0000 μm	1.5767 μm	1.5767 μm	-0.0000 μm	1.5767 μm
46	5.098 mm	0.0000°	0.0000 μm	1.6128 μm	1.6128 μm	-0.0000 μm	1.6128 μm
47	5.353 mm	0.0000°	0.0000 μm	1.6489 μm	1.6489 μm	-0.0000 μm	1.6489 μm
48	5.608 mm	0.0000°	0.0000 μm	1.6850 μm	1.6850 μm	-0.0000 μm	1.6850 μm
49	5.863 mm	0.0000°	0.0000 μm	1.7211 μm	1.7211 μm	-0.0000 μm	1.7211 μm
50	6.118 mm	0.0000°	0.0000 μm	1.7572 μm	1.7572 μm	-0.0000 μm	1.7572 μm
51	6.373 mm	0.0000°	0.0000 μm	1.7933 μm	1.7933 μm	-0.0000 μm	1.7933 μm

Explanations:

- y : Width
- φ.t : Static torsion
- f.t : Displacement due to torsion
- f.b : Displacement due to bending
- f.tot : Total displacement (f.b+f.t)
- f.C : Change due to flank line modification

Load distribution

Contact stiffness = 15.023 N/mm/μm

Young's modulus = 202000.0/202000.0 N/mm<sup>2</sup>

	y	δ	g	w
1.	-6.3725 mm	8.3400 μm	12.1894 μm	183.1175 N/mm
2.	-6.1176 mm	7.6581 μm	12.8712 μm	193.3603 N/mm
3.	-5.8627 mm	6.9779 μm	13.5514 μm	203.5787 N/mm
4.	-5.6078 mm	6.3467 μm	14.1827 μm	213.0614 N/mm
5.	-5.3529 mm	5.7351 μm	14.7943 μm	222.2498 N/mm
6.	-5.0980 mm	5.1545 μm	15.3749 μm	230.9724 N/mm
7.	-4.8431 mm	4.6114 μm	15.9180 μm	239.1309 N/mm
8.	-4.5882 mm	4.0862 μm	16.4431 μm	247.0197 N/mm
9.	-4.3333 mm	3.6068 μm	16.9225 μm	254.2219 N/mm
10.	-4.0784 mm	3.1503 μm	17.3791 μm	261.0808 N/mm
11.	-3.8235 mm	2.7214 μm	17.8079 μm	267.5228 N/mm
12.	-3.5686 mm	2.3334 μm	18.1959 μm	273.3518 N/mm
13.	-3.3137 mm	1.9634 μm	18.5660 μm	278.9111 N/mm
14.	-3.0588 mm	1.6357 μm	18.8936 μm	283.8328 N/mm
15.	-2.8039 mm	1.3342 μm	19.1951 μm	288.3622 N/mm
16.	-2.5490 mm	1.0572 μm	19.4721 μm	292.5237 N/mm
17.	-2.2941 mm	0.8243 μm	19.7051 μm	296.0232 N/mm
18.	-2.0392 mm	0.6093 μm	19.9201 μm	299.2530 N/mm
19.	-1.7843 mm	0.4335 μm	20.0959 μm	301.8942 N/mm
20.	-1.5294 mm	0.2870 μm	20.2423 μm	304.0940 N/mm
21.	-1.2745 mm	0.1618 μm	20.3676 μm	305.9751 N/mm
22.	-1.0196 mm	0.0839 μm	20.4454 μm	307.1451 N/mm
23.	-0.7647 mm	0.0240 μm	20.5054 μm	308.0453 N/mm
24.	-0.5098 mm	0.0000 μm	20.5294 μm	308.4060 N/mm
25.	-0.2549 mm	0.0086 μm	20.5207 μm	308.2764 N/mm

26.	-0.0000 mm	0.0352 $\mu\text{m}$	20.4942 $\mu\text{m}$	307.8770 N/mm
27.	0.2549 mm	0.1124 $\mu\text{m}$	20.4170 $\mu\text{m}$	306.7174 N/mm
28.	0.5098 mm	0.2075 $\mu\text{m}$	20.3218 $\mu\text{m}$	305.2881 N/mm
29.	0.7647 mm	0.3353 $\mu\text{m}$	20.1940 $\mu\text{m}$	303.3684 N/mm
30.	1.0196 mm	0.4990 $\mu\text{m}$	20.0303 $\mu\text{m}$	300.9092 N/mm
31.	1.2745 mm	0.6807 $\mu\text{m}$	19.8487 $\mu\text{m}$	298.1803 N/mm
32.	1.5294 mm	0.9097 $\mu\text{m}$	19.6197 $\mu\text{m}$	294.7402 N/mm
33.	1.7843 mm	1.1599 $\mu\text{m}$	19.3695 $\mu\text{m}$	290.9814 N/mm
34.	2.0392 mm	1.4395 $\mu\text{m}$	19.0899 $\mu\text{m}$	286.7812 N/mm
35.	2.2941 mm	1.7582 $\mu\text{m}$	18.7711 $\mu\text{m}$	281.9925 N/mm
36.	2.5490 mm	2.0950 $\mu\text{m}$	18.4344 $\mu\text{m}$	276.9340 N/mm
37.	2.8039 mm	2.4758 $\mu\text{m}$	18.0536 $\mu\text{m}$	271.2135 N/mm
38.	3.0588 mm	2.8810 $\mu\text{m}$	17.6483 $\mu\text{m}$	265.1252 N/mm
39.	3.3137 mm	3.3124 $\mu\text{m}$	17.2169 $\mu\text{m}$	258.6445 N/mm
40.	3.5686 mm	3.7863 $\mu\text{m}$	16.7431 $\mu\text{m}$	251.5263 N/mm
41.	3.8235 mm	4.2780 $\mu\text{m}$	16.2513 $\mu\text{m}$	244.1383 N/mm
42.	4.0784 mm	4.8106 $\mu\text{m}$	15.7187 $\mu\text{m}$	236.1373 N/mm
43.	4.3333 mm	5.3710 $\mu\text{m}$	15.1584 $\mu\text{m}$	227.7194 N/mm
44.	4.5882 mm	5.9542 $\mu\text{m}$	14.5752 $\mu\text{m}$	218.9582 N/mm
45.	4.8431 mm	6.5831 $\mu\text{m}$	13.9463 $\mu\text{m}$	209.5105 N/mm
46.	5.0980 mm	7.2299 $\mu\text{m}$	13.2994 $\mu\text{m}$	199.7930 N/mm
47.	5.3529 mm	7.9143 $\mu\text{m}$	12.6150 $\mu\text{m}$	189.5115 N/mm
48.	5.6078 mm	8.6298 $\mu\text{m}$	11.8996 $\mu\text{m}$	178.7641 N/mm
49.	5.8627 mm	9.3648 $\mu\text{m}$	11.1646 $\mu\text{m}$	167.7224 N/mm
50.	6.1176 mm	10.1487 $\mu\text{m}$	10.3806 $\mu\text{m}$	155.9451 N/mm
51.	6.3725 mm	10.9343 $\mu\text{m}$	9.5950 $\mu\text{m}$	144.1433 N/mm

Explanations:

$\delta$  : Gap

g : Flank overlap

w : Line load

Force application point, Y direction:  $y = -0.210 \text{ mm}$  ( $F = 3350.4 \text{ N}$ )

To take into account the load distribution in the shaft calculation: Force center point offset:  $\Delta y = -0.210 \text{ mm}$

$w_{\text{max}} = 308.406 \text{ N/mm}$ ,  $w_m = 257.726 \text{ N/mm}$

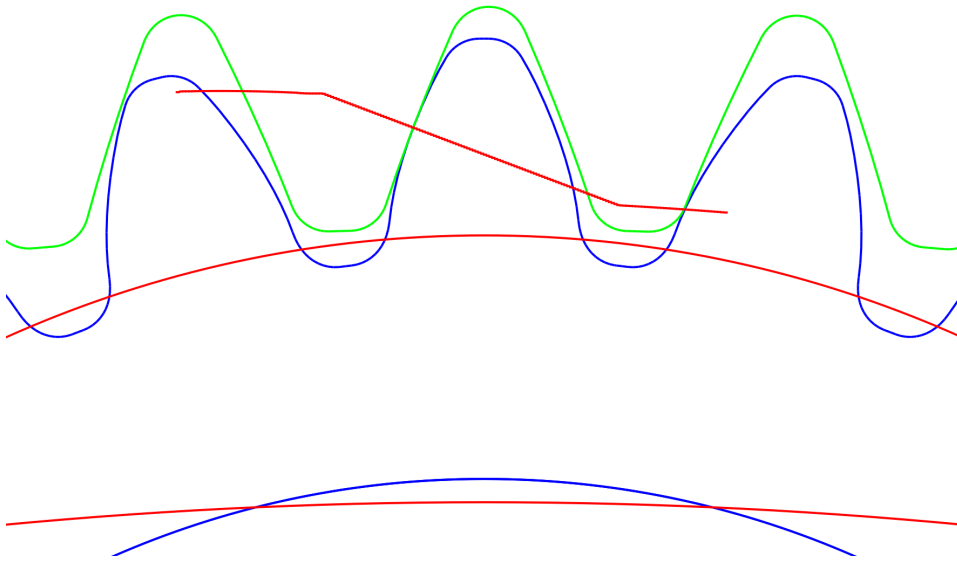
$w_m = K_V * K_A * K_Y * (F_t/b) / \cos(\alpha_{wt})$

$K_V = 1.0285$ ,  $K_A = 1.250$ ,  $K_Y = 1.000$

$K_{H\beta} = w_{\text{max}}/w_m = 1.1966$  (Calculation according to ISO 6336-1, Appendix E)

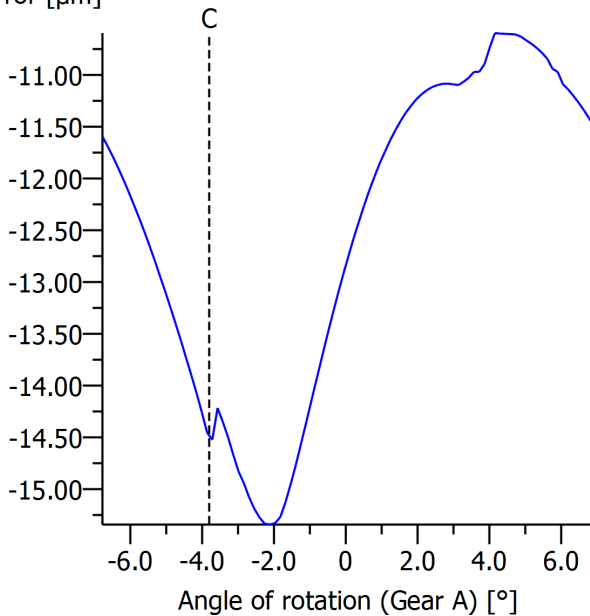
Side I, II:  $w_I / w_m = 0.7105$   $w_{II} / w_m = 0.5593$

Notice: The influence of the exceeding facewidth is not taken into account in the calculation of  $K_{H\beta}$ .



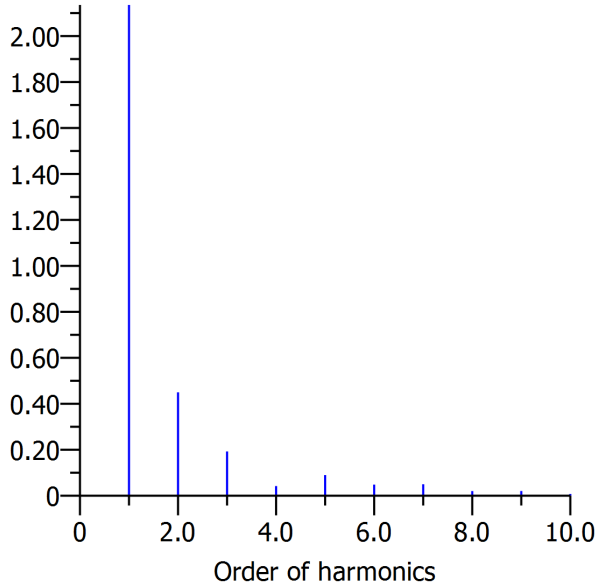
da1 = 21.4134 mm, df1 = 17.9716 mm, As1 = -0.0239 mm, da2 = -83.2226 mm, df2 = -86.7139 mm, As2 = -0.0442 mm  
Figure: Meshing Gear 1 - Gear 2

Transmission error [ $\mu\text{m}$ ]



wt = 100 %, a = -32.400 mm, fpt = 0.000  $\mu\text{m}$ ,  $\mu = 0.111$  Working flank: Left flank  
The transmission error contains the backlash  
Figure: Transmission error

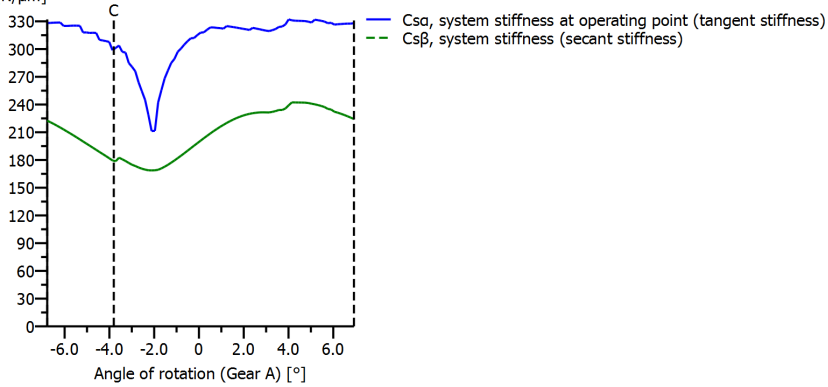
Amplitude [ $\mu\text{m}$ ]



Order of harmonics Amplitude [ $\mu\text{m}$ ]. 2.1353192. 0.4498113. 0.1925344. 0.0419075. 0.0897266.  
 0.0482577. 0.0498018. 0.0201579. 0.02048110. 0.007504wt = 100 %, a = -32.400 mm, fpt = 0.000  $\mu\text{m}$ ,  $\mu$  =  
 0.111Working flank: Left flank

Figure: Amplitude spectrum of transmission error

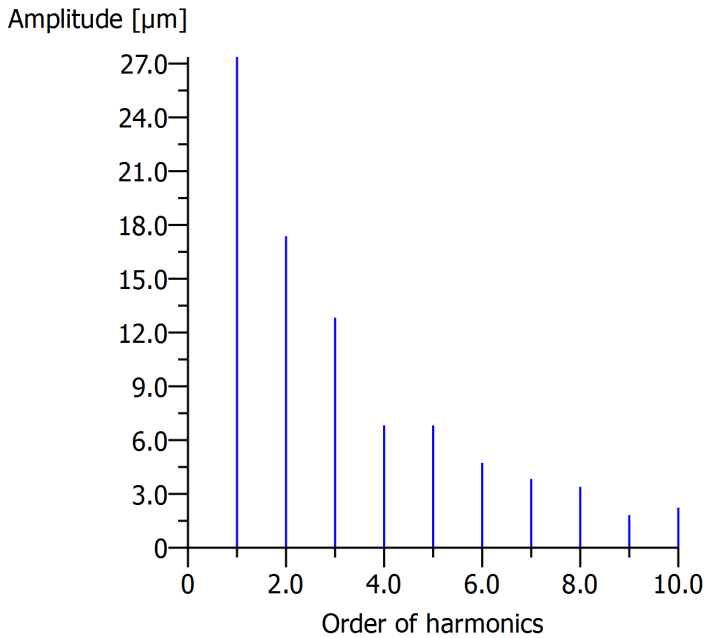
System stiffness [ $\text{N}/\mu\text{m}$ ]



wt = 100 %, a = -32.400 mm, fpt = 0.000  $\mu\text{m}$ ,  $\mu$  = 0.111Working flank: Left flank  $C_{\alpha\_mean} = 310.8727559 \text{ N}/\mu\text{m}$   $C_{\beta\_mean} = 209.0476425 \text{ N}/\mu\text{m}$   
 $C_{\alpha} = C_{\gamma\alpha} * b$   $C_{\beta} = C_{\gamma\beta} * b$

Figure: Stiffness curve

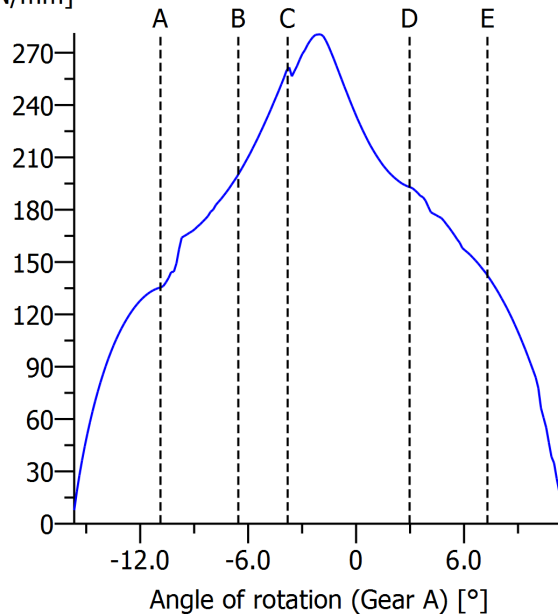




Order of harmonics Amplitude [N/mm/μm]1. 27.3693332. 17.3693193. 12.8331164. 6.8234135.  
6.8197916. 4.7310817. 3.8334378. 3.3925889. 1.82293710. 2.232019wt = 100 %, a = -32.400  
mm,fpt = 0.000 μm,μ = 0.111Working flank: Left flank

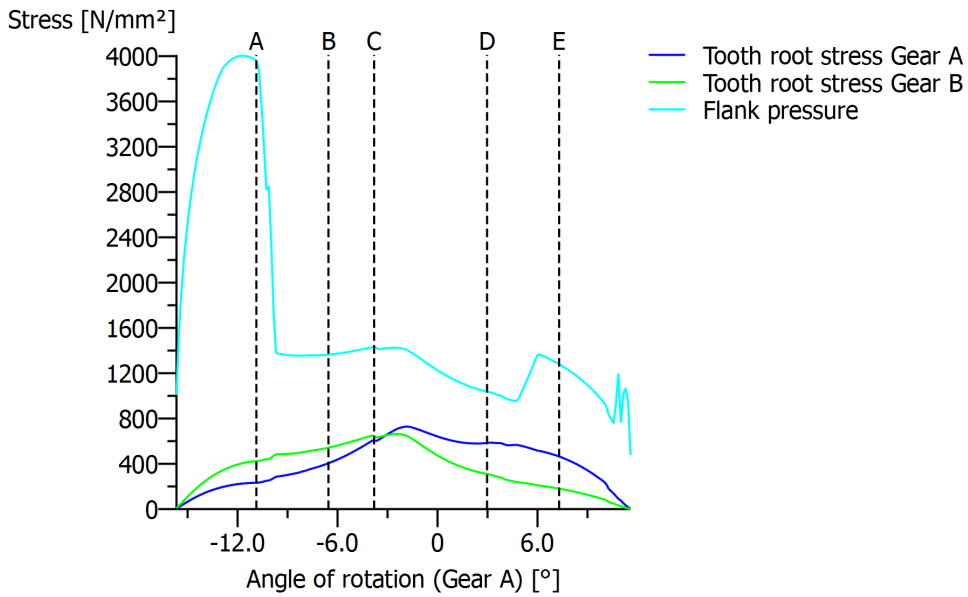
Figure: Amplitude spectrum of contact stiffness

Normal force (line load) [N/mm]

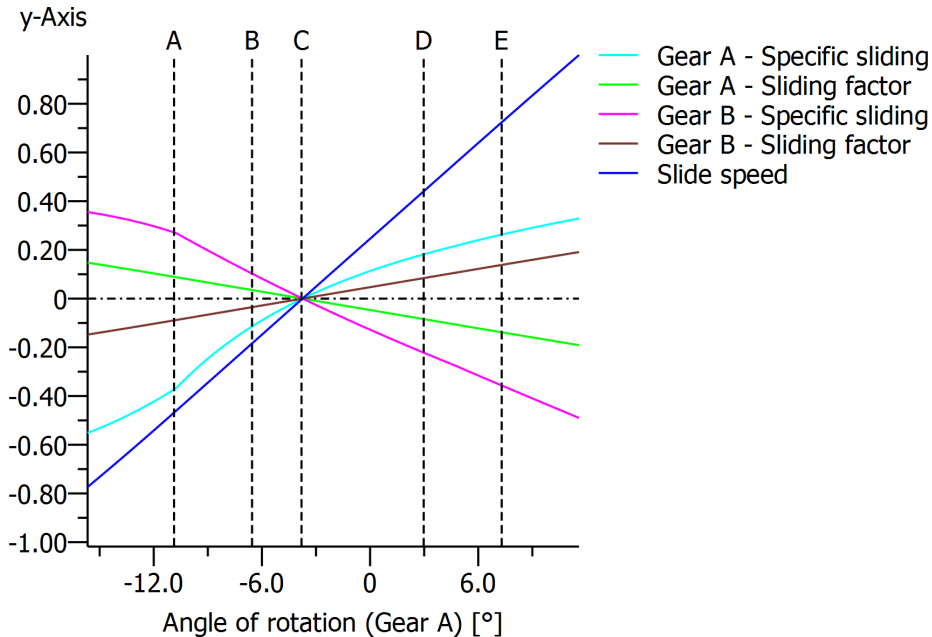


wt = 100 %, a = -32.400 mm,fpt = 0.000 μm,μ = 0.111Working flank: Left flank

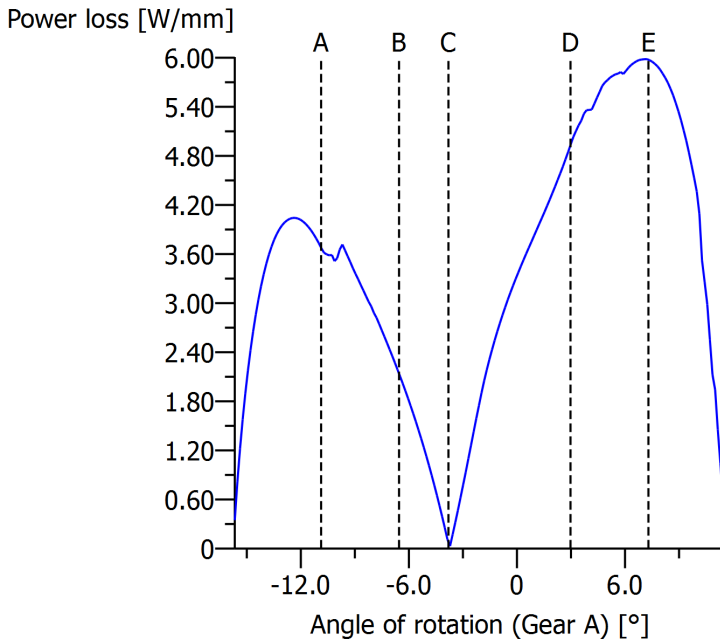
Figure: Normal force curve (Line load)



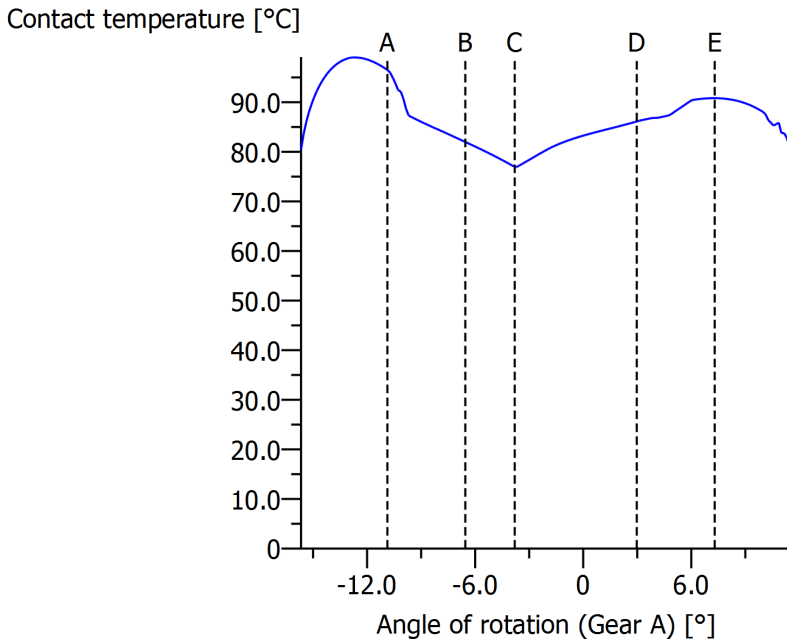
wt = 100 %, a = -32.400 mm, fpt = 0.000 μm, μ = 0.111 Working flank: Left flank  
Figure: Stress curve



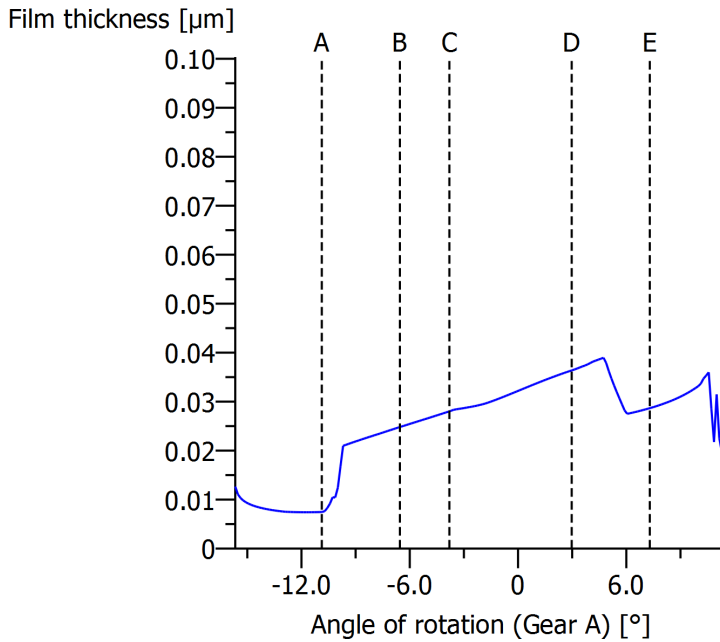
wt = 100 %, a = -32.400 mm, fpt = 0.000 μm, μ = 0.111 Working flank: Left flank Maximum sliding velocity: 0.420 m/s  
Figure: Kinematics



wt = 100 %, a = -32.400 mm, fpt = 0.000  $\mu\text{m}$ ,  $\mu = 0.111$  Displaying power losses per mm facewidth Working flank: Left flank  
Figure: Specific Power Loss

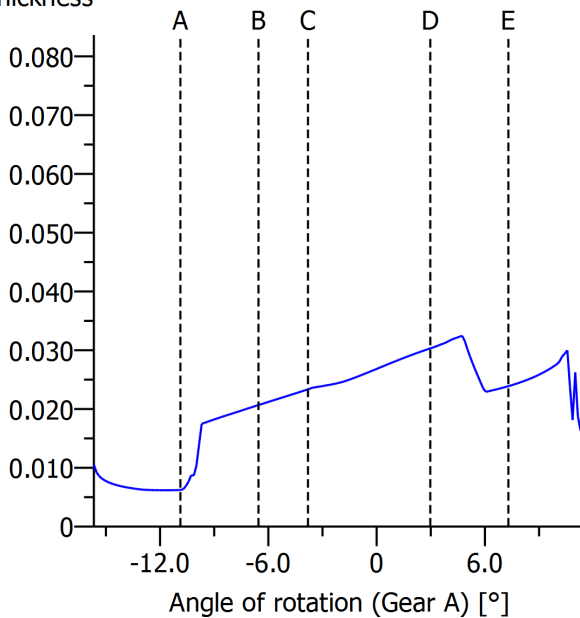


wt = 100 %, a = -32.400 mm, fpt = 0.000  $\mu\text{m}$ ,  $\mu = 0.091$  the oil = 70.0 °C, the M = 76.8 °C, etaM = 8.14 mPa\*s Working flank: Left flank  
Figure: Contact temperature



wt = 100 %, a = -32.400 mm, fpt = 0.000 µm,  $\mu = 0.091$  the oil = 70.0 °C, theM = 76.8 °C, etaM = 8.14 mPa\*shMini(ISO) = 0.007 µm, Ra = 1.200 µm Working flank: Left flank  
Figure: Lubricating film (ISO TR 15144)

**Specific film thickness**



wt = 100 %, a = -32.400 mm, fpt = 0.000 µm,  $\mu = 0.091$  the oil = 70.0 °C, theM = 76.8 °C, etaM = 8.14 mPa\*shMini(ISO) = 0.007 µm, Ra = 1.200 µm, lamGFmin = 0.006 Working flank: Left flank  
Figure: Specific film thickness (ISO TR 15144)